Development of New Self-centring Rocking Systems by Incorporating Resilient Slip Friction Mechanisms: Applications in Structures and Storage Tanks

Kaveh Sahami

A thesis submitted to
Auckland University of Technology in fulfilment of the
requirements for the degree of Doctor of Philosophy (PhD) in
Structural/Earthquake Engineering,

Supervisors:
Dr. Pouyan Zarnani
Prof. Pierre Quenneville

School of Future Environments, Department of Built Environment
Engineering Auckland University of Technology (AUT), New Zealand
December 2025

Abstract

Rocking systems, encompassing walls, columns and frames, have emerged as effective structural configurations in mitigating seismic hazards by providing the desirable displacement ductility, demonstrated by their robust bilinear elastic response. Initially conceptualized for gravity load applications, their resilience across various natural disasters (including hurricanes, tornadoes, and earthquakes) has substantiated their competence as primary lateral load-resisting structures. In recent decades, this conventional concept has been augmented by incorporation of energy dissipation mechanisms and hold-down systems to enhance the structure hysteresis performance by reducing the amplitude of oscillation during an event. This has fostered a low-damage, stable, and reliable seismic performance. The fundamental efficacy of rocking systems is attributed to the rotational freedom provided to structures, facilitating the synchronicity with seismic motions and consequently mitigating the impact of seismic forces on structural components and their connections.

To ensure the stability of such systems, integration with stabilizing mechanisms is imperative. Moreover, the inclusion of additional damping mechanisms is critical for maintaining deflections within permissible limits. The utilization of self-centring friction dampers, which includes both restoring and energy damping features, is particularly advantageous for rocking system applications. This research focused on the seismic performance of two distinct applications of rocking systems equipped with self-centring friction dampers: cylindrical steel liquid storage tanks and rocking panel walls.

The initial phase of this study investigated the rocking behaviour of conventionally designed cylindrical steel tanks, equipped with an innovative hold-down system to reduce the earthquake load demand and enhance their seismic resilience. This phase was commenced with the experimental component testing to validate the performance of a specially designed self-centring friction damper suitable for this application. Subsequently, a comparative seismic performance analysis was conducted on several case studies of cylindrical steel storage tanks, comparing the effects of the proposed anchorage system with the current state-of-practice such as necked rods and buckling-restrained hold-downs.

The second phase of the study proposed a novel rocking panel by integration of self-centring dampers, functioning as shear keys on both sides of the panel (rather than hold-downs). The objective was to introduce a new damage-free rocking system as a primary lateral resisting mechanism, applicable to both new structures and retrofitting of existing earthquake-prone building. Initially, the effectiveness of this system was validated through numerical modelling, followed by the design and testing of a large-scale rocking concrete panel incorporating the proposed configuration.

Attestation of Authorship

I hereby declare that this submission is my own work and that, to the best of my knowledge and belief, it contains no material previously published or written by another person (except where explicitly defined in the acknowledgements), nor material which to a substantial extent has been submitted for the award of any other degree or diploma of a university or other institutions of higher learning.

Signature: Kaveh Sahami

Date: 15th Nov 2024

Disclaimer

This thesis is prepared by Kaveh Sahami during a four-year PhD program in his best personal capacity and knowledge. Any opinions, findings, conclusions, and recommendations expressed in this material are those of the author and do not necessarily reflect the views of the sponsors. The responsibility of correct employment/accommodation of the opinions, recommendations, and formulations of this thesis would fall only and solely on the structural engineer(s) and the involved parties, and the author of the thesis shall not be liable for any design outcome.

Kaveh Sahami

Date: 15th Nov 2024

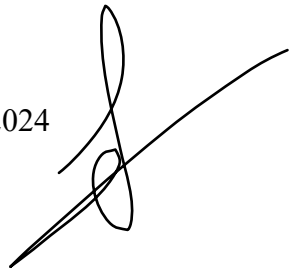

Dedication

This thesis is wholeheartedly and lovingly dedicated to:

My dearest Samira, the love of my life and my steadfast companion,

Your support has been the guiding light in my journey, for which I am profoundly grateful.

To the heart of our lives, Lovin, whose warmth brightens our world and inspires us every day.

And to my treasured family:

Momma,

Papa,

Roya,

Abtin,

Your unwavering love and encouragement have been my greatest inspiration and the source of my strength.

Table of Contents

List of figures

List of tables

Chapter 1: Introduction

1.1. Need for Next-Generation Lateral Load Resisting Systems

In the ever-evolving field of structural engineering, the resilience of buildings against dynamic lateral loads such as severe earthquakes and strong winds is a paramount concern. The dominant practices in contemporary lateral load systems, while effective to a degree, exhibit limitations in terms of energy dissipation, adaptability, and damage control. This chapter explores the necessity for next-generation lateral load resisting systems (LLRS's) in structures, emphasizing the innovations that can significantly enhance the structural resilience and sustainability.

1.1.1. Mainstream Methodologies Incorporated in LLRS's & the Challenges

The backbone of modern structural safety against lateral forces primarily consists of systems like shear walls, bracing systems, and moment-resisting frames. Each of these systems offers unique benefits. For instance, shear walls provide rigidity and strength, bracing systems offer ease of installation and cost-effectiveness, and moment-resisting frames allow for architectural flexibility. However, the performance of these systems under extreme conditions reveals critical vulnerabilities, including susceptibility to irreversible damage and limited energy dissipation capacity.

In the context of existing LLRS's, a primary challenge for these systems is the occurrence of plastic deformation often resulting in irreversible damage (though to be controlled) following significant seismic events making them vulnerable to aftershock sequences. This damage frequently necessitates extensive and costly repairs, and in severe cases, may require complete reconstruction of the affected structure.

Another critical aspect that is increasingly coming to the forefront is the environmental sustainability. The need to integrate eco-friendly design practices and materials in the construction as well as minimising the maintenance requirements of the structural systems adopted is becoming increasingly important. This focus on sustainability not only aligns with the global environmental objectives but also addresses the growing demand for green building practices and materials in the construction industry. The development of lateral load resisting systems that are resilient to seismic forces and less in need of repair or rebuild could reduce the carbon footprint following major events. Such

environmentally sustainable systems could represent a significant advancement in the field, offering a pathway towards more holistic and future-oriented structural engineering solutions.

1.1.2. The Imperative for Next-Generation Systems Emerging

The need for next-generation lateral load resisting systems is driven by the pursuit of enhanced resilience, adaptability, and environmental sustainability. Innovations in materials, such as the use of high-performance concrete or advanced steel compositions, promise improved strength and flexibility. Design advancements like base isolation and energy dissipating systems not only aim to preserve the structural integrity but also to limit the damage during disasters, ensuring a quicker recovery and reduced costs.

Recent case studies have underscored the effectiveness of advanced seismic protection systems, particularly those incorporating energy dissipation devices. For instance, structures equipped with base isolation technology have demonstrated notable resilience in seismically active regions. Additionally, the integration of innovative smart materials, which possess the ability to self-repair minor cracks and damage, indicates a promising future in which buildings are capable of preserving their structural integrity. This shift in building design towards self-maintaining and energy-dissipating technologies is a significant step forward in enhancing the seismic resilience of structures.

1.2. Residual Drift as an Indicator of Potential Need for Post Event Recovery

The concept of residual drift has emerged as a critical metric for assessing the aftermath of seismic events on buildings. The residual drift is defined as the permanent deformation or displacement remaining in a structure after a seismic event. It serves as an essential indicator of the building potential post-event recovery. This section delves into the importance of understanding and measuring the residual drift, its implications on structural integrity, and its role in guiding effective recovery and rehabilitation strategies.

1.2.1. Understanding the Residual Drift & its Implications

The residual drift is primarily a consequence of inelastic deformations during seismic activities. Unlike the elastic deformations, where a structure returns to its original state, inelastic deformations lead to permanent changes in the structure geometry. The extent of residual drift is influenced by various factors, including the intensity of the seismic

event, the building design, the materials used, and the quality of construction. The measurement of residual drift provides invaluable insights into the extent of damage and the structural health of the building impacted by earthquake.

The presence of significant residual drift in a structure can have far-reaching implications. Firstly, it can compromise the building safety, making it uninhabitable or prone to collapse during aftershocks. Secondly, it has economic implications, as buildings with high residual drift often require extensive repairs or even demolition and reconstruction. Lastly, it could impact the urban resilience given a high incidence of residual drift in a region and need for demolition and rebuild could lead to a housing crisis and hinder a quick recovery from seismic events.

The analysis of residual drift is pivotal in shaping post-event recovery strategies. It helps engineers and decision-makers determine whether a building can be repaired or needs to be replaced. In addition, understanding residual drift patterns aids in the development of more resilient building designs. This includes the integration of features such as base isolation, energy-dissipating devices, and more flexible materials that can reduce the extent of inelastic deformations during earthquakes.

1.2.2. Case Studies and Research Findings

Several case studies post major earthquakes – such as the Northridge or the Christchurch earthquakes – have demonstrated the value of analysing the impact of residual drift level. Buildings with minimal residual drift were often quickly repaired and reoccupied, while those with significant drift required more extensive interventions. The research in this domain continuously contributes to refining the building codes and practices, emphasising the designs that not only prevent collapse but also minimize the residual drift.

The residual drift serves as a crucial factor in assessing the building ability to recover from seismic events. Understanding and mitigating the residual drift is not just about repairing structures; it's about building resilience into the very fabric of urban environments. As the world faces increasing seismic risks due to urbanization, controlling the residual drift in structural design and post-event evaluation becomes imperative. This approach will provide safer, more resilient communities and industries capable of withstanding and quicker recovering from seismic challenges. According to FEMA P-58, moment-resisting frames can typically endure higher drift levels, with the threshold for

non-repairable damage around 3%. In contrast, braced frames and shear walls, especially those designed with high stiffness, may reach the non-repairable damage limit at lower drifts, often around 2%.

1.3. Friction Mechanism as an Approach for Energy Dissipation

In the pursuit of engineering structures capable of withstanding seismic and dynamic loads, the role of energy dissipation mechanisms is paramount in reducing the earthquake load demand. Among the various strategies such as deploying steel yieldable fuses and fluid viscous dampers, the friction mechanisms stand out as effective means for energy dissipation. This section explores the principles behind friction mechanisms used in structures, their effectiveness as energy dissipators, and their contribution to the overall resilience of buildings and infrastructures.

1.3.1. Effectiveness in Comparison with Other Energy Dissipation Systems

The effectiveness of friction mechanisms in energy dissipation is evidenced in several aspects. Firstly, they reduce the amplitude of vibrations during seismic events, thus protecting the structural integrity. Secondly, their capacity to dissipate energy helps in controlling both the transient and residual movements of the structure, contributing to its stability and longevity. Additionally, these systems are typically designed to be easily replaceable with repeatable performance within the designed range, which allows for quick restoration of their energy dissipation capacity against major seismic events.

When compared to other energy dissipation systems such as viscous dampers or base isolators, friction mechanisms offer unique advantages. They are often more cost-effective, require less maintenance, and have a simpler design, making them applicable for a wide range of structures. However, their performance is highly dependent on the material characteristics and the specific design of the damper, which can be a limitation in certain applications.

1.3.2. Aligning Seismic Resilience with Environmental Sustainability

The incorporation of energy dissipation devices in structural design not only advances seismic resilience but also aligns with the principles of environmental sustainability, a crucial consideration in contemporary architectural and engineering practices. These energy dissipation systems, such as base isolators and damping devices, reduce the forces transmitted to a structure during seismic events, thereby minimizing structural damage

and extending the lifespan of buildings. This reduction in damage correlates with a decreased need for resource-intensive repairs and rebuilds, contributing to a more sustainable use of materials and resources.

Moreover, the longevity and durability imparted by these devices mean that structures require less frequent renovation or reconstruction, leading to a reduction in construction waste and lower consumption of raw materials over the building lifecycle. Additionally, the application of such technologies can be seen as an investment in the long-term sustainability of urban infrastructure, potentially reducing the environmental footprint associated with periodic seismic retrofitting.

In a broader context, the integration of energy dissipation devices reflects a growing trend towards building designs that consider not only immediate functional requirements but also long-term environmental impact. This approach is in line with sustainable development goals, seeking to harmonize the built environment with ecological considerations. As such, the role of energy dissipation devices extends beyond mere structural safety, contributing to a holistic vision of sustainable and resilient urban development.

1.3.3. Future Trends and Research Directions

Looking forward, the development of friction mechanisms continues to be a dynamic field of research. Current trends focus on optimizing materials and designs to improve performance and adaptability. Innovations in smart materials and self-centring friction systems are being explored to create more responsive and efficient energy dissipation solutions.

Friction mechanisms as a source of energy dissipation are integral to the design of resilient structures. Their ability to effectively dissipate seismic energy, coupled with advantages such as cost-effectiveness and ease of maintenance, positions them as a crucial component in modern structural design. Continued research and innovation in this field are essential to enhance the capacity of structures to withstand and recover from the dynamic forces they encounter, ensuring safety and sustainability in the built environment.

1.4. Low Damage Design Philosophy

Low damage design philosophy stems from the recognition that the traditional approach of designing structures to remain elastic under seismic loads is often economically and practically unfeasible. Instead, this approach aims to allow controlled inelastic behaviour in specific areas while protecting critical structural components from damage. The key is to ensure that the building can be quickly and economically repaired and reoccupied after a seismic event, minimizing the downtime and long-term economic impacts.

1.4.1. Methodologies in Low Damage Design

Various methodologies underpin the low damage design philosophy. These include the use of base isolation systems, which decouple the building from ground motion; energy dissipation devices that absorb and dissipate seismic energy; and the use of sacrificial elements designed to yield or deform or displace, protecting the main structural system. Additionally, the employment of self-centring allows structures, reducing residual deformations after severe earthquakes.

1.4.2. Benefits and Challenges

The benefits of low damage design are multifold. Primarily, it significantly reduces the economic and social impacts of earthquakes by allowing rapid post-event recovery. It also contributes to sustainability by reducing the need for extensive repairs or reconstruction. However, the challenges are notable as well. Implementing low damage design can be more costly upfront, requires advanced engineering and detailed analysis, and may involve the use of novel materials and technologies that have not been extensively tested in real-world scenarios.

1.4.3. Case Studies and Applications

Various successful applications of low damage design can be found globally. In New Zealand, for instance, the Christchurch rebuild following the 2010 and 2011 sequences of earthquakes has incorporated these principles extensively. The buildings designed with base isolators and damage-resistant technologies have shown excellent performance in subsequent seismic events. Such case studies provide valuable real-world data supporting the effectiveness of the low damage design approach.

The low damage design philosophy represents a significant step forward in creating resilient, sustainable communities capable of withstanding seismic events with minimal disruption. By focusing on rapid recovery and reduced long-term impacts, this approach aligns with the broader goals of sustainable development and resilience in the face of increasing environmental challenges. As such, it is an essential consideration for the future of structural engineering and urban planning.

1.5. Research motivation: Embracing Low Damage Philosophy with Self-Centring Friction-Based Energy Dissipation Devices

The motivation for this research is rooted in the pursuit of integrating low damage design philosophy with the implementation of self-centring damping devices using the friction as the primary source of energy dissipation for structural systems. This approach is driven by the need to enhance the resilience of buildings against seismic events, ensuring not only the safety and stability of structures but also their post-event functionality and repairability. Self-centring energy dissipation devices offer a promising solution by combining the benefits of reduced residual deformations and efficient energy absorption during seismic activities. The incorporation of these devices aligns with the low damage design objectives, aiming to minimize structural damage, expedite repair processes, and significantly reduce the economic and social impacts of earthquakes. This research seeks to explore the efficacy of these devices, investigate their performance in various structural configurations, and evaluate their contribution to the overarching goals of sustainable and resilient urban development. The expected outcomes include enhanced guidelines for designing earthquake-resistant structures that embody the principles of low damage design, ultimately leading to safer, more durable, and economically viable built environments.

In this study, the focus has been on exploring the implementation of self-centring friction-based mechanisms within rocking systems. The research specifically targets two new seismic resistant rocking systems for shear walls and cylindrical tanks impacting the resilience in the communities and industries. To achieve these objectives, friction-based self-centring devices have been integrated as shear links for the shear wall and as hold-downs for the tank concepts. These devices function as a safety fuse, playing a crucial role in augmenting the resilience of the targeted structures. The incorporation of these mechanisms is a step toward enhancing their ability to withstand seismic events by

allowing them to return to their original positions post-deformation, thereby mitigating the potential for structural damage.

The implementation of the friction-based self-centring devices within rocking shear walls and cylindrical tanks aligns with the low-damage design philosophy that is increasingly vital in seismic engineering design. This philosophy prioritizes minimizing structural damage during seismic events, thereby reducing repair costs and downtime following severe earthquakes.

1.6. Organization of the Thesis

The thesis contains nine chapters and an appendix as explained below:

Chapter 1 presents the introduction and motivation behind this research project.

Chapter 2 offers the literature review on seismic solutions and self-centring methodologies as implemented in both historical and modern structural designs.

Chapter 3 details the paper published in the proceedings of 2019 NZSEE conference on seismic performance of rocking concrete shear walls with innovative rotational resilient slip friction joints.

Chapter 4 presents the paper of seismic performance of rocking braced frame equipped with resilient slip friction joints as shear keys, published in the proceedings of 2020 WCEE.

Chapter 5 discusses the innovations in rocking shear wall experimental testing: design, assembly, and analysis.

Chapter 6 delves into the development and case studies of Resilient Slip Friction Dampers as an anchorage solution for cylindrical steel tanks.

Chapter 7 presents the 2020 WCEE paper on an innovative damage-free anchorage system for cylindrical steel storage tanks.

Chapter 8 showcases the 2021 ASME paper of using an innovative low damage anchorage system for industrial tanks and vessels with different aspect ratios.

Chapter 9 Conclusions and Future Studies

Appendix provides the structural drawings of the experimentally tested components and system, also including the details of the test setup design.

Due to the paper-based nature of this thesis, it should be noted that there will be some unavoidable duplication of information.

Chapter 2: Research Background

2.1. Introduction

In the field of structural engineering, "self-centring" refers to a design principle or a technology enabling structures to return, or nearly return, to their original positions after being subjected to significant loads or displacements, such as those caused by seismic events or strong winds. This capability is crucial for maintaining the structural integrity and usability of a building post-disaster.

The concept of self-centring hinges on the idea of elastic response under stress. In contrast to traditional structural designs, where plastic deformations can lead to permanent displacements, self-centring systems are designed to undergo controlled elastic deformations. After the load is removed, these systems can revert to their original state due to their inherent elastic properties or additional mechanisms like post-tensioning. Self-centring technology often involves innovative materials and engineering techniques, such as post-tensioned precast concrete, shape memory alloys, or specially designed friction-based devices. Key characteristics of self-centring designs include:

1. Resilience to Seismic: Self-centring structures are inherently more resilient to dynamic forces. They are designed to absorb and dissipate energy during seismic events or high winds, reducing the risk of catastrophic failure. This resilience is crucial in safeguarding lives and minimizing property damage.

2. Reduced Permanent Deformations: Traditional structural designs often suffer permanent deformations post-seismic events, necessitating extensive repairs or even complete reconstruction. Self-centring systems, by contrast, are designed to be returned to their original state, greatly reducing the likelihood of permanent deformation and the associated costs and disruptions.

3. Economic Efficiency: The ability of self-centring structures to withstand significant stress without substantial damage can lead to considerable economic benefits. These include reduced repair and reconstruction costs, lower insurance premiums due to decreased risk, and minimized disruption to business operations and residential occupancy.

4. Sustainability: From an environmental perspective, self-centring designs contribute to sustainability. Structures that can be quickly repaired or require less intensive reconstruction consume fewer resources and generate less waste. This aspect is increasingly important in the context of global environmental concerns and the push for green building practices.

5. Enhanced Post-Disaster Recovery: Buildings designed with self-centring principles can be integral to quicker post-disaster recovery efforts. Structures that remain functional or require minimal repairs can expedite the overall recovery process in affected communities, reducing the socio-economic impacts of natural disasters.

In summary, the incorporation of self-centring mechanisms in structural design represents an advancement in creating buildings that are not only safe and durable but also economically and environmentally sustainable, particularly in the face of increasing challenges posed by natural disasters.

2.2. Historical Context and Evolution

The historical context and evolution of self-centring mechanisms in structural design reflect a long-standing pursuit of resilience and adaptability in architecture and engineering. This evolution can be traced back to ancient civilizations and spans up to the sophisticated technologies of the modern era.

In this section, we undertake a thorough review of historical progress within the scope of our research, accomplished by esteemed scholars and researchers. Our scholarly investigation is centred on the significant advancements achieved in the domain of self-centring systems, with a particular emphasis on their application in both **buildings** and **cylindrical steel tanks** engineering.

2.3. Rocking Structural Systems

Numerous ancient structures in seismically active regions, such as Greece, Iran, and Chile, have demonstrated remarkable resilience to lateral forces, including those from earthquakes and wind, primarily due to their reliance on rocking mechanisms. Although it may be argued that these mechanisms were not intentionally designed for seismic resistance, the enduring stability and self-recentring capacity of these structures post-seismic events are irrefutable. This type of seismic resilience could be exemplified by

certain Greek temples and slender Chilean structures. These historical examples, surviving through millennia, stand as testament to the inherent effectiveness of rocking mechanisms in withstanding seismic forces, even in cases where such design intentions might not have been explicit (Makris and Vassiliou, 2014). This evidence from antiquity not only highlights the natural incorporation of seismic resilience in early architectural forms but also underscores the potential of such mechanisms in modern structural designs.

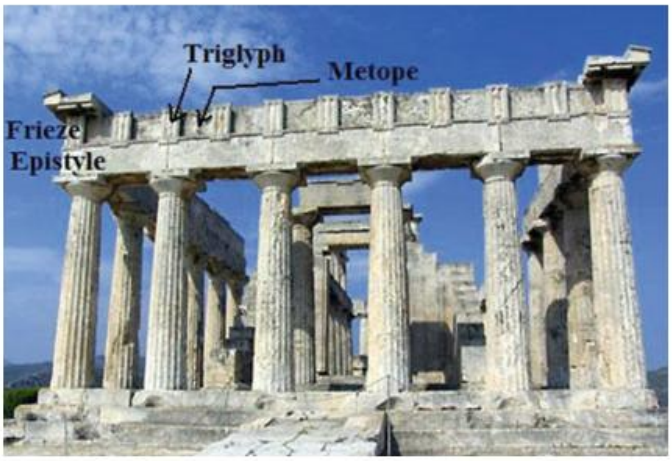

Figure 2-1: View of a temple of Aphaia, Greece. Free-standing columns, standing for more than 2500 years (Makris and Vassiliou 2014)

The foundational exploration into the dynamics of rigid rocking bodies, which significantly advanced our understanding of the mechanics of rocking in structural engineering, was initiated by Muto et al. (1960). Their research involved meticulous small-scale experimental tests on structures exposed to ground excitation. This experimental endeavour led them to establish a comprehensive theoretical framework that articulated the behaviour of rocking in rigid bodies. A pivotal finding from Muto et al.'s work was the discovery that a rocking body has the capacity to withstand lateral static loads up until the point where its center of mass approaches the so-called 'rocking toe.' This crucial insight was rigorously validated through a series of shake table tests on small-scale specimens, supplemented by theoretical analyses focused on rigid bodies under sinusoidal base excitations. The implications of their findings were particularly significant for slender multi-storey buildings in Japan, indicating a reduced likelihood of such structures overturning during earthquakes, thanks to their intrinsic rocking capabilities.

Building upon these foundational insights, Housner (1963) introduced the concept of rocking structures as an effective lateral load resisting system by mitigating the seismic

demands. His observations shed light on the reduced damage in flexible, slender structures compared to their more rigid counterparts, a phenomenon he attributed to the inherent ductility of the former. Housner's impactful research illuminated the potential of structures to not only survive seismic events through rocking, but also to reposition themselves post-quake. However, he also acknowledged a notable gap in knowledge - the challenge of designing structures that could achieve controlled rocking with a minimized risk of overturning.

Encouraged by Housner's findings, a wave of research initiatives was launched, targeting both concrete and steel structural systems. These efforts were geared towards developing mechanisms that could enhance the self-centring capabilities of rocking systems and integrate damping solutions to effectively decrease the deflection demands.

A significant milestone in this evolving field was achieved by Clough et al. in 1977. Their experimental investigation involved a half-scale three-story steel rocking moment frame. Unique to their design was the allowance for vertical movement at the column base, facilitated by specially designed pin connections that could accommodate a degree of uplift motion. The primary source of resisting moment in their setup was attributed to gravity loads. Upon comparing their findings with a fixed-base scenario, Clough et al. observed a considerable reduction in the forces exerted on structural members and the overall acceleration experienced by the stories. Notably, they reported a maximum drift ratio of 2.4%, with an accentuated acceleration observed in the first story, a consequence of base impact coupled with the influence of higher mode effects. Their study also leveraged numerical models to predict the displacement and force responses, although the accuracy of these models was found to be highly depending on the damping parameters employed.

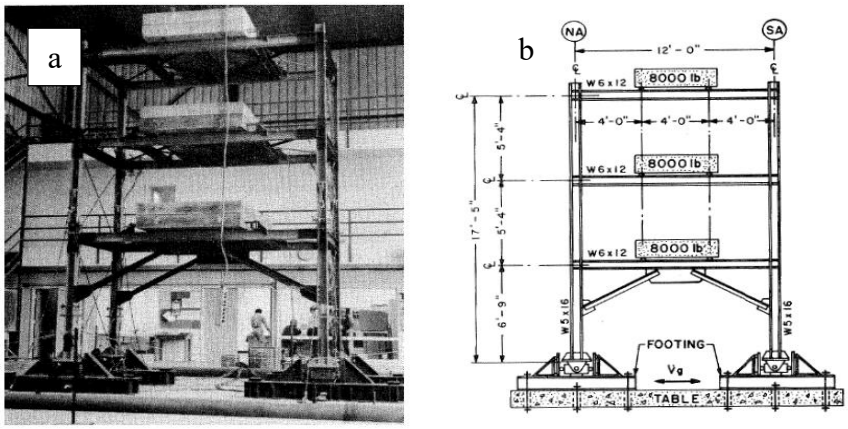

Figure 2-2: The three-story rocking frame specimen: (a) test setup; (b) schematic Clough et al. (1977)

In 1977, Huckelbridge conducted another study involving a nine-story steel moment frame, which provided pivotal insights into the behaviour of structures employing rocking systems. His experimental investigation revealed that the lower peak forces were associated with higher displacement levels in the frame. This inverse relationship between force and displacement underscored the unique dynamic characteristics of rocking systems in seismic scenarios.

Furthermore, Huckelbridge's study was extended to consider the vertical component of ground motion. By replicating the tests under these conditions, he found consistent results, reinforcing the initial findings. This aspect of the study was crucial in understanding the multi-directional nature of seismic forces and their impact on structural systems.

The findings of the study were further verified through detailed numerical analysis. A key finding from this analysis was the close alignment of the tangent stiffness-proportional damping of approximately 0.7% in the fundamental mode with the experimental results. This correlation between theoretical predictions and practical observations highlighted the reliability of numerical models in simulating the seismic response of rocking systems.

Interestingly, when Huckelbridge conducted his tests on the rocking system with and without the vertical component of ground motion, the outcomes were strikingly similar. This observation suggested that the rocking system performance was not significantly influenced by the vertical seismic component, at least within the scope of the tested conditions. However, it is important to note that the relatively low gravity load on the frame might have contributed to this outcome, indicating that the system response could vary under different loading conditions.

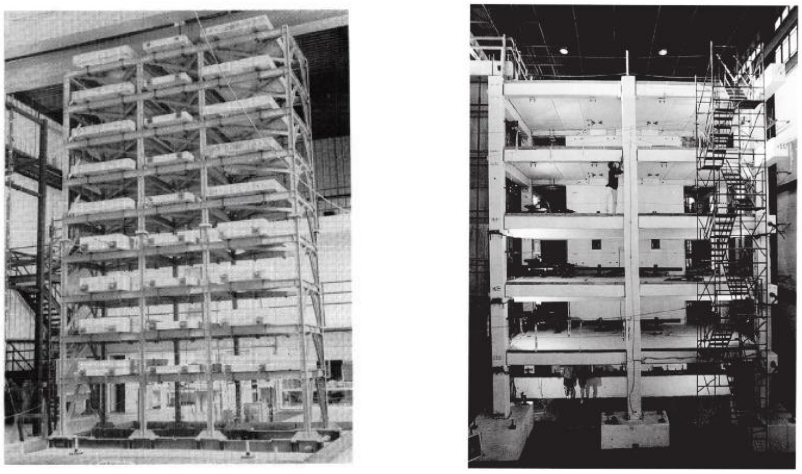

Figure 2-3: (a) The nine-story rocking frame (Huckelbridge and Clough 1977); (b) The rocking frame specimen (Priestley 1991)

While the potential of rocking systems was acknowledged as early as the 1970s, it was not until the advent of the Precast Seismic Structural Systems (PRESSS) program in the 1990s that these systems gained substantial attention within the structural engineering community. The primary objective of the PRESSS program was to innovate precast concrete seismic force resisting systems, striving for a balance between seismic performance and construction economics, a balance not typically achieved by traditional systems.

Traditional precast concrete systems are engineered to mitigate nonlinear responses in the connections between elements. However, the challenges associated with following the common process of monolithic construction in precast concrete members, along with the costs associated with ductility detailing and post-earthquake repairs, necessitated a new approach. The PRESSS program embarked on developing alternative connections designed to localize nonlinear responses exclusively within the connections (Priestley, 1991). A notable aspect of these connections was their reliance on a rocking response, manifested either at beam-column interfaces or at horizontal joints connecting precast wall panels and the foundation. This innovative approach was revolutionary given it was the first instance where unbonded post-tensioning was utilized to augment the lateral load capacity of rocking systems.

One of the significant outcomes of the PRESSS program was the testing of a 60%-scale five-story building equipped with a precast concrete rocking wall system (Priestley et al., 1999). The testing of this structure involved coupling two adjacent walls with U-shaped steel devices, designed to yield in flexure due to the relative displacement between the wall units. The wall systems successfully withstood pseudo-dynamic tests, resisting forces up to 50% greater than the design-level seismic event, while only incurring cosmetic damage. However, the tests also revealed amplifications in overturning moments, story shears, and floor forces due to higher mode effects. The insights gained from this comprehensive research were culminated in the publication of the PRESSS design handbook in New Zealand (2010).

Complementing the PRESSS program, Kurama et al. (1999) conducted in-depth numerical studies to examine the behaviour of unbonded post-tension rocking walls using finite element software. Analyzing ground motions with a 2% probability of exceedance in 50 years, Kurama reported several critical findings:

- The base shear in time history analysis was found to be 2.9 times higher than that calculated using the pushover method.
- A friction coefficient of 0.7 was deemed sufficient for shear force transfer without the need for hold-downs.
- Peak displacements were 40% greater compared to conventional walls, but importantly, without any residual displacements, which are typically present in conventional walls.

Further advancements were made by Kurama in 2000 and 2002, focusing on the integration of viscous or friction dampers. This addition improved displacement reduction to a range of 37% to 57%, with the higher reduction rates observed in taller shear walls. Kurama's subsequent work in 2002 considered a design response modification factor (R=5) for designing post-tensioned rocking walls without dampers and compared these results with scenarios incorporating dissipation devices. The inclusion of dampers was reported to significantly reduce both the displacement (by nearly 50%) and force demands on the structural members.

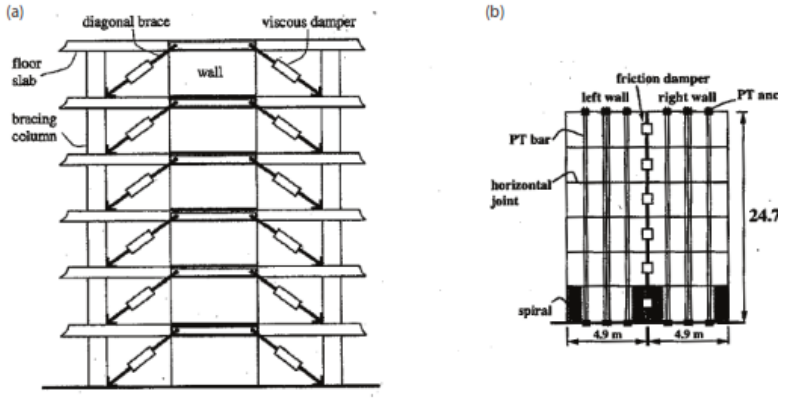

Figure 2-4: (a) with viscous damper; (b) with friction damper (Kurama 2000)

Iwashita et al. (2002) conducted an innovative shake table test on a 1/9-scale four-story moment frame. This research was aimed at rigorously investigating the performance of rocking shear walls with varying aspect ratios under seismic conditions. One of the key observations from Iwashita et al.'s experiment was the impact of uplift phases on the forces experienced by structural members. Intriguingly, the study revealed that during the uplift phase of the rocking shear wall, higher intensities of ground motion did not substantially increase the forces exerted on the frame members. This finding is crucial as it suggests that the rocking mechanism inherent in shear walls can effectively mitigate the impact of severe seismic forces on structural components, a characteristic that is immensely beneficial in earthquake-prone regions.

Furthermore, Iwashita et al. noted a distinct difference in the effectiveness of the rocking motion based on the aspect ratio of the walls. Their results indicated that walls with an aspect ratio of 7 exhibited more pronounced benefits from the rocking motion compared to those with an aspect ratio of 3.5. This observation is particularly insightful as it underscores the impact of aspect ratio in the design of rocking shear walls. It suggests that optimizing the aspect ratio can significantly enhance the seismic resilience of structures equipped with rocking shear walls.

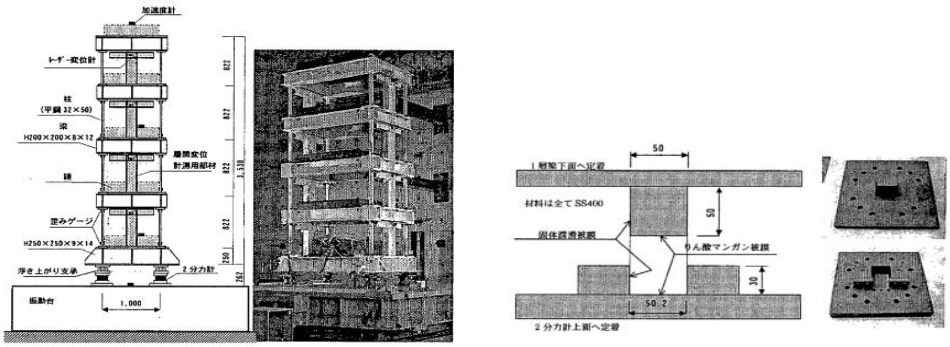

Figure 2-5: Iwashita moment frame test: (a) test setup; (b) rocking base detail (Iwashita, Kimura et al. 2002)

Midorikawa et al. (2006) embarked on a project to design and test a yieldable base plate, aimed at energy dissipation in rocking frame systems. Their study focused on a half-scale three-story building, providing a practical context for their investigations. The central aspect of their research was to evaluate the effectiveness of yieldable base plates in reducing seismic forces and enhancing the overall performance of rocking frames during earthquakes. The team designed a series of base plates with varying thicknesses and subjected them to rigorous testing. They observed that thicker base plates resulted in a more significant reduction in base forces. This outcome aligns with the principle that the increased material thickness in structural components often leads to enhanced energy absorption capabilities, which is crucial in seismic design.

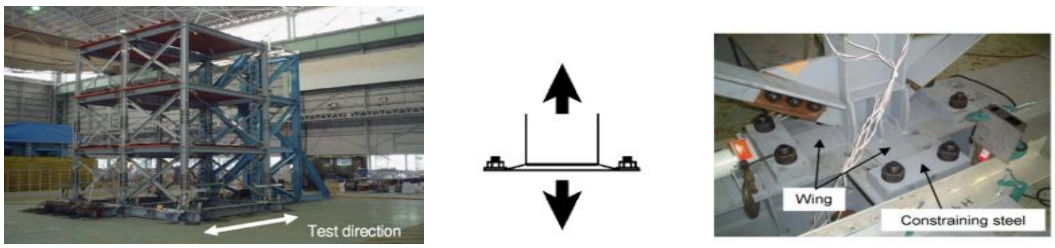

Figure 2-6: (a) Three-story rocking frame; (b) base plate; (c) base connection details (Midorikawa, Takeuchi et al. 2010)

In a landmark study in 2001, Wada et al. introduced an innovative concept in seismic design: the use of column splices to enhance the flexibility of rocking systems. This novel approach was primarily aimed at reducing the forces exerted on the columns of structures

during seismic events. The key to this innovation was the design of a new splice joint, which incorporated a yieldable plate. This plate was not just a structural element; it was also a critical damping component, designed to absorb and dissipate seismic energy, thereby reducing the overall response of the structure to seismic forces.

The introduction of the yieldable plate in the splice joint represented a significant advancement in the field of seismic engineering. By yielding under seismic loads, this plate acted as a damper, effectively absorbing a portion of the seismic energy that would otherwise be transmitted through the columns. This energy dissipation capability was crucial in enhancing the overall seismic performance of the structure, leading to reduced structural demands and potential damage during an earthquake.

Wada et al.'s research included quasi-static tests to evaluate the effectiveness of this new splice joint design. The results of these tests were compelling, demonstrating the splice joint ability to significantly reduce forces in the columns and enhance the structure seismic resilience. The practicality and effectiveness of this concept were further validated when it was implemented in an industrial building in Japan. This real-world application provided valuable insights into the splice joint performance in actual seismic conditions and showcased its potential as a viable solution for enhancing seismic resilience in buildings.

Figure 2-7: (a) Frame with conventional columns; (b) Frame with stepping columns; (c) industrial building Japan; (d) connection splice (Wada, Yamada et al. 2001)

In 2006, Roke et al. conducted an experiment on Controlled Rocking Steel Braced Frames (CRSBFs). These frames were uniquely equipped with post-tensioning tendons and supplementary energy dissipation devices, strategically located on both sides of the wall and connected to boundary columns. This design approach effectively decoupled the rocking system from the gravity columns, a novel concept in seismic design.

The experiment involved a 60%-scale four-story model, designed to meticulously simulate the behaviour of CRSBFs under seismic conditions. A key feature of this setup was the transfer of lateral loads to the rocking system via knuckles, which then transmitted

these forces to the foundation through specially designed bumpers. The structure was subjected to ground motions scaled to represent 475-year seismic events. The observed structural drift was approximately 2%, with only minor yielding noted in the post-tensioning (PT) cables. Remarkably, the system maintained its stiffness and strength throughout the tests, with the exception of some loss of prestressing force due to yielding of the PT bars under certain Maximum Considered Earthquake (MCE)-level and extreme MCE-level ground motions. However, this yielding did not compromise the system self-centring capability and was easily rectifiable by restressing the PT bars.

Building upon their experimental findings, Roke et al. (2009) developed a design procedure for CRSBF systems using the quasi-static method, explicitly accounting for the effects of higher modes. They applied this procedure in a case study involving a six-story frame, initially designed solely based on the first mode. Time history analysis of this frame revealed a 3.6-fold increase in axial force demand in the bracing system compared to the design based on the first mode alone. This result highlighted the importance of considering higher mode effects in the design of CRSBFs to ensure adequate structural performance and safety.

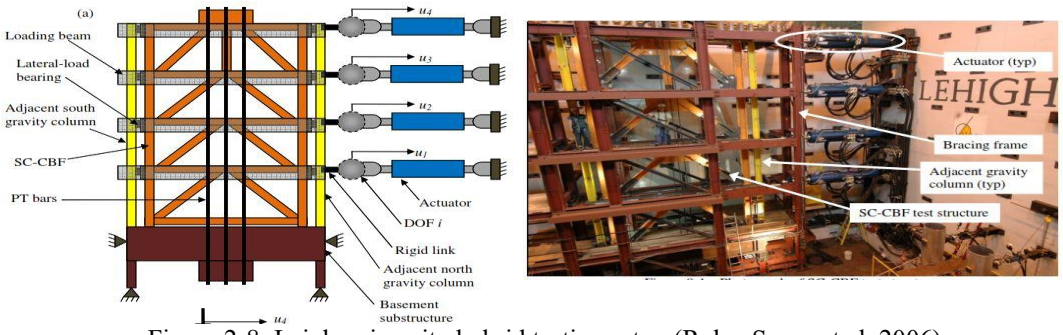

Figure 2-8: Leigh university hybrid testing setup (Roke, Sause et al. 2006)

Marriot et al.'s research focused on the design and testing of novel damping solutions for structural applications. Their study centered around the implementation of Externally Mounted Mild Steel, Tension and Compression Yielding (TCY) dampers, along with viscous dampers, to enhance the seismic resilience of structures. In their innovative approach, depicted in Figure 2-9, Marriot et al. evaluated various combinations of TCY and viscous dampers. A notable feature of their system was the use of an epoxy-injected steel confining tube. This tube was strategically placed to cover the tapered part of the TCY dampers. The inclusion of this confining tube was crucial in enhancing the performance of the dampers, particularly in terms of durability and energy dissipation capacity.

However, one of the challenges identified in the study was the susceptibility of these dampers to buckle under certain conditions. This issue highlights the need for a robust design and detailed engineering to prevent buckling and ensure the dampers function as intended during seismic events. Marriot et al.'s work thus sheds light on the complexities and considerations involved in developing advanced damping systems for seismic applications.

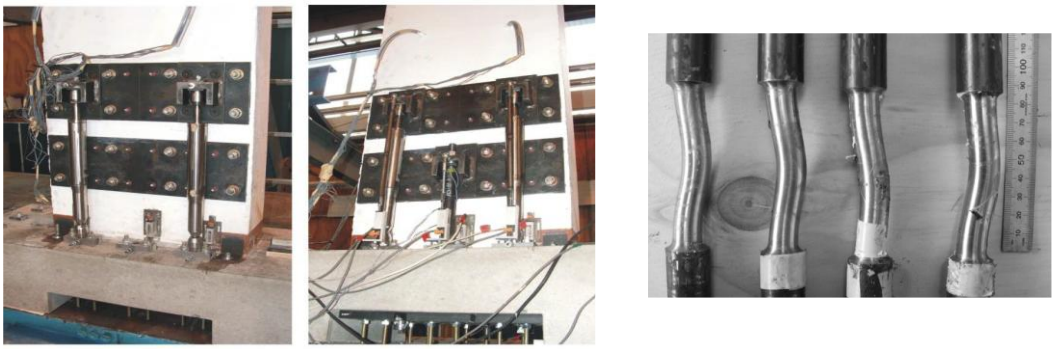

Figure 2-9: (a) Post tensioned wall with viscous and TCY mild steel damper; (b) Buckled external TCY dissipaters (Marriot et al)

By the significant advances made in the study of unbonded post-tensioned (PT) walls during the Precast Seismic Structural Systems (PRESSS) program, Sritharan et al. proposed a novel system known as Precast Wall with End Columns (PreWEC). This system was conceptualized as a response to the complexities and cost considerations associated with the use of U-shaped connectors in coupled wall systems.

In the PreWEC system, as illustrated in Figure 2-10, the innovative approach involves coupling the wall with end columns through the use of welded mild steel oval-shaped connections, referred to as “O connectors”. This design strategy aimed to simplify the connection mechanism while maintaining or enhancing the seismic performance of the wall system.

Despite the theoretical efficacy of the PreWEC system in handling design earthquake levels, practical implementation revealed some challenges. During the experimental investigations, various unexpected failure modes of the O connectors were observed. These failure modes highlighted the need for a deeper understanding of the behaviour of these connectors under seismic loading and prompted further examination of their design and structural integrity. Such findings are crucial for refining the design and ensuring the reliability and safety of the system in real-world applications.

Sritharan et al.'s work on the PreWEC system contributes to the ongoing development of seismic-resistant precast structures. This research not only advances the field of structural engineering but also serves as a reminder of the critical role of experimental validation in the development of safe and effective seismic design solutions.

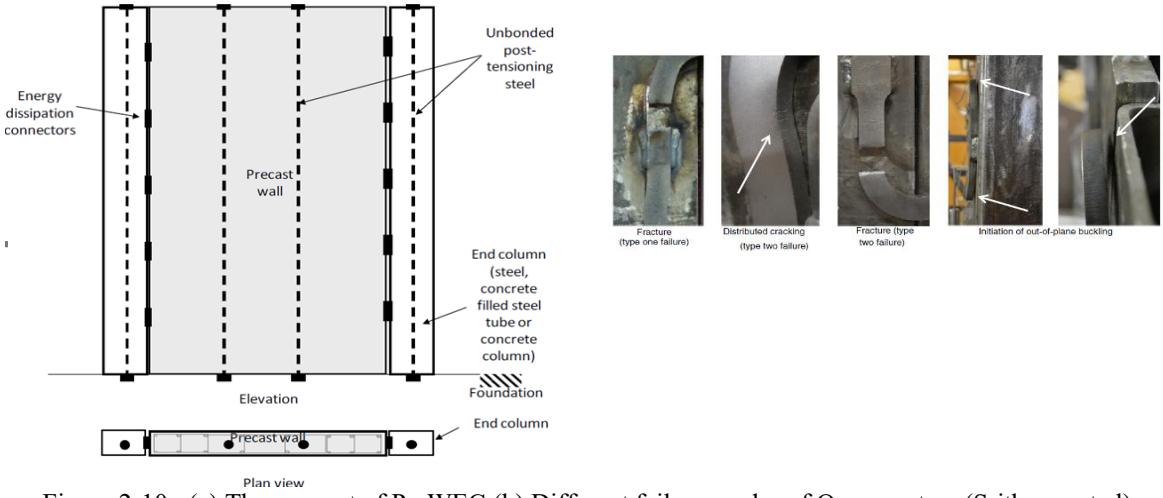

Figure 2-10: (a) The concept of PreWEC (b) Different failure modes of O connectors (Sritharan et al)

At the University of Illinois at Urbana-Champaign, a significant study conducted by Eatherton, Hajjar et al. (2008) delved into the performance of Controlled Rocking Steel Braced Frames (CRSBFs), incorporating post-tensioned cables and yielding dampers. This research was aimed at achieving an optimal balance between the self-centring forces and energy dissipation in seismic-resistant structures.

In this system, as depicted in Figure 2-11, the tendons were strategically positioned at the center of the frames, while the dampers, functioning like shear keys, were placed between the columns. The CRSBFs system employed three main components:

1. Steel Frames: These frames were designed to remain essentially elastic and allowed to rock about the column bases. A distinctive feature of the column base detail was its ability to allow the column uplift while restraining the horizontal motion, achieved through the use of bumpers or an armoured foundation trough.

2. Vertical Post-Tensioning Strands: These strands provided active self-centring forces. They were initially stressed to less than half of their ultimate strength, allowing for additional elastic straining during the rocking of the frames.

3. Replaceable Energy Dissipating Elements: Serving as structural fuses, these elements were designed to yield under seismic loads, effectively limiting the forces

imposed on the rest of the structure. The fuses could be configured either between two frames in a dual frame setup or at the base of a single frame.

One of the key characteristics of this controlled rocking system was its flag-shaped hysteretic response, typical of self-centring systems. The post-tensioned frame contributed to a bilinear elastic response, characterized by initial stiffness due to elastic deformations in the frame and secondary stiffness arising from additional elastic elongation of the post-tensioning strands after uplift. In contrast, the fuse could exhibit full hysteretic load-deformation behaviour. The combined effect of these components resulted in a flag-shaped hysteresis loop that returns to near zero displacement when the load is removed.

During testing, the system was designed to engage the fuse in the damper at a roof drift of 3%, although the test extended to 4%. However, the PT system experienced failure at strains corresponding to a drift as low as 0.85%, contradicting component tests that showed elongation capacities greater than 4.5%. In subsequent phases, the strain capacity of the strands was improved by 1.3%. The structure demonstrated the ability to remain self-centered up to a 2500-year seismic event, although post-tensioning yielded significantly at this level of roof drift being 3.9% (Eatherton and Hajjar, 2011).

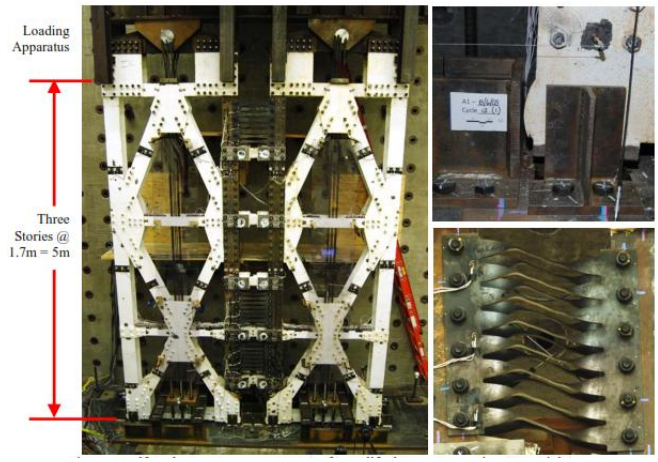

Figure 2-11: Half Scale Test Setup at UIUC (Left), Uplifted Base Connection (Top Right), Deformed Fuse (Bottom Right) (Eatherton, Hajjar et al. 2008)

In 2013, Wiebe conducted a pioneering study that involved testing a 30% scale model of an eight-storey post-tensioned frame, providing significant insights into the impact of higher mode effects on the frame design. This research was critical in advancing the understanding of how higher modes influence the capacity design of post-tensioned frames in seismic scenarios.

One of the key findings from Wiebe's study was the realization that the capacity design of the frame could be considerably affected by higher modes. While design tools, such as modified response spectrum analysis techniques, were available to estimate design forces, the study highlighted a crucial challenge: the rocking behaviour of the frame did not entirely limit the forces exerted on it. As a result, designers were faced with the task of determining the intensity of the response in their designs. This decision was particularly important because excessive design forces, if not adequately addressed, could compromise the structural integrity of the frame. To address this challenge, Wiebe proposed two innovative approaches aimed at mitigating the effects of higher modes:

1. Multiple Rocking Joints: This approach involved integrating several rocking joints within the frame. The idea was that by distributing the rocking mechanism across multiple points, the frame response to seismic forces could be more effectively controlled. This distribution would help in dampening the impact of higher modes, thereby reducing the overall forces experienced by the frame.

2. Shear Control Brace: The second approach proposed by Wiebe was the implementation of a nonlinear brace at the first story of the frame, referred to as a shear control brace. This brace was designed to engage nonlinearly under seismic loads, providing an additional mechanism to control the forces and displacements within the frame, particularly those induced by higher mode effects.

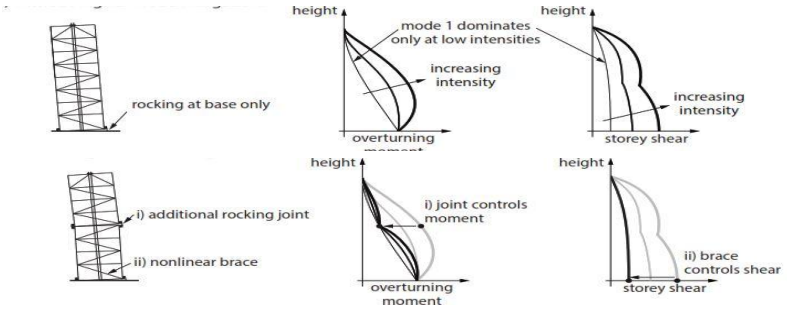

Figure 2-12: Two concepts for higher mode mitigation; (a) Without higher mode mitigation; (b) With higher mode mitigation (Wiebe 2013)

The base rocking joint was primarily responsible for most of the system deformation, manifesting as low-frequency oscillations dominated by the first mode. However, the mechanisms aimed at mitigating the higher modes operated at significantly higher frequencies and with much smaller deformations, as they responded primarily to the higher modes of the structure. Notably, these higher mode mitigation techniques did not result in any residual drifts or structural damage, indicating their effectiveness and reliability.

The research found that the upper rocking joint increased peak roof displacement by an average of 18%, while the nonlinear brace at the first story increased it by about 6%. These mitigation mechanisms were particularly effective in reducing peak storey shears, floor accelerations, and overturning moments for ground motions with large amplitudes or substantial high-frequency content. However, their impact was less pronounced for ground motions that did not significantly excite the higher modes.

Further, the study observed that while both the upper rocking joint and the nonlinear first-storey brace reduced storey shears and brace forces, the nonlinear brace achieved greater force reductions near the base of the structure. In terms of reducing overturning moments throughout the frame, the upper rocking joint was generally more effective. Combining these two mechanisms provided the best overall control of both storey shears and overturning moments.

The outcomes of this comprehensive research formed the development of the New Zealand design guide for CRSBF systems. The guide proposes different ductility factors (μ) of 4 and 6 for load-bearing and non-load bearing systems, respectively. This reflects the different requirements of these structural systems in mitigating seismic forces.

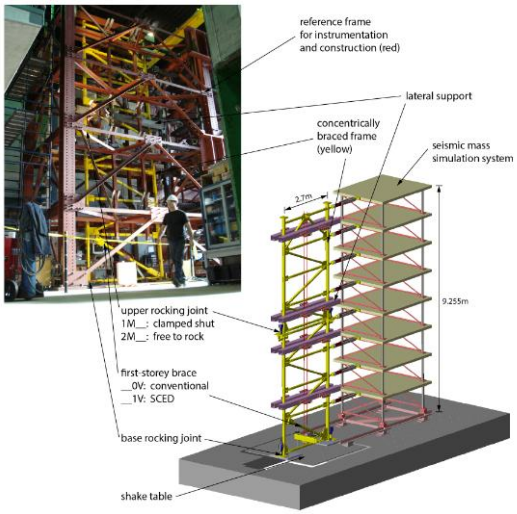

Figure 2-13: Test Setup (Wiebe 2013)

In 2015, Zarnani and Quenneville introduced a groundbreaking innovation in seismic damping technology: the Resilient Slip Friction Joint (RSFJ). This new generation of friction damper is notable for its dual functionality, providing both restoring force and energy dissipation in a single, compact joint. The initial application of the RSFJ was in a rocking timber wall, where it served as a hold-down mechanism. This application was studied by Hashemi et al. (2017).

One of the most remarkable features of the RSFJ, as observed in the rocking timber wall application, was its ability to achieve fully self-centring behaviour. This outcome was achieved despite the absence of additional vertical loads on the wall, a testament to the unique characteristics of the RSF joints. Additionally, the RSFJ exhibited a stable hysteretic response, effectively dissipating a significant amount of energy through friction.

The connection of the RSF joints to the Cross-Laminated Timber (CLT) panel was achieved using self-tapping screws. In 2018, Hashemi confirmed the efficiency of this connecting method through experimental data, demonstrating that it provided sufficient rigidity for the system. This aspect of the RSFJ design further emphasises its practicality and adaptability in various structural applications.

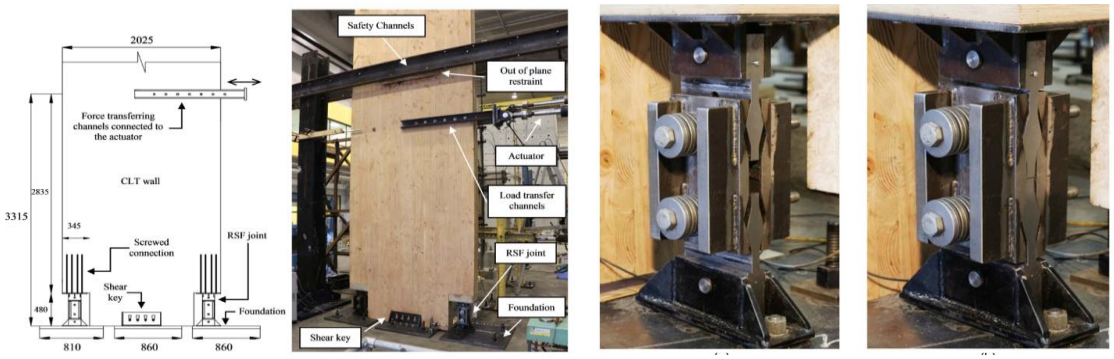

Figure 2-14: CLT walls with RSF joints (Hashemi 2018)

2.3.1. Friction Damper

As the present research focuses on the development of rocking systems combined with energy dissipation devices, it is important to review the evolution and fundamental concepts of friction dampers. Accordingly, this section presents a brief overview of selected friction damper technologies that have been previously proposed and investigated. The aim is to provide background information on the mechanisms, behaviour, and applications of friction-based energy dissipation devices to support the discussion and development of the system examined in this thesis.

Friction-based energy dissipation devices are widely employed as passive control systems to enhance the seismic performance of structural systems. These devices dissipate seismic input energy through controlled sliding between contact surfaces, generating stable and nearly rectangular hysteretic responses under cyclic loading.

The overview of friction damper systems presented in this section is largely based on the state-of-the-art review by Jaisee et al. (2021), which provides a systematic summary of the development and application of friction-based seismic energy dissipation devices. The descriptions of the principal damper configurations and the related figures discussed in this section mostly are adapted from that study.

Pall Friction Damper (PFD)

The development of friction-based seismic energy dissipation devices began with the introduction of the Pall friction damper, which represents one of the earliest practical applications of friction damping in structural systems. Pall et al. (1980) initially proposed the use of sliding friction joints to dissipate seismic energy in structural frames. The concept was based on the principle that seismic energy could be dissipated through frictional sliding rather than through yielding of primary structural members.

Further development of the device was presented by Pall and Marsh (1982), proposed a modified configuration in which friction elements were installed at the intersection of cross-braces, Figure xxx. In this arrangement, friction pads are clamped between steel plates and sliding occurs once the applied force exceeds a predetermined slip load. The system is designed so that sliding occurs only during significant seismic events, while the structure remains elastic under moderate loads.

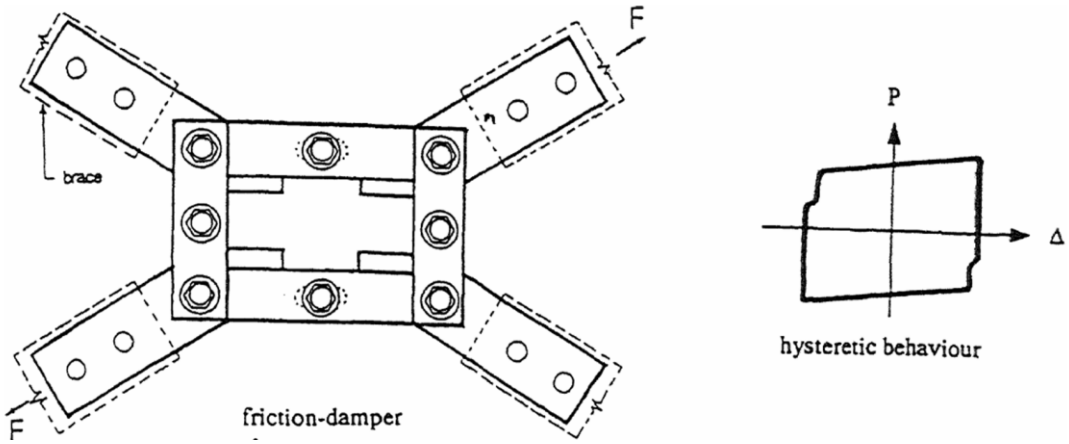

Figure 2-15: Typical configuration of Pall friction damper and its hysteretic behaviour (adapted from Jaisee et al., 2021).

Following the development of the Pall friction damper, researchers explored simpler and more practical friction-based devices that could be easily fabricated and installed in

structural systems. One such development was the slotted bolted connection (SBC) proposed by Fitzgerald et al. (1989).

The SBC consists of steel plates connected using high-strength bolts inserted into slotted holes. Frictional resistance is generated by the clamping force of the bolts, and sliding occurs when the applied force exceeds the frictional resistance. Belleville washers are often used to maintain stable bolt tension and consistent friction behaviour. Experimental studies showed that SBC systems exhibit nearly elastic-perfectly plastic behaviour and provide reliable energy dissipation under cyclic loading (Grigorian et al., 1993).

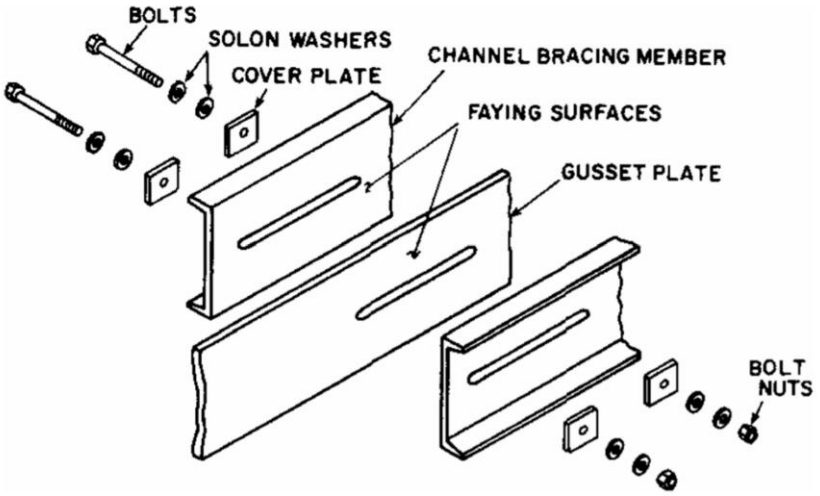

Figure 2-16: Slotted bolted friction connection (adapted from Jaisee et al., 2021).

A more advanced friction damping mechanism was developed by Sumitomo Metal Industries in Japan, known as the Sumitomo friction damper (SFD). This device incorporates wedge elements, friction pads, and springs housed within a cylindrical assembly. In this system, compressed springs generate normal forces that press friction pads against a cylinder surface. Sliding between these components produces frictional resistance and dissipates seismic energy. Shaking-table tests conducted by Aiken and Kelly (1990) demonstrated that the damper exhibits stable rectangular hysteretic loops and maintains consistent performance regardless of loading amplitude, frequency, or number of cycles.

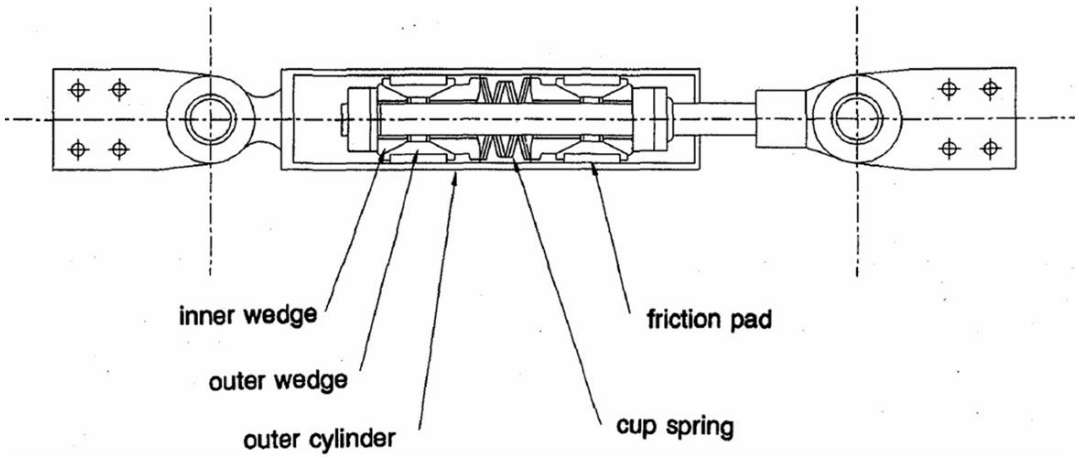

Figure 2-17: Configuration of Sumitomo friction damper (adapted from Jaisee et al., 2021)

Further advancements in friction-based damping systems focused on combining friction mechanisms with self-centering behaviour. The Energy Dissipating Restraint (EDR) represents such a development. The device consists of wedges, springs, and internal stops housed within a cylindrical casing. Sliding friction generated by wedge mechanisms dissipates seismic energy, while internal springs provide self-centering capability (Nims et al., 1993).

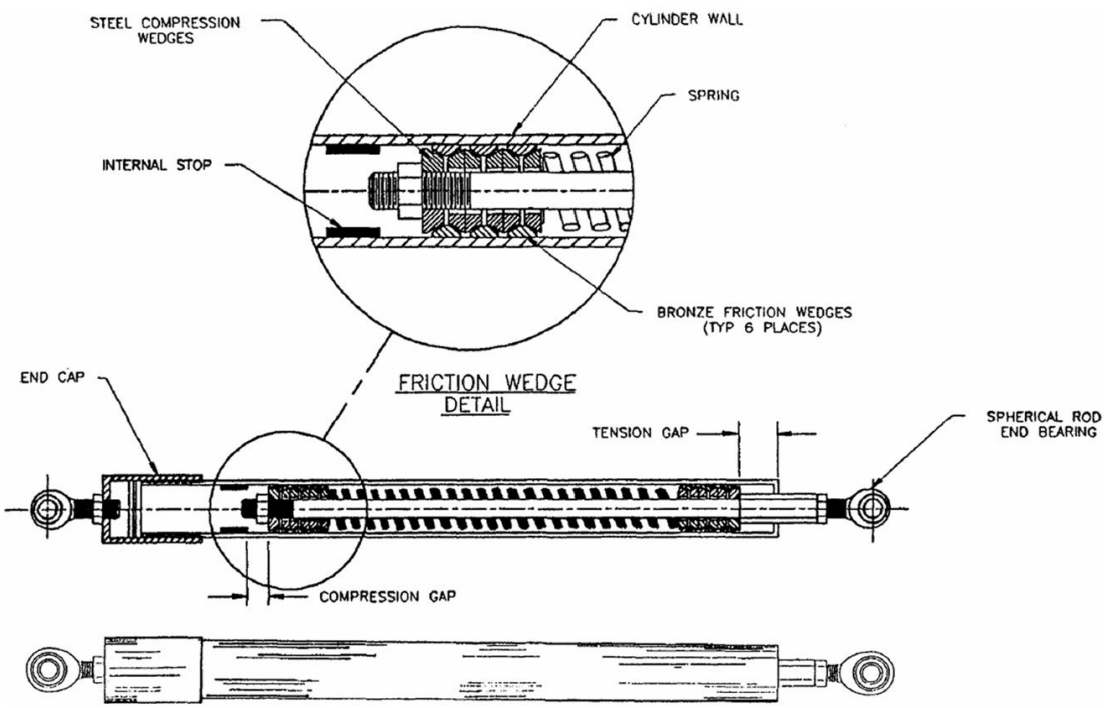

Figure 2-18: Energy dissipating restraint device (adapted from Jaisee et al., 2021)

Later developments explored alternative configurations for friction dampers that could improve energy dissipation efficiency and simplify installation. One such system is the rotational friction damper (RFD) introduced by Mualla and Belev (2002). The device consists of steel plates clamped together with friction pads and bolts, allowing rotational sliding when the applied force exceeds the friction resistance. Experimental studies showed that the system effectively reduces structural displacements and inter-storey drift under seismic loading.

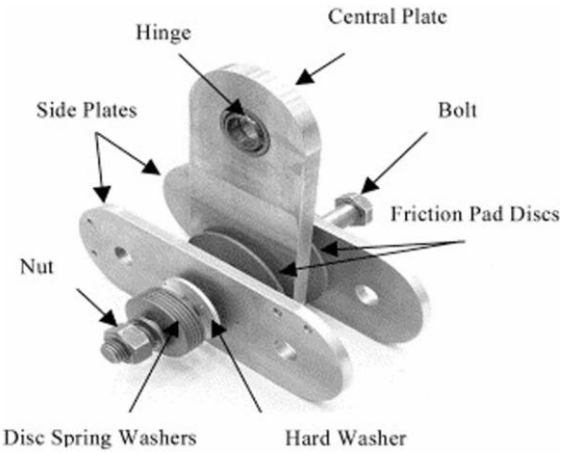

Figure 2-19: Rotational friction damper configuration (adapted from Jaisee et al., 2021)

More recent developments have focused on improving reliability and simplifying device configuration. The cylindrical friction damper (CFD) proposed by Mirtaheri et al. (2011) dissipates energy through friction between a shaft and a cylindrical sleeve. Unlike many earlier devices, the CFD does not rely on bolted friction interfaces, which simplifies the design and manufacturing process. Experimental studies demonstrated stable hysteretic behaviour and consistent slip loads even after repeated loading cycles.

Figure 2-20 Cylindrical friction damper concept (adapted from Jaisee et al., 2021)

Recent research in seismic design has focused on low-damage or damage-free structural systems. The FREEDAM system represents a significant advancement in this direction by integrating friction dampers directly into beam-column connections. In this system, conventional ductile connections are replaced with friction interfaces consisting of steel plates, friction pads, and high-strength bolts. During seismic loading, sliding occurs at the friction interfaces, dissipating energy while preventing plastic damage in the primary structural members (Latour et al., 2015). This approach represents an important step toward resilient structural systems capable of maintaining functionality after major earthquakes.

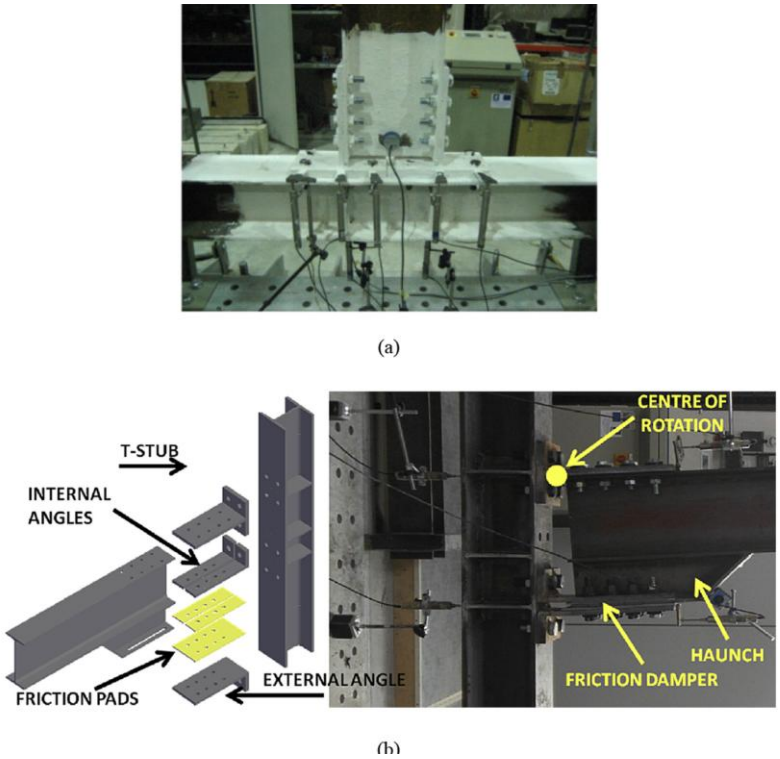

Figure 2-21: FREEDAM friction-based beam-column connection (adapted from Jaisee et al., 2021)

Ring spring dampers are friction-based energy dissipation devices consisting of stacked inner and outer steel rings with tapered mating surfaces. Under axial compression, sliding occurs along the inclined friction interfaces, producing energy dissipation and axial deformation. This mechanism typically results in a flag-shaped hysteretic response that is mainly activated in compression (Filiatrault et al., 2000; Christopoulos and Filiatrault, 2006). Due to the combination of frictional energy dissipation and inherent restoring capability, ring spring dampers can provide stable hysteretic behaviour and self-centering performance, making them suitable for seismic applications where reduced structural damage is desired.

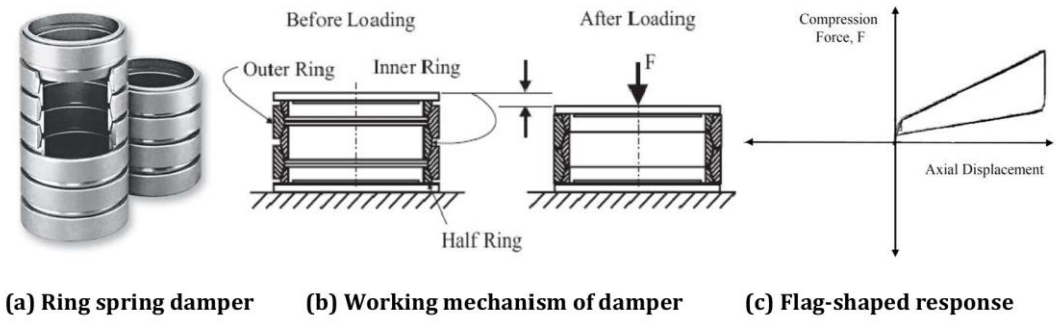

Figure 2-22: Ring spring damper configuration showing (a) stacked inner and outer rings forming the spring assembly, (b) sliding mechanism along the conical friction surfaces during compression loading, and (c) typical flag-shaped force–displacement response of the device. Adapted from Mashal (PhD thesis) based on Filiatrault et al. (2000)

Ring spring dampers have also been applied in controlled rocking structural systems. Guerrini et al. (2012) studied their use in a dissipative controlled rocking (DCR) connection, where the device was installed at the top of a cantilever column with unbonded post-tensioning tendons at the base. The damper was designed to activate before yielding of the tendons, allowing larger drift demands while protecting the post-tensioning steel and providing restoring forces to assist re-centering after unloading.

A modified form of the device, known as the Shapia damper, alters the ring stack configuration to produce a more symmetric cyclic response. In this arrangement, the ring assembly is confined within end cups so that compression develops during both tensile and compressive loading, resulting in a symmetric flag-shaped hysteretic behaviour (Christopoulos and Filiatrault, 2006).

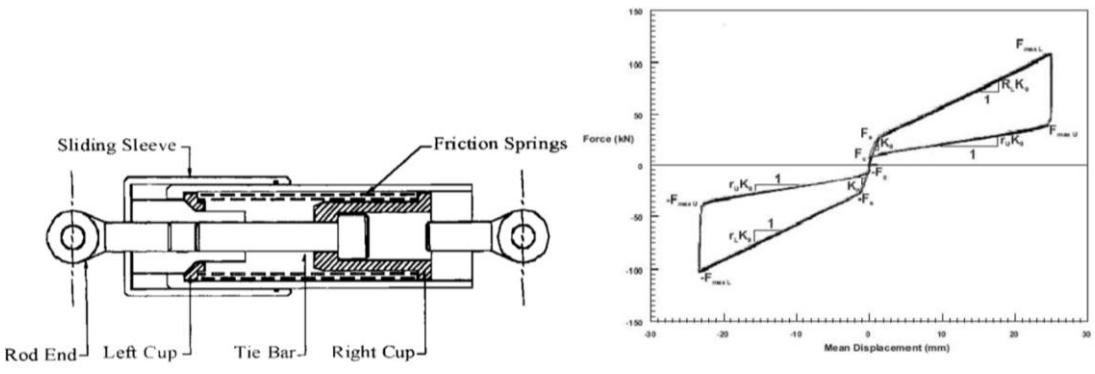

Figure 2-23: Shapia friction damper configuration showing (a) main mechanical components of the device and (b) symmetric flag-shaped hysteretic response under cyclic loading. Adapted from Mashal (PhD thesis) based on Filiatrault et al. (2000) and Christopoulos and Filiatrault (2006).

2.4. Rocking Cylindrical Tanks

The motivation to research the seismic behaviour of steel cylindrical tanks was further intensified by the emergence of the structure rocking concept, a paradigm shift that became increasingly relevant following the reported damages to such tanks in New Zealand and North America. These incidents highlighted not only a gap in industry knowledge but also the potential benefits of incorporating rocking motion principles into the tank design. The concept of rocking structures, which allows for controlled movement during seismic events to dissipate energy and reduce stress, presented an innovative approach that could address the vulnerabilities exposed in these incidents.

The seismic design of storage tanks has undergone a significant evolution over the past few decades, transitioning from basic concepts of stability and rigidity to sophisticated, performance-based approaches. The integration of rocking motion into the tank design represented a shift towards more dynamic and adaptive systems. This approach allowed tanks to rock back and forth during an earthquake, dissipating energy and reducing the forces transmitted through the tank body. It emphasized the importance of controlled movement and energy dissipation in enhancing seismic resilience. This section explores the development of various anchorage systems for tanks, namely free anchorage, partially restrained, and fully anchored tanks, tracing their historical context.

Furthermore, there have been numerous reports of typical damage to tanks following seismic events. In addition, some research have been conducted, with a particular emphasis on innovative approaches for tank foundation connections. This body of work, which plays a pivotal role in enhancing the understanding of seismic impacts on tank structures and contributes to the development of more resilient foundation connection methodologies, has been comprehensively reported in the following section.

Early Concepts

In the initial stages of tank design, the primary focus was on structural stability with little consideration for seismic forces. Tanks were either left unanchored, allowing for free movement, or were fully anchored to restrict any motion. This simplistic approach was underpinned by a limited understanding of seismic impacts and the behaviour of tanks under such conditions. However, the landscape of seismic design began to shift dramatically following major earthquakes in the 1970s and 1980s (Razzaghi & Eshghi,

2015). These events exposed the vulnerabilities of existing tank designs and the necessity for re-evaluation of seismic resilience in tank structures.

Free Anchorage Tanks

Free anchorage tanks, originally designed to move unrestrictedly during seismic events, were among the first to be reassessed. The early belief was that allowing tanks to move freely could help avoiding damage. However, subsequent research indicated that such uncontrolled movement could lead to catastrophic failures. This led to a refined approach where free movement was not entirely prohibited but controlled to an extent. Modern free anchorage designs aim to strike a balance, allowing for some flexibility to absorb seismic forces while preventing excessive movement that could lead to structural failures.

Fully Anchored Tanks

Fully anchored tanks, initially thought to be the safest option, undergone a significant re-evaluation. The rigid approach of these designs was found to be susceptible to absorb higher rate of seismic transmitted force under certain seismic scenarios. This realization encouraged innovations in anchorage systems, leading to modern designs that are robust yet flexible enough to withstand significant seismic forces. These systems aim to prevent uplift and reduce stress concentrations, thereby enhancing the overall resilience of the tank.

The Emergence of Partially Restrained Tanks

Partially restrained tanks emerged as an intermediate solution between the two extremes of free and fully anchored systems. These designs acknowledged that some degree of flexibility could be beneficial in dissipating seismic energy. Over time, the design of partially restrained tanks has evolved, driven by technological advancements and a deeper understanding of seismic behaviour.

The Era of Performance-Based Design

The introduction of performance-based design philosophies marked a new era in seismic tank design. This approach involved designing tanks based on expected performance under different seismic intensities, leading to more detailed and tailored anchorage systems.

In the subsequent section, we will report the research that has contributed to the current understanding of the seismic behaviour of steel cylindrical tanks. Additionally, we will discuss the documented instances of damage experienced by these structures following seismic events. This review aims to shed light on the advancements in seismic design principles and the practical implications of seismic activity on such storage facilities.

A Review of Influential Research

The pioneering work in understanding tank behaviour under seismic conditions dates back to Housner (1957), who was instrumental in developing a methodology for evaluating seismic actions on storage tanks. In his initial research, Housner assumed the tank to be rigid and analysed the hydrodynamic effects of the liquid as two distinct actions: Impulsive and Sloshing motions. This methodology formed the foundation of several standards, including the American Petroleum Institute (API) provisions (2003, 2007), New Zealand standards (NZNSEE 1986 Red Book), and the Seismic Design of Storage Tanks NZSEE 2009.

Subsequent to extensive damage observed in liquid storage tanks during the Chile earthquake (1960), Alaska earthquake (1964), and Parkfield earthquake (1966), research was conducted to investigate the causes. Veletsos and Yang (1977), along with Haroun and Housner (1981), discovered that the hydrodynamic pressure was significantly influenced by the flexible behaviour of tank walls. Veletsos conceptualized the liquid tank as a cantilever beam subjected to horizontal seismic forces. This approach effectively extended Housner's formulation but also considered the effects of barrel flexibility and decoupled the impulsive and convective components of liquid motion based on their respective frequencies.

Two additional factors influencing hydrodynamic pressure are the tank interaction with the soil and its uplift motion. Depending on the tank flexibility and the liquid level height, these factors can alter the pattern of hydrodynamic pressure along the storage wall and base plate. These effects were further studied by Veletsos and Tang (1990), and Malhotra (1995).

Building upon these findings, a design approach for the seismic response of both anchored and unanchored liquid storage tanks was developed by Fischer (1979) and Rammerstorfer et al. (1988). Their results contributed to Part 4 of Eurocode 8, Annex A (European Committee for Standardization 2006b), providing engineers with guidelines for designing

cylindrical tanks. This body of research collectively enhances the understanding of seismic behaviour in liquid storage tanks, contributing to safer and more resilient designs in seismic-prone areas.

The data regarding the damage incurred to cylindrical steel liquid tanks has been compiled from three scholarly papers, which present different instances of damage observed during seismic events in 2013 and 2016 in Marlborough, New Zealand, and in 2014 in the Northwest of American Canyon, California. These papers, authored by Rosewitz & Kahanek (2017), Dizhur et al. (2017) and Fischer et al. (2016), provide detailed accounts and analyses of the types and extents of damage sustained by these structures. This compilation offers valuable insights into the vulnerability of cylindrical steel liquid tanks to seismic forces, underscoring the need for enhanced design and construction practices to improve their resilience in earthquake-prone regions.

New Zealand Marlborough Region

The Marlborough region, situated at the Northeastern tip of New Zealand South Island, has been a focal point of seismic activity in recent years, with several significant earthquakes affecting the area. Notably, the region experienced the MW 6.6 Cook Strait earthquake on 21 July 2013, the MW 6.6 Lake Grassmere earthquake on 26 August 2013, and the MW 7.8 Kaikoura earthquake on 14 November 2016 (Rosewitz & Kahanek, 2017). These seismic events have resulted in considerable shaking and have posed challenges to the region infrastructure and industries.

Marlborough holds a prominent position in the New Zealand wine industry, having seen remarkable growth over the past two decades. It is currently the largest wine-producing region in the country, with 141 wineries that contribute to more than 75% of New Zealand total wine production. The significance of this industry is further highlighted by the fact that, as of 2016, wine exports were valued at $1.6 billion (NZD), making it the New Zealand sixth largest export commodity (Dizhur et al., 2017).

In the aftermath of the 2013 seismic events, detailed assessments were conducted at over 20 wineries in the region, which collectively owned more than 4,000 stainless steel tanks. These assessments, aimed at evaluating the damage for insurance purposes, revealed that while the seismic damage to winery buildings was generally minor or non-existent, the tanks themselves fared worse. Reports from the 2013 earthquake indicated that nearly half of these tanks exhibited visible deformations or other forms of minor damage. More

concerning was the rupture of over 70 tanks, leading to significant wine loss. Additionally, many catwalks that were directly connected to the tanks also sustained damage, further complicating the recovery and operational processes at these wineries (Dizhur et al., 2017).

The New Zealand Wine reported substantial wine loss due to the Kaikoura earthquake in 2016. This loss was estimated to be around 2.0% of the Marlborough total production, equating to approximately 5.3 million liters of wine. Initial estimates suggested that about 20% of the wine tank storage capacity in Marlborough was affected to varying degrees. A more detailed assessment indicated that at least 1,000 tanks suffered damage ranging from minor to major, with around 150 of these tanks were deemed irreparable. By the vintage of 2017, the industry estimated that the tank capacity sidelined due to the earthquake was between 30-40 million liters, representing 10-13% of the capacity available before the Kaikoura earthquake (Dizhur et al., 2017).

These findings highlight the vulnerability of stainless-steel wine storage tanks to seismic events and highlight the need for improved design and retrofitting strategies to enhance their resilience in earthquake-prone regions.

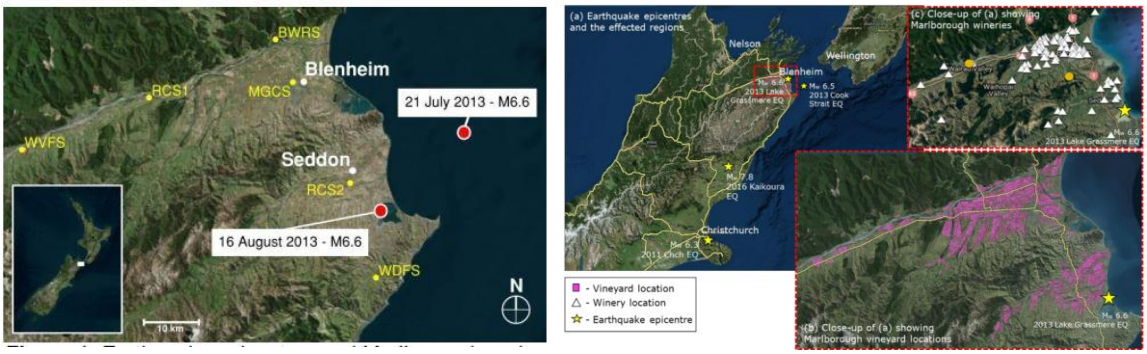

Figure 2-24: Location of MW6.6 Cook Strait Earthquake 2013(Rosewitz & Kahanek, 2017) (left); Location of MW 7.8 Kaikoura Earthquake and affected zone (Dizhur et al., 2017). (right)

Shaking in Napa Valley region

The South Napa earthquake, which occurred on August 24, 2014, had significant implications for the wine industry, particularly in terms of damage to stainless steel cylindrical tanks used for wine storage and fermentation. This seismic event, with a moment magnitude (Mw) of 6.0, was centered northwest of American Canyon, California, situated between two geological fault lines: the West Napa Fault and the Carneros-Franklin Faults, near the north shore of San Pablo Bay. Despite its moderate magnitude, the earthquake generated substantial ground acceleration, reaching a

maximum of 1.0g, as reported by Brocher et al. (2014). Figure 2-16 illustrates the earthquake's epicenter and the shaking intensities experienced across the Napa Valley region (CISN 2015).

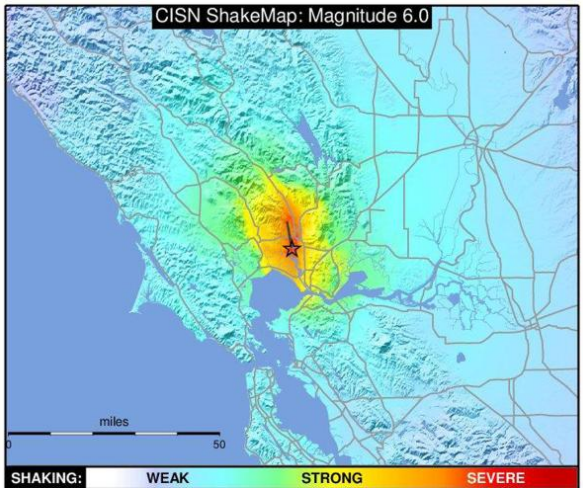

Figure 2-25: ShakeMap showing extent of shaking in Napa Valley region

The damage observed in wineries and storage facilities throughout the region was notably consistent, encompassing three primary types: (1) anchorage failure of wine storage tanks, (2) buckling of the walls of these storage tanks, and (3) collapse of wine barrel racks. These types of damage highlight the vulnerability of wine production infrastructure to seismic activities and the need for improved design and anchorage solutions to mitigate such risks in the future (Fischer et al., 2016).

Tank damages reported in Marlborough and Napa Valley

This section focuses on the damage reported in both the Marlborough and South Napa regions, specifically highlighting issues related to the anchoring detail design of wine storage tanks. Figure 2-17 provides schematic representations of the main type of tank utilized in wine production: ground-supported tanks (Rosewitz & Kahanek, 2017).

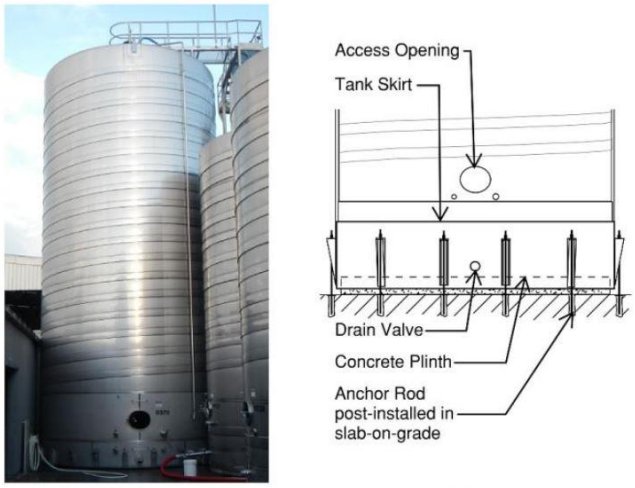

Figure 2-26: Ground-supported tanks and components (Rosewitz & Kahanek, 2017)

Barrel Failure

The construction of tank barrels in the wine industry involves meticulous craftsmanship, particularly in the use of sheet metal "strakes". These strakes, each up to 1,500 mm wide, are butt welded together to form the tank barrel. The types of damage observed in these tank barrels are varied and include shell buckling, indentations from pounding, and deformations at the points where catwalk tabs connect. Shell buckling manifests in two primary forms: diamond buckling and elephant foot buckling. Diamond buckling, illustrated in Figure 2-19, is characterized by membrane compression buckling, whereas elephant foot buckling, shown in Figure 2-18, is identified as the elastic-plastic collapse of the tank wall. Understanding these various construction techniques and potential damage types is crucial for assessing the resilience of wine storage tanks and for guiding the design of more robust and earthquake-resistant storage solutions (Rosewitz & Kahanek, 2017).

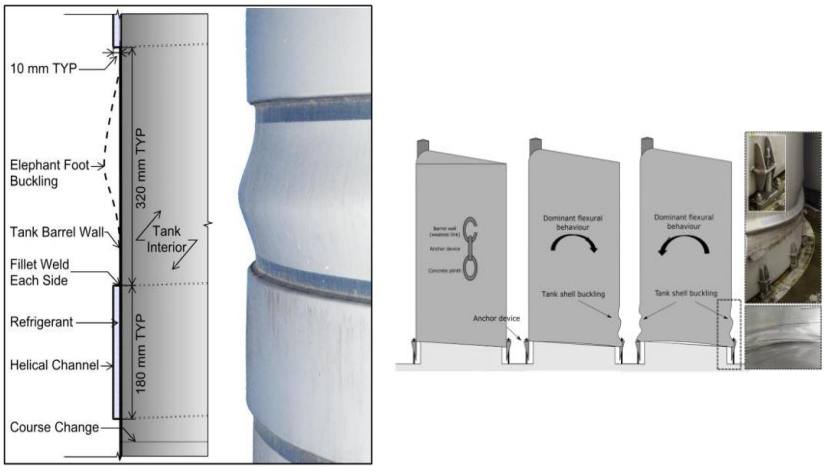

Figure 2-27: Observed Elephant Foot Buckling Between Refrigerant Channels (Rosewitz & Kahanek, 2017)

Figure 2-28: Observed diamond buckling of the tanks at varying heights (Dizhur et al., 2017)

The occurrence of different forms of buckling in the barrels of storage tanks is primarily attributed to the escalation in transmitted forces, specifically hoop forces, vertical bending moments, or axial membrane forces. Hoop forces typically result in circumferential stresses around the tank, influencing the barrel tendency to buckle in a pattern that aligns with the tank curvature. Vertical bending moments, on the other hand, introduce stresses that can lead to buckling patterns aligned with the vertical axis of the tank. Axial membrane forces, which act along the length of the tank, can also contribute to buckling, especially when these forces exceed the structural capacity of the barrel material (NZSEE, 2009).

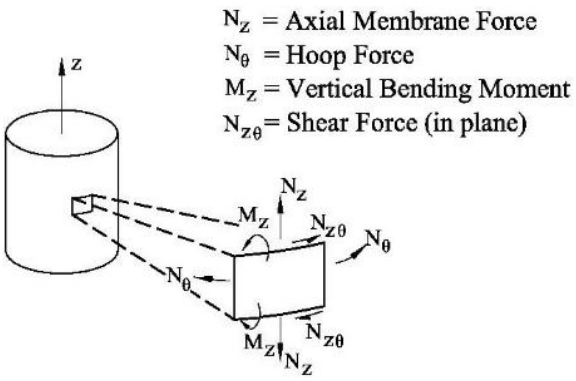

Figure 2-29: Shell Created Force and Moment (NZSEE, 2009)

Anchorage Failure

In the examination of anchor rod failures in storage tanks, several distinct types were observed, each presenting unique failure characteristics (Rosewitz & Kahanek, 2017):

1. Rupture: This type of failure involves the breaking of the anchor rod itself, as illustrated in Figure 2-21A. Rupture typically occurs when the tensile stress in the rod exceeds its material strength.

2. Concrete Pull-Out: Here, the failure is characterized by the anchor rod being pulled out from the concrete, as depicted in Figure 2-21B. This failure mode suggests that the bond strength between the concrete and the anchor rod or the concrete compressive strength was insufficient to resist the applied forces.

3. Epoxy Pull-Out: Similar to concrete pull-out, this failure involves the detachment of the anchor rod from its epoxy bonding within the concrete.

4. Anchor Rod Buckling: This type of failure occurs when the rod buckles under compressive forces, as shown in Figure 2-21C. Buckling indicates that the critical buckling load of the anchor rod was surpassed, possibly due to excessive compressive forces or inadequate rod support.

5. Anchor Rod Thread Shearing: In this scenario, the threads of the anchor rod shear off, often due to excessive tensile or shear forces.

Figure 2-30: (A) Anchor rod tearing; (B) Pull-out of the anchor bolt; (C) Buckling of the anchor rod; (D) Pull-out of the anchor bolt (Rosewitz & Kahanek, 2017)

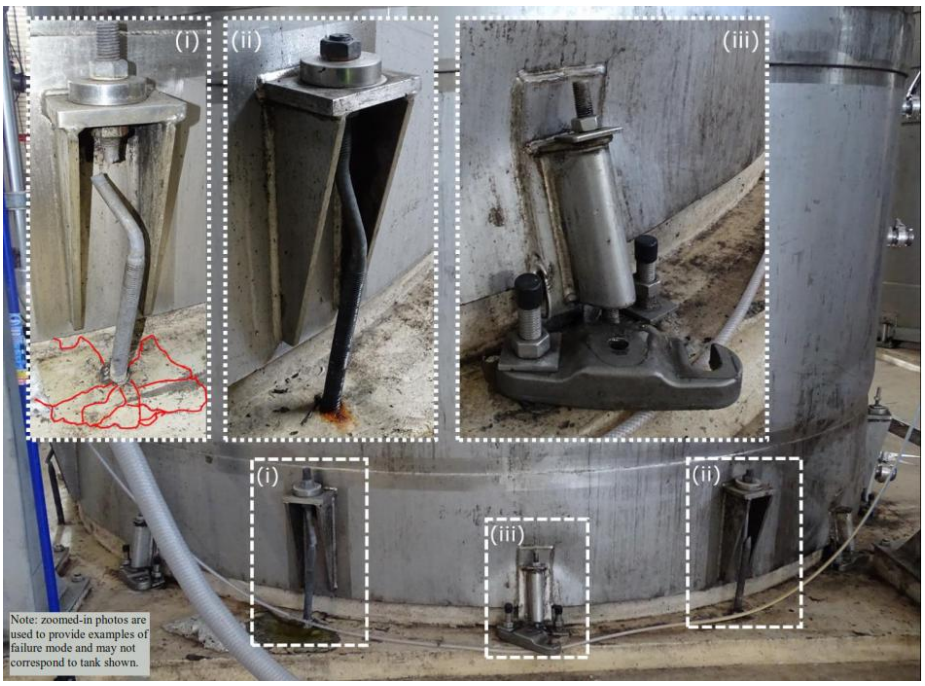

Figure 2-31: (i) buckling of the anchor rod and dislodgement from anchoring bolts; (ii) rupture of anchor rod; (iii) stripped thread and fully coming off the holding nut; (iv) evidence of tank base distortion in 'knuckle-squash' type deformation (Dizhur et al., 2017)

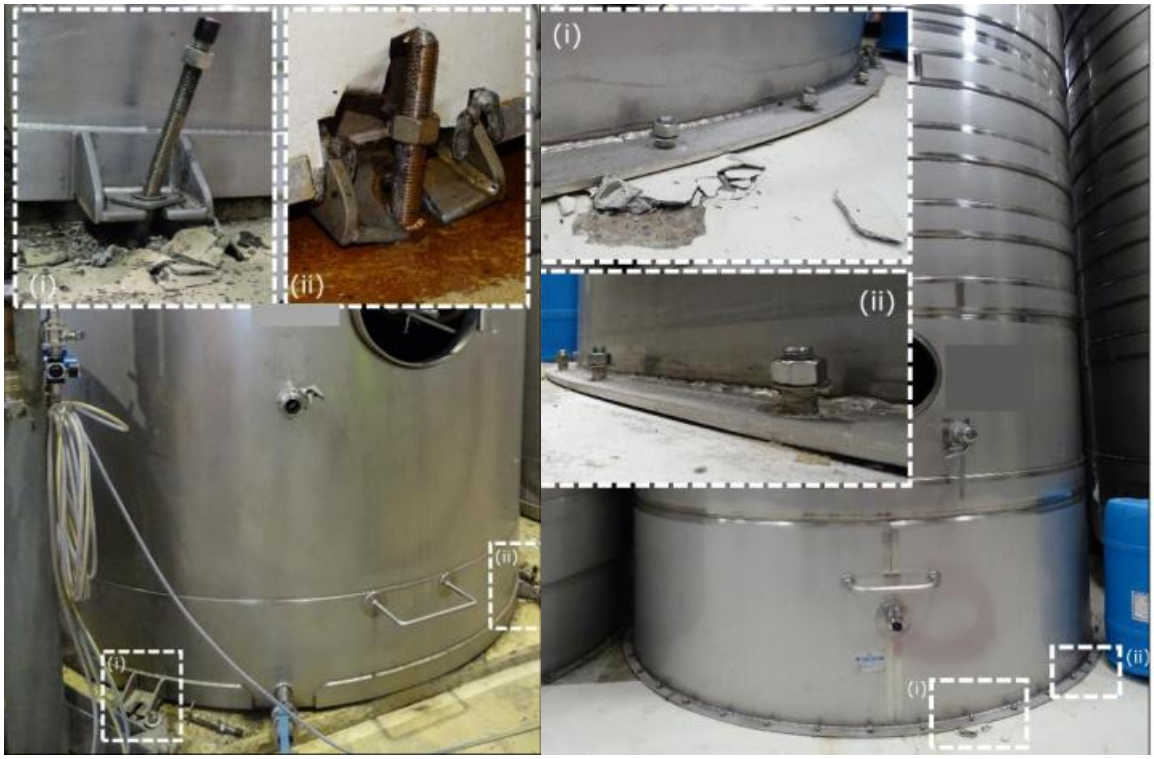

Figure 2-32: Pull-out of anchors from concrete and yielding, rupture and compression failure of anchor rod (Dizhur et al., 2017)

Collapse of Tanks

In certain wineries, instances of complete tank collapse were documented, which were predominantly attributed to excessive rocking and displacement of the tanks during the earthquake. This phenomenon points to the considerable impact that seismic forces can

have on the structural integrity of storage tanks. In particular, situations were observed where the collapse of one tank triggered a 'domino effect,' leading to the subsequent collapse of adjacent tanks. This chain reaction was found to be more likely in configurations where full tanks were positioned next to empty ones, as illustrated in Figure 2-24, (Dizhur et al., 2017).

Figure 2-33: Complete collapse of different sized tanks (Dizhur et al., 2017 and Fischer et al., 2016)

Complete collapses of storage tanks are generally anticipated in structures with a higher slenderness ratio. However, there have been instances where collapses occurred in tanks with lower aspect ratios as well. Notably, these failures were observed in both unanchored and anchored systems, indicating that anchorage alone may not be sufficient to prevent collapse under certain seismic conditions.

This pattern of damage underscores the critical importance of self-centring forces in the seismic design of storage tanks. The presence of self-centring forces, particularly in yielding mechanisms, can significantly enhance the resilience of these structures. The implementation of self-centring resilient systems could mitigate the risk of collapse by allowing the structure to return to its original position following seismic-induced displacements.

For a comprehensive overview of the reported damages from various seismic events (as depicted in Figure 2-25), the reference by Fischer et al. (2016) provides valuable information. This resource offers an in-depth analysis of different damage types and patterns observed in past earthquakes, contributing to a broader understanding of the vulnerabilities and potential mitigation strategies in the seismic design of storage tanks.

Earthquake	Year	General building structural damage	Cylindrical steel tank damage
San Juan	1977	Adobe structures Unreinforced masonry building damage (only new buildings under construction)	Anchorage failure Elephant foot buckling Weld rupture Tank collapse
Greenville–Mt. Diablo	1980	Residential timber-frame homes	Anchorage failure Tank wall buckling
Morgan Hill	1984	Unreinforced masonry building damage	Tanks walked Damage to piping connection Anchorage failure Local rupture of tank wall Racking of catwalk against tanks
Loma Prieta	1989	Unreinforced masonry buildings with timber frames	Damage to piping connection Tank wall buckling
San Simeon	2003	Unreinforced masonry building damage Wine barrels fell off racks	Ruptured tank walls
Maule	2010	Reinforced concrete building damage Unreinforced masonry building damage	Buckling of supporting legs Movement of tank resulting in falling off foundation Damage to piping connection Anchorage failure Elephant foot buckling of tank walls Diamond-shape buckling of tank walls
Christchurch	2011	Unreinforced masonry building damage Building façade damage	Not documented

Figure 2-34: Summary of Previous Earthquakes and Resulting Structural Damage (Fischer et al., 2016)

2.4.1. New Approaches for Tanks Hold-down Connections

The concept of employing isolators to attenuate input energy in liquid storage tanks has been a subject of extensive research. Various types of isolators, commonly utilized in the building industry, are adaptable for use in liquid tank systems. For instance, one notable example is the Friction Pendulum Bearing (FPB), as illustrated in a Figure 2-26. A friction isolation system incorporating an FPB typically functions through two primary mechanisms: the friction sliding effect and a restoring force generated by the isolator geometric design (Zhang et al., 2014).

This approach capitalizes on the FPB's unique properties to both absorb seismic energy through frictional sliding and to contribute to the tank post-seismic repositioning through its inherent geometrically induced restoring force. Such isolators offer a promising solution for enhancing the seismic resilience of liquid storage tanks, aligning with advanced seismic mitigation strategies in structural engineering.

Figure 2-35: Tank and joints detail (Zhang et al., 2014)

Another innovative concept in this domain, as depicted in Figure 2-27, utilizes a combination of sliding surfaces and yielding elements to achieve sufficient damping (De Angelis et al., 2008). This particular type of isolation system harnesses the sliding mechanism to dissipate energy through frictional resistance. Concurrently, the yielding elements within the system are designed to deform plastically under seismic loads. This plastic deformation is a critical aspect of the system damping capacity, as it absorbs and dissipates seismic energy, thereby reducing the force transmitted to the tank.

Seismic base isolation, while effective for many structures, faces practical challenges when applied to large-sized tanks. The primary concern is the significant increase in the size and complexity of the isolation system required to accommodate the large mass and dimensions of such tanks. This not only escalates the cost considerably but also introduces engineering challenges related to the design and installation of the isolators. Additionally, the dynamic behaviour of the liquid contents in large tanks (sloshing) during seismic events can interact adversely with the isolation system, potentially undermining its effectiveness. This fluid-structure interaction requires highly specialized design considerations to ensure the safety and integrity of the tank, further complicating the application of base isolation. Moreover, the maintenance and inspection of these complex systems in large tanks can be challenging and costly, adding to the operational concerns. Therefore, while base isolation is a promising seismic protection strategy, its application in large-sized tanks demands careful consideration of these practical and technical issues.

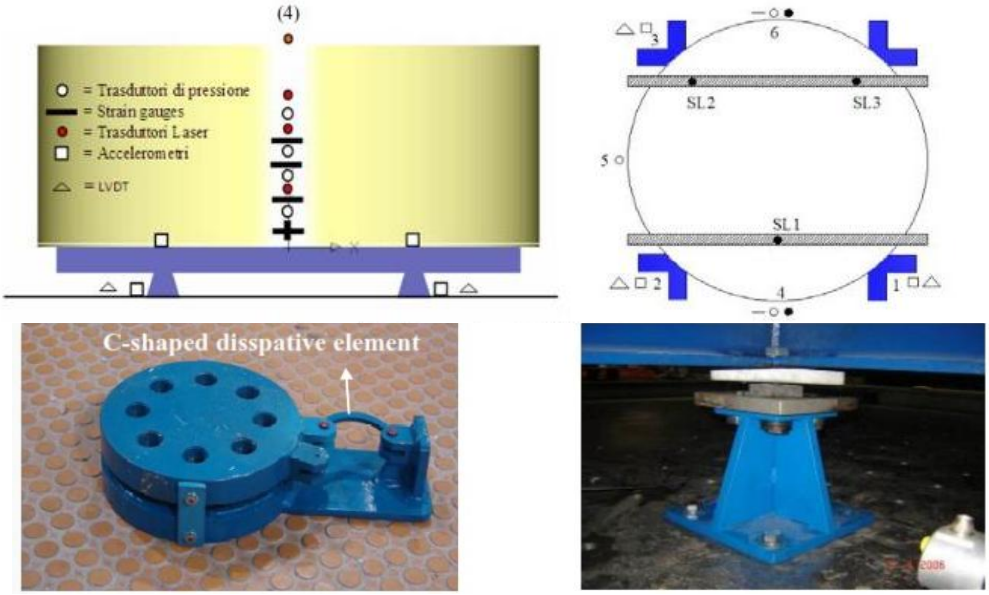

Figure 2-36: (a) Experimental Set- up; (b) Sliding bearing with dissipative damper; (c) High Damping Rubber Bearing (De Angelis et al., 2008)

Friction Damper

Figure 2-28 illustrates an innovative approach to anchor down a tank to its foundation, utilizing a friction joint mechanism. This design concept typically involves the use of a shaft or pipe that functions as a slide, along which a friction clamp is positioned. The friction clamp is carefully calibrated to exert a force that provides a specific level of resistance to movement, (Malhotra, P. K., 2000). The key aspect of this system is the use of friction to control the movement of the tank during seismic events. By adjusting the force induced by the friction clamp, the system can be fine-tuned to offer the desired balance between mobility and stability. This balance is crucial for ensuring that the tank has enough freedom to move in response to seismic forces, thereby reducing stress concentrations, while also preventing excessive displacement that could lead to structural failure.

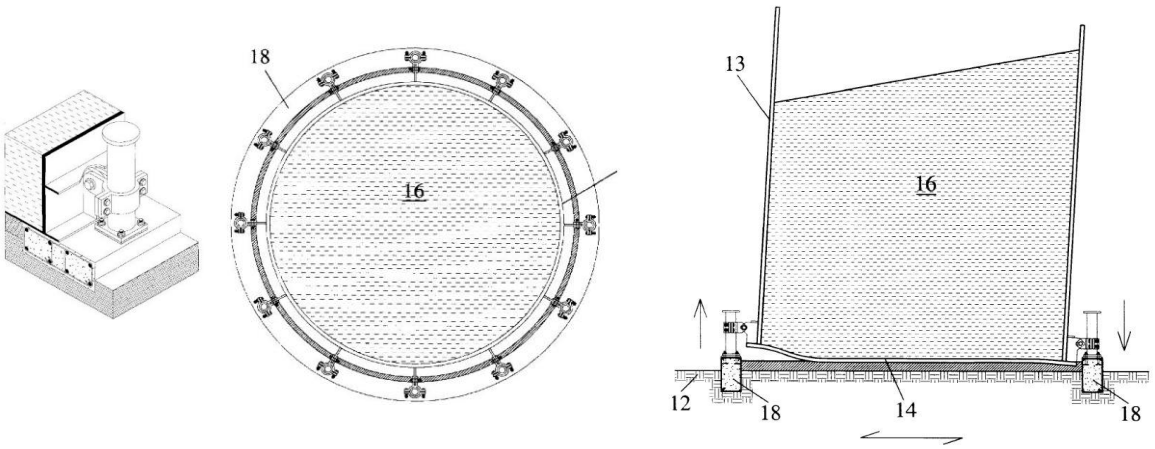

Figure 2-37: Display another concept for a slip friction connector (Malhotra, P. K., 2000)

Figure 2-29 showcases an additional seismic mitigation system that was experimentally tested at the University of Auckland (Ormeño et al, 2015). This system represents another approach in the ongoing efforts to enhance the seismic resilience of storage tanks.

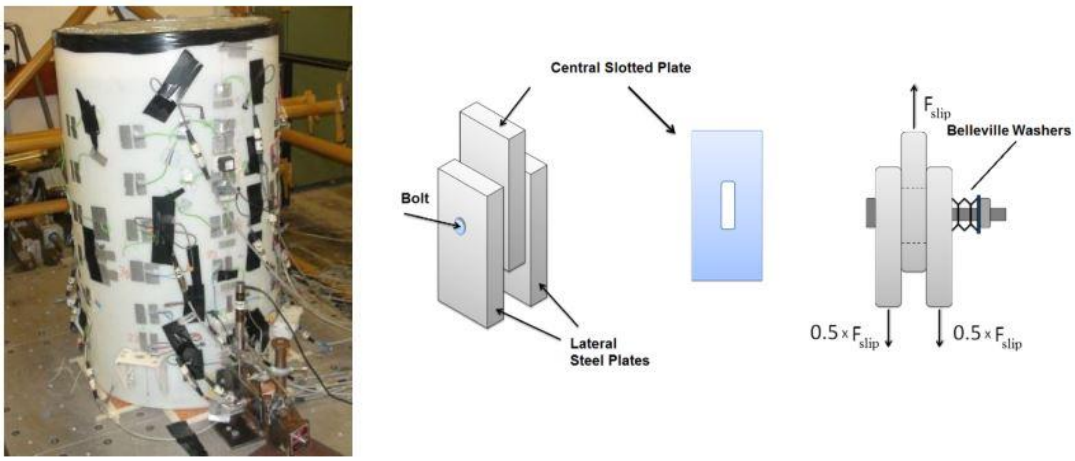

Figure 2-38: Symmetric slip-friction connector (Ormeño et al, 2015)

Steel Hysteretic Type

The ductile anchor system showcased in the experimental setup provides a controlled yielding mechanism in both tension and compression (Onguard Seismic Systems, n.d). The principle behind this approach is to allow the internal gauged steel bar to absorb the impact of the seismic forces through controlled yielding deformation. By doing so, it acts as a sacrificial element that takes on the extreme stresses, hence represents a seismic fuse. This feature is instrumental in preventing more extensive damage to the tank, as the fuse dissipates a significant amount of energy that would otherwise be transferred to and potentially compromise the integrity of the primary structural elements of the tank.

Post-earthquake, it is essential to inspect this ductile anchor system, particularly the seismic fuse component. Given its role as an energy absorber, the seismic fuse may undergo significant deformation or damage during its operation. Therefore, a thorough inspection is necessary to assess its condition. If the seismic fuse is found to have been compromised or excessively deformed, it should be replaced to ensure the continued efficacy and safety of the anchor system.

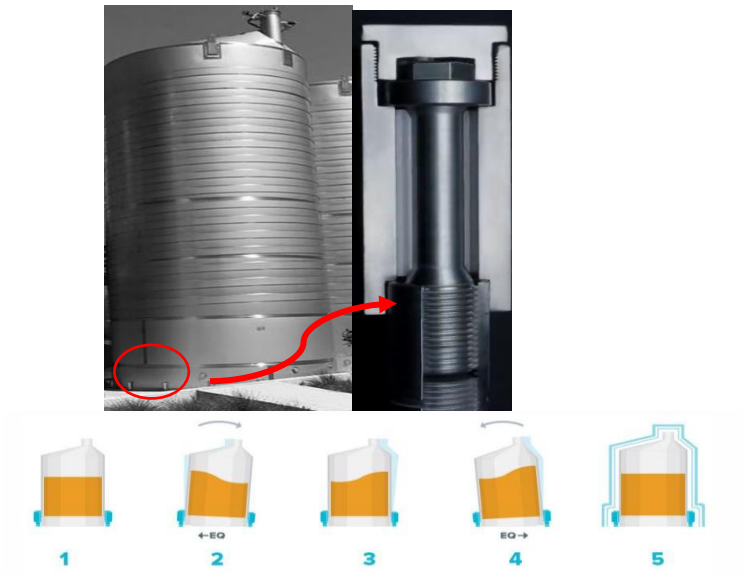

Figure 2-39: Controlled yielding concept, Onguard Seismic Systems, n.d.

Further expanding on the concept of yielding in seismic design, there are additional innovative ideas being explored, as shown in Figure 2-40. One such concept includes the use of U-shaped steel joints (Colombo & Almazán, 2014). These joints are designed to accommodate the movement and deformation during seismic events, effectively absorbing and dissipating seismic energy. The U-shape allows for a certain degree of flexure and movement, providing a controlled yielding mechanism that enhances the overall ductility of the system.

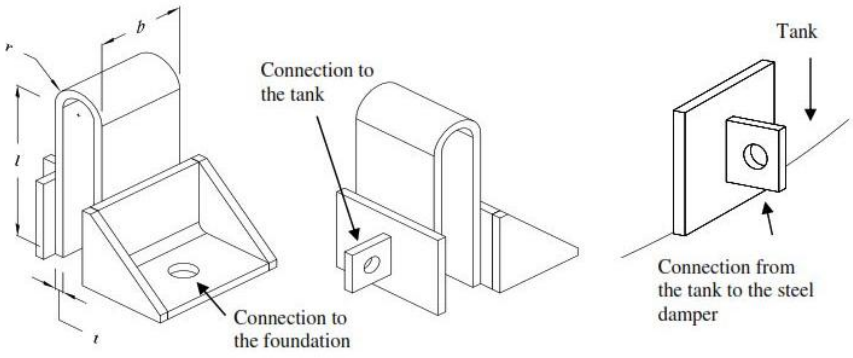

Figure 2-40: U shape Steel Damper (Colombo & Almazán, 2014)

To provide further context for the concept of mini buckling-restrained braces (mini-BRB), several related configurations previously investigated in the literature are briefly presented in this section. Although these devices have not been applied as hold-down mechanisms for tanks, they illustrate potential approaches for developing compact energy dissipation mechanisms and may represent a potential topic for future research.

The following discussion on buckling-restrained dissipaters is adapted from Mashal's PhD thesis entitled Post-Tensioned Earthquake Damage Resistant Technologies for Accelerated Bridge Construction. The concepts summarized here are based on previous studies including Christopoulos et al. (2002), Amaris Mesa (2010), Marriott (2009), Sarti et al. (2013), and White (2014).

Buckling-Restrained Fused-Type Dissipater (BRF)

The Buckling-Restrained Fused-type (BRF) dissipater can be considered a compact form of a buckling-restrained brace (BRB), developed to provide localized energy dissipation within structural systems. Due to its relatively small and modular configuration, the device can be incorporated into a variety of structural applications. Previous research has explored the use of BRF dissipaters in both building structures and rocking systems designed for low-damage seismic performance (Christopoulos et al., 2002; Amaris Mesa, 2010; Marriott, 2009; Sarti et al., 2013).

A typical BRF dissipater consists of a steel core bar, an outer confining tube, and a filling material such as epoxy or grout. The steel core is usually formed from a round bar that is locally reduced in cross-section over a specific "fused" length. This region is intended to concentrate inelastic deformation when the device is subjected to axial loading. In practice, approximately a 20 % reduction in the cross-sectional area is commonly adopted to ensure that yielding occurs in the fused region rather than the threaded portions of the bar (White, 2014). The fused length is typically determined based on displacement demand while limiting peak strain to approximately 5 % (Pampanin et al., 2010).

To prevent global buckling of the core bar during compression, the bar is placed inside a confining tube and the annular gap is filled with epoxy or grout. The confining tube together with the filling material restrains the core against buckling, allowing the device to sustain cyclic deformation with stable hysteretic behaviour (Sarti et al., 2013).

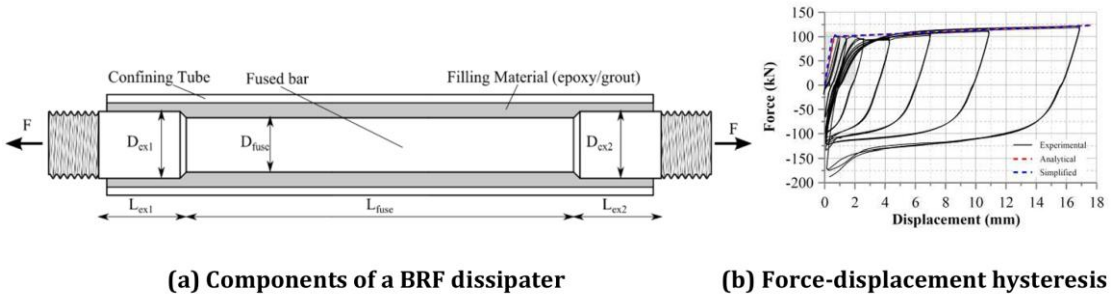

Figure 2-41: Buckling-Restrained (BRF) dissipater showing (a) main components (b) typical force-displacement hysteretic response. Adapted from Mashal (PhD thesis) based on Sarti et al. (2013).

Experimental investigations by Amaris Mesa (2010) showed that BRF dissipaters exhibit stable behaviour when subjected to tensile deformation. However, when subjected to compression, interaction between the steel core and the surrounding filling material may lead to increased stiffness and force. This behaviour can result in asymmetric hysteretic response due to premature interaction between the core and confining materials.

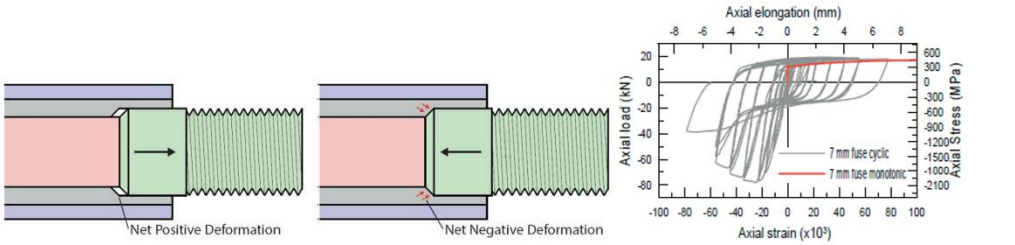

Figure 2-42: Behaviour of BRF dissipaters under cyclic loading showing (a) response under net positive deformation, (b) interaction between the steel core and filling material during compression, and (c) resulting asymmetric hysteretic response. Adapted from Mashal (PhD thesis) based on Amaris Mesa (2010) and White (2014).

Overall, BRF dissipaters offer advantages such as simple fabrication using readily available steel bars, stable hysteretic behaviour under tensile loading, and effective buckling restraint. However, limitations include the need for filling materials, potential stiffness increase under compressive loading, and susceptibility to low-cycle fatigue during repeated cyclic deformation.

Buckling-Restrained Dry-Type Dissipaters (BRD)

To address some limitations associated with BRF dissipaters, alternative configurations known as buckling-restrained dry-type (BRD) dissipaters have been proposed. In these

devices, the filling material between the steel core and the confining tube is eliminated, which simplifies fabrication and assembly. Instead, buckling restraint is achieved through mechanical interaction between the steel bar and the surrounding tube (White, 2014).

Split Tube Dissipater

In the split-tube configuration, the confining tube is initially split longitudinally during fabrication. After inserting the fused steel bar inside the tube, the split tube is welded to complete the assembly. Small clearances are typically provided near the ends to allow compressive deformation without excessive interaction between the bar and tube. Experimental testing demonstrated that this configuration can sustain cyclic deformation with stable hysteretic behaviour.

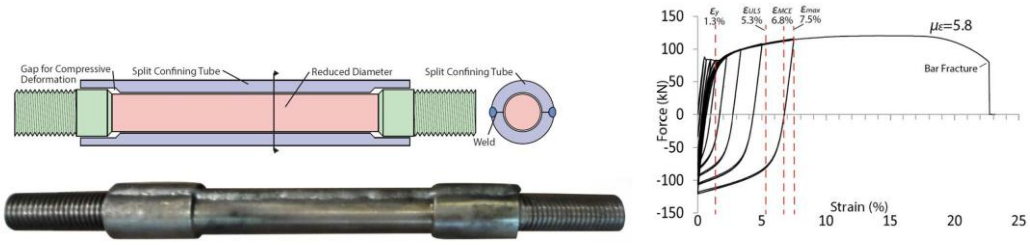

Figure 2-43: Split-tube type BRD dissipater showing configuration of the fused steel bar and confining tube, and force–strain hysteretic response. Adapted from Mashal (PhD thesis) based on White (2014).

Although the device performs well under cyclic loading, the fabrication process requires splitting and welding of the confining tube, which may increase manufacturing complexity and cost.

Deformed Tube Dissipater

Another variation is the deformed-tube dissipater, where the steel bar is inserted into a tube whose diameter is subsequently reduced through mechanical deformation. This method eliminates the need for welding while maintaining confinement of the steel bar. Although this configuration eliminates welding, fabrication may require specialized equipment for tube deformation.

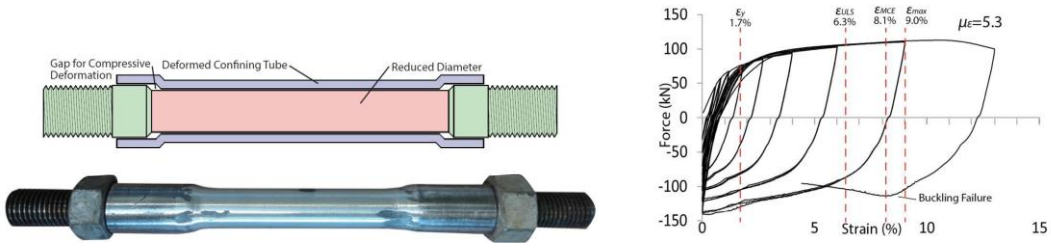

Figure 2-44: Split-tube type dissipater configuration and cyclic force–strain hysteretic response of the deformed-tube dissipater Adapted from Mashal (PhD thesis) based on White (2014).

Supported Bar Dissipater

The supported-bar configuration introduces intermediate supports along the fused length of the steel bar to reduce the effective buckling length. These supports improve buckling resistance while allowing inelastic deformation to occur in the segments between supports.

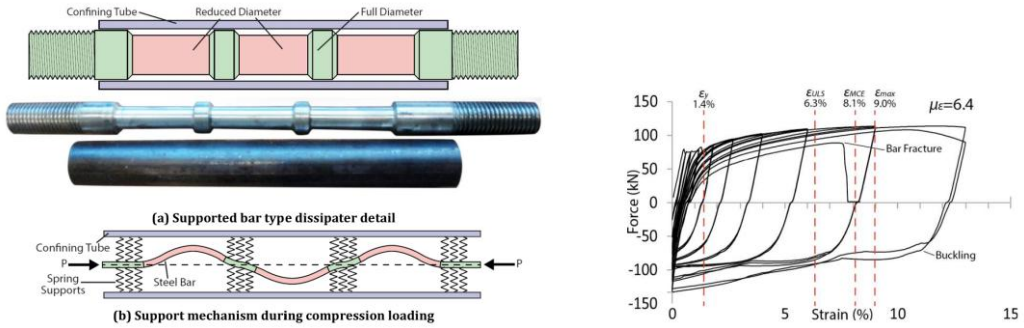

Figure 2-45: Supported-bar type BRD dissipater: configuration, compression support mechanism, and cyclic hysteretic response. Adapted from Mashal (PhD thesis) based on White (2014).

Experimental testing showed that buckling may still occur between the support points when subjected to large compressive strains.While this configuration offers relatively simple fabrication, the device length may increase due to the presence of support points along the bar.

Grooved Dissipater

A further development is the grooved-bar dissipater, where grooves are machined along the bar to create predetermined yielding locations. These grooves concentrate plastic deformation and energy dissipation. Experimental studies showed that configurations with three grooves provide favourable hysteretic performance and displacement ductility. The device exhibits stable cyclic behaviour and relatively limited stiffness increase under

compression. Despite its favourable performance, possible limitations include low-cycle fatigue failure near the grooves and local buckling around the cut regions.

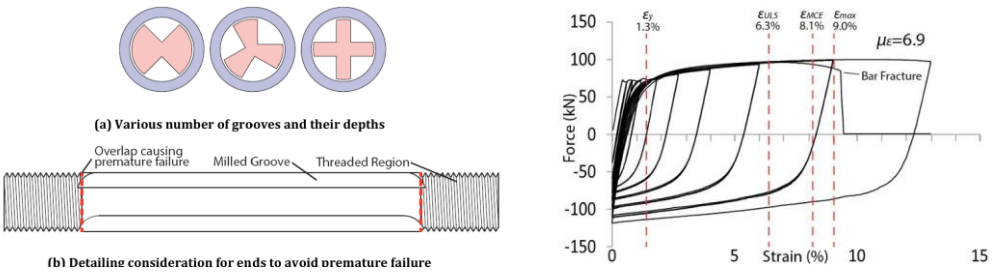

Figure 2-46: Grooved-type dissipater showing (a) groove configurations, (b) end detailing to prevent premature failure, and hysteretic response under cyclic loading. Adapted from Mashal (PhD thesis) based on White (2014).

These concepts relying on a sacrificial element which necessitates subsequent maintenance and replacement, presenting a challenge in post-earthquake recovery. The concern is further compounded by the potential for aftershocks following a primary seismic event. The tanks, already weakened by the mainshock, may be ill-equipped to withstand additional seismic forces, raising the risk of severe damage or even collapse during subsequent aftershocks.

The phenomenon of mainshock-aftershock sequences is particularly concerning in seismically active regions. In such areas, tanks could be subjected to multiple seismic events in rapid succession, without adequate time for repairs or reinforcement between occurrences. The cumulative effect of these events may elevate the risk of structural damage or collapse beyond that posed by a single seismic event. In this context, the role of post-earthquake safety assessments becomes paramount. These assessments are essential for determining the structural integrity of tanks, enforcing restrictions on occupancy for damaged components, and identifying those requiring immediate repair.

Another crucial aspect in the design of seismic mitigation systems is the capability for self-centring. Post-earthquake repositioning is a key concern, particularly in yielding mechanisms that necessitate a restoring force to return the system to its pre-seismic state. The ability to self-center not only contributes to the structural stability post-event but also ensures the safety and usability of the tanks.

2.5. Summation and Key Research Objectives in Seismic Resilience Enhancement

This chapter is concluded by highlighting the focus of the present research on concept developing of two new controlled rocking systems for shear walls (or frames), and steel cylindrical tanks. Both concepts are driven by the goal of proposing a practical system that enhances the lateral resilience of structures and tanks, adhering to a low-damage design philosophy. Central to both parts is the adoption of self-centring energy dissipation, aimed at minimizing the post-event recovery and mitigating the residual displacement. While the literature suggests that rocking frames and shear walls typically rely on sacrificial mechanisms necessitating maintenance post-earthquake and may be limited in efficiency due to higher mode effects, this research strives to propose new systems that address these limitations and could offer more choices for seismic-resistant solutions.

2.6. References

1. Makris, Nicos, Vassiliou, Michalis F. (2015). "Dynamics of the rocking frame with vertical restrainers." Journal of Structural Engineering 141.10: 04014245.
2. Clough, Ray W., and Arthur A. Huckelbridge. "Preliminary experimental study of seismic uplift of a steel frame." Earthquake Engineering Research Center, College of Engineering, University of California (1977).
3. Huckelbridge, A. A., and R. Clough. "Earthquake simulation tests of a nine-story steel frame with columns allowed to uplift." University of California, Berkeley (1977).
4. Kurama, Y., et al. "Seismic behaviour and design of unbonded post-tensioned precast concrete walls." Earthquake Engineering & Structural Dynamics 44.3 (1999): 72-89.
5. Kurama, Y. "Seismic design of unbonded post-tensioned precast concrete walls with supplemental viscous damping." Earthquake Spectra 97.4 (2000): 648-658.
6. Priestley, M. N. "Overview of PRESSS research program." Journal of Performance of Constructed Facilities 36.4 (1991): 50-57.
7. Iwashita, K., et al. "Shaking table test of a steel frame allowing uplift." (2002): 47-54.

8. Midorikawa, M., et al. "Seismic Performance of Controlled Rocking Frames with Shear Fuse and PT Wire Anchorage-Shaking table tests on controlled rocking steel frames using multipurpose inertial mass system: Part I." (2010): 1547-1556.
9. Wada, A., et al. "Passive controlled slender structures having special devices at column connections." 7th International Seminar on Seismic Isolation, Passive Energy Dissipation and Active Control of Vibrations of Structures (2001).
10. Roke, D., et al. "Self-centring seismic-resistant steel concentrically-braced frames." Proceedings of the 8th US National Conference on Earthquake Engineering, EERI, San Francisco, April (2006).
11. Roke, D., et al. "Damage-free seismic resistant self-centring steel concentrically-braced frames." (2009).
12. Eatherton, M., et al. "Controlled rocking of steel-framed buildings with replaceable energy-dissipating fuses." Proceedings of the 14th world conference on earthquake engineering (2008).
13. Eatherton, M. R., and J. F. J. E. S. Hajjar. "Residual drifts of self-centring systems including effects of ambient building resistance." Journal of Structural Engineering 27.3 (2011): 719-744.
14. Wiebe, L. D. A. "Design of controlled rocking steel frames to limit higher mode effects." (2013).
15. Zarnani, P. and Quenneville, P. "A resilient slip friction joint", Patent No. WO2016185432A1, NZ IP Office (2015).
16. Hashemi, A., F. D., S. Yousef-Beik, H. Abadi, P. Zarmani, and P. Quenneville. "Recent Developments of the Resilient Slip Friction Joint (RSFJ) Technology for Seismic Proofing New and Existing Buildings." (2018).
17. Razzaghi, M. S., & Eshghi, S. (2015). Seismic Design of Steel Tanks. In Seismic Design of Steel Structures (pp. 221-234). Springer.
18. Housner, G. W. (1957). Dynamic pressures on accelerated fluid containers. Bulletin of the Seismological Society of America, 47(1), 15-35.
19. American Petroleum Institute (API) provisions. (2003, 2007). Welded Steel Tanks for Oil Storage.
20. New Zealand standards (NZNSEE 1986 Red Book).
21. Seismic Design of Storage Tanks NZSEE. (2009). Recommendations of a Study Group of the New Zealand Society for Earthquake Engineering, Wellington, New Zealand.

22. Veletsos, A., & Yang, J. (1977). Earthquake response of liquid storage tank. Advances in Civil Engineering through Engineering Mechanics. Proc. Engrg. Mech. Div. Specialty Con., Raleigh, N.C, ASCE, New York, N.Y., 1-24.
23. Haroun, Medhat A., and George W. Housner. "Seismic design of liquid storage tanks." Journal of the Technical Councils of ASCE 107.1 (1981): 191-207.
24. Veletsos, A., & Tang, Y. (1990). Soil-structure interaction effects for laterally excited liquid storage tanks. Earthquake Engineering & Structural Dynamics, 19(4), 473-496.
25. Malhotra, P.K. (1995). Base uplifting analysis of flexibly supported liquid-storage tanks. Earthquake Engineering & Structural Dynamics, 24(12), 1591–1607.
26. Fischer, F. D. (1979). Dynamic fluid effects in liquid-filled flexible cylindrical tanks. Earthquake Engineering & Structural Dynamics, 7(6), 587-601.
27. Scharf, K., Rammerstorfer, F. G., & Fischer, F. D. (1989). The scientific background of the Austrian recommendation for earthquake-resistant liquid storage tank design. Structural Dynamics and Soil-Structure Interaction, 281-313.
28. Part 4 of Eurocode 8, Annex A (European Committee for Standardization 2006b).
29. NZSEE: Seismic Design of Storage Tanks: 2009
30. Rosewitz, J., & Kahanek, C. (2017). PERFORMANCE OF WINE STORAGE TANKS: LESSONS FROM THE EARTHQUAKES NEAR MARLBOROUGH. Bulletin of the New Zealand Society for Earthquake Engineering, Vol. 50, No. 2.
31. Dizhur, D., Simkin, G., Giaretton, M., & Loporcaro, G. (2017). PERFORMANCE OF WINERY FACILITIES DURING THE 14 NOVEMBER 2016 KAIKOURA EARTHQUAKE. Bulletin of the New Zealand Society for Earthquake Engineering, Vol. 50, No. 2, June 2017.
32. Fischer, E. C., Liu, J., & Varma, A. H. (2016). Investigation of Cylindrical Steel Tank Damage at Wineries during Earthquakes: Lessons Learned and Mitigation Opportunities. Practice Periodical on Structural Design and Construction / Volume 21 Issue 3 - August 2016.
33. Zhang, R., Weng, D., & Ge, Q. (2014). Shaking table experiment on a steel storage tank with multiple friction pendulum bearings. Structural Engineering and Mechanics, Volume 52, Number 5, December 10, 2014, pages 875-887.

34. De Angelis, M., Giannini, R., & Paolacci, F. (2008). Experimental investigation on the seismic response of a steel liquid storage tank equipped with a floating roof by shaking table tests. The 14th World Conference on Earthquake Engineering, October 12-17, 2008, Beijing, China.
35. Malhotra, P. K. (2000). Method of protecting liquid storage tanks from seismic shocks and an anchor especially adapted for the same. United States Patent No. 6085472.
36. Ormeño, M, Geddes,M, Larkin, T, Chouw, N. Experimental study of slip-friction connectors for controlling the maximum seismic demand on a liquid storage tank. Engineering Structures 103:134-146 15 Nov 2015.
37. Onguard Seismic Systems. (n.d.). Seismic Protection. Retrieved January 12, 2024, from https://onguardseismic.com/
38. Colombo, J. I., & Almazán, J. L. (2014). Seismic fragility curves for the shell–base connection of unanchored steel liquid storage tanks with energy dissipation devices. In Proceedings of the Tenth U.S. National Conference on Earthquake Engineering: Frontiers of Earthquake Engineering (pp. [page numbers]). July 21-25, Anchorage, Alaska.
39. Pall, A. S., Pall, R. T., & Marsh, C. (1980). Friction dampers for seismic control of large panel structures. Journal of Structural Engineering, ASCE.
40. Pall, A. S., & Marsh, C. (1981). Experimental study of friction damping devices for seismic control of structures. Journal of Structural Engineering, ASCE.
41. Pall, A. S., & Marsh, C. (1982). Response of friction-damped braced frames. Journal of Structural Engineering, ASCE, 108(ST6), 1313–1323.
42. Constantinou, M. C., & Symans, M. D. (1993). Experimental and analytical investigation of seismic response of structures with supplemental friction dampers. Earthquake Engineering and Structural Dynamics, 22, 273–292.
43. Fitzgerald, T. F., Anagnos, T., Goodson, M., & Zsutty, T. (1989). Slotted bolted connections in aseismic design for concentrically braced frames. Earthquake Spectra, 5(2), 383–391.
44. Grigorian, C. E., Popov, E. P., & Yang, T. S. (1993). Slotted bolted connection energy dissipators. Earthquake Spectra, 9(3), 491–504.
45. Aiken, I. D., & Kelly, J. M. (1990). Earthquake simulator testing and analytical studies of two energy absorbing systems for multistory structures. Earthquake Engineering Research Center, University of California, Berkeley.

46. Aiken, I. D., Nims, D. K., Whittaker, A. S., & Kelly, J. M. (1993). Testing of passive energy dissipation systems. Earthquake Spectra, 9(3), 335–370.
47. Nims, D. K., Richter, P. J., & Bachman, R. E. (1993). The use of energy dissipating devices for seismic design of structures. Earthquake Spectra, 9(3), 467–487.
48. Mualla, I. H., & Belev, B. (2002). Performance of steel frames with a new friction damper device under earthquake excitation. Engineering Structures, 24(3), 365–371.
49. Liao, W. I., Loh, C. H., & Wan, S. (2004). Shaking table tests of structures with rotational friction dampers. Earthquake Engineering and Structural Dynamics, 33(7), 693–710.
50. Mirtaheri, M., Torabian, S., & Yousefi, A. (2011). Cylindrical friction damper for seismic energy dissipation in structures. Engineering Structures, 33(11), 3202–3211.
51. Latour, M., D'Aniello, M., Zimbru, M., & Rizzano, G. (2015). FREEDAM: A friction damper device for moment resisting frames. Journal of Constructional Steel Research, 109, 159–172.
52. Jaisee, S., Yue, F., & Ooi, Y. H. (2021). A state-of-the-art review on passive friction dampers and their applications. Engineering Structures, 235, 112022.
53. Christopoulos, C., & Filiatrault, A. (2006). Principles of Passive Supplemental Damping and Seismic Isolation. IUSS Press, Pavia, Italy.
54. Filiatrault, A., Tremblay, R., & Kar, R. (2000). Performance evaluation of friction spring seismic damper. ASCE Journal of Structural Engineering, 126(4), 491–499.
55. Guerrini, G., Restrepo, J. I., Massari, M., & Vervelidis, A. (2012). Self-centering precast concrete dual-shell steel columns. Proceedings of the 15th World Conference on Earthquake Engineering, Lisbon, Portugal.
56. Mashal, M. (Year). Post-Tensioned Earthquake Damage Resistant Technologies for Accelerated Bridge Construction. Doctor of Philosophy Thesis, University of Canterbury, Christchurch, New Zealand.
57. Christopoulos, C., Filiatrault, A., Uang, C., & Folz, B. (2002). Post-tensioned energy dissipating connections for moment-resisting steel frames. Journal of Structural Engineering, 128(9), 1111-1120.

58. Amaris Mesa, A. D. (2010). Developments of Advanced Solutions for Seismic Resisting Precast Concrete Frames. PhD Thesis, University of Canterbury, Christchurch, New Zealand.
59. Marriott, D. (2009). The Development of High-Performance Post-Tensioned Rocking Systems for the Seismic Design of Structures. PhD Thesis, University of Canterbury, Christchurch, New Zealand.
60. Sarti, F., Smith, T., Palermo, A., Bonardi, D., & Carradine, D. (2013). Experimental and analytical study of replaceable buckling-restrained fuse-type mild steel dissipaters. Proceedings of the New Zealand Society for Earthquake Engineering Conference, Wellington, New Zealand.
61. White, S. (2014). Controlled Damage Rocking Systems for Accelerated Bridge Construction. Master Thesis, University of Canterbury, Christchurch, New Zealand.
62. Pampanin, S., Marriott, D., & Palermo, A. (2010). PRESSS Design Handbook. New Zealand Concrete Society, Auckland, New Zealand.
63. Latham, D. A., Reay, A. M., & Pampanin, S. (2013). Kilmore Street Medical Centre: Application of an advanced flag-shape steel rocking system. Proceedings of the New Zealand Society for Earthquake Engineering Conference, Wellington, New Zealand.

Chapter 3: Seismic Performance of Rocking Concrete Shear Walls with Innovative Rotational Resilient Slip Friction Joints

K. Sahami[1], P. Zarnani[2], P. Quenneville[3]

(1) PhD student, Dept of Built Environment Engineering, Auckland University of Technology, New Zealand, kaveh.sahami@aut.ac.nz
(2) Lecturer, Dept of Built Environment Engineering, Auckland University of Technology, New Zealand, pouyan.zarnani@aut.ac.nz
(3) Professor, Dept of Civil and Environmental Engineering, University of Auckland, New Zealand, p.quenneville@auckland.ac.nz

Paper published in 2019 pacific conference on Earthquake Engineering

3.1. Abstract

With the prevalence of the concept of damage avoidance design, rocking walls were one of the primary solutions to minimize structural components' damage as well as decreasing the time and cost of building rehabilitation after severe earthquakes. In this study, in order to achieve a self-centring damage avoidance rocking system, a new generation of Rotational Resilient Slip Friction Joint (Rotational-RSFJ) has been employed as a shear link between reinforced concrete shear walls and their boundary columns.

This type of friction damper dissipates energy through the rotational sliding of grooved surfaces pre-stressed using disc springs, which can also provide the required self-centring to restore the building to its original position without residual drifts. In this paper, initially the joint component has been analytically and numerically investigated, and then the results have been used to develop an analytical model for the performance prediction of the proposed rocking shear walls as a new lateral load resisting system. Such new self-centring system not only does not require post-event maintenance, but also attenuates the complexity of analysing and implementing of conventional resilient rocking walls using post-tensioning tendons.

Eventually, a five-story prototype building using the proposed lateral load resisting system comprising of single and coupled rocking walls has been numerically analysed.

Also, the effectiveness of such a concept has been investigated for rocking systems with multiple ductile joints in different stories. The results demonstrated the efficiency of the proposed system that is mainly attributed to high ductility, self-centring and the ability to dissipate energy of Rotational-RSFJs.

Keywords: Rotational-RSFJ, Self-centring, Rocking shear wall, Energy dissipation, Low damage design

3.2. Introduction

Concrete shear walls, due to their high seismic performance and cost-efficient material, are widely used in the building industry. While shear walls provide sufficient resistance and stiffness, thereby rarely experiencing collapse during earthquakes, they have been reported to suffer various degrees of structural and non-structural damages. These damages have led to significant property losses, particularly in connections to floors and foundations (Fintel, 1995). In the conventional design approach, engineers accommodate the required ductility through material nonlinearity, which implies accepting potential residual drift and damage in buildings after severe events, necessitating post-event repairs.

The initial studies on rocking motion focused on investigating the overturning resistance of a rigid body, demonstrating that a rocking block is capable of rebounding until its center of gravity reaches the edge of the foundation (Muto K, 1960). Housner (1963) introduced the concept of rocking structures as a system resistant to lateral forces. Aslam (1978) proposed adding a post-tensioning mechanism to provide self-centring capabilities for rocking systems. Subsequently, Priestley (1995) conducted a series of non-linear dynamic time history analyses on moment-resisting structures equipped with prestressing tendons, aiming to eliminate residual drift. Further research by Stone et al. (1995) introduced a hybrid system that combined mild steel reinforcement for energy dissipation with a self-centring mechanism provided by unbonded post-tensioned tendons. Moreover, the PREcast Seismic Structural Systems (PRESSS) research program (Priestley, 1991) developed several prestressed frames in the United States to achieve a self-centring system with minimal damage and residual drift. A key feature of the PRESSS program was employing unbonded post-tensioning to tie precast components together, including in beam-to-column connections and shear walls.

Another critical factor in structural response during cyclic loading is the capacity to dissipate energy, traditionally provided by the nonlinear behaviour of material in the structure. In rocking structures, as per the low damage concepts, while the tendons were designed to remain elastic, the structures were equipped with additional devices for earthquake energy dissipation. Part of the PRESSS program included using various types of shear connectors, such as U-shaped flexural plates (UFPs), in coupled wall systems to transfer shear force and dissipate input energy (Priestley et al., 1999). Providing necessary damping for a rocking system was the focus of several researches. Marriott (2008) proposed using viscous fluid dampers or tension-compression yielding steel dampers externally, in parallel to post-tensioned tendons. Buckling-Restrained Braces (BRB) were also suggested for use in Propped Rocking Wall Systems (Nicknam, 2015). However, all these rocking shear wall systems relied on PT systems for providing restoring force and required an additional type of passive damper as a sacrificial element for energy dissipation. The loss of prestressing significantly impacts the overall performance of such systems. Challenges like creeping, vulnerability to ambient factors such as temperature, and practical installation challenges, especially for tall shear walls, are notable in PT systems.

Zarnani and Quenneville (2015) introduced a new generation of friction dampers that combine restoring force and energy dissipation in one compact joint. This resilient slip friction joint (RSFJ) was initially studied in a rocking timber wall application as a hold-down (Hashemi et al., 2017) and later employed in a practical project (Nelson airport terminal, NZ). Darani et al. (2018) extended this concept to rocking concrete shear walls as a damage-free solution requiring no service or post-event maintenance. In this paper, an innovative seismic device, branded as Rotational Resilient Slip Friction Joint (Rotational-RSFJ) and considered a new generation of RSFJ, has been developed. R-RSFJ retains the RSFJ concept for providing self-centring and damage avoidance characteristics but benefits from rotational movement like the common Rotational Damper (Mualla et al., 2002), significantly enhancing its deflection capacity. These features make R-RSFJ suitable for incorporation into rocking shear walls, presenting a damage-free resisting system. By adopting R-RSFJs as shear links between reinforced concrete shear walls and their boundary columns, the resisting force is distributed along the wall, reducing the bending moment demand. This not only avoids high-stress concentration at conventional hold-down connections but also significantly reduces wall size.

3.3. Rotational Resilient Slip Friction Joint (R-RSFJ)

3.3.1. Analytical Modelling of Rotational-RSF Joint

The mechanical operation of the Rotational-RSFJ closely mirrors that of the RSFJ. In both devices, the restoration force originates from specially designed steel grooved plates, which are secured using high-strength bolts and disc springs. The energy input is dissipated through the frictional resistance encountered during the slipping of these grooved plates. Utilizing the free body diagrams depicted in Figure. 3-1, a design procedure has been formulated to predict the performance of the RSF joint, as detailed by Hashemi et al. (2017). The slip force (F_slip) and residual force (F_res) are calculable through equations (1) and (2), respectively:

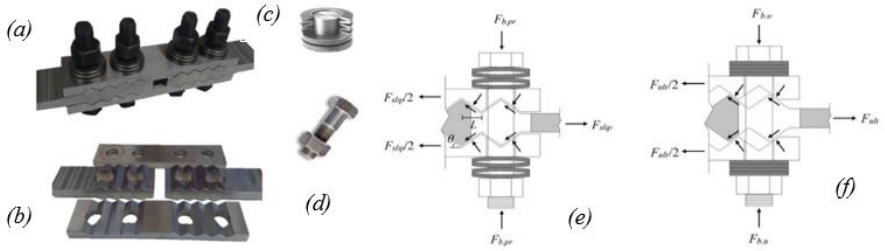

Figure 3-1: a) Assembly of the RSF Joint; b) Cap plates and slotted centre plates; c) Disk springs; d) High strength bolts; e) Free body diagrams RSF join on the brink of slippage; f) at ultimate defection (Hashemi 2017)

$$F_{RSFJ,slip} = 2n_b F_{b,pr}\left(\frac{\sin\theta + \mu_s \cos\theta}{\cos\theta - \mu_s \sin\theta}\right) \qquad \text{Equation 3-1}$$

$$F_{RSFJ,res} = 2n_b F_{b,pr}\left(\frac{\sin\theta - \mu_k \cos\theta}{\cos\theta + \mu_k \sin\theta}\right) \qquad \text{Equation 3-2}$$

In the equation, nb represents the number of bolts on each splice, and θ denotes the groove angle. Fb.pr is the clamping force resulting from pre-stressing. μs and μk are the static and kinetic coefficients of friction, respectively. In this context, μk is considered to be 0.85 times μs, as per Hashemi, Zarnani et al. (2017). The overall hysteresis behaviour of the RSFJ is depicted in Figure 3-2a. Here, Fult, loading and Fult, unloading refer to the system forces at the maximum displacement of the disk springs and the force exerted by the bolts, respectively.

$$F_{b,u} = F_{b,pr} + K_s \Delta_s \qquad \text{Equation 3-3}$$

The values of Fult, loading and Fult, unloading are determined by substituting the bolt forces in Equations 1 and 2 with those from Equation 3, and interchanging μs and μk with μk and μs, respectively. The Rotational-RSFJ (R-RSFJ) consists of friction circular grooved disk plates, which are clamped by pre-stressed bolts. To facilitate a maximum rotation of 45 degrees, each disk is divided into four sections, and the grooves are oriented in two opposite directions to accommodate both tension and compression movements. The groove angle is varied along the curved sliding surfaces to ensure the most efficient frictional contact. These disk plates are positioned on two cap plates and a central plate, which facilitate rotational movement. The total rotation of the joint is dependent on the deflection capacity of the disk springs, and by adjusting the length of the lever arm (between the middle and cap plates), the total deflection of the joint can be controlled. The detailed design and functionality of the R-RSFJ are illustrated in Figure 3-2:

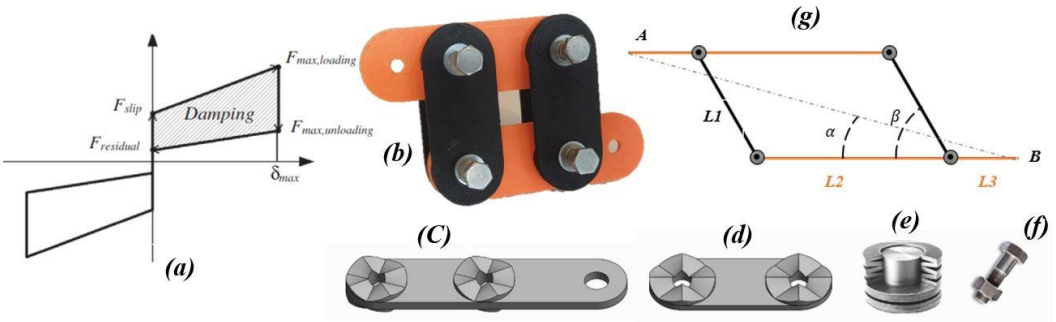

Figure 3-2: (a) hysteresis behaviour of RSFJ ;(b) R-RSF joint component; (c) middle plate; (d) cap plate; (e) conical disk spring; (f) high strength bolt; (g) Simplified analytical model.

L1 represents the length of the middle plates, while L2 indicates the distance between the two cap plates. Therefore, the sum L2+L3 signifies the total length of the cap plates. The angles β and α are defined as the angle between the cap and middle plates, and the angle of the applied load, respectively. By monitoring the variations in these angles, α and β, the total deflection of the system can be accurately calculated.

$$L = \frac{2L_3 + L_2 + L_1 \cos(\beta)}{\cos(\alpha)} \qquad \text{Equation 3-4}$$

Where the parameter α can be obtained by:

$$\alpha = Arctan\left(\frac{L_1 \sin(\beta)}{2L_3 + L_2 + L_1 \cos(\beta)}\right) \qquad \text{Equation 3-5}$$

So, the deflection and the joint force at each step are derived and expressed by Eq. 6 and Eq. 7.

$$\Delta = L - L_{ini} \qquad \text{Equation 3-6}$$

$$F = \frac{4M}{(2L_3 + L_2)\, sin(\alpha)} \qquad \text{Equation 3-7}$$

3.4. Numerical modelling of Rotational-RSF Joint

In order to compare the analytical results with Finite Element (FE) analysis, the behaviour of a joint component has been studied using the FE analysis software, Abaqus. The properties of the analysed joint are summarized in Table 3-1.

For the cap plates and middle plates, high-strength steel (Fy=690MPa and Fu=860MPa) with deformable solid parts (meshed by C3D8R finite element) was used. The friction coefficient was considered to be a consistent value of μ=0.18 for both static and kinetic conditions, and contact is modeled with 'Hard contact' for normal behaviour, along with tangential behaviour allowing for relative sliding. The rods and the stack are also assumed to function as a spring.

The force was applied in two steps: (i) disk spring pre-stressing force, and (ii) displacement history application.

The von Mises stress contour of the joint at nearly 100mm compressive deflection and the joint performance are illustrated in Figure 3-3. As shown the joint hysteresis loop predicted by the analytical model matches the FE outputs with high accuracy.

Table 3-1 Rotational-RSFJ characteristics

Parameter	Value
Cap plate thickness (mm)	12
Middle plate thickness (mm)	20
β (degree)	108
Friction Disk diameter (mm)	125

Pin hole diameter (mm)	36
Coefficient of Friction	0.18
Disk spring ultimate force (KN)	132
Disk spring deflection capacity (mm)	1.75
No. of disk spring per bolt per side	9

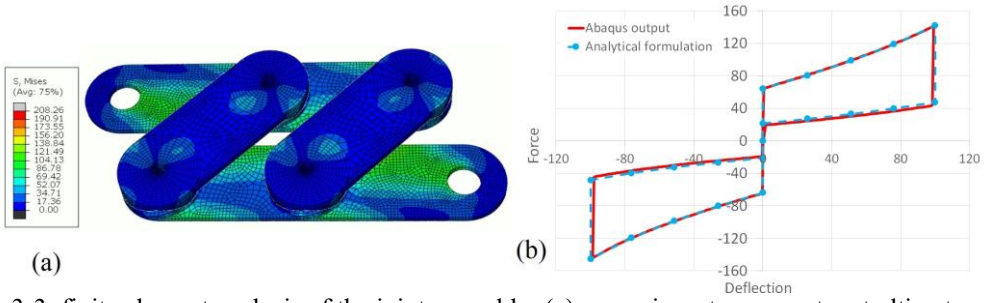

Figure 3-3: finite element analysis of the joint assembly: (a) von-mises stress counter at ultimate compression; (b) comparison of the analytical with FE analysis

3.5. Rocking Wall Equipped Rotational RSF Joint

All rocking systems require a hold-down mechanism combined with an energy dissipating feature to achieve the desired level of seismic performance. In conventional rocking shear walls, to meet these conditions, PT tendons are used along with a type of sacrificial element to dissipate the input energy. However, the complexity of implementing unbonded post-tensioning, especially in tall shear walls, and the potential loss of tension in strands have always been concerns for engineers. Additionally, systems with yielding mechanisms are vulnerable to severe aftershocks, necessitating specific inspections and maintenance after the event. The rotational movement and high deflection capacity of the R-RSFJ make it feasible for this joint to be used with boundary columns, providing structures with sufficient restoring force and damping mechanism simultaneously. This eliminates the need for regular inspections and post-event maintenance.

3.6. Single Rocking Shear Wall Equipped With R-RSFJ and End Columns

The proposed configuration for a single rocking wall equipped with R-RSFJs is depicted in Figure 3-4. In this configuration, the wall and columns are attached to the floor, and

bracket beams are utilized to connect shear links to both the wall and end columns. The rocking moment is calculated by taking the moment of the rocking base

$$M_{rock} = M_{weight} + M_{damper} = W\frac{l}{2} + n_d\left[F_{DL_i}(l+d) + F_{DR_i}(d)\right] \quad \text{Equation 3-8}$$

where $n_d$is the number of dampers in each side of the walls, F_{DL_i}, $F_{DR_i}$are the force of dampers in left and right sides of the rocking toe. Assuming that the bracket beams, columns, and wall are all rigid compared to RSFJs, the deflection in dampers in right side (δ_{DR}) and left side (δ_{LR}) of the wall is determined.

$$\delta_{DR} = (L+d)\,sin(\theta) \quad \text{Equation 3-9}$$

$$\delta_{DL} = d\,sin(\theta) \quad \text{Equation 3-10}$$

While the wall rotates at an angle θ, the deflections of the joint on each side of the wall are the same, resulting in equal forces on both sides. The general hysteretic response of the system is depicted in Figure 3-4b. Before reaching the slipping point ($M \leq M_{slip}$), the stiffness of each link connected to other elements can be determined by:

$$k_{ini} = (\frac{1}{k_{col,axial}} + \frac{1}{k_{bb,bending}} + \frac{1}{k_{wall,axail}} + \frac{1}{k_{R-RSFJ,initial}})^{-1} \quad \text{Equation 3-11}$$

$k_{col,axial}$: axial stiffness of column with the height equal to the level of corresponding damper ($\frac{EA}{h_i}$)

$k_{bb,bending}$: bending stiffness of bracket beam ($\frac{b_{bb}h_{bb}^3}{12}$)

$k_{wall,axial}$: axial stiffness of wall with the height equal to the level of corresponding damper and with length of around 10% of wall total length ($\frac{EA_w}{h_i}$)

While h_i is the link level, b_{bb}, h_{bb} denote the thickness and height of the bracket beam, respectively. After the slipping point, as the stiffness of the R-RSFJs decreases considerably($k_{rock} \ll k_{ini}$), he stiffness of the links becomes significantly smaller compared to other elements. Therefore, the rocking stiffness can be directly derived using the following equation:

$$k_{rock} = n_d k_{d,ini}[(L+d)^2 + (d)^2] \quad \text{Equation 3-12}$$

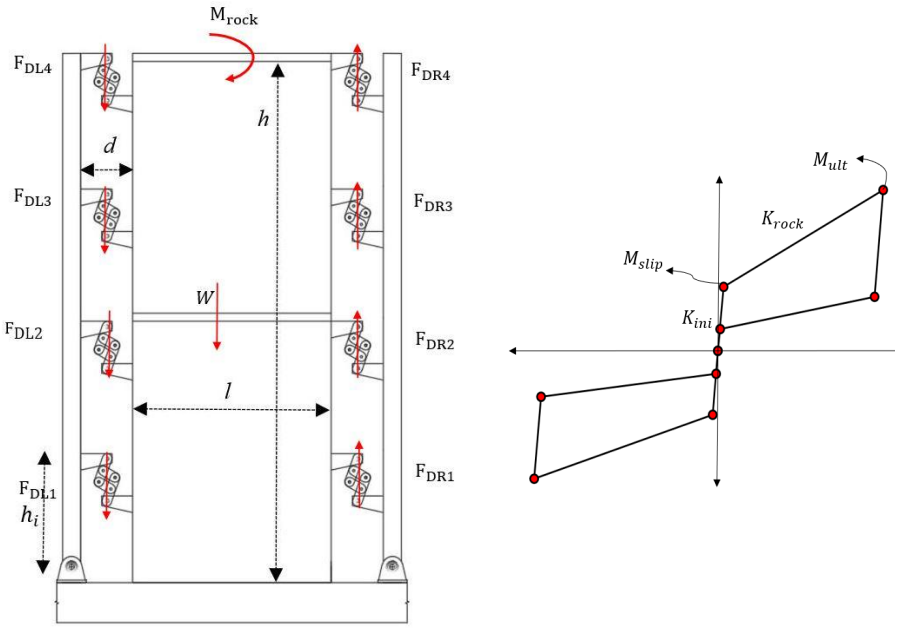

Figure 3-4: a) Schematic of single wall system; b) general hysteretic response of rocking wall with R-RSF joints

3.7. Coupled Rocking Shear Wall Equipped With R-RSFJ and End Columns

In the coupled walls system, the boundary element in the middle can be removed, allowing the walls to be connected directly by the shear links. Similar to a single shear wall, all columns and walls undergo the same horizontal displacement since they are connected to the floor. Coupled shear walls, following this configuration, exhibit the same behavioural pattern as a single shear wall. Therefore, the moment at the rocking base and the rocking stiffness are given by:

$$M_{rock} = M_{weight} + M_{damper} = Wl + n_d\left[n_w F_{DL_i}(l+d) + F_{DR_i}(d)\right] \quad \text{Equation 3-13}$$

$$k_{rock} = n_d k_{d,ini}[n_w(L+d)^2 + (d)^2] \quad \text{Equation 3-14}$$

n_w represents the number of coupled walls. When comparing the capacity of coupled walls with two single walls of identical length, it's notable that, if architectural requirements allow sufficient space for coupled walls, the same capacity can be achieved while eliminating the middle column and a row of shear links, corresponding to the number of coupled walls.

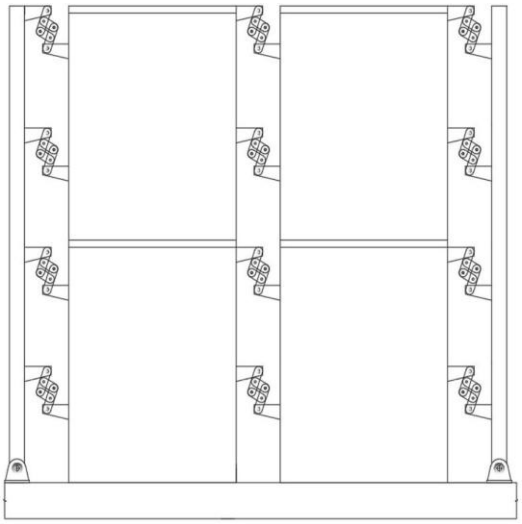

Figure 3-5: Schematic of coupled wall system

3.8. Prototype Building and Numerical Modelling

To assess the seismic behaviour of rocking wall systems equipped with R-RSFJs, both single and coupled wall concepts have been considered for the lateral load-resisting system of a five-story office building. The total height of the prototype building is 20 meters, with each story being 4 meters high, and it has a floor plan measuring 16 meters by 32 meters, as depicted in Figure 3-6. The building is situated in Wellington on shallow soil (type C) and is of normal importance level (with seismic factors as per NZS 1170.5 summarized in Table 3-3. In terms of seismic force resistance, the system in the longitudinal direction incorporates six single shear walls, while in the transverse direction, it includes three coupled shear walls.

Table 3-2 Wall, column and end column details

Single and couple wall (each wall)		Boundary Concrete column		Bracket Plate	
Total height	2000 (mm)	Depth	350 (mm)	Depth	300 (mm)
Length	3000(mm)	Width	350 (mm)	Width	20 (mm)
Thickness	300 (mm)				

Table 3-3 Seismic factors according to NZS 1170.5

Coefficient	Selected value
Design Life	50 years
Importance Level	II
Site subsoil Class	C
Seismic Hazard (Z)	0.4
Return Period Factor (ULS)	1
Return Period Factor (SLS)	0.25

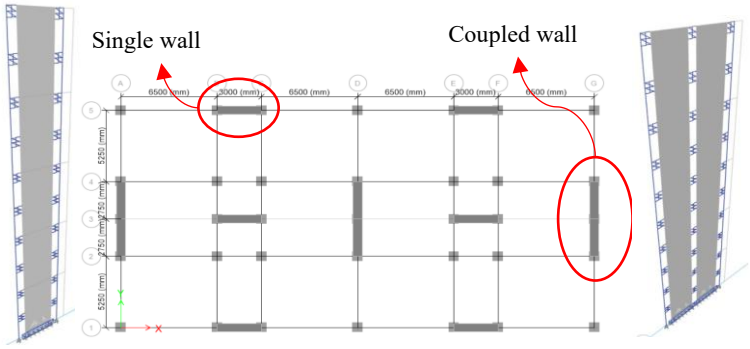

Figure 3-6: plan view of prototype building

The total dead load of the building comprises the self-weight of all structural elements, including floor slabs, beams, columns, shear walls, and a superimposed load consisting of ceilings and floor finishes, which was taken as 6 kPa. Additionally, a superimposed live load due to occupancy and partitions, as per NZS 1170.5, was assumed to be 3 kPa. The seismic weight of the building at each level is calculated in accordance with Clause 4.2 of NZS 1170.5. Nonlinear dynamic numerical simulations were carried out using CSI Etabs, where all members were modeled using common frame and shell elements. The Rotational-RSF joints were represented by a Damper – Friction spring link element, available in CSI Etabs. For the base connections and shear keys, which transfer shear forces to the foundation, a nonlinear gap link with high compressive stiffness and zero gap was employed. In this model, columns and beams were considered to resist gravity loads; therefore, connections of beams to columns and columns to the base are modeled by pin connections. For the nonlinear dynamic time-history analyses, a suite of seven ground motions was scaled to match the NZS 1170.5 spectrum with return periods of 500 and 2500 years, corresponding to ULS and MCE, respectively. The records and scale factors are detailed in Table 3-4.

Table 3-4: The selected ground motions and scale factor

Earthquake ground motion	PGA	PGA Scaled ULS	PGA Scaled MCE
El Centro (1951)	0.3	0.62	1.12
Landers (1992)	0.74	0.45	0.81
Northridge (1994)	0.61	0.46	0.83
Kobe (1995)	0.35	0.52	0.94
Chi-Chi (1999)	0.36	0.76	1.37
Bam (2003)	0.16	0.44	0.79
Christchurch (2011)	0.1	0.73	1.31

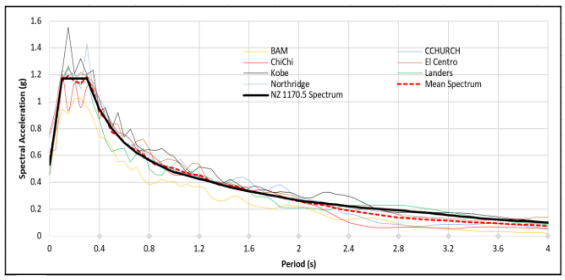

Figure 3-7: Spectral acceleration of matched ground motions with NZS1170.5 ULS Level

3.9. Hysteretic Response of Single and Coupled Shear Wall

The rocking system is recommended to be designed such that it does not begin to experience uplift at the Serviceability Limit State (SLS) earthquake level or the Ultimate Limit State (ULS) level for wind load, as suggested by SCNZ.110 (2015). Consequently, the slip force and the number of R-RSFJs should be adjusted to satisfy the required resisting force. To design the system efficiently in terms of the forces and deflection capacities of the R-RSFJs, the Displacement Based Design (DBD) method has been used. The building was designed to achieve a roof drift of 2.5% at approximately the same base shear as the ULS level, according to the NZ 1170.5 parameters (Table 3). Additionally, to assess the performance of the rocking system, the dampers were designed to have a corresponding deflection of 3.75% at the Modified Mercalli Intensity (MCE). Therefore, based on Eq. 9, the required displacement capacity would be 94 mm for both single and coupled systems. Four R-RSFJs per story were considered, with calibrated parameters presented in Table 3-5, to satisfy the required design parameters indicated in Table 3-6.

Table 3-5:Parameter of Rotational-RSFJs

Parameter	Value
L1 (mm)	250
L2 (mm)	250
L3 (mm)	100
Cap plate thickness (mm)	15
Middle plate thickness (mm)	25
Friction Disk diameter (mm)	120
Initial degree of adjustment	38
Coefficient of Friction	0.18
Disk spring ultimate force	132
No. of disk spring per bolt per side	9
Disk spring deflection capacity	1.75
Angle of groove (degree)	22

Table 3-6: Design Parameter and numerical parameter of R-RSFJs

Slipping Force (KN)	60
Ultimate Force (KN)	155
Residual Force (KN)	30
Maximum Displacement (mm)	94
Friction Link Parameter (Numerical Modelling)	
Initial stiffness (KN/mm)	14
Loading slipping stiffness (KN/mm)	1.05
Unloading slipping stiffness (KN/mm)	0.54
Pre-compression displacement (mm)	-57.1
Stop displacement (mm)	94

In terms of calibrating the RSFJ parameters in CSI Etabs, the slipping and residual forces are determined by multiplying the pre-compression displacement by the loading and unloading slipping stiffnesses. A comparison between the analytical and numerical results of the hysteresis flag-shape is shown in Figure 3-8a. Additionally, the hysteretic responses of the two systems are illustrated in Figure 3-8b. It can be observed that both systems exhibit almost identical behaviour. However, in the coupled shear wall, the middle column is removed, resulting in a 25% reduction in the total number of R-RSFJs for this configuration.

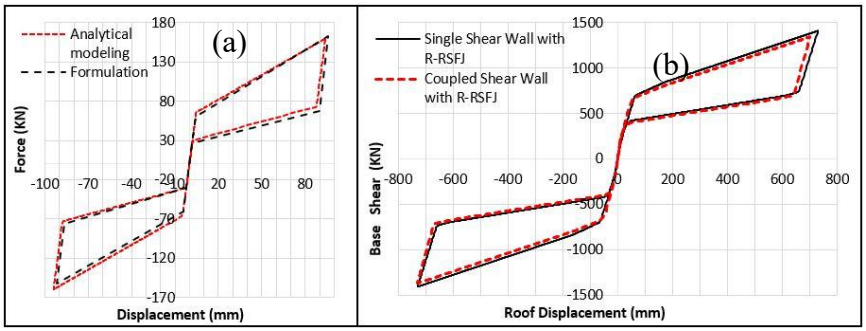

Figure 3-8: a) analytical and numerical performance of joint; b) hysteretic response of single and coupled wall

3.10. Seismic Performance of Introduced System

3.10.1. Residual Displacement and Maximum Inter-story Drift

As material nonlinearity is avoided in the introduced concept, the dynamic behaviour of the system directly depends on the seismic behaviour of the joints. Therefore, since the R-RSFJs exhibit fully self-centring behaviour, the structure is expected to be pulled back to its initial position by the joints' restoring force. As demonstrated in Figure 3-9, the roof shows complete self-centring, indicating that no residual displacement or inter-story drift was experienced in the prototype structure.

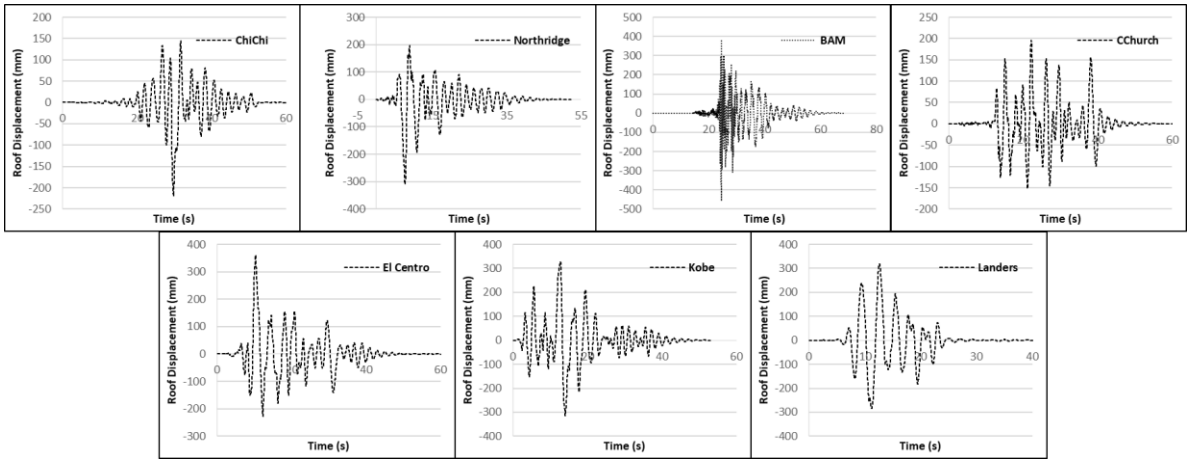

Figure 3-9: Roof displacement of structure subjected to ULS scaled ground motion

Figure 3-10 displays the maximum inter-story drifts when subjected to seven ground motion accelerations scaled to ULS and MCE levels. Since both systems exhibit similar dynamic behaviour, the inter-story drift percentages in both are nearly identical. For the ULS level, the maximum drift in both systems is less than 2.5%, and for the MCE scaled ground motions, the drifts remain within the allowable inter-story drift limit of 3.75%.

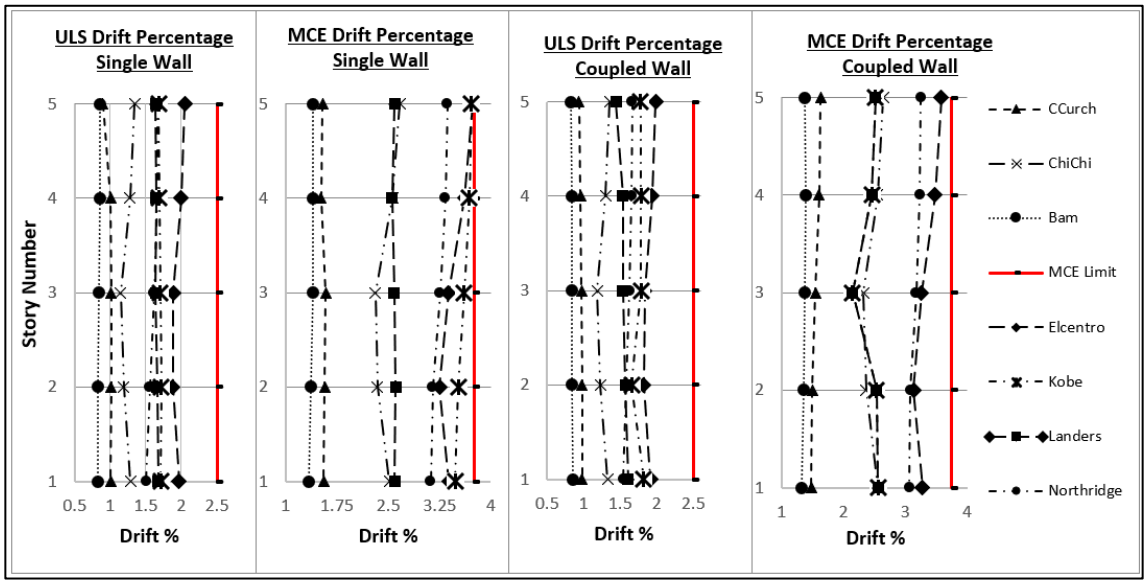

Figure 3-10:: Envelope of drift of single and coupled wall systems subjected to record scaled to ULS and MCE

3.10.2. Higher Mode Effect and Overturning Moment

In rocking systems, depending on their dynamic characteristics, the maximum overturning moment often occurs at the upper level of the base, which raises concerns in the case of higher mode effects (Wiebe, Christopoulos et al. 2013). These higher mode effects also significantly influence the amount and pattern of story forces. To illustrate the dynamic behaviour of the proposed rocking system with R-RSFJ, the first three shape modes and responses of just one leg of a single wall subjected to Kobe Ground Motion (matched to ULS level) are represented in Figures 3-11 and 3-12. These graphs display the instances of maximum displacement, base shear, and bending moment. It should be noted that the conclusions drawn from this section are not limited to the chosen ground motion; hence, to avoid prolongation, only the results from one record are presented.

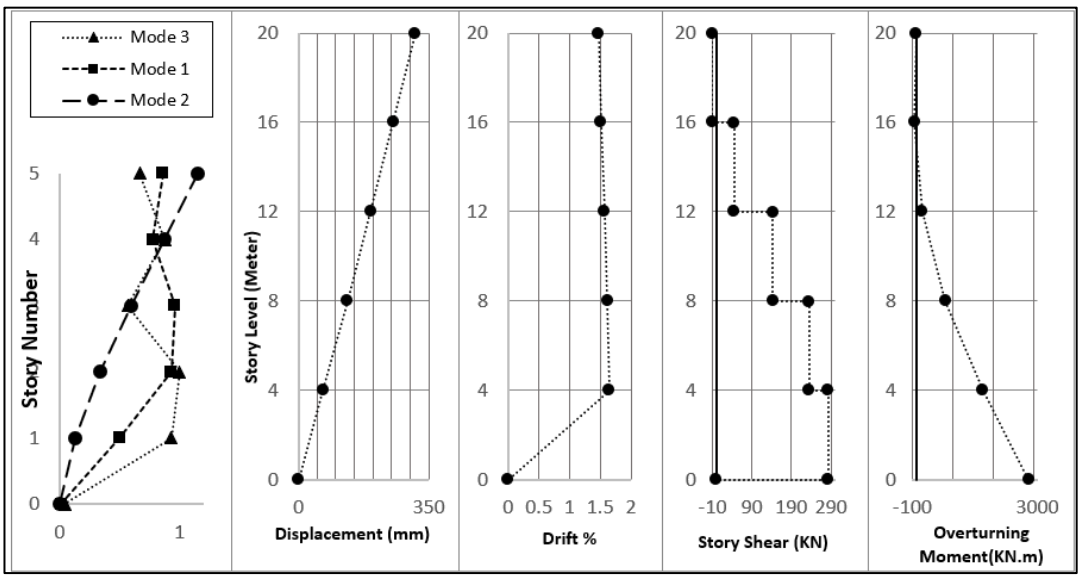

Figure 3-11: Structure mode shapes and response in moment of maximum displacement and drift in Kobe Ground motion (matched to ULS level)

As illustrated in Figure 3-11, in rocking wall systems equipped with R-RSFJs, the maximum displacement and drift are influenced by the first mode, which occurs simultaneously. Therefore, from a design perspective, it is reasonable to estimate the maximum displacement and its corresponding drift based on the first mode. However, as shown in Figure 3-12, the maximum base shear and wall bending moment are influenced by higher modes and typically do not occur at the same time. This aspect reduces the effectiveness of isolation in conventional rocking systems. By distributing the resisting force along the wall through the application of a resisting moment, the demand for wall bending moment, a critical parameter in the design of tall rocking shear walls, is decreased. Figure 3-13. shows the maximum induced bending moment and its corresponding moment transferred to the shear wall. The difference between these two values reflects the effectiveness of the R-RSFJs in terms of reducing the bending moment demand. In the prototype structure, considering all ground motions, the maximum overturning moment (which occurred in the second story) has been decreased on average by around 40% with the use of R-RSFJs. When considering all stories, the reduction is almost 52%.

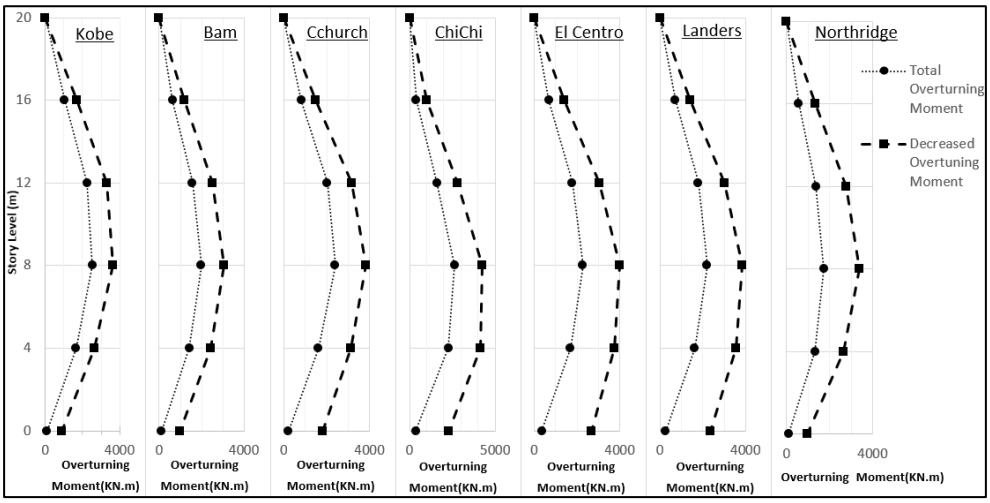

Figure 3-12: Maximum induced overturning moment and it's decreased amount due to R-RSFJs

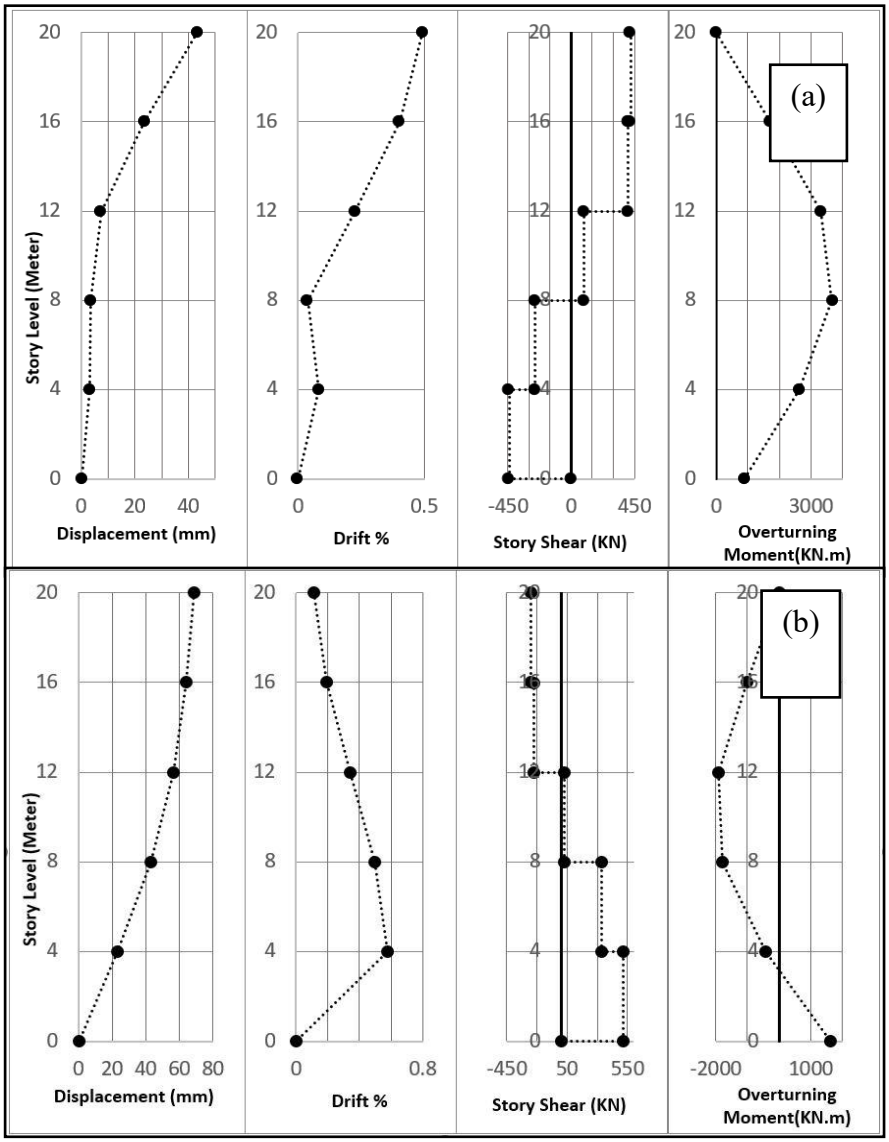

Figure 3-13: a) Structure response in moment of maximum bending moment; b) maximum base shear in Kobe Ground motion (matched to ULS level)

3.10.3. Multiple Rocking Sections

One approach to mitigating higher mode effects in a rocking system is the use of multiple rocking joints (Wiebe, Christopoulos et al. 2013). This concept has even been applied in practical projects, where RSFJs were used as hold-downs at the base and mid-height of timber walls (Hashemi, Darani et al. 2018). Considering that the R-RSFJs are placed along the wall in all stories, the wall could be segmented at each story level. The connections between these isolated walls would have a mechanism similar to that of the base joints, allowing rotational movement while transmitting the shear force to the lower level. Therefore, to study the effectiveness of this approach, the wall in the single wall system is segmented at all story levels. Figure 3-14 illustrates the mean values of maximum base shear, bending moment, and displacement subjected to the selected ground motions. It is important to note that the bending moment refers to the moment demand in one span of the single wall system. In terms of base shear, the results show an average decrease of 38%. In terms of overturning moment, the maximum overturning moment in the second story decreased by about 69%, while considering all stories, this reduction was nearly 62%. The displacement across the stories also decreased by around 20%. By eliminating the higher mode effect and softening the structure – which leads to a decrease in input energy through the isolating shear walls at each story – there was a reduction in base shear, overturning moment, and even story displacement in this system.

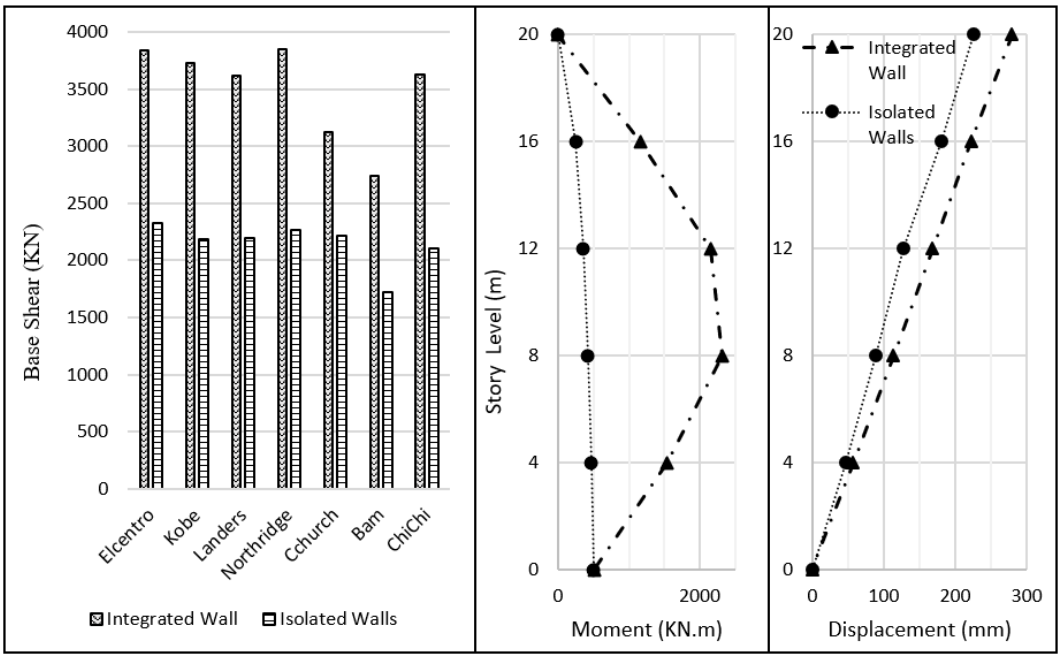

Figure 3-14: The mean value of maximum base shear, bending moment and displacement of single wall system

3.11. Summary and Conclusion

In this section of thesis, a new generation of rotational self-centring friction damper has been introduced, and its performance has been investigated both analytically and numerically. This innovative Rotational Resilient Slip Friction Joint (R-RSFJ) was incorporated into a rocking shear wall system with the objective of achieving a damage avoidance resisting system. Such a system, when used with boundary columns, could be applied to both single and coupled shear walls. In this concept, the Rotational-RSFJ acts as both a shear link and an energy dissipation device. To evaluate the seismic performance of this system, a five-story prototype building with single and coupled rocking shear walls equipped with R-RSFJs has been analysed. The results from time history analysis of the structure, subjected to seven ground motions, confirm the efficiency of the proposed system in terms of fully self-centring the structure, satisfying the inter-story drift limits for ULS and MCE, and achieving a considerable reduction in maximum bending demands. Additionally, the potential of isolating the walls in stories to mitigate higher mode effects was explored. Isolating the walls resulted in a decline of about 38% in base shear, 69% in maximum bending moment, and 20% in maximum roof displacement. Finally, it is noteworthy that this concept presents significantly less construction complexity compared to the conventional approach of using PT tendons, especially for tall rocking shear walls. Experimental testing is planned to further validate the proposed concept.

A suite of earthquake ground motions was selected to represent a range of seismic characteristics; however, the findings are valid for the earthquakes considered in this study. The results may differ if alternative ground motions, source locations, or scaling methods are used, and care should therefore be taken to ensure that selected records are representative of the seismicity and region of interest.

3.12. Acknowledgements

The authors wish to express their gratitude to the Ministry of Business, Innovation and Employment of New Zealand (MBIE) for the financial support provided for this research project.

3.13. References

1. Aslam, M. (1978). "Earthquake rocking response of rigid bodies."

2. Chanchi, J., MacRae, G.A., Clifton, G.C., Chase, G. (2010). "Quantifying Seismic Sustainability Of Steel Framed Structures." Proceedings of the Steel Structures Workshop.
3. Darani, F. M., Zarnani, P., Haemmerle, E., Hashemi, A., Quenneville, P. (2018). "Application of new resilient slip friction joint for seismic damage avoidance design of rocking concrete shear walls." New Zealand Society for Earthquake Engineering (NZSEE) Conference.
4. Hashemi, A., Darani, F., Yousef-Beik, S., Abadi, H., Zarmani, P., Quenneville, P. (2018). "Recent Developments of the Resilient Slip Friction Joint (RSFJ) Technology for Seismic Proofing New and Existing Buildings."
5. Hashemi, A., Zarmani, P., Masoudnia, R., Quenneville, P. (2017). "Seismic resistant rocking coupled walls with innovative Resilient Slip Friction (RSF) joints." 129: 215-226.
6. Housner, G. W. (1963). "The behaviour of inverted pendulum structures during earthquakes." Bulletin of the Seismological Society of America 53(2): 403-417.
7. Marriott, D., Pampanin, S., Bull, D., Palermo, A. (2008). "Dynamic testing of precast, post-tensioned rocking wall systems with alternative dissipating solutions."
8. Muto, K., U.H., Sonobe, T. (1960). "Study of the overturning vibration of slender structures." Proceedings of the 2nd World Conference on Earthquake Engineering, Tokyo and Kyoto, Japan.
9. Nicknam, A. (2015). "Seismic analysis and design of buildings equipped with propped rocking wall systems." State University of New York at Buffalo.
10. Priestley, M. (1995). "Myths and Fallacies in Earthquake Engineering--Conflicts Between Design and Reality." 157: 231-254.
11. Priestley, M., Sritharan, S., Conley, J.R., Pampanin, S. (1999). "Preliminary results and conclusions from the PRESSS five-story precast concrete test building." 44(6): 42-67.
12. Priestley, M. (1991). "Overview of PRESSS research program." 36(4): 50-57.
13. Sritharan, S., Aaleti, S., Henry, R.S., Liu, K., Tsai, K. (2015). "Precast concrete wall with end columns (PreWEC) for earthquake-resistant design." Earthquake Engineering Structural Dynamics 44(12): 2075-2092.
14. Stone, W., Cheok, G., Stanton, J. (1995). "Performance of hybrid moment-resisting precast beam-column concrete connections subjected to cyclic loading." 92(2): 229-249.

15. Wiebe, L., Christopoulos, C., Tremblay, R., Leclerc, M. (2013). "Mechanisms to limit higher mode effects in a controlled rocking steel frame. 2: Large-amplitude shake table testing." 42(7): 1069-1086.
16. Zarnani, P., Quenneville, P. (2015). "A resilient slip friction joint." Patent No. WO2016185432A1, NZ IP Office.
17. Mualla, I., Belev, B. (2002). "Performance of steel frames with a new friction damper device under earthquake excitation." Engineering Structures, Vol 24(3), 365-371.
18. Makris, Nicos, Vassiliou, Michalis F. (2015). "Dynamics of the rocking frame with vertical restrainers." Journal of Structural Engineering 141.10: 04014245.
19. Clough, Ray W., Huckelbridge, Arthur A. (1977). "Preliminary experimental study of seismic uplift of a steel frame." Earthquake Engineering Research Center, College of Engineering, University of California.
20. Kelley, J., Tsztoo, D.J.E.E.R.C. (1977). "Earthquake simulation testing of a stepping frame with energy-absorbing devices." Report No. EERC 77-17.
21. Midorikawa, M., et al. (2010). "Seismic Performance of Controlled Rocking Frames with Shear Fuse and PT Wire Anchorage-Shaking table tests on controlled rocking steel frames using multipurpose inertial mass system: Part I." 75(654): 1547-1556.
22. Roke, D., et al. (2006). "Self-centring seismic-resistant steel concentrically-braced frames." Proceedings of the 8th US National Conference on Earthquake Engineering, EERI, San Francisco, April.
23. Eatherton, M., et al. (2008). "Controlled rocking of steel-framed buildings with replaceable energy-dissipating fuses." Proceedings of the 14th World Conference on Earthquake Engineering.
24. Eatherton, M.R. (2010). "Large-scale cyclic and hybrid simulation testing and development of a controlled-rocking steel building system with replaceable fuses." University of Illinois at Urbana-Champaign.
25. Wiebe, Lydell Deighton Andree. (2013). "Design of controlled rocking steel frames to limit higher mode effects." University of Toronto.
26. Wiebe, L.D.A. (2015). "Design and construction of controlled rocking steel braced frames in New Zealand." Improving the Seismic Performance of Existing Buildings and Other Structures 2015: 810-821.
27. Zarnani, Pouyan, Quenneville, Pierre. (2015). "A resilient slip friction joint." Patent No. WO2016185432A1, NZ IP Office.

28. Hashemi, A., Darani, F., Yousef-Beik, S., Abadi, H., Zarmani, P., Quenneville, P. (2018). "Recent Developments of the Resilient Slip Friction Joint (RSFJ) Technology for Seismic Proofing New and Existing Buildings."
29. Bagheri, H., Hashemi, A., Quenneville, S.M.M., Yousef-Beik, P., Zarnani, P. (2018). "Experimental test of a new self-centring tension-only brace using the Resilient Slip Friction Joint." New Zealand Society for Earthquake Engineering (NZSEE) Conference.
30. Sahami, K., Veismoradi, S., Zarnani, P., Quenneville, P. (2019). "Seismic Performance of Rocking Concrete Shear

Chapter 4: Introducing a Low Damage System Incorporation Rocking Braced Frame and Resilient Slip Friction Joints as Shear Links

K. Sahami[1], P. Zarnani[2], P. Quenneville[3]

(1) PhD student, Dept of Built Environment Engineering, Auckland University of Technology, New Zealand, kaveh.sahami@aut.ac.nz
(2) Lecturer, Dept of Built Environment Engineering, Auckland University of Technology, New Zealand, pouyan.zarnani@aut.ac.nz
(3) Professor, Dept of Civil and Environmental Engineering, University of Auckland, New Zealand, p.quenneville@auckland.ac.nz

Paper published at 17th World Conference on Earthquake Engineering, 17WCEE.

4.1. Abstract

Since ancient times, structures have been engineered with rocking mechanisms, including rocking columns or walls, as one of the applicable structural systems. Initially considered primarily for gravity systems, these mechanisms have proven their effectiveness as main lateral systems as well, having withstood various natural hazards such as hurricanes, tornadoes, and earthquakes. In recent years, inspired by this traditional concept and in an effort to achieve a low-damage lateral system, the rocking motion has been integrated with energy dissipation mechanisms and hold-down systems to ensure stable and reliable seismic performance. Two of the most common approaches are employing pre-tension cables as a system retainer, along with yielding or friction mechanisms, or mounting a self-centring system like the Resilient Slip Friction Joint (RSFJ) as a hold-down in the rocking toes. The RSFJ is a self-centring friction damper that, unlike other passive control systems, not only dissipates input energy but also restores the structure to its original position.

In this paper, to achieve a self-centring, damage-avoidance rocking frame system, the RSFJ has been employed as a shear link between the braced frame and its boundary columns. This system can be used for either a single or coupled braced frame and offers an alternative to conventional rocking systems, reducing their design complexity and implementation challenges. This configuration also covers taller rocking systems. The

study first explains this mechanism and assesses its performance. Then, to evaluate the seismic performance of the introduced system, results are compared with a braced frame equipped with an lead rubber bearing (LRB) isolation system at the ground level. For the case study, a seven-story prototype building equipped with a conventional special braced frame and both isolation concepts has been analysed. The results demonstrate that the proposed rocking system can provide structures with a fully self-centring, low-damage lateral system, which is crucial for evaluating the time and cost required for building rehabilitation and the vulnerability of structures to severe aftershocks. Additionally, as both base isolating and rocking systems rely on shifting the effective mode to reduce transmitted forces, compared to the braced frame, the induced overturning moment is at a lower rate. However, to improve efficiency given the influence of higher mode effects on rocking systems, the impact of having multiple rocking levels has also been studied.

Keywords: RSFJ, Resilient Slip Friction Joint, Self-centring, Rocking braced frame, Energy dissipation, Low damage design

4.2. Introduction

Some ancient structures in Greece, Iran, and other seismic-prone areas have withstood lateral forces, including earthquakes and wind, by relying on rocking mechanisms. Although it might be claimed that these mechanisms were not intentionally designed for seismic resistance, their ability to resist and return to position after seismic events is undeniable. Notable examples include Greek temples and certain slender structures in Chile [1]. Muto et al. [2] were among the first to analyse the rocking mechanism of a rigid body, conducting small-scale experimental tests subject to ground excitation and theoretically deriving the relationship of rocking in a rigid body. They concluded that a rocking body resists lateral static load until the center of mass reaches the rocking toe.

The concept of rocking structures as effective lateral resisting systems to mitigate seismic demand was initially introduced by Housner [3]. He observed less damage in flexible slender structures compared to stiffer ones, attributing this to the ductility of such systems. Clough et al. [4] tested a half-scale three-story steel rocking moment frame, showing a reduction in member force and story acceleration compared to fixed-base scenarios. Addressing displacement concerns, Kelly et al. [5] incorporated a yielding type damper at the base of the structure, which activated during uplift and dissipated energy through material nonlinearity. As expected, this resulted in a lower deflection demand while maintaining the base shear level similar to the rocking system without fuse elements.

Midorikawa et al. [6] designed a yieldable base plate for a rocking frame in a half-scale three-story building, finding that thicker base plates reduced force but increased displacement demands. Roke et al. [7] developed controlled rocking steel frames (CRSBFs) with post-tensioning tendons and supplementary energy dissipation, effectively separating the rocking system from gravity columns. Roke provided a procedure for designing CRSBFs using a quasi-static method that considered higher mode effects. In a case study of a six-story frame, time history analysis indicated a 3.6 times greater axial force demand in the bracing system than predicted. The simplified method proposed by Roke et al. [7] estimated a higher force design than this demand.

The University of Illinois at Urbana-Champaign [8] studied CRSBFs with post-tensioned cables for self-centring forces and yielding dampers for energy dissipation. They found that while the PT system failed at strains as low as 0.85%, the structure remained self-centered up to a 2500-year seismic event (Eatherton and Hajjar [9]). Wiebe [10] tested a

30% scale eight-story post-tensioned frame, proposing multiple rocking joints and shear control braces to mitigate higher mode effects. His research informed the New Zealand design guide for CRSBFs [11], which suggested ductility factors of four for load-bearing systems and six for non-load-bearing systems.

Zarnani and Quenneville [12] introduced a new generation of friction damper, the Resilient Slip Friction Joint (RFSJ), combining restoring force and energy dissipation. Initially applied in rocking timber walls [13], it was later used in tension-only braces [14] and practical projects like the Nelson airport terminal in New Zealand. Darani et al. [15] extended this concept to rocking concrete shear walls with RSFJ hold-downs. Sahami et al. [16] introduced rocking walls with self-centring shear keys (rotational-RSFJs), reducing the likelihood of high-stress zones in single and coupled shear walls and mitigating higher mode effects. This study extends this idea to a braced frame rocking system, comparing the results with another isolation concept, the lead rubber bearing (LRB) isolation.

4.3. Resilient Slip Friction Joint (RSFJ)

In RSFJ restoring force comes from a specific steel grooved plates which are tied through high strength bolts and disk springs. By slipping of grooved plates, the input energy is dissipated through frictional resistance. Based on the free-body diagrams presented in Figure 4-1, the design procedure is developed for the prediction of the performance of the RSF joint [13]. The slip force (F_{slip}) and residual force (F_{res}) are determined by the following equations:

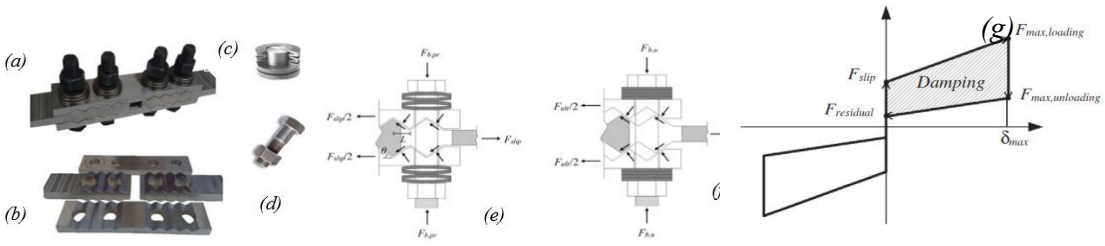

Figure 4-1: a) Assembly of the RSF Joint; b) Cap plates and slotted centre plates; c) Disk springs; d) High strength bolts; e) Free body diagrams RSF join on the brink of slippage; f) at ultimate defection; g) The general hysteresis behaviour of RSFD [13]

$$F_{RSFJ,slip} = 2n_b F_{b,pr}\left(\frac{\sin\theta + \mu_s \cos\theta}{\cos\theta - \mu_s \sin\theta}\right) \qquad \text{Equation 4-1}$$

$$F_{RSFJ,res} = 2n_b F_{b,pr}\left(\frac{\sin\theta - \mu_k \cos\theta}{\cos\theta + \mu_k \sin\theta}\right) \quad \text{Equation 4-2}$$

Where n_b is the number of bolts on each splice, θ is groove angle, $F_{b,pr}$ is clamping force of prestressing and the μ_s and μ_k are the static and kinetic coefficient of friction respectively, while considered $\mu_k = .85\mu_s$ [13].

The general hysteresis behaviour of RSFJ is illustrated in Figure 4-1(g). $F_{ult,loading}$ and $F_{ult,unloading}$ are the system forces at the maximum disk springs displacement and bolts force.

$$F_{b,u} = F_{b,pr} + K_s\Delta_s \quad \text{Equation 4-3}$$

4.4. Structural Isolation, Effective Approach to Decrease Seismic Transmitted Force

Unlike responses to gravity loads, structural responses to seismic actions are dependent on the dynamic specifications of a structure. Strengthening structures often involves stiffening them, which consequently leads to a higher level of earthquake energy absorption. This creates a cycle where structural strength must ultimately overcome the induced forces. The more a structure is in harmony with seismic movements, the fewer internal interactions and reactions it experiences. This principle underlies the development of isolation systems, which are now considered one of the most effective approaches, especially for acceleration-sensitive structures like hospitals and telecommunication centers. Base isolation systems achieve this by using sliding motion to shift the fundamental period to a higher level, thereby reducing the force level. Another approach following this concept is rocking systems, where the rocking motion allows the structure to harmonize with seismic excitation through rotational movement, leading to lower energy absorption. This mechanism has been identified as a key factor in preserving many ancient structures that lack a rigid base and are free to slide and rock on the ground.

All rocking systems require a hold-down mechanism in conjunction with an energy dissipating mechanism to achieve the desired level of seismic performance. Conventional rocking systems typically employ post-tensioning (PT) tendons with some form of sacrificial element for dissipating input energy. However, challenges such as the complexity of implementing unbonded post-tensioning, particularly in tall structures, and

the loss of tension in strands have always been concerns for engineers. Moreover, systems with yielding mechanisms are vulnerable to severe aftershocks, necessitating specific inspections and maintenance post-event. The Resilient Slip Friction Joint (RSFJ) addresses these issues by being used with boundary columns to provide both sufficient restoring force and damping mechanisms simultaneously, thereby eliminating the need for regular inspections and post-event maintenance.

4.4.1. Single Rocking Braced Frame

The proposed configuration for a single rocking frame with RSFJs is shown in Figure 4-2. Braced frame and columns in this configuration are attached to the floor and bracket beams are used to connect shear links to frame and end columns. The rocking moment can be found by taking the moment about the rocking base:

$$M_{rock} = M_{weight} + M_{damper} = W\frac{l}{2} + n_d\left[F_{DL_i}(l+d) + F_{DR_i}(d)\right] \qquad \text{Equation 4-4}$$

where n_d is the number of dampers in each side of the columns and F_{DL_i}, F_{DR_i} are the dampers force in the left and right sides of the rocking toe. Assuming that the bracket beams, columns are all rigid compared to RSFJs, the deflection in dampers in the right side (δ_{DR}) and left side (δ_{LR}) of the frame is determined.

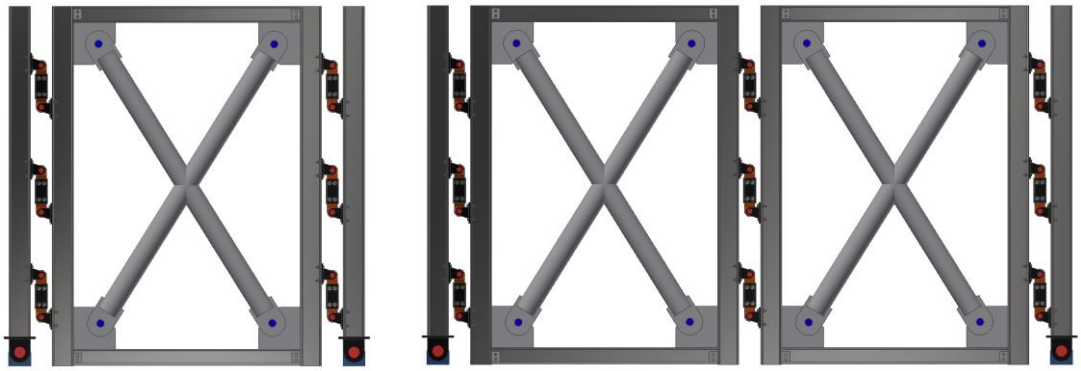

Figure 4-2: Schematic of single and coupled braced frame

$$\delta_{DR} = (L+d)\sin(\theta) \qquad \text{Equation 4-5}$$

$$\delta_{DL} = d\sin(\theta) \qquad \text{Equation 4-6}$$

While d is the gap between the frame and boundary columns, L is the width of the frame and θ rotating angle. The general hysteretic response of the system is shown in Fig. 3. Before the slipping point ($M \leq M_{slip}$), stiffness of each link connected to other elements can be determined by:

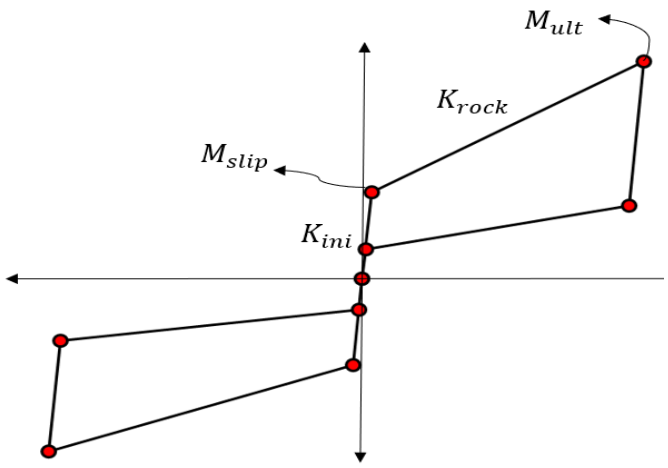

Figure 4-3: General hysteretic performance of rocking system equipped with RSFJs

$$k_{ini} = \left(\frac{1}{k_{col,axial}} + \frac{1}{k_{bb,bending}} + \frac{1}{k_{frame,axail}} + \frac{1}{k_{RSFJ,initial}}\right)^{-1} \quad \text{Equation 4-7}$$

$k_{col,axial}$: axial stiffness of column

$k_{bb,bending}$: bending stiffness of bracket beam ($\frac{b_{bb}h_{bb}^3}{12}$)

$k_{frame,axial}$: axial stiffness of column in the frame

While b_{bb}, h_{bb} are thickness and height of bracket beam. After slipping point, as the stiffness of RSFJs decreases considerably ($k_{rock} \ll k_{ini}$), the stiffness of the links is significantly smaller in comparison to other elements so that rocking stiffness could be directly derived by:

$$k_{rock} = n_d k_{d,ini}\left[(L+d)^2 + (d)^2\right] \quad \text{Equation 4-8}$$

4.4.2. Coupled Rocking Braced Frame

In the coupled braced frames system, it's possible to remove the boundary element in the middle, allowing the frames to be directly connected by shear links. Similar to the single braced frame setup, all columns and frames experience the same horizontal displacement since they are anchored to the floor. This configuration ensures that coupled braced frames follow the same behavioural pattern as single braced frames. Consequently, the calculations for the rocking base moment and rocking stiffness in coupled braced frames are as follows:

$$M_{rock} = M_{weight} + M_{damper} = Wl + n_d \left[n_w F_{DL_i} (l+d) + F_{DR_i} (d) \right]$$ Equation 4-9

$$k_{rock} = n_d k_{d,ini} \left[n_w (L+d)^2 + (d)^2 \right]$$ Equation 4-10

n_w is the number of coupled frames. Comparing coupled braced frames capacity with two single frames all identical in length - if architectural requirements provide enough space for coupled frames - the same capacity could be achieved while the middle column and a row of the shear link according to the number of coupled frames have been eliminated.

4.5. Case Study of a Seven-Story Office Building

The primary goal of this study, besides introducing a new mechanism for rocking systems, is to estimate the performance of a rocking braced frame in comparison to both a conventional braced frame and a base isolation system, the latter being a well-established and efficient structural solution. The first step involved designing a seven-story special braced frame building in accordance with ASCE/SEI 7-16 standards. Subsequently, the building was equipped with an LRB isolation system to achieve the desired fundamental period. Based on the performance outcomes of the LRB system, both the rocking system and the shear keys were then designed and adjusted accordingly.

4.5.1. 4.1 Braced Frame System

A seven-story office building with overall height 24.5 meters (3.5-meter height for each story) with plan dimension of 42 m by 42 m, as shown in Figure 4-4 and six bays of braced frame in external perimeter in each direction have been considered.

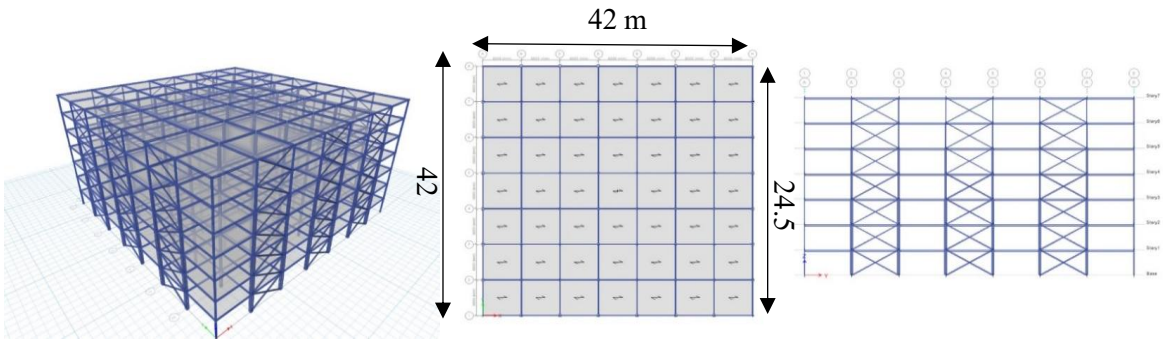

Figure 4-4: prototype office building

The assumed seismic factors for steel special concentrically braced frames are summarized in Figure 4-5.

Seismic Coefficient	Value
I_e (Importance Factor)	1.25
R (Response Modification Factor)	6
C_d (Deflection Amplification Factor)	5
Ω_0 (Overstrength Factor)	2

S_s	1.6 g	S_{MS}	1.92	S_{DS}	1.28	F_v	1.5
S_1	0.5 g	S_{M1}	0.75	S_{D1}	0.5	F_a	1.2

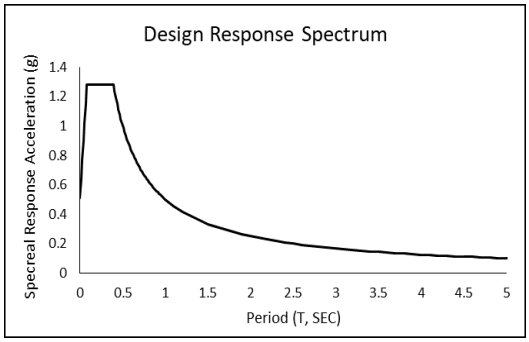

Figure 4-5: Seismic coefficient and response spectrum curve

Considering the superimposed dead load and live load of 500 and 400 $^{kg}/_{m^2}$ the base shear calculated by the following equations:

$$V = C_s.m.g \rightarrow C_s = \frac{S_{DS}}{\left(\frac{R}{I_e}\right)}$$ Equation 4-11

$$S_{M1} = F_v\, S_1 \ , \ S_{MS} = F_a\, S_s$$ Equation 4-12

$$S_{D1} = {}^{2}/_{3}\, S_{M1} \ , \ S_{DS} = {}^{2}/_{3}\ S_{MS}$$ Equation 4-13

The first mode period, as determined by the numerical model for both directions, is equal to 0.9 seconds. To meet the code's strength and drift limitations for the first four stories, pipes with dimensions 200X12 were chosen, and for the next three stories, pipes measuring 150X12 were selected. Based on the coefficient method, the target displacement for the push-over analysis was derived.

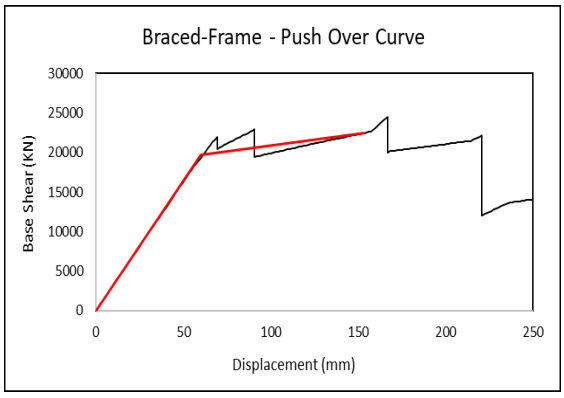

Target Displacement (mm)	153
Base Shear (KN)	22440
C0	1.21
C1	1
C2	1
Sa, g	0.9
Ti	0.74
Dy(mm)	60
Vy(KN)	1974

Figure 4-6: Push-over result of special braced frame

When the structure is pushed to its target displacement, the performance of the braces under compression and tension is depicted in Figure 4-7. It is observed that almost all braces in compression within the first three stories reach their ultimate capacity at a displacement of 150 mm.

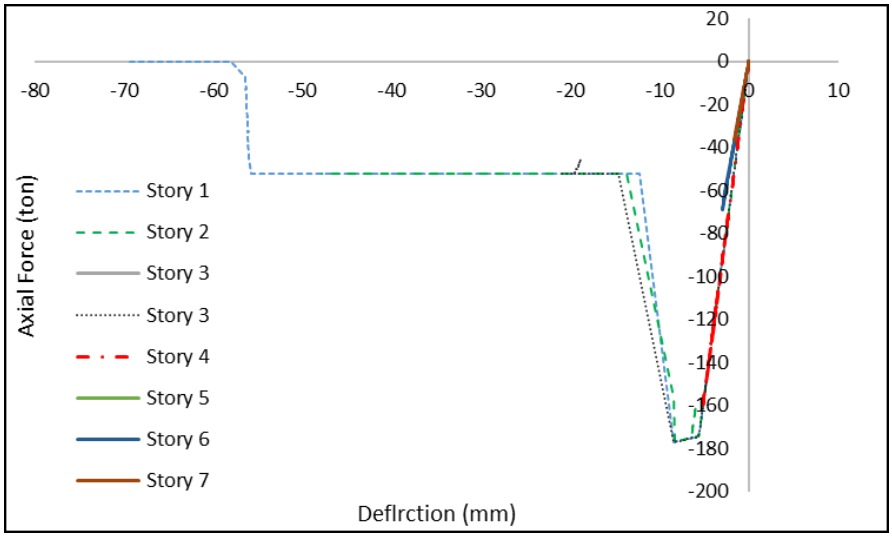

Figure 4-7: Hinge responses of braces (axial force)

4.5.2. LRB Isolation System

The design of the LRB joints for the prototype building has been done based on chapter 17 of ASCE/SEI 7-16. For the first step, a target period and desire damping are considered to be 2.75 and 15% respectively. The total number of columns is 64, and the LRB specifications should be designed to reach those values. First, the effective stiffness is determined as below:

$$K_{Dmin} = \frac{4\pi^2}{g} \times \frac{W}{T_D{}^2} = 41507 \text{ KN} \qquad \text{Equation 4-14}$$

$$K_{Dmax} = 1.3\, K_{Dmin} = 53960 \text{ KN} \qquad \text{Equation 4-15}$$

Then maximum and design displacement calculated as:

$$\beta = 15\% \rightarrow B = 1.35$$

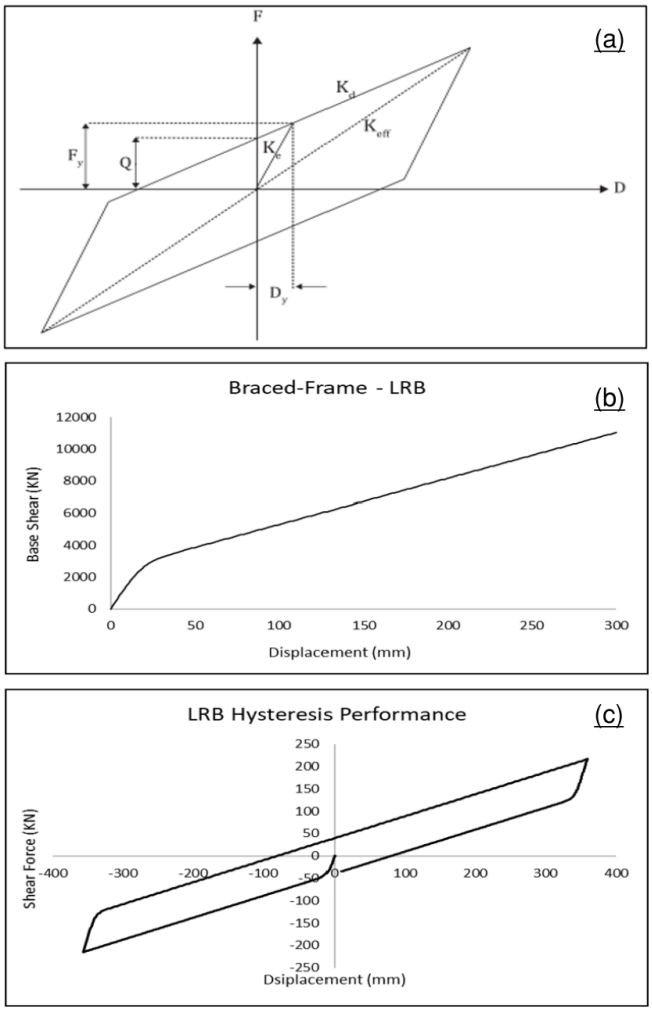

Figure 4-8: (a) LRB general hysteresis performance [17];

(b) Push over curve of LRB system;

(c) Hysteresis curve of defined LRB

$$D_D = \frac{g}{4\pi^2} \times \frac{S_{D1} T_D}{B_D} = 253 \text{ mm} \qquad \text{Equation 4-16}$$

$$D_M = \frac{g}{4\pi^2} \times \frac{S_{M1} T_M}{B_M} = 379 \text{ mm} \qquad \text{Equation 4-17}$$

Then the shear force for isolation unites, isolated structure and structure below are achieved:

$$V_b = K_{Dmax} D_D = 13650 \text{ KN} \qquad \text{Equation 4-18}$$

$$V_{MCE} = K_{Dmax} D_M = 20490 \text{ KN} \qquad \text{Equation 4-19}$$

$$V_s = \frac{V_b}{R_I}, 1 < \frac{3}{8R_I} < 2 \rightarrow V_s = 6830 \text{ KN} \qquad \text{Equation 4-20}$$

Then LRB details including K_e, K_d and F_y calculated as 4918 KN.m, 492 8 KN.m and 44.1 KN respectively.

4.5.3. Rocking Braced Frame Equipped with RSFJs

The primary objective of this study was to investigate the seismic behaviour of rocking braced frames equipped with RSFJs and to compare these with two isolation concepts. Given that base isolation is renowned as an efficient structural system for low and mid-rise buildings, it serves as an appropriate benchmark for comparison. To design the rocking braced frame, we utilized the force demand from the push-over analysis of the LRB system to design the RSF joints, ensuring compliance with code limitations on strength and drift. The details of the RSF joints were determined based on the overturning moment obtained from the push-over analysis of the structure with LRB joints, as per Equation (4), and are presented in Table 4.1.

Table 4-1: RSFD details calculation and specifications

L (m)	6
D (m)	0.4
F_{DL}	$0.3F_{DR}$
n_w	1
n_d	21
$M_{rocking}$ (KN. m)	227
F_{total} (KN)	3482
F_{damper} (KN)	165
Deflection (mm)	90

Slipping Force (KN)	45
Ultimate Force (KN)	180
Residual Force (KN)	48
Maximum Displacement (mm)	100

As observed, the hysteresis performances of the two isolation approaches have been closely aligned. However, the performance of the rocking system is expected to be influenced by higher mode effects, which are not a significant concern in the base isolation system. Therefore, a realistic assessment of seismic performance requires Nonlinear Time History (NTH) analysis.

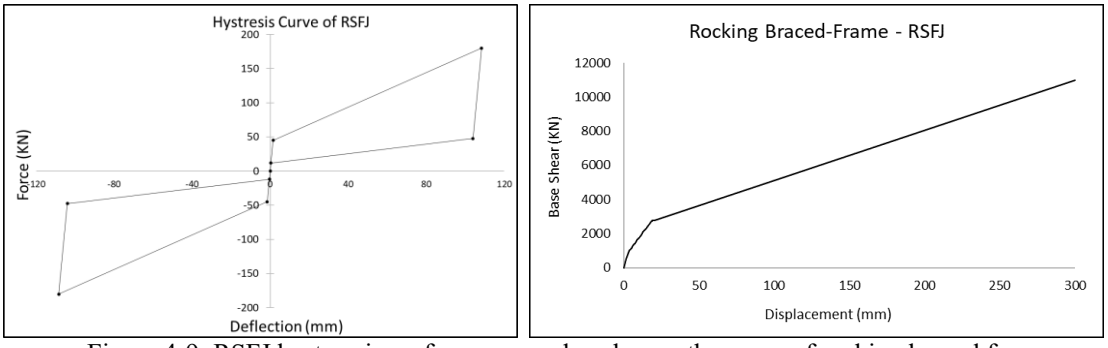

Figure 4-9: RSFJ hysteresis performance and push over the curve of rocking braced frame

Concerning brace performance, it was previously noted that the diagonal braces in the first three stories experienced buckling. However, in both isolation concepts, none of the braces reached the buckling or yielding phase, indicating a distinct difference in structural response under seismic conditions.

4.6. NTHA of The Three Structural Systems

For the nonlinear dynamic time-history analyses, a suite of seven ground motions was scaled to match the ASCE/SEI 7-16 spectrum, considering $S_1 = 0.5$, $S_s = 1.6$, Soil type C and $I_e = 1.25$. The analytical model was developed using CSI ETABS software.

Earthquake ground motion	PGA
El Centro (1951)	0.3
Landers (1992)	0.74
Northridge (1994)	0.61
Kobe (1995)	0.35
Chi-Chi (1999)	0.36
Bam (2003)	0.16
Christchurch (2011)	0.1

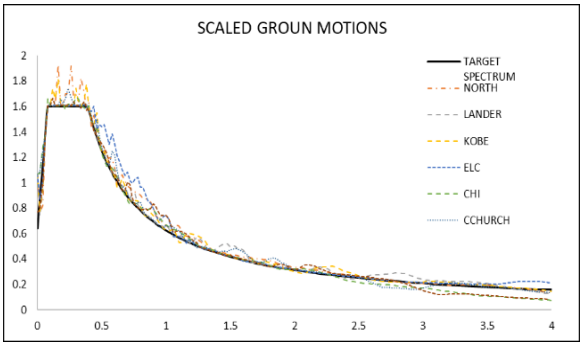

Figure 4-10: The selected ground motions and scale factor

As illustrated in Figure 4-11, the structure exhibits no residual displacement, due to the self-centring feature of the RSFJs, which are capable of returning the structure to its initial position. Consequently, there is typically no permanent structural damage as long as the RSF joints are appropriately designed for the seismic force level. For this structure, the drift limit was considered to be 2%, a threshold not exceeded by any of the records.

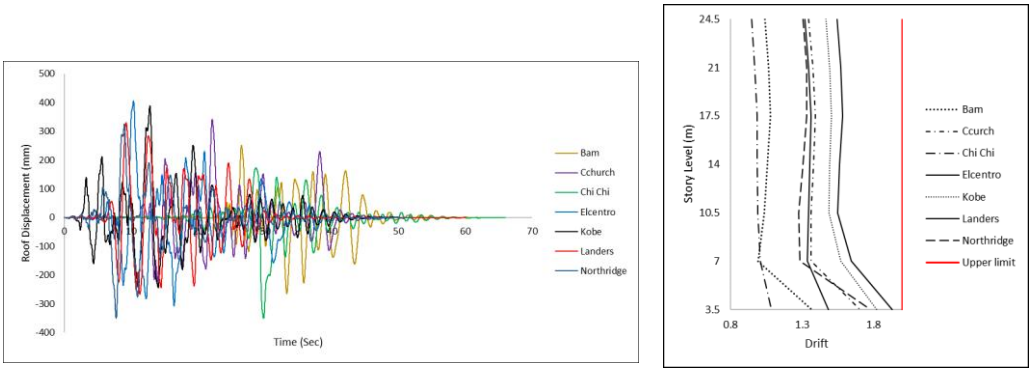

Figure 4-11: Roof time history displacement and inter-story drift subjected to selected ground motion

Comparing the results of the three designed systems, the base shear in the LRB isolation system averages 33% of that in the special braced frame. For the rocking frame, this figure is around 55% (see Figure 4-12). The differences between base isolation systems and rocking frames are attributed to the nature of their movement. While the base isolation

method allows the structure to slide, rocking is about rotation, with the overturning moment being a key design parameter. In the proposed rocking mechanism, the resisting force is distributed along the height of the structure. This distribution means that while the base shear is higher, its effective height is lower, resulting in an overturning moment that is lower compared to the base isolation system. On average, the overturning moment for base isolation and rocking frames are 23% and 18%, respectively, of that in the braced frame (as depicted in Figure 4-12).

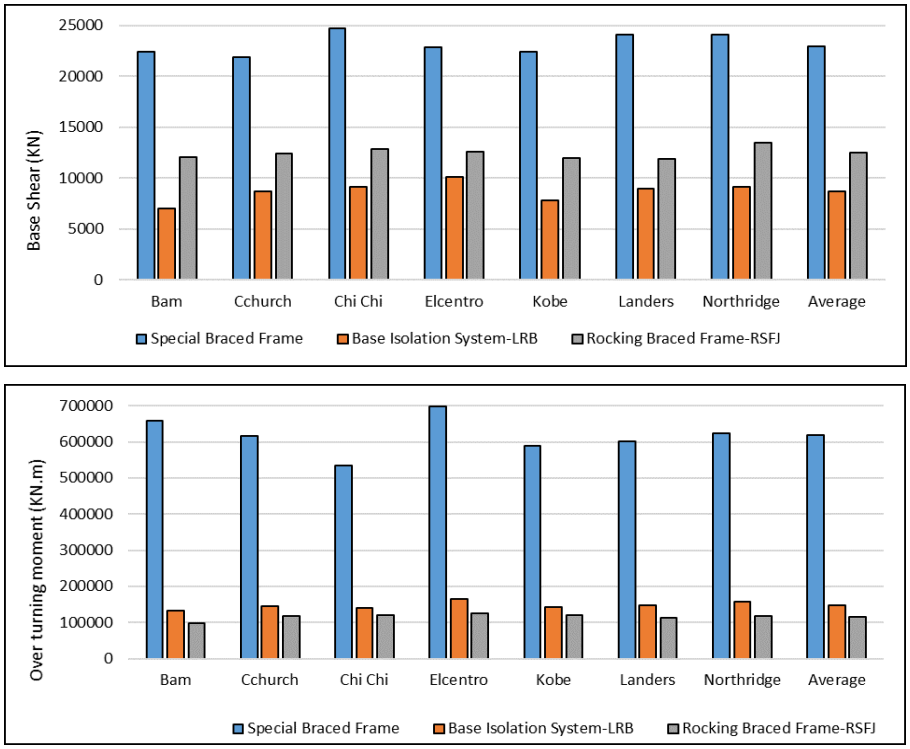

Figure 4-12: Base shear and an overturning moment of the three structural system

4.7. The Effect of Multiple Rocking Spots

An effective approach to enhancing the performance of rocking systems involves considering different levels for rocking motion. Unlike base isolation systems, where higher mode contributions are less critical, they are essential in rocking systems. In this study, various levels of rocking were defined to compare the results. By allowing rotation at all stories, the base shear is reduced by approximately 24%, which represents the lower rate of reduction. Based on the first three modes, where the structure tends to bend, allowing the structure to rotate at these points could decrease the bending demand. Specifically, focusing on the second and fourth floors, which correspond to the second

and third mode shapes, offers an optimal placement for rocking joints. These spots are strategically chosen as they are closest to the minimum amount across all levels.

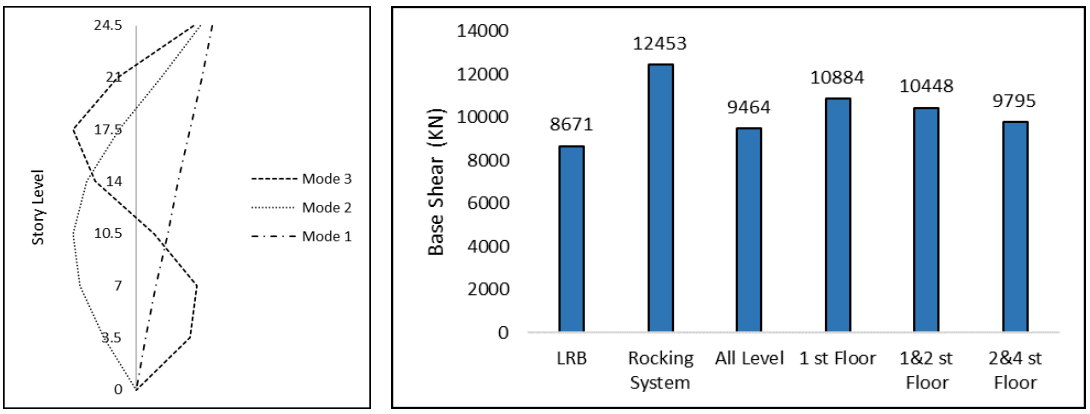

Figure 4-13: Modal shaped and base shear results for multiple isolation levels

4.8. Summary and Conclusion

In this chapter of thesis, we introduce a novel approach for rocking braced frames. This proposed configuration relies on RSFJs as shear keys, connecting the braced frame to boundary columns. Unlike conventional rocking systems that derive the required restoring force from post-tension technology and add damping through yielding dampers, this study employs RSFJs to integrate all these features. Distributed along the frame, this system presents an alternative to conventional methods, reducing design complexity and implementation challenges, and is particularly advantageous for taller rocking systems. Applicable for single, coupled, or core braced frames, as well as concrete shear or timber walls, this system allows for multiple rocking levels in different stories, effectively attenuating the impact of higher modes.

To evaluate the performance of this proposed system, and in comparison with conventional braced frames and LRB base isolation systems, we investigated the seismic behaviour of a seven-story office building. The results indicate that the rocking system equipped with RSFJ technology significantly improves the dynamic performance of the structure. According to Nonlinear Time History Analysis (NTHA) of seven ground motions, compared to the conventional braced frame, the LRB isolation and rocking system led to reductions in base shear by 67% and 45%, respectively. Considering the overturning moment, these reductions are approximately 18% and 23%, which are crucial factors in the design of rocking braced frames. The proposed mechanism is fully self-centring and satisfies inter-story drift limitations. It offers considerable advantages in

construction simplicity, especially for taller structures, due to its potential for multiple rocking levels. Further experimental testing is planned to validate this concept.

The earthquake ground motions adopted in this study were selected to capture variability in seismic demand. Consequently, the conclusions are dependent on the specific set of records analysed and may vary if alternative ground motions, source regions, or scaling approaches are employed. This dependency is inherent to nonlinear time-history analysis in general, and careful consideration should therefore be given to the representativeness of the selected seismic inputs with respect to the site and regional seismic conditions.

4.9. Acknowledgements

The authors extend their gratitude to the Ministry of Business, Innovation, and Employment of New Zealand (MBIE) for financially supporting this research project.

4.10. References

1. Makris, Nicos, and Michalis F. Vassiliou. (2015). "Dynamics of the Rocking Frame with Vertical Restrainers." Journal of Structural Engineering, 141.10: 04014245.
2. Muto, K., U. H., & Sonobe, T. (1960). "Study of the Overturning Vibration of Slender Structures." Proceedings of the 2nd World Conference on Earthquake Engineering, Tokyo and Kyoto, Japan.
3. Housner, G. W. (1963). "The Behaviour of Inverted Pendulum Structures During Earthquakes." Bulletin of the Seismological Society of America 53(2): 403-417.
4. Clough, Ray W., & Huckelbridge, Arthur A. (1977). Preliminary Experimental Study of Seismic Uplift of a Steel Frame. Earthquake Engineering Research Center, College of Engineering, University of California.
5. Kelley, James M. (1977). "Earthquake Simulation Testing of a Stepping Frame with Energy-Absorbing Devices." Report No. EERC 77-17.
6. Midorikawa, M., Takeuchi, T., Hikino, T., Kasai, K., Deierlein, G., Ohbayashi, M., Yamazaki, R., & Kishiki, S. (2010). "Seismic Performance of Controlled Rocking Frames with Shear Fuse and PT Wire Anchorage - Shaking Table Tests on Controlled Rocking Steel Frames Using Multipurpose Inertial Mass System: Part I." Journal of Structural and Construction Engineering, 75(654): 1547-56.

7. Roke, D., et al. (2006). "Self-Centring Seismic-Resistant Steel Concentrically Braced Frames." Proceedings of the 8th US National Conference on Earthquake Engineering, EERI, San Francisco, April.
8. Eatherton, M., et al. (2008). "The Controlled Rocking of Steel-Framed Buildings with Replaceable Energy-Dissipating Fuses." Proceedings of the 14th World Conference on Earthquake Engineering.
9. Eatherton, M. R. (2010). "Large-Scale Cyclic and Hybrid Simulation Testing and Development of a Controlled-Rocking Steel Building System with Replaceable Fuses." University of Illinois at Urbana-Champaign.
10. Wiebe, Lydell Deighton Andree. (2013). Design of Controlled Rocking Steel Frames to Limit Higher Mode Effects. Toronto: University of Toronto.
11. Wiebe, L. D. A. (2015). "Design and Construction of Controlled Rocking Steel Braced Frames in New Zealand." Improving the Seismic Performance of Existing Buildings and Other Structures in 2015. pp. 810-821.
12. Zarnani, Pouyan, & Quenneville, Pierre. (2015). "A Resilient Slip Friction Joint." Patent No. WO2016185432A1, NZ IP Office.
13. Hashemi, A., Darani, F. D., Yousef-Beik, S., Abadi, H., Zarmani, P., & Quenneville, P. (2018). "Recent Developments of the Resilient Slip Friction Joint (RSFJ) Technology for Seismic Proofing New and Existing Buildings."
14. Bagheri, H., Hashemi, A., Quenneville, P., Yousef-beik, S.M.M., & Zarnani, P. (2018). "An Experimental Test of a New Self-Centring Tension-Only Brace Using the Resilient Slip Friction Joint." New Zealand Society for Earthquake Engineering (NZSEE) Conference.
15. Darani, F. M., Zarnani, P., Haemmerle, E., Hashemi, A., & Quenneville, P. (2018). "Application of New Resilient Slip Friction Joint for Seismic Damage Avoidance Design of Rocking Concrete Shear Walls." New Zealand Society for Earthquake Engineering (NZSEE) Conference.
16. Sahami, K., Veismoradi, S., Zarnani, P., & Quenneville, P. (2019). "Seismic Performance of Rocking Concrete Shear Walls with Innovative Rotational Resilient Slip Friction Joints." New Zealand Society for Earthquake Engineering (NZSEE) Conference.
17. American Society of Civil Engineers. (2017). Minimum Design Loads for Buildings and Other Structures, Standard ASCE/SEI 7-16. American Society of Civil Engineering.

Chapter 5: Experimental Verification of the proposed new rocking wall: Design, Testing, and Analysis

To complement these studies, an experimental test was scheduled to further demonstrate and validate the proposed concept. This experimental phase was essential for verifying the theoretical and computational results, confirming the feasibility of the concept.

To achieve this, considering the practical limitations of the AUT Structures lab, a single panel wall was designed to resist approximately 100kN of lateral load, with a maximum drift of 2.5% as advised by New Zealand building codes as upper displacement level for buildings. Based on the derived equations from the analytical studies explained in Chapter 3, the Resilient Slip Friction (RSF) joints with capacity of 60 kN and 60 mm of displacement were designed to support the rocking wall as shear links coupled with the adjacent columns. These joints were initially component tested to validate the desired performance achieved by calculation. At the system level, the experimental program was designed to be conducted in three phases:

Phase One: The rocking wall system underwent a cyclic loading regime in the in-plane direction of the wall to simulate real repetitive seismic shaking with increasing intensity. This approach aimed to assess the overall performance of the system as the main lateral load resisting system and validate the assumed behaviour of incorporated components.

Phase Two: This phase involved out-of-plane shaking of the setup, assuming a perpendicular arrangement of the system to the seismic shake. The deflection compatibility of the system was investigated under the assumption that columns and walls were tied together.

Phase Three: The final phase focused on capturing the failure mode of the system beyond the design level, which is explored further in the subsequent section. A secondary fuse mechanism was incorporated into the RSFJ devices to activate during beyond-design-level shaking events, providing additional damping and functioning as a fuse to enable ductile failure. The setup was pushed to the ultimate actuator stroke, which was 3 times the RSFJs elastic deflection.

5.1. Test Setup: Single Rocking Wall with Links to Adjacent Columns

The dimensions of the wall for the experimental setup were determined based on a realistic case study as well as the spatial constraints and facilities available at the AUT laboratory.

The dimensions of the wall were considered as:

- Height: 3500 mm
- Length: 1500 mm
- Thickness: 250 mm

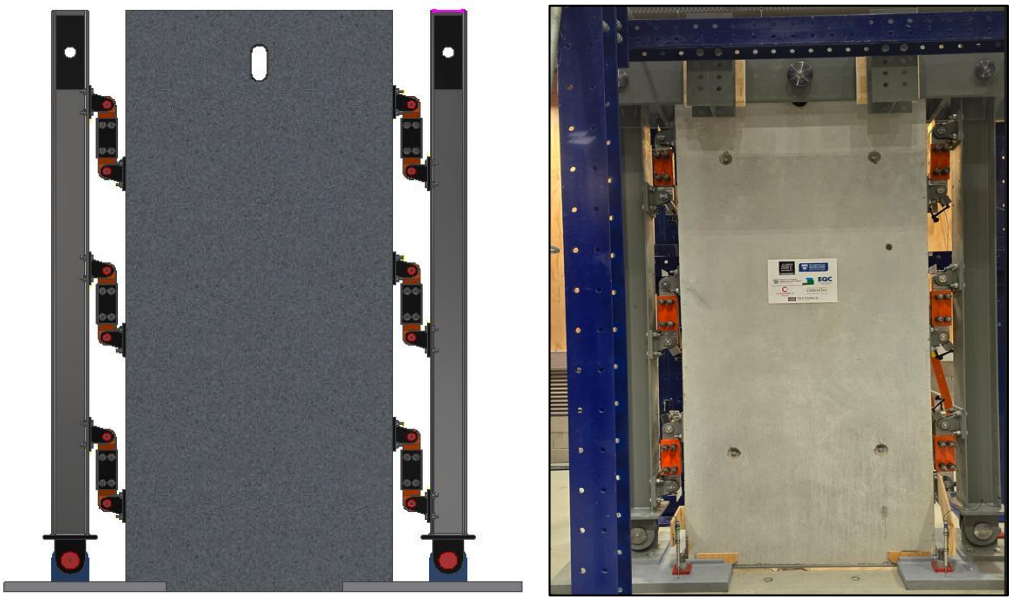

Figure 5-1: Schematic view of the test setup

The incorporated actuator was characterized by a maximum force capacity of 250 KN and a stroke of ±125 mm. The configuration for the experimental setup is outlined in Figure 5-1 and 5-2. This configuration had been designed to mimic real-world conditions, ensuring that the results are as relevant and applicable as possible.

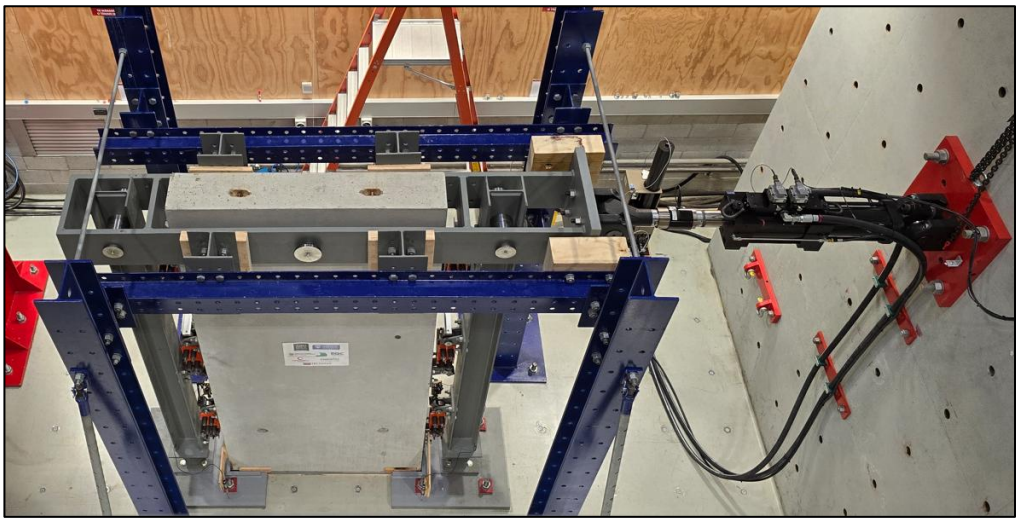

Figure 5-2: Top view of assembled test setup

In the proposed structural concept, a total of six Resilient Slip Friction Joints (RSFJs) were utilized as shear link elements. These joints were mounted on both sides of the wall to optimize their effectiveness (Figure 5-4). Additionally, steel columns were integrated into the design to function as boundary elements (Figure 5-3), providing structural support and stability. The column base connection and the RSFJs end connections to the wall and column were designed as pins, allowing them to rotate freely in response to the wall movement. The connection of the RSFJs to the concrete wall was achieved by drilling holes and epoxying bars into the panel wall.

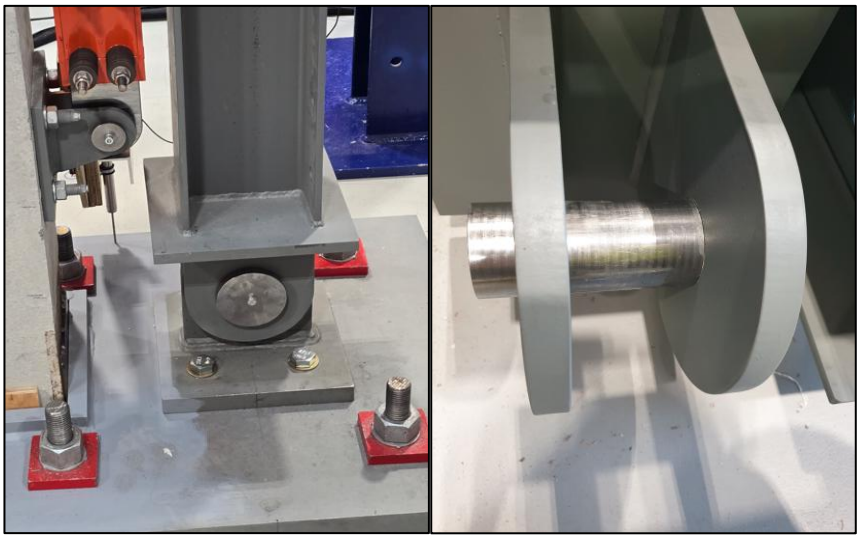

Figure 5-3: Column base pin connection

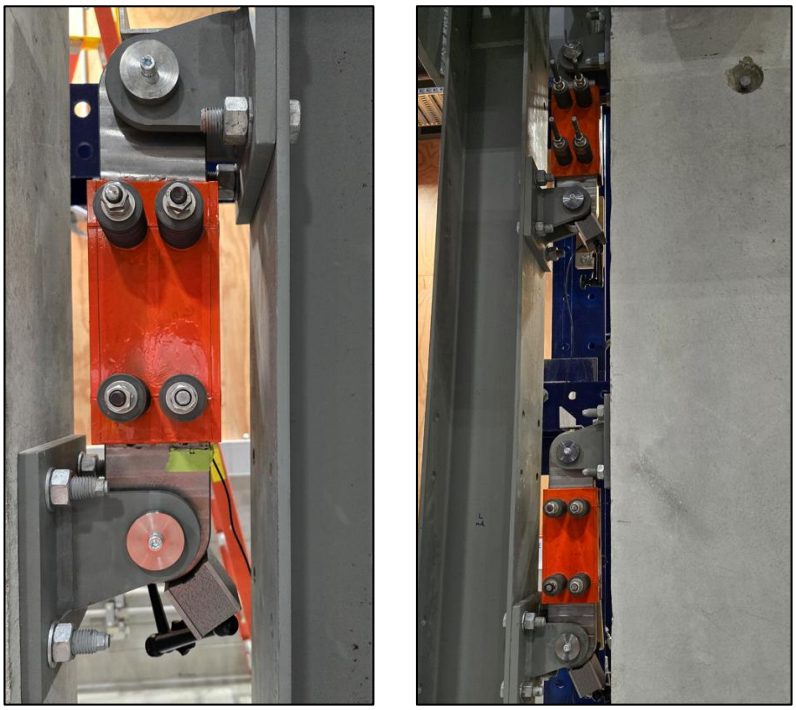

Figure 5-4: RSFJs with pin connections on both ends

A loading beam was designed to link the actuator to the columns and wall, which were assumed to be pulled together, mirroring real-case scenarios where both the wall and column are tied through the diaphragm system (Figure 5-5). This beam was not only connected to the wall and adjacent columns via pin connections to allow for coordinated displacement but also was served to transmit the force from the actuator to the system. This design ensured the displacement compatibility and permitted free lateral movement. It is worth mentioning that the application of this concept extends beyond concrete shear walls and is adaptable to braced frames and timber walls as well.

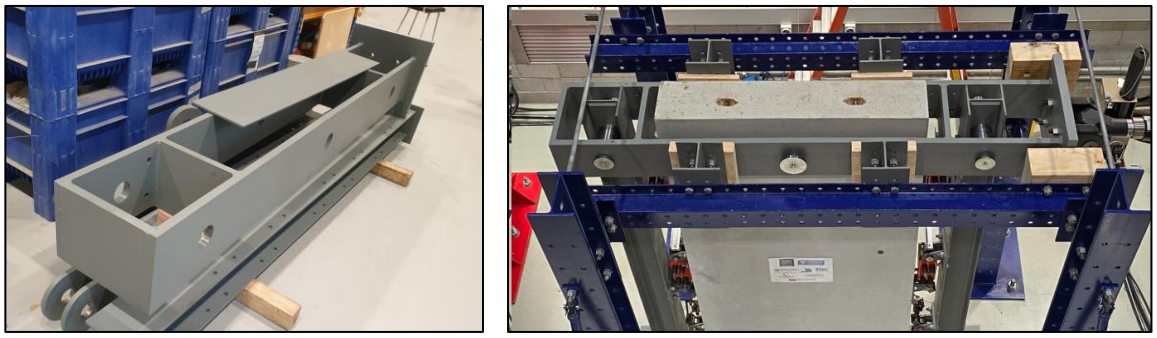

Figure 5-5: Loading beam designed to pull-push the wall and adjacent columns with pin connections

The design of the RSFJs was determined by the desired performance as per the structural analysis. The design process is expressed through the following calculations:

$$\delta_D = (L + d)\sin(\theta)$$

$$\Delta_{actuator} = 90\ mm \rightarrow \frac{90}{3500} = 0.025 \rightarrow \delta_D = (1500 + 300) \times 0.025 = \sim 45\ \text{mm}$$

$$F_{actuator} = 100\ KN \rightarrow M = 100 \times 3.5 = 350 KN.m = M_{rock}$$

$$M_{rock} = W\frac{l}{2} + n_d\left[F_{DL_i}(l + d) + F_{DR_i}(d)\right] = 40\ (^{1.5}/_{2}) + 3\ (\ F_{DL_i} \times 1.8 + 0.4\ F_{DL_i} \times 0.3) = 30 + 5.76F_{DL_i} \rightarrow F_{DL_i} \cong 55kN$$

Considering a slipping force of 20 kN, the RSFJs were designed based on the following specifications:

Table 5-1: Design Parameter and numerical parameter of RSFJs

Slipping Force (KN)	20
Ultimate Force (KN)	55
Ultimate Force Unloading (KN)	5
Maximum Displacement (mm)	50

5.2. Evaluating the Hysteresis Loop

To evaluate the hysteresis behaviour of the wall, a push-over analysis was conducted for a single cycle, capturing both the complete compression and expansion phases of the joints. This approach illustrated the hysteresis loop for one cycle, providing insights into how the wall system behaves under both compressive and tensile forces (Figure 5-6 and 5-7). The model presented incorporated pin connections, and the top nodes of the wall and column were assumed to be laterally tied together. The RSFJ link elements were tuned according to the assumed flag shape. The model was pushed on either side up to 100 mm based on this configuration.

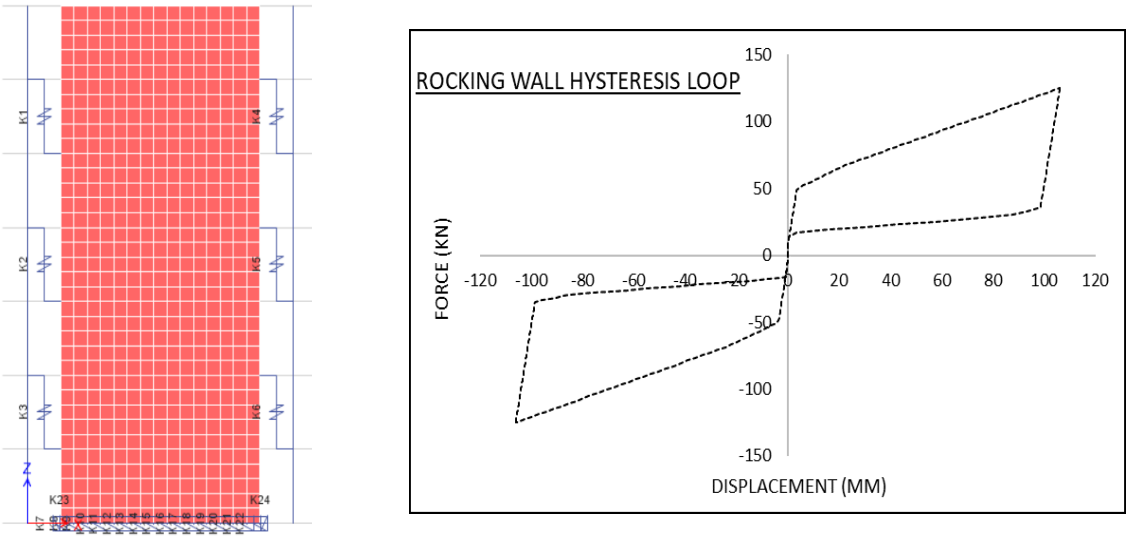

Figure 5-6: Test setup Etabs model (left); Hysteresis response of pushover analysis (right)

The corresponding response for each damper device is evaluated as below:

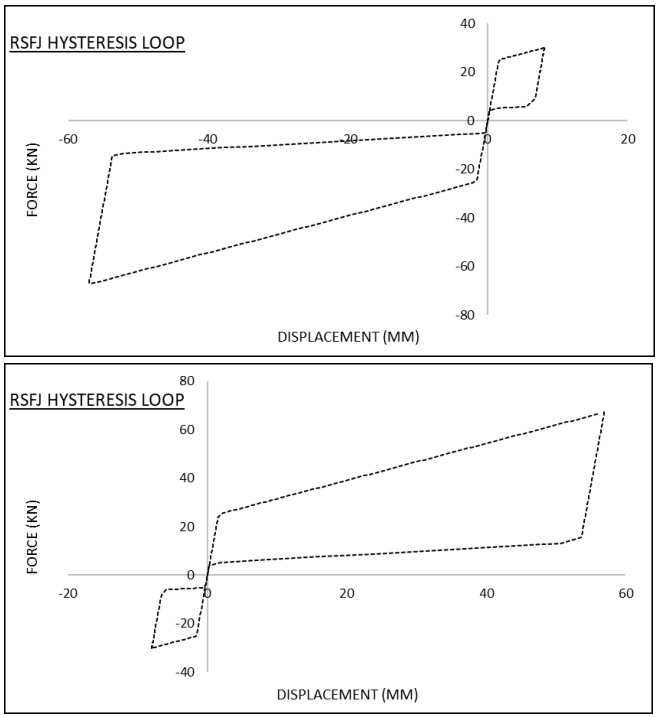

Figure 5-7: Hysteresis loop of each RSFJs in both sides of the wall

5.3. RSFJs Component Testing

In this research, the Resilient Slip Friction Joints (RSFJs) were subjected to an assembly and tuning process, tailored to align with the exact design specifications established at the outset (Figure 5-8). This calibration phase was instrumental in ensuring that each joint conformed to the anticipated design parameters. Following the assembly, the RSFJs were put through pull-push tests, validating the calibration process.

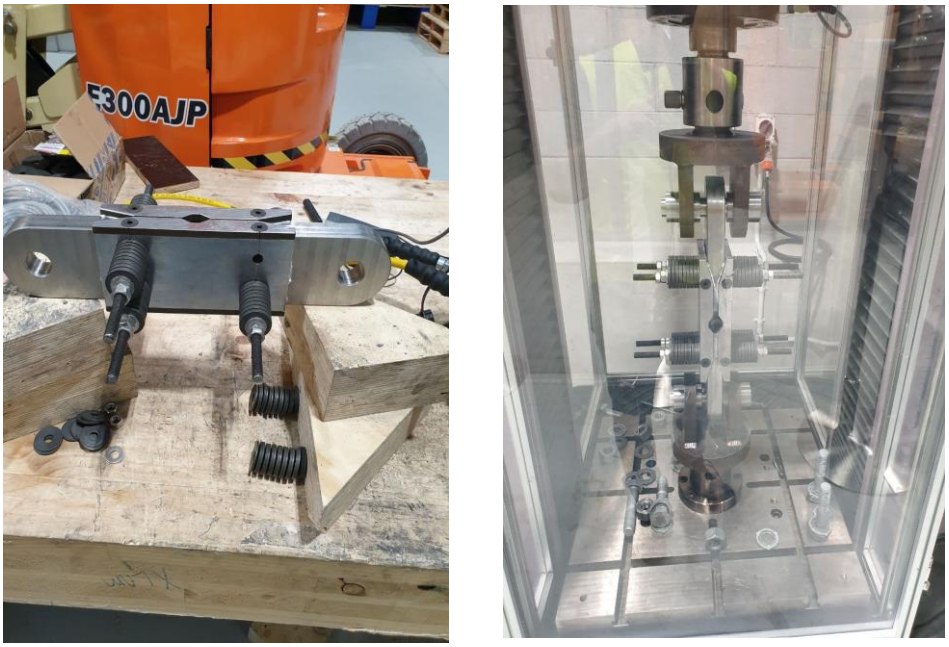

Figure 5-8: Assembling and testing of RSFJ units.

The outcomes of the experimental analysis conducted on six distinct RSFJ units are presented in the following graph. The aim was to align their responses closely, so that under comparable conditions, each unit would demonstrate a performance that was nearly identical with others. Based on the graphs provided, the RSFJs were pushed to nearly 50mm in both extension and compression (Figure 5-9). Extending beyond 55mm appears to bring the system into its ultimate elastic range, initiating a secondary phase characterized by nonlinear behaviour governed by the rods deflection. Once this phase begins, it will impact subsequent cycles, as the rod elongation is assumed to be irreversible

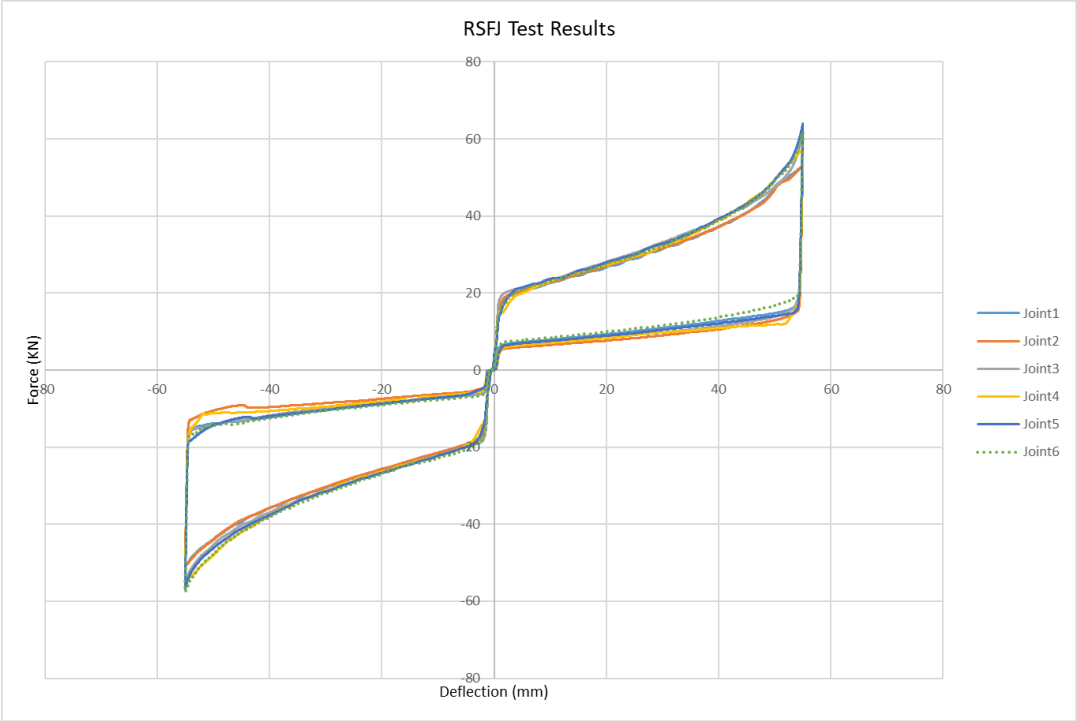

Figure 5-9: Result of six RSFJ units tuned to the design specs

The secondary phase was assumed to follow the non-linear path similar to what tested previously (Figure 5-10) as per Hashemi et al. (2019). The maximum displacement was expected to be 50% greater than the ultimate elastic displacement, while it correlates with a 25% increase in the ultimate force.

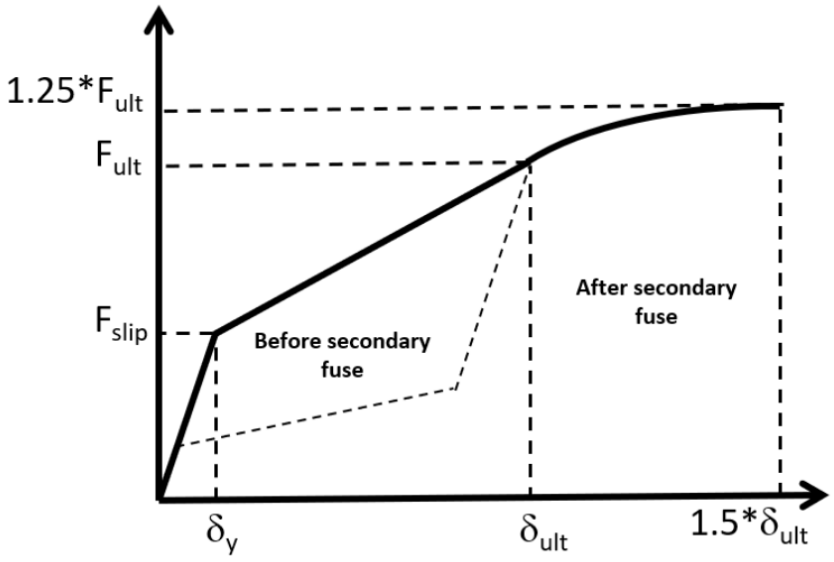

Figure 5-10: RSFJ performance with the secondary fuse (Hashemi et al., 2019)

5.4. Concrete Wall In-Plane Rocking Performance

5.4.1. Displacement Regime

For the first phase, the setup was positioned parallel to the actuator to evaluate the in-plane hysteresis performance. The testing protocols were designed in line with ASCE 7 standards, adapted to the maximum frequency of 0.35 Hz achievable by the incorporated actuators. This approach involves 10 cycles at 33% of ultimate displacement, followed by 5 cycles at 66%, and 3 cycles representing the full displacement capacity as depicted in Figure 5-11.

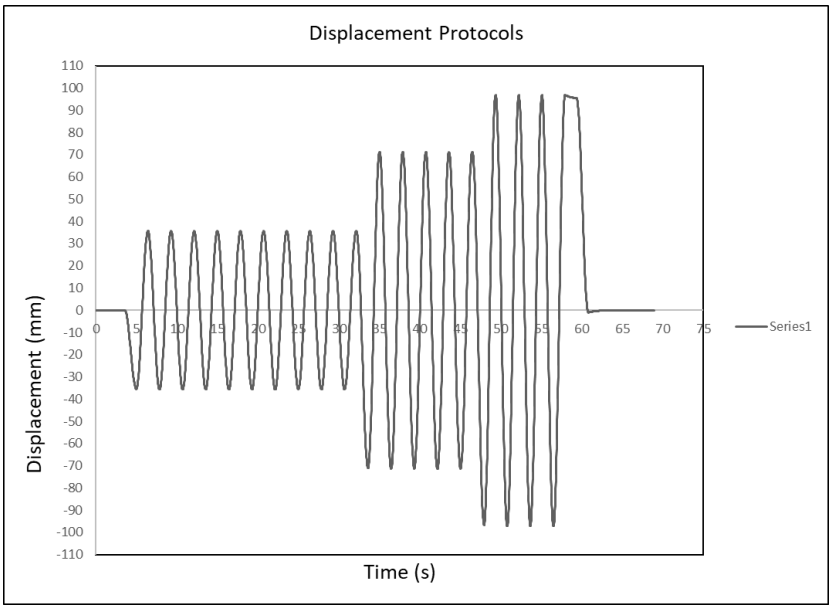

Figure 5-11: Displacement protocols considered for the test (0.35 Hz)

5.4.2. Instrumentation

The RSFJs were instrumented with LVDTs to measure both the tension and compression displacements. The uplift at the rocking corners of the walls was also measured with LVDTs, while the in-plane movement at the top of the wall and out-of-plane movement in the middle of the wall were tracked using draw wire sensors as shown in Figure 5-412. This measurement was conducted to ensure that the actuator motion remained centered, avoiding any impactful eccentricity that could affect the results. Collectively, the data from these instrumentation points provided a view of the behaviour of the setup under different test conditions.

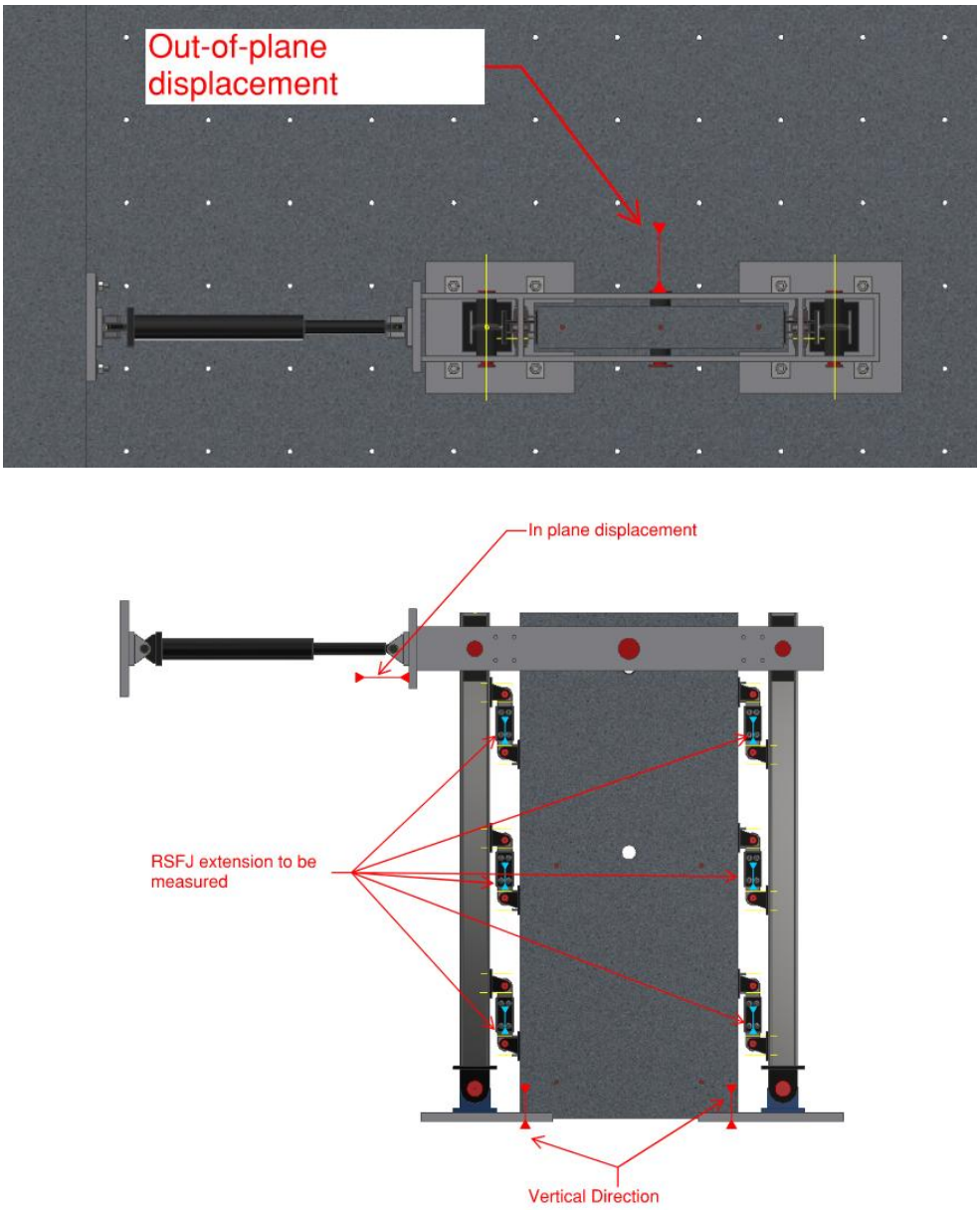

Figure 5-12: Instrumentation Placement Diagram

5.4.3. Testing results

To validate the accuracy of the analytical equations and to analyse the effects of frequency and cycle count on the wall dynamic performances, a detailed series of experiments were conducted. The testing protocol was structured as follows:

Two Cycles at Low Frequency: The tests included two cycles at amplitudes of 50 mm and 95 mm, conducted at a low frequency of 0.1 Hz. This setup aimed to assess the wall performance under minimal dynamic conditions, allowing for observation of the basic response without rapid oscillations.

Two Cycles at Medium Frequency: Similar to the first step, but with an increased frequency of 0.25 Hz. This increment in frequency helped to gauge the impact of faster oscillations while maintaining the same displacement amplitudes.

Two Cycles at Higher Frequency: The cycles were again tested at amplitudes of 50 mm and 95 mm but at an increased frequency of 0.35 Hz. This test further explored the upper limits of frequency impact within a short cycle duration, providing insights into the behaviour under more aggressive dynamic conditions.

Eighteen Cycles According to ASCE Protocols: This extended test, conducted at frequency of 0.35 Hz, involved amplitudes of 35 mm, 70 mm, and 95 mm. Adhering to the American Society of Civil Engineers (ASCE) protocols as depicted in 5.4.1, this set of tests was designed to cover the results over a prolonged period and multiple intensities, which is showcasing a structure subjected to continuous dynamic loads.

5.4.4. Summary of Pull and Push Test Results

The hysteresis loop obtained from the conducted pull and push tests provides (Figure 5-13) a detailed depiction of the energy dissipation and cyclic performance of this new rocking system under the considered loading regime. The results were in accordance with the anticipated outcomes based on prior calculations and the joint deflections observed were within the expected range.

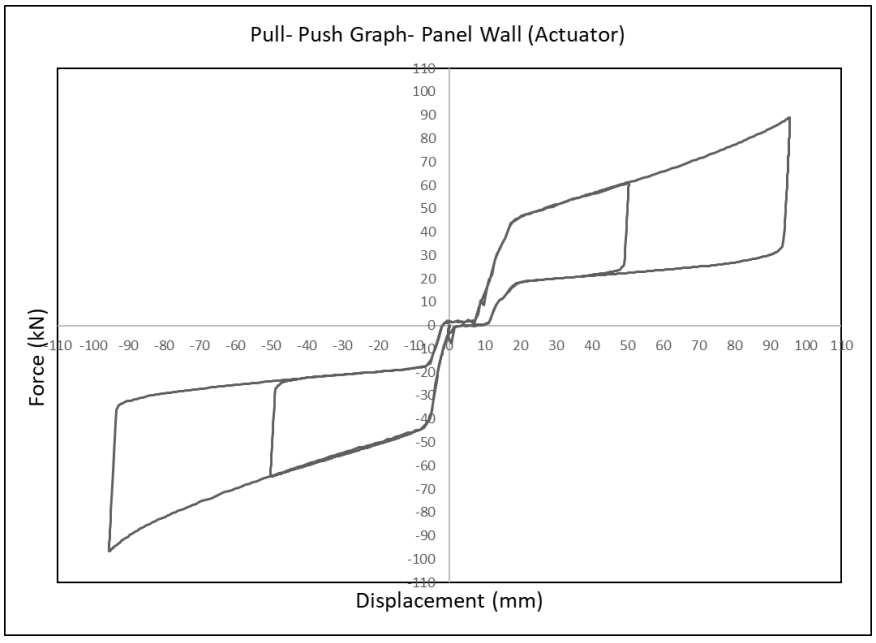

Figure 5-13: Hysteresis behaviour of the new rocking wall system under 0.1 Hz loading

The wall experienced a lateral movement of approximately 95 mm, which corresponds to a 2.5% drift. This level of drift is considered as the maximum acceptable for conventional design practices. The Figure 5-15 shows the displacements recorded by the LVDTs installed on the RSFJs and the rocking centers (ie, center of rotation), indicating whether the devices were extending or compressing. It is worth to note that the forces shown in the graph are derived from the actuator force used in the pull-push testing setup. Furthermore, the labelling of the outputs follows the numbering arrangement specified below.

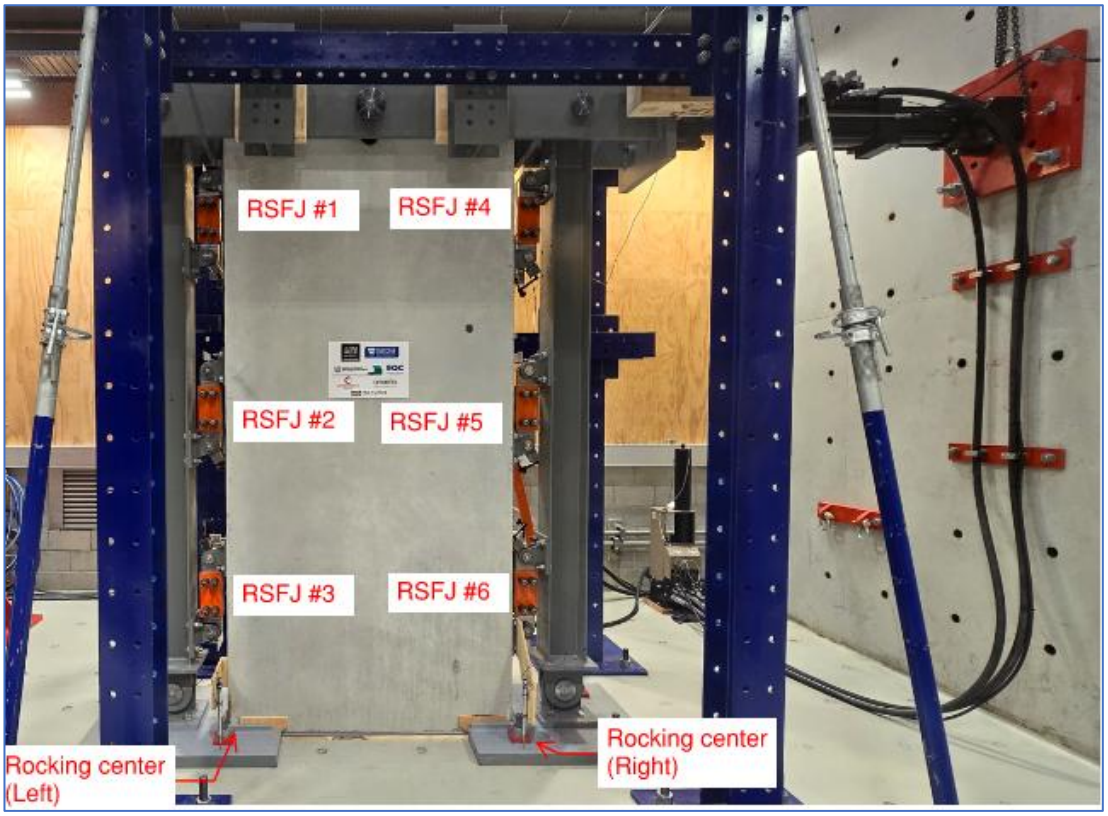

Figure 5-14: Identification of the RSFJ's by numbering

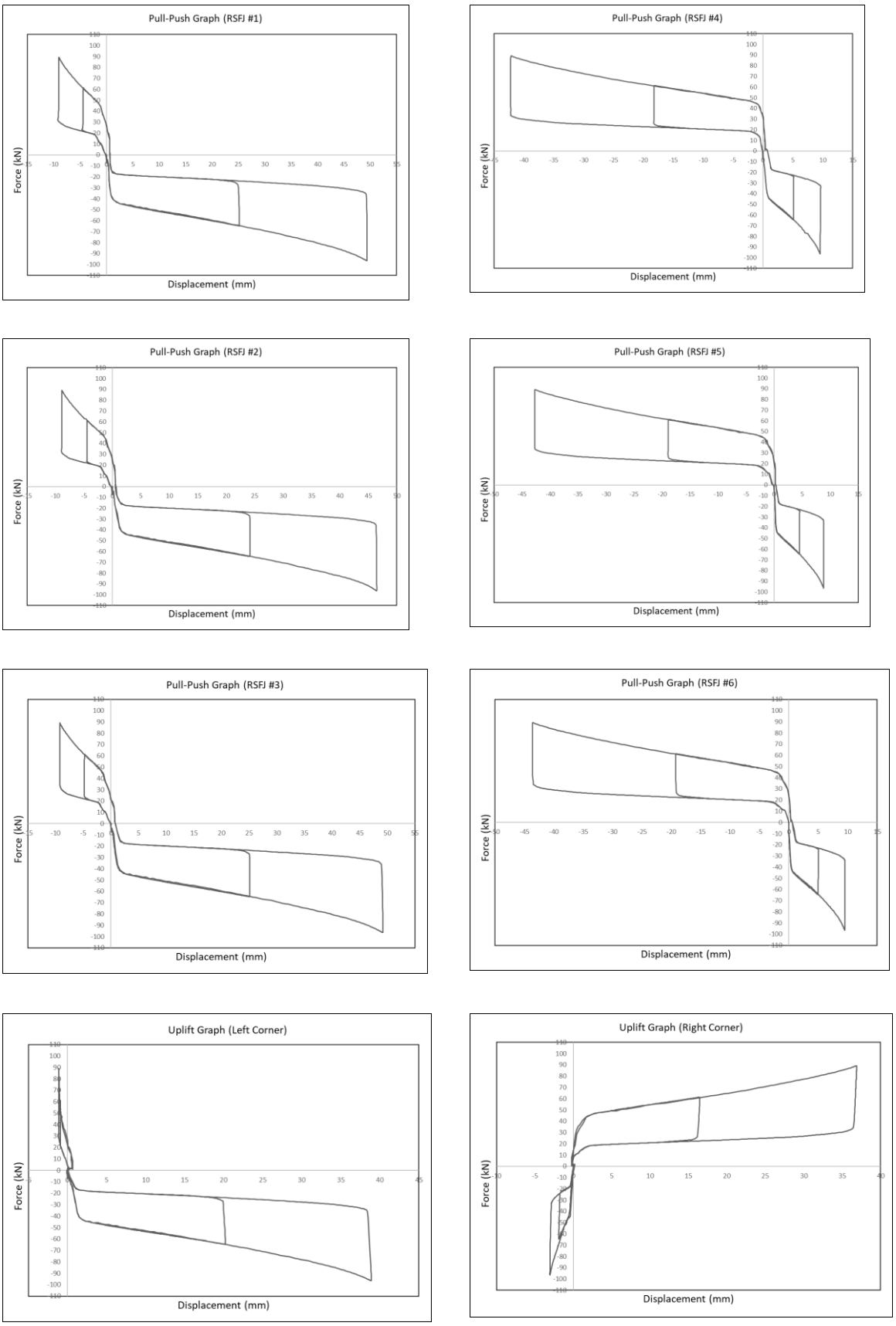

Figure 5-15: Measured displacement of LVDTs installed on RSFJs or at the base of rocking centers on the wall

On average, the RSFJs on the opposite side of the rocking center reached their maximum extension, opened to a distance between 45 and 50 mm. Conversely, the RSFJs on the rocking center side deformed less as expected, measuring around 10 mm which is the ratio of $d/(d+l)$ as indicated in Equations 4-5 and 4-6. Additionally, there was an upward movement at the base of about 40 millimetres. Both expansion and contraction were observed in these joints, ensuring adequate movement and energy dissipation during the push and pull tests.

There were minor differences in the displacement of RSFJs on one side, with variations on the order of 5 mm. These variations are attributed to an accumulation effect of tuning and connection tolerances. This pattern has been observed across a series of tests, suggesting that these minor discrepancies could be a characteristic of the setup and the testing method used.

5.4.5. Higher Frequency Impact

To explore the impact of testing frequency on the setup, the frequencies were varied: 0.1, 0.25, and 0.35 Hz. The results, as illustrated in figure 5-16, appear to closely match and indicate that these changes in frequency do not have a significant impact on the rocking performance of the wall.

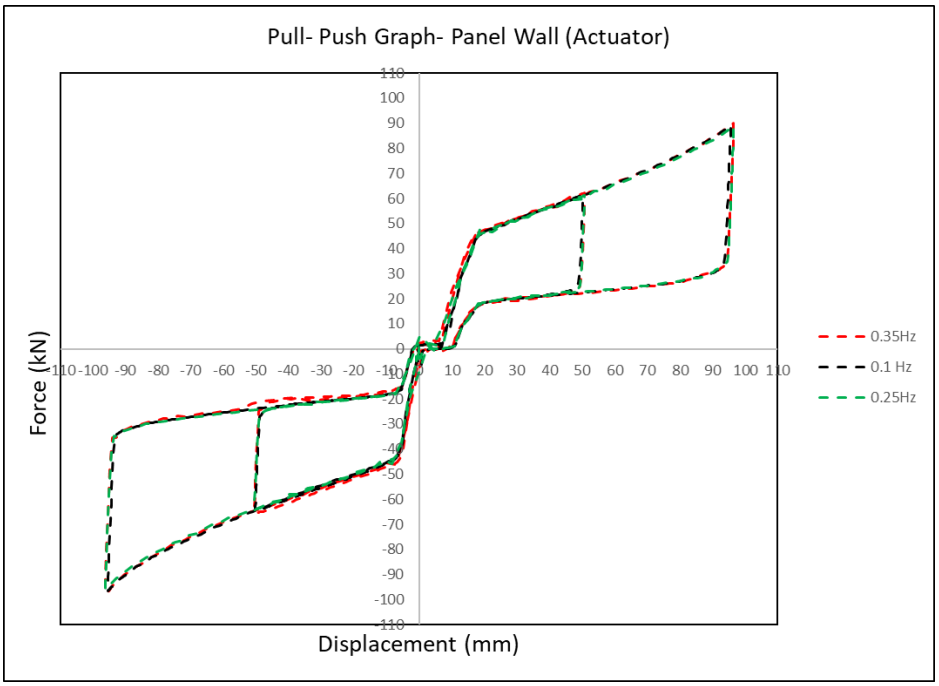

Figure 5-16: Setup hysteretic response under various loading frequency

5.4.6. Testing outcome as per ASCE protocols (0.35 Hz)

The system performance was designed to meet the ASCE requirements, which involve imposing a higher number of cycles with a targeted displacement that simulates the demands of actual earthquake motion. The results are depicted in figure 5-17. The hysteresis loop observed during the test appears to be repeatable, providing the expected levels of ductility and damping. However, with higher frequencies, there was an impact of the wall touching the ground. This aspect could be further investigated in more comprehensive tests by including accelerometers to measure the exact vertical acceleration, especially since such impacts may need to be considered for taller buildings for the residents comfort.

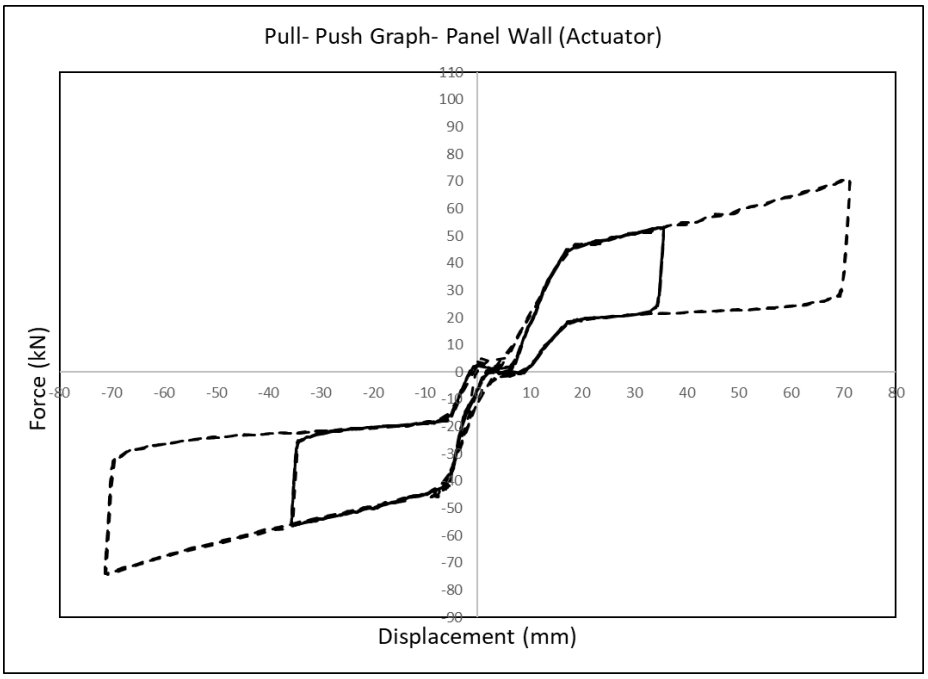

Figure 5-17: System in-plane hysteretic response under ASCE protocols

Additionally, the out-of-plane displacement of this system was measured to ensure that the actual movements did not cause a significant impact and were not substantially off-centre. As shown (Figure 5-18), the out-of-plane movement was controlled within a 5 mm range, thanks to the propping system implemented that included a 5 mm gap to keep the actuator aligned with the wall line. This setup helped to maintain the structural integrity and performance expectations under the simulated earthquake conditions.

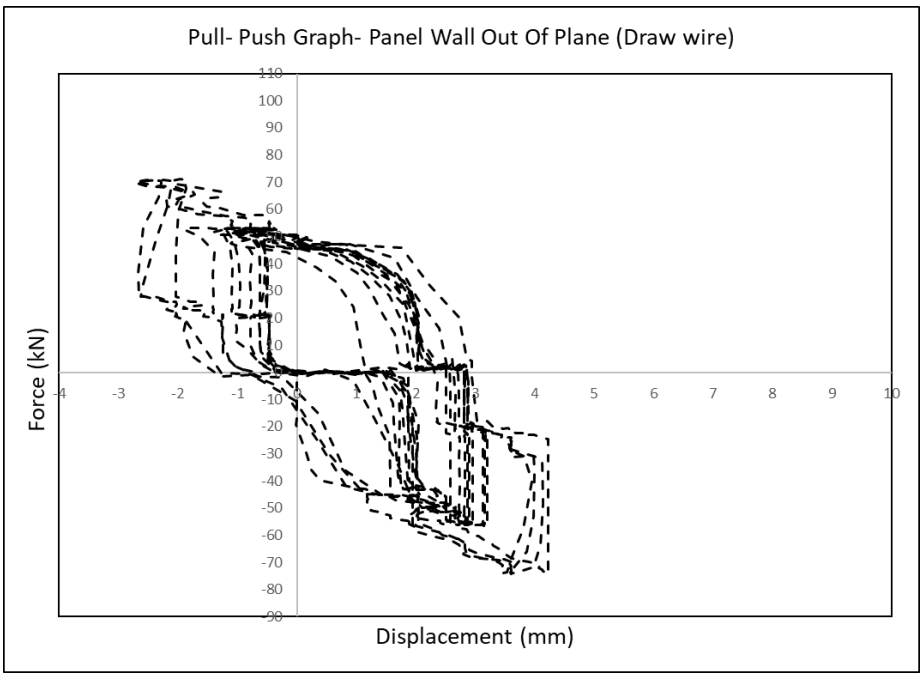

Figure 5-18: Setup out-of-plane pull-push response under ASCE protocols

The RSFJs displacement outputs and uplift measured at the rocking center are illustrated in the following. Graphs:

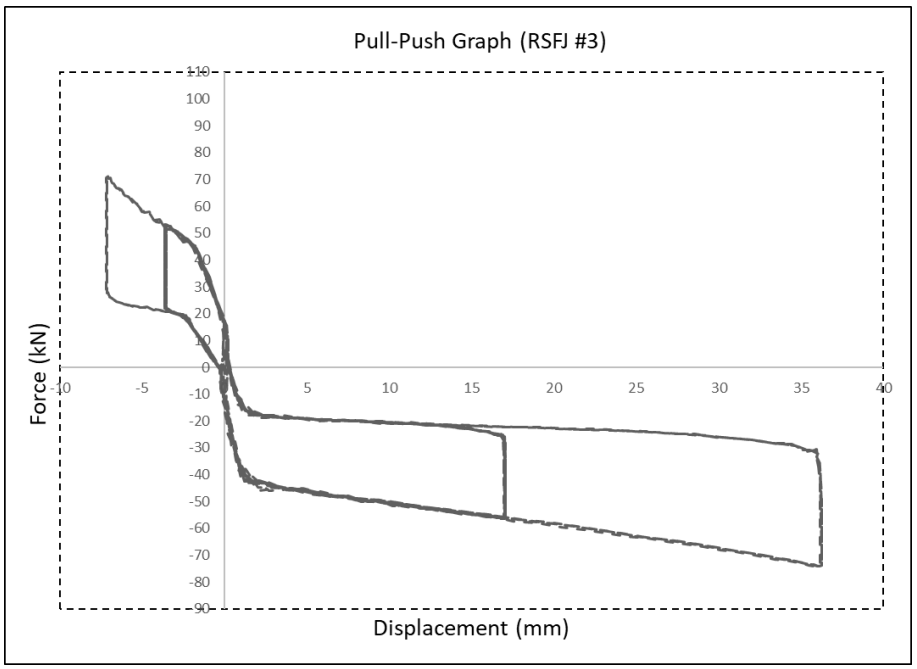

Figure 5-19: Hysteresis curve of the RSFJs mounted on the either side of the wall

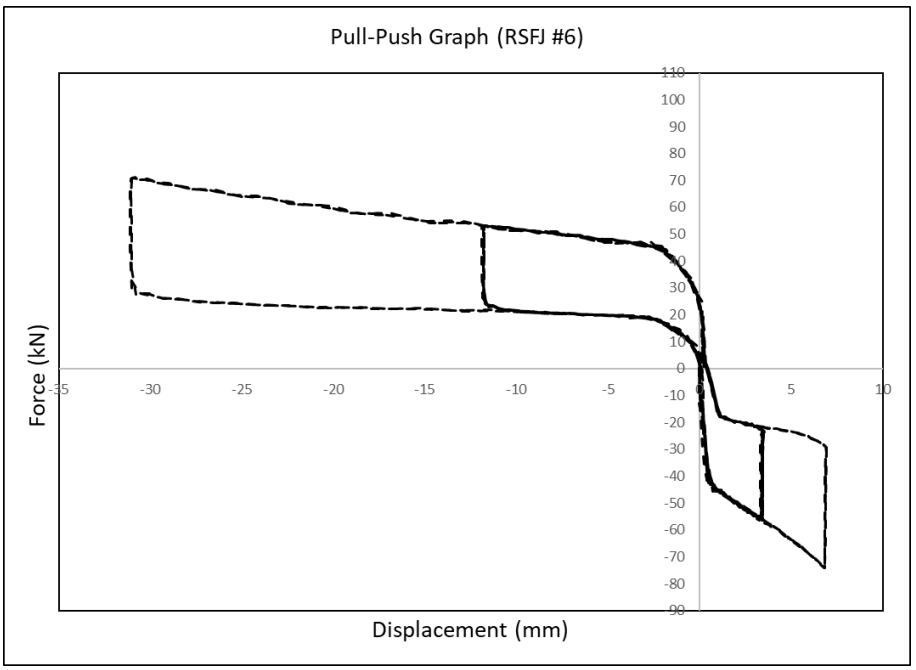

Figure 5-20: Hysteresis curve of the RSFJs mounted on the either side of the wall

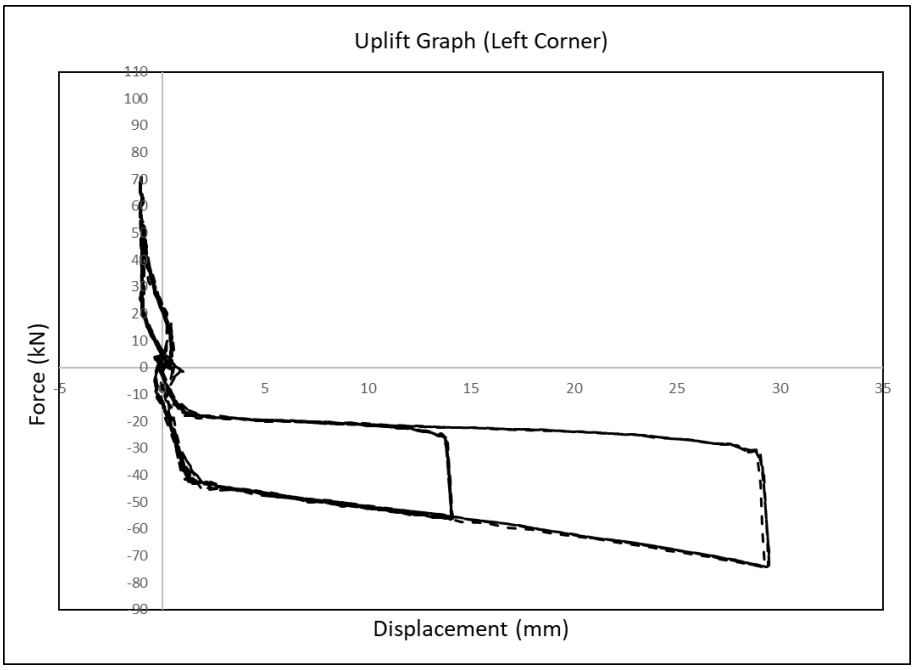

Figure 5-21: Measured uplift at the rocking center at either corner of the concrete wall

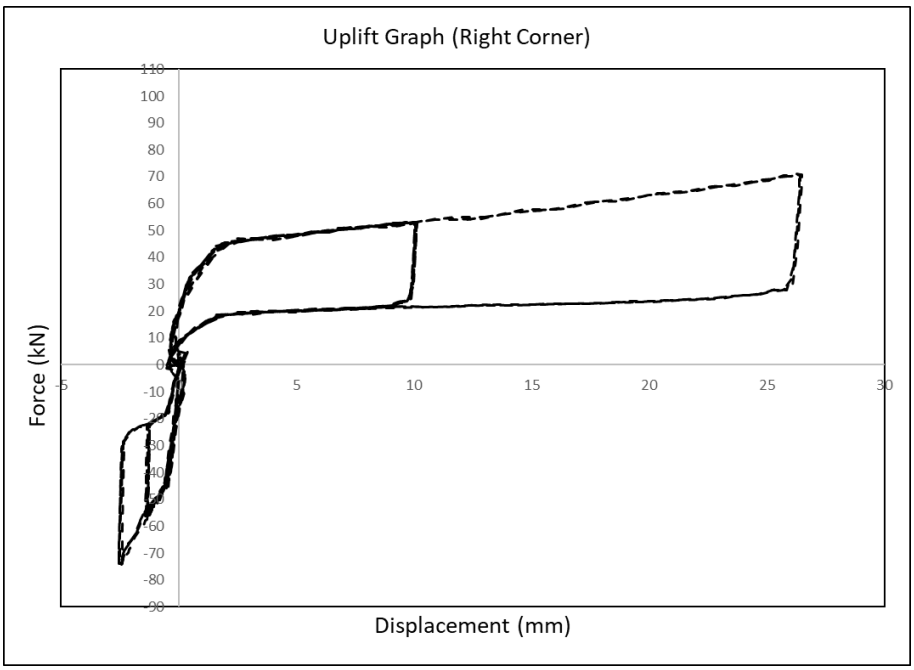

Figure 5-22: Measured uplift at the rocking center at either corner of the concrete wall

5.5. Concrete Wall Out-of-Plane Rocking Performance

To investigate how this new system responds to the out-of-plane movements at the similar deflection demand of 2.5% drift, the same setup was subjected to loading (Figure 5-23). This is particularly relevant when earthquake direction is not aligned with the wall setup, and the system must have deformation compatibility to absorb movements in a perpendicular direction without causing significant damage. To achieve this, the test setup was rotated 90 degrees to allow the actuator to be attached in the out-of-plane direction. The load path is assumed to be transferred from the actuator to the top connector beam, which then engages with the concrete wall and columns.

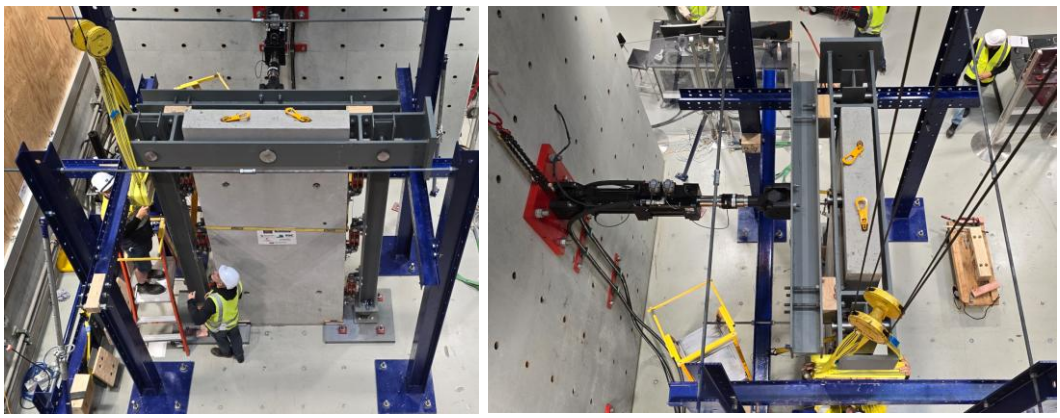

Figure 5-23: Concrete wall Out of plane loading setup

Due to the swivel bearing used in the column base pin connection, it was expected that the wall and column would move freely, requiring only enough force to overcome their weight to initiate the rotating motion. Assuming the combined weight of the wall and connections contributes between 40 to 50 kN, we expected a resultant resistance force of approximately 2.08kN ($\frac{50kN \times 0.125m}{3m} = 2.08kN$). The setup was subjected to three cycles of push-pull testing with displacements of 35 mm, 75 mm, and 100 mm. The results obtained are as follows:

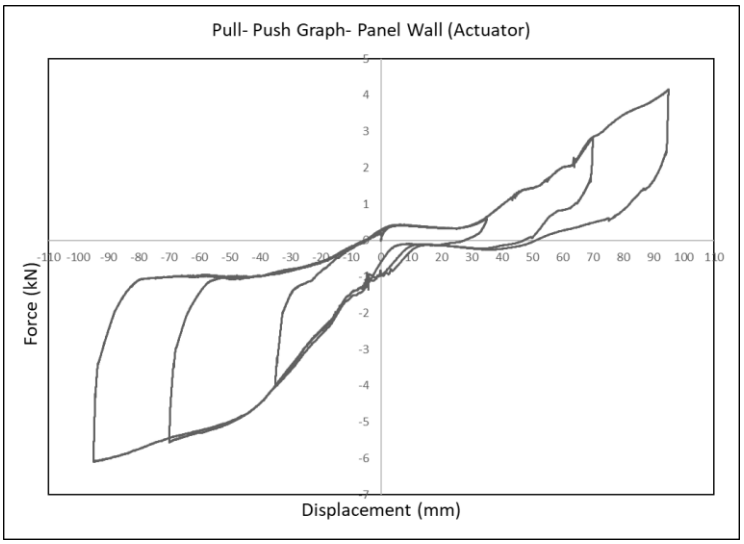

Figure 5-24: Measured displacement against the force in the out-of-plane direction

As expected, the setup moved without needing to engage the RSFJs, and both the columns and wall rotated around the base (Figure 5-25). However, the actuator load was higher than the weight contribution, likely due to the frictional resistance provided by the shimming plates inserted to fill the gap between the concrete wall and base plates. These plates were intended to prevent wall slippage while allowing for wall base rotation. Consequently, the concrete wall had to bear and press against these plates, introducing additional frictional resistance beyond the weight resistance as shown in figure 5-26.

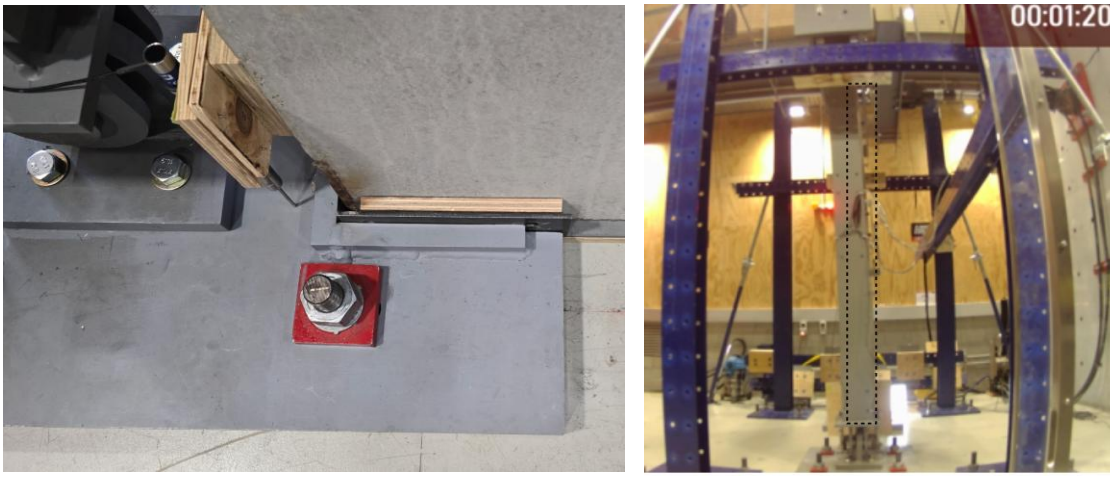

Figure 5-25: Wall corner shoe brackets in contact with the base plate to transfer shear (left); Inclined wall position (Right)

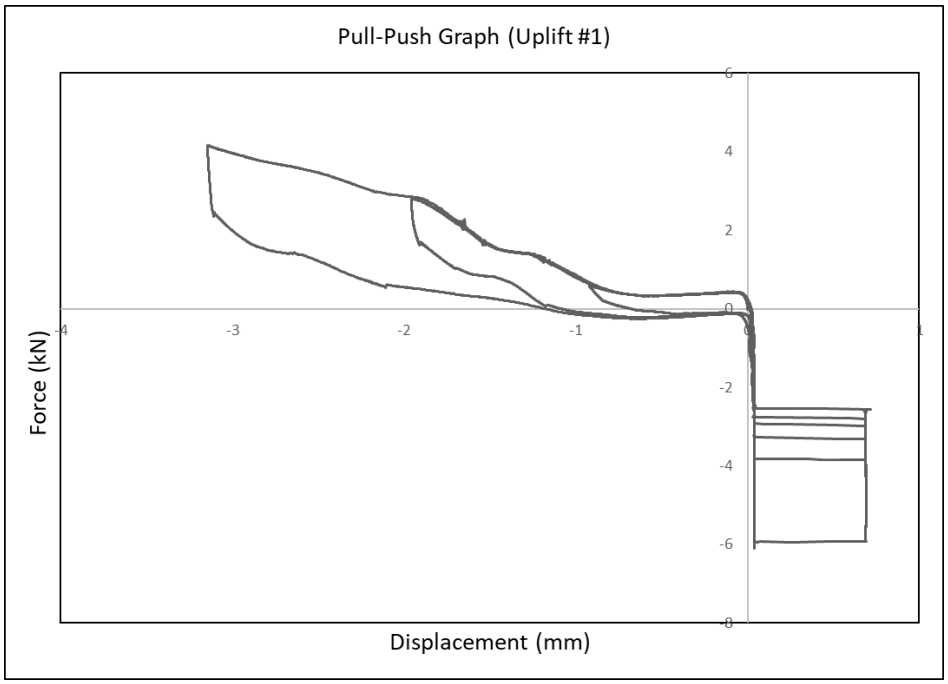

Figure 5-26: Uplift measured on the wall base

5.6. System Performance Evaluation under Extreme Displacement Conditions

In scenarios involving stronger-than-expected earthquakes, the structural system can ideally be designed to follow a ductile failure mode, which absorbs more energy and allows the structure to deflect more safely rather than losing strength and eventually collapsing. Achieving such performance involves creating a hierarchy of failure, designing the system so that the desired failure mode occurs before any brittle failure. Adopting this philosophy, the RSFJs can be engineered to act like a fuse within the system, absorbing damage and thereby allowing a ductile, desirable failure to protect other components that are costly or difficult to repair.

As illustrated in the graph Fig 5-10, the secondary phase of RSFJ behaviour includes the rod plastic elongation (without compromising the self-centring feature), which provides up to 50% more deflection capacity beyond the designed value. This incorporation ensures that if one side of the wall reaches maximum extension initially, the arrangement engages the far side further as one side extends into the secondary fuse phase. This concept provides the system with reserved displacement capacity (ie, extra energy dissipation capacity), which can be relied upon during stronger cycles beyond the design level. Engaging in such a phase makes the behaviour irreversible and necessitates repairs through replacing the RSFJ rods yielded, but the advantage is that the location and type of damage are predictable and easier to address.

To evaluate the performance of this new system beyond the design level, the actuator stroke limit was considered. As such, some of the RSFJ's disc springs were removed to adjust the joints for a target horizontal wall movement of 30mm, reaching the ultimate linear phase of the RSFJ devices (in contrast to the 95mm achieved in previous tests). The setup was then subjected to a maximum displacement of 120mm in one direction, nearly three times the linear phase value (Figure 5-27). This test aimed to assess the behavior of the setup under extreme conditions. Within this displacement range, it was expected that the RSFJs on the far side of the rocking toe would yield and elongate until rupture. This scenario reflects the reserved capacity in practical cases beyond the ultimate limit state (ULS) level, tuned to the end of the linear phase. The associated connections and adjacent members should be designed to accommodate the overstrength resulting from the rods overstrength factor due to yielding. The graph below illustrates the captured response across multiple cycles, reaching up to 120mm displacement. It should be noted that the observed overstrength factor for the system could be reduced by selecting rods with yielding capacity closer to the discs flat load. This optimisation was not considered for the test given the secondary fuse activation of the system (beyond ULS) was not initially part of the research scope (added later).

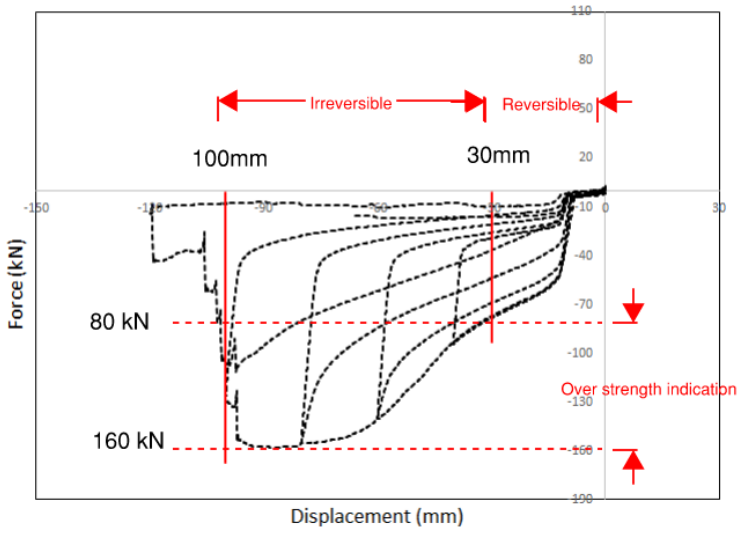

Figure 5-27: Performance of System under Extreme Displacement Conditions (beyond ULS)

As shown in figures 5-28 and 5-29, all three joints on the left side experienced rod rupture and lost their resistance. Unfortunately, due to the limitations of the lab machinery, it was not possible to push the setup further to capture the failure of the RSFJs on the other side of the rocking toe. However, it is expected that, with further displacement, these joints would engage more and provide an additional level of resistance.

Figure 5-28: Post-Test Condition: Left-Side Joints Ruptured, Right-Side Joints Intact

Figure 5-29: RSFJ with Ruptured Rods

5.7. Limitation of Applying the Proposed Experimental Research Plan on Real Building

In this research, our primary focus was on the dynamic behaviour and performance of rocking systems in seismic conditions. However, it is important to note that the scope of our study was specifically confined to the fundamental aspects of rocking system dynamics. Real-world applications of these systems often involve additional complexities, such as the intricacies of connections to the building floor and the impact of concurrent actions from various forces.

This section acknowledges specific aspects of rocking systems that are essential for a comprehensive understanding and application yet fall beyond the scope of our current research. Future studies should address these elements to improve the effectiveness and reliability of rocking systems under robust seismic-resistant designs.

5.7.1. Deformation Compatibility of Diaphragm

For the structural design of a rocking system, careful consideration is required in determining how the lateral loads from the floor diaphragms will be effectively transferred to the rocking system, particularly while accommodating the uplift of the

rocking system. This consideration is influenced based on whether the rocking system is intended to bear the gravity loads.

Load-Bearing Rocking Systems: In scenarios where the rocking system also bears gravity loads, a portion of the gravity system must be uplifted with the rocking system. This necessitates a detailed analysis of both the deformations imposed on the gravity system and the resistance of this system to the rocking motion. Ensuring that the gravity system can accommodate these deformations without compromising structural integrity is crucial. Furthermore, the connection detailing between the diaphragm and the rocking system in load-bearing systems demands attention to ensure seamless load transfer and movement compatibility.

Non-Load-Bearing Rocking Systems: If the rocking system is designed not to carry gravity loads, specific detailing is required to transfer inertial loads from the floors to the rocking system. This must be achieved while allowing for differential vertical movement between the rocking system and the gravity system. This approach involves engineering solutions that enable the decoupling of the rocking system from the gravity load-bearing elements of the structure. Some of the relevant studies have been summarized in the following section.

5.7.2. Previous studies on Rocking System Connection to Diaphragm

Eatherton and Hajjar (2010), as a part of their study on steel Controlled Rocking Systems (CRS's), suggested the split of the load collecting beam into two parallel lines around the CRS (Figure 5-30). In this method, floor forces are transferred through steel plates, which are designed to bend about their weak axes during the uplift of the CRS or by employing a yoke with sliders. This design is illustrated in the subsequent figures.

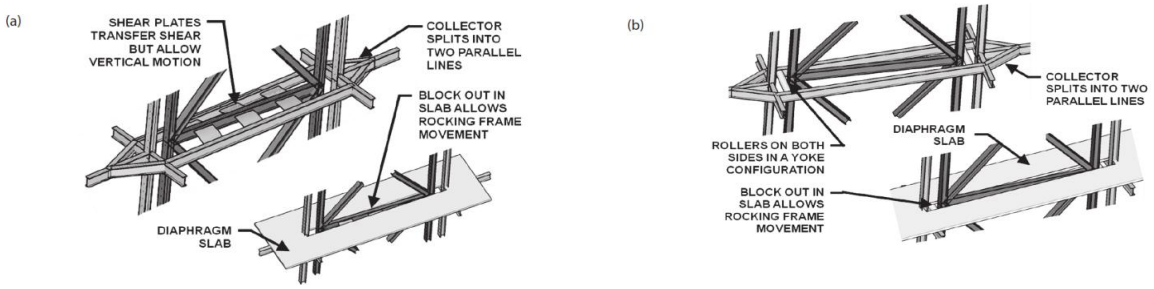

Figure 5-30: (a) flexible steel plates; (b) yoke and rollers; images from Eatherton and Hajjar [2010]

In another project Latham et al., 2013 (Kilmore Street Medical Centre) introduced the protruding tongue plate detail, as depicted in Figure 5-28. This design included the addition of ties between floor levels, ensuring that the floor slabs do not uplift with the rocking frames. This detail was critical in maintaining the structural integrity and stability of the floors while allowing the frames to undergo the necessary uplifting movement during seismic events.

Figure 5-31: Seismic frame collector beam with slot for tongue plates (Latham et al. [2013])

The following Figure 5-32 presents a series of innovative suggestions proposed by Henry in 2011, specifically tailored for precast diaphragm systems. Henry's proposals focus on optimizing the design of precast diaphragms to address common challenges and to leverage the benefits of precast construction. This included considerations for improving load transfer, enhancing seismic resilience, and ensuring efficient assembly and integration with other structural components. The suggestions encompass a range of design aspects, from connection detailing to material selection, each aimed at enhancing the overall performance and functionality of precast diaphragms.

In addition to addressing practical design considerations, Henry's suggestions also emphasize the importance of aligning precast diaphragm design with contemporary seismic engineering principles (Figure 5-32). This alignment is crucial for ensuring that these structural elements not only contribute to the overall stability and integrity of buildings but also perform optimally under seismic loads.

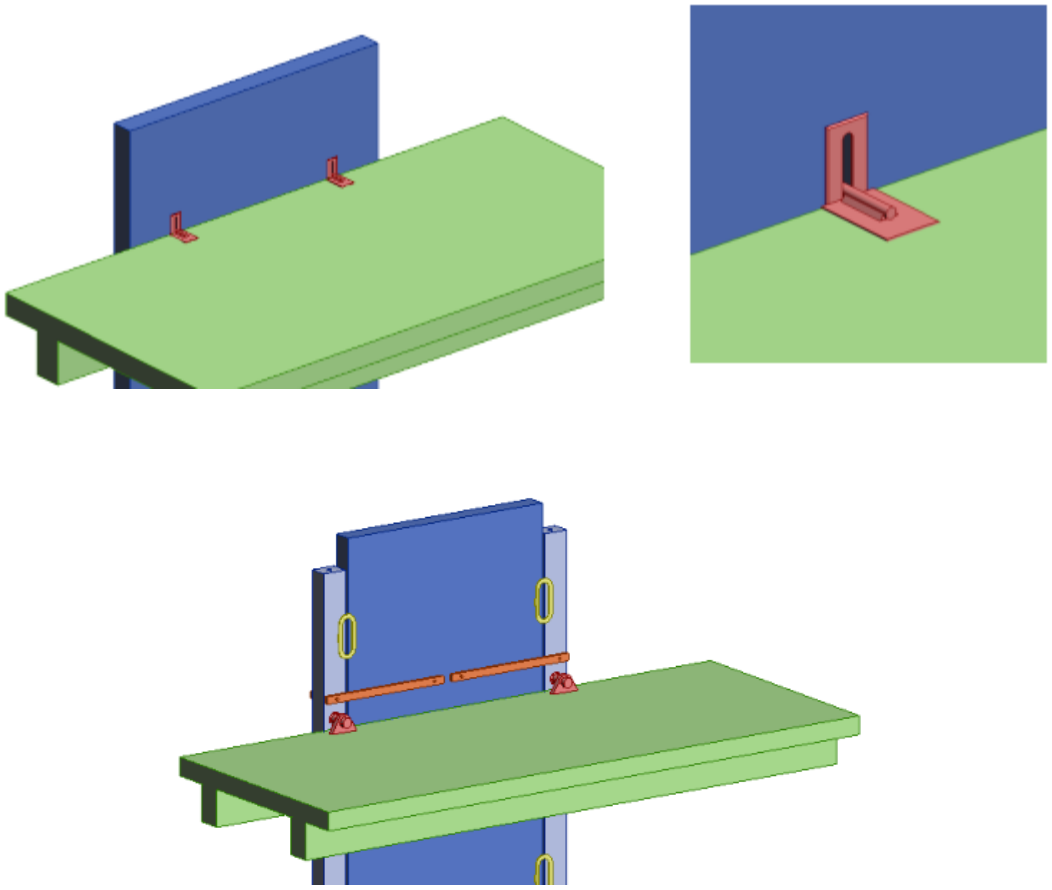

Figure 5-32: Proposed details for diaphragm connection to rocking walls (Henry et al., 2011)

For load-bearing systems, conventional detailing practices are typically employed, albeit with the anticipation of some level of damage to the diaphragm. Henry et al. (2011) undertook a series of dynamic time-history analyses to evaluate the seismic behaviour of slab-to-rocking system connections. The results of these analyses indicated that, at a 2% design level lateral drift, extensive cracking in the concrete floor and some yielding of the reinforcing steel were observed. However, it was noted that the damage generally remained within serviceability limits and could be feasibly repaired. The extent of damage anticipated at the wall-to-floor connection, however, was found to be dependent on the specific building layout and the length of the wall. It should be noted that the building response underwent alterations when the interaction between the wall and the floor was accounted for, leading to up to a 50% increase in lateral strength at the design level lateral drift. This over-strength poses potential implications for the seismic design of the building, particularly concerning possible shear or sliding failure of the wall.

In another project at the University of California, San Diego, Schoettler et al. (2009) sought to develop a diaphragm seismic design methodology (DSDM) by conducting

shake-table tests on a prototype precast concrete parking structure. The tested structure, illustrated in Figure 5-30, was constructed using precast column and beam elements, three precast flooring systems, and two hybrid self-centring walls. The floor diaphragms included hollow-core with in-situ topping, double T's with in-situ topping, and double T. Although the primary focus of the tested structure was to observe the behaviour of the precast floor diaphragms, the interaction between the wall and floor diaphragm was also under consideration. Researchers opted to isolate the floors from the vertical uplift of the wall using slotted insert connectors. These connectors were expected to transfer horizontal inertia forces from the floors to the wall while allowing independent uplift of the wall. This design effectively prevented damage to the floor system due to wall uplift, enabling researchers to concentrate on the in-plane behaviour of the diaphragms. Preliminary results affirmed that these connectors performed effectively under low-intensity earthquake loads but failed under maximum considered input motions due to the uplift of the wall panel exceeding the slot available stroke. No damage was noted in the floor diaphragms adjacent to the walls, and the hybrid walls behaved as anticipated from earlier pseudo-static tests, as reported by Henry et al. (2011).

Figure 5-33: Shake-table test of DDSM precast building at San Diego (Schoettler et al. 2009)

The test setup in this study is based on the assumption of a non-load-bearing type of rocking system. However, in scenarios involving load-bearing rocking frames, there are two distinct approaches observed in design and implementation.

Firstly, one approach involves the detailed design of specialized connections that facilitate uplift without causing interruption to the system functioning. This design

strategy focuses on ensuring that the connections can accommodate the unique movements associated with rocking systems, especially during seismic events.

Secondly, an alternative approach accepts a certain degree of damage as a consequence of seismic activity, while ensuring that this damage remains within serviceability limits. In such cases, the potential damage is factored into the design, and the structure is engineered to remain functional and safe even with some level of post-seismic damage.

Regardless of the approach, it is imperative that the effects of these connections, particularly in terms of their stiffness, are appropriately considered and integrated into the design process. This aspect of design is critical to ensure that the rocking frame performs as intended under seismic loads.

In our research, the test setup was of a non-bearing type, meaning that the effects of the diaphragm, in terms of stiffness and strength, were not considered. This distinction is critical when considering the application of this setup in practical projects, as highlighted by Henry et al. (2011).

It should be noted that this part of the structural design, particularly the detailed study of connections in load-bearing rocking systems, appears to be an area ripe for further research and is not a focus of the experimental aspect of this particular study.

5.7.3. Connection to Foundation

In the described test setup, where the columns are not designed to bear gravity loads, the base column connections have been specifically engineered to exhibit pin performance. This design approach is essential in replicating the ideal conditions of a pin connection, which is crucial for accurately assessing the behaviour of the system under test conditions.

In practical projects, achieving a perfectly pinned connection is relatively uncommon with typical pined connection detail, and as such, the effects of potential stiffness in the connections and the compatibility of displacements become critical factors in the detailed design phase. This consideration is important because deviation from ideal pin behaviour can influence the overall performance of the structure, especially under seismic loads.

The detailed design process must, therefore, evaluate the characteristics of the column connections. This evaluation includes understanding the extent to which these

connections can mimic true pin performance and identifying any inherent stiffness that might affect the system behaviour.

In summary, while the test setup aims to replicate ideal conditions with real pin performance at the base column connections, the complexities and challenges of achieving such conditions in real-world projects necessitate thorough and careful design considerations.

5.7.4. Higher Mode Effect

The primary focus of this test setup is to validate deflection compatibility and the overall design methodology of single panel wall. Consequently, the investigation into the effects of higher modes, which are crucial in understanding the complete seismic response of the structure, falls outside the scope of this physical testing.

As discussed in the previous chapter, the numerical analysis is considered as an effective tool to address this limitation. However, while incorporating numerical analysis is crucial for understanding the structural response, particularly regarding higher mode effects, physical testing provides valuable insights into deflection compatibility and validates certain aspects of the design method. These insights can be used to calibrate and complete the numerical model, which can then be considered for further study.

5.8. Soil-Structure Interaction

Soil-structure interaction (SSI) effects influence the seismic response of superstructures. Understanding the dynamic behaviour of various soil types under seismic loads is essential, including soil stiffness, damping characteristics, and changes in these properties during an earthquake. The efficiency of rocking systems, given their inherent flexibility, can be impacted by SSI. Research should focus on optimizing the performance of rocking frames by considering soil conditions and identifying potential limitations associated with incorporating such ductile behaviour. While this was not within the scope of this research, further studies may highlight some constraints related to SSI.

5.9. References

1. Hashemi, A., et al. (2019). The Resilient Slip Friction Joint (RSFJ) Technology: Recent Developments and Completed Projects. Presented at the 2019 SESOC Conference, New Zealand. Retrieved from 2019 SESOC Conference.
2. Eatherton, M. R., & Hajjar, J. F. (2010). Large-scale cyclic and hybrid simulation testing and development of a controlled-rocking steel building system with replaceable fuses. *Report No. NSEL-025
3. Latham, D., Reay, A., & Pampanin, S. (2013). Kilmore Street Medical Centre: Application of a post-tensioned steel rocking system. Paper presented at the Steel Innovations Conference 2013, Christchurch, New Zealand.
4. Henry, R.S., Ingham, J.M., & Sritharan, S. (2012). Wall-to-floor interaction in concrete buildings with rocking wall systems. 2012 NZSEE Conference.
5. Schoettler, Matthew & Belleri, Andrea & Zhang, Dichuan & Restrepo, Jose & Fleischman, Robert. (2009). Preliminary results of the shake-table testing for the development of a diaphragm seismic design methodology. PCI Journal. 54. 100-124. 10.15554/pcij.01012009.100.124.

Chapter 6: Development and Case Studies of Resilient Slip Friction Dampers As an Anchorage System for Cylindrical Steel Tanks

The motivation behind this research stems from the need to resolve the high force demand and associated damage issues prevalent in fully anchored tank systems. In contrast to unanchored tank systems, which lack controlled deflection and movement, the proposed solution aims to regulate these aspects within a desired range, thereby preventing tank collapse. Moreover, this proposed system aims to offer an improved solution over existing ductile systems, which are often prone to incurring damage and necessitate replacement following seismic events. Central to this novel approach is the enhancement of the resilience of liquid storage tanks, particularly in their capacity to withstand aftershocks. Additionally, it introduces a self-centring mechanism, a feature frequently absent in conventional anchorage designs. This advancement not only addresses the vulnerabilities of current systems but also represents a significant step forward in the field of seismic-resistant construction, offering a more robust and durable solution for liquid storage tanks.

Nevertheless, for practical implementation, this approach necessitates careful consideration of the durability of steel materials and their compatibility with the environmental conditions prevalent in the wine industry. The proposed connection, being an external linkage, will be exposed not only to environmental elements but also to the chemical constituents of wine or dairy and the cleaning agents used for tank maintenance. Furthermore, the design must accommodate the cylindrical geometry of the tanks to ensure a seamless and effective connection. To address these challenges, a novel Resilient Slip Friction Damper (RSFD), as patented by Darani et al., has been utilized to establish a robust connection between cylindrical, ground-supported tanks and their foundations.

6.1. Resilient Slip Friction Damper (RSFD)

The innovative connector adopted in this study aims to overcome the aforementioned disadvantages. Initial patent consists of an elongate hollow casing. Within this casing is an elongate spring and damping assembly (Figure 6-1). This assembly is capable of linear translation within the casing, engaging frictionally with its interior surfaces to provide

damping functionality. The configuration of this novel connector is detailed in the accompanying figure, illustrating its design and operational mechanism.

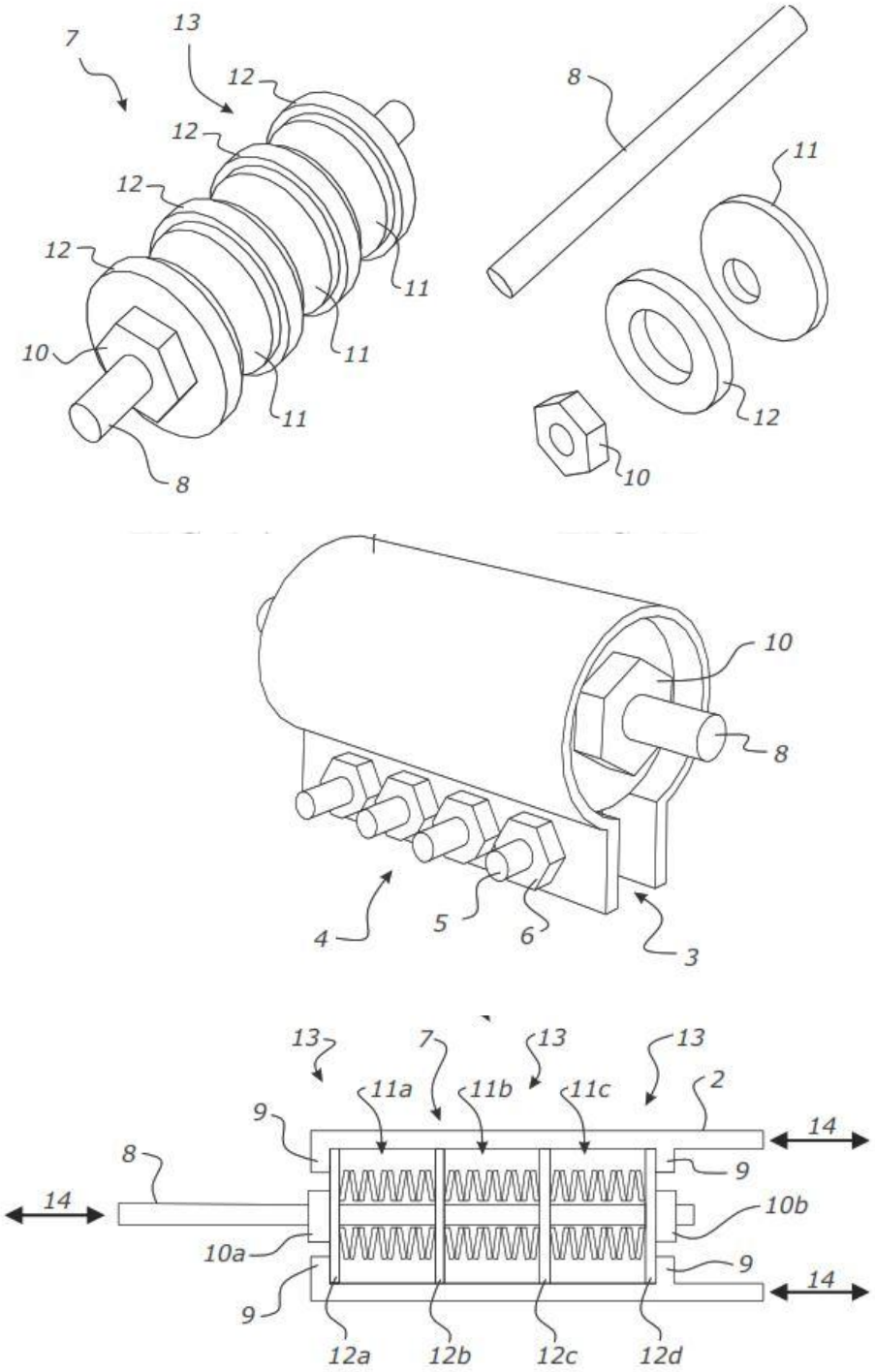

Figure 6-1: Details of proposed concept of self-centring connector, (Darani et al. (2021).

The formulation and of joint is derived as below Mohammadi Darani et al. (2021):

	Equation	Description
(1)	$F_{friction} = 2\pi\mu F_{pr,bolt} n_{bolt}$	Total friction force
(2)	$F_{pr,rod} > F_{friction}$	Self-centring condition
(3)	$F_{slip,0} = F_{pr,rod} + \frac{f_{friction}}{n}$	First slip force
(4)	$F_{slip,1} = F_{slip,0} + \frac{f_{friction}}{n}$ and $\Delta_{slip,1} = \frac{f_{friction}}{n * k_1}$	Second slip force and its corresponding displacement
(5)	$F_{slip,i} = F_{slip,i-1} + \frac{f_{friction}}{n}$ and $\Delta_{slip,i} = \sum_{j=1}^{i-1} \Delta_j + \frac{f_{friction}}{n * k_i}$	The i^{th} slip force and its corresponding displacement. It should be noted that the sign "Σ" refers to the displacement of other disk stacks which should be added to the i^{th} one.
(6)	$\Delta_j = \min\left\{\frac{F_j}{k_j}, \Delta_{max,j}\right\}$	Displacement of j^{th} spring stack at the slip of i^{th} friction disk.
(7)	$F_j = F_{slip,i} - j * \frac{f_{friction}}{n}$	Force in the j^{th} spring stack at the slip of i^{th} friction disk.
(8)	$F_{ult} = F_{slip,m-1} + k_m * \Delta_{max,m}$	Ultimate loading capacity.
(9)	$F_{restoring,m} = k_m * \Delta_{max,m} - \frac{f_{friction}}{n}$	Restoring force at the maximum displacement.
(10)	$F_{restoring,m-1} = F_{restoring,m} - \frac{f_{friction}}{n}$ and $\Delta_{restoring,m-1} = \Delta_{ult} - \Delta_{slip,1}$	Restoring force at the second re-centring slip.
(11)	$F_{restoring,i} = F_{restoring,i+1} - \frac{f_{friction}}{n}$ and $\Delta_{restoring,m-1} = \Delta_{ult} - \Delta_{slip,i}$	Restoring force at the i^{th} re-centring slip.
(12)	$F_{residual} = F_{restoring,0} = F_{pr,rod} - \frac{f_{friction}}{n}$	The residual unloading force in the damper.

As per patented concept the hysteresis behaviour is expected to be fit with below graph:

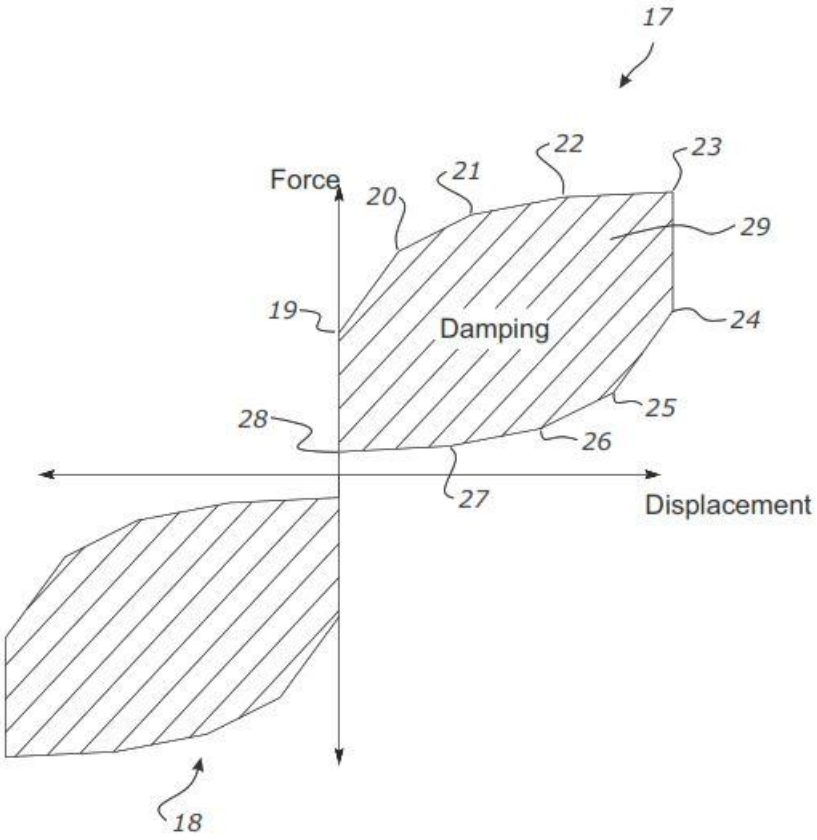

Figure 6-2: hysteresis behaviour of self-centring connector Mohammadi Darani et al. (2021)

Compared to other friction and yielding-based seismic design concepts, the proposed connection in this study offers a damage-free solution, reducing the need for both short-term and long-term inspection and maintenance. This innovative approach is predicated on the principle that as long as seismic activity remains within the designed range, the joint will not sustain damage. The frictional aspect of this system functions effectively as an energy dissipator, which plays a crucial role in diminishing the forces transferred to other structural members during seismic events. This energy dissipation is vital in protecting the overall integrity of the structure and reducing the likelihood of damage.

Another critical element in the design of rocking structures is the provision of a restoring force. This force is necessary to reposition the structure back to its initial state post-earthquake. In the proposed concept, this restoring force is achieved through the strategic use of disk springs. The inclusion of a sufficient number of these springs ensures that the structure is not only capable of withstanding seismic forces but also has the inherent ability to self-correct and return to its original position.

6.2. Advanced Resilient Slip Friction Damper

To adapt the innovative Resilient Slip Friction Damper (RSFD) concept for the specific requirements of steel tank applications, the original design underwent a series of strategic modifications, resulting in an assembly comprised of two distinct parts. The upper section of the RSFD features a slotted design, a crucial modification that imparts the flexibility needed for effective clamping. This flexibility is key to generating the intended frictional resistance, a fundamental aspect of the damper's seismic energy dissipation function. The slotted upper piece is securely fastened to a robustly designed cap and a lower section. This lower part serves as a casing for the disk springs, crafted to be solid and sturdy to ensure that the disk spring stack operates with unhindered movement within its sleeve.

In addition to these structural enhancements, the design incorporates circulation holes. These holes play a vital role in maintaining the internal environment of the cylinder, specifically designed to prevent the accumulation of damp air inside, which could potentially impact the damper's performance.

In terms of material selection, the Resilient Slip Friction Damper (RSFD) has been designed using a grade of stainless steel that aligns with that of the tank systems. This choice of material is pivotal for ensuring durability and addressing the practical aspects of the application. The use of stainless steel is particularly advantageous due to its resistance to corrosion and its strength, making it an ideal choice for environments where it may be exposed to various chemical substances or weather conditions.

Furthermore, all the bolts and nuts utilized in the assembly of the RSFD are also fabricated from stainless steel. This uniformity in material selection is critical for maintaining compatibility under environmental circumstances where the damper might be exposed to harsh conditions. Stainless steel's inherent properties, including its resistance to corrosion and its ability to withstand various chemical interactions, are essential for the long-term functionality and reliability of the RSFD in the specific context of steel tank applications. This consistency in material choice across all components of the RSFD ensures that the entire system can uniformly respond to environmental challenges, thereby enhancing the overall integrity and lifespan of the damper system.

As part of the development process, a prototype exemplifying this revised RSFD design was created. This initial model was engineered to be compact, with specifications including a 40 kN force capacity and an estimated displacement range of around 15mm

(Figure 6-3 and 6-4). This smaller-scale version of the RSFD underwent comprehensive testing. These tests were critical in assessing the operational capabilities and resilience of the damper under simulated conditions, thereby providing valuable insights into its performance characteristics and potential applications in enhancing the seismic resilience of steel storage tanks.

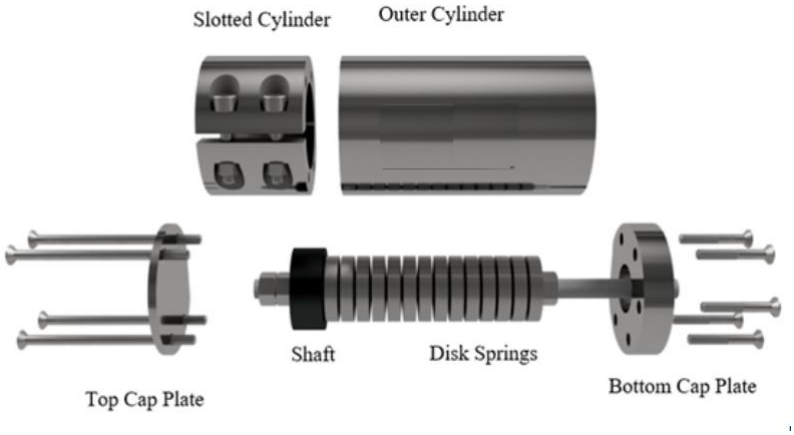

Figure 6-3: RSFD prototype components

Figure 6-4: Assembled RSFD Prototype Undergoing Testing in Universal Testing Machine (UTM)

The graph below clearly demonstrates that the intended flag-shaped behaviour of the Resilient Slip Friction Damper (RSFD) was successfully achieved and subsequently validated through cyclic testing.

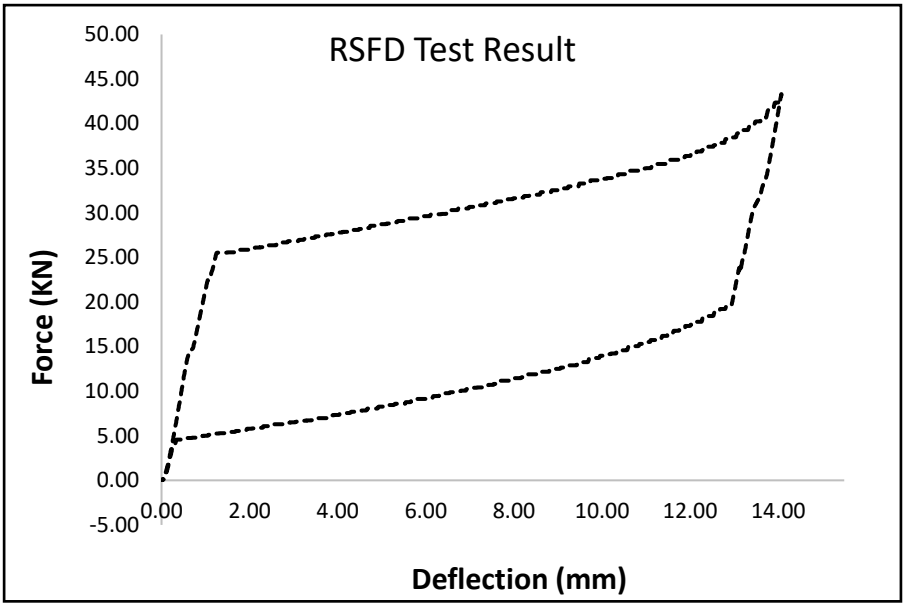

Figure 6-5: Hysteresis loop of prototype RSFD

The next generation of Resilient Slip Friction Devices (RSFDs) has been developed as part of a commercial project, intricately tied to the research and development initiatives of Tectonus, a company specializing in seismic resilience technologies. This advanced iteration of RSFDs represents a significant leap in the application of seismic mitigation devices, marrying innovative engineering with practical, real-world applications. The development phase involved rigorous testing and refinement, ensuring that the device met the stringent demands of seismic resilience in industrial tanks. Subsequently, Tectonus successfully integrated these enhanced RSFDs into several real-case projects, marking a pivotal step in the adoption of this technology in the field. This transition from theoretical design and development to practical implementation underscores the potential of these devices to significantly improve structural integrity and safety in seismically active regions.

In the development of the next-generation RSFD, several key modifications were introduced to enhance its functionality and ease of assembly. One notable addition is a welding block on the bottom cylinder, enabling direct attachment to the tank barrel. This design change facilitates a more seamless integration of the RSFD with the tank structure.

Additionally, to simplify the assembly process, the bottom cylinder cap was redesigned as a single segment. The top cylinder cap now features threading, which streamlines

production and assembly. This two-piece construction is also advantageous in terms of thermal management; the heat generated during the welding process does not affect the friction between the shaft and the outer cylinder, thereby maintaining consistent friction resistance.

A sealing plate has been incorporated to fill the gaps around the bolt cleats, effectively preventing direct liquid penetration into the cylinder (Figure 6-6). This feature is particularly crucial in safeguarding the internal components of the RSFD from potential damage caused by exposure to liquids.

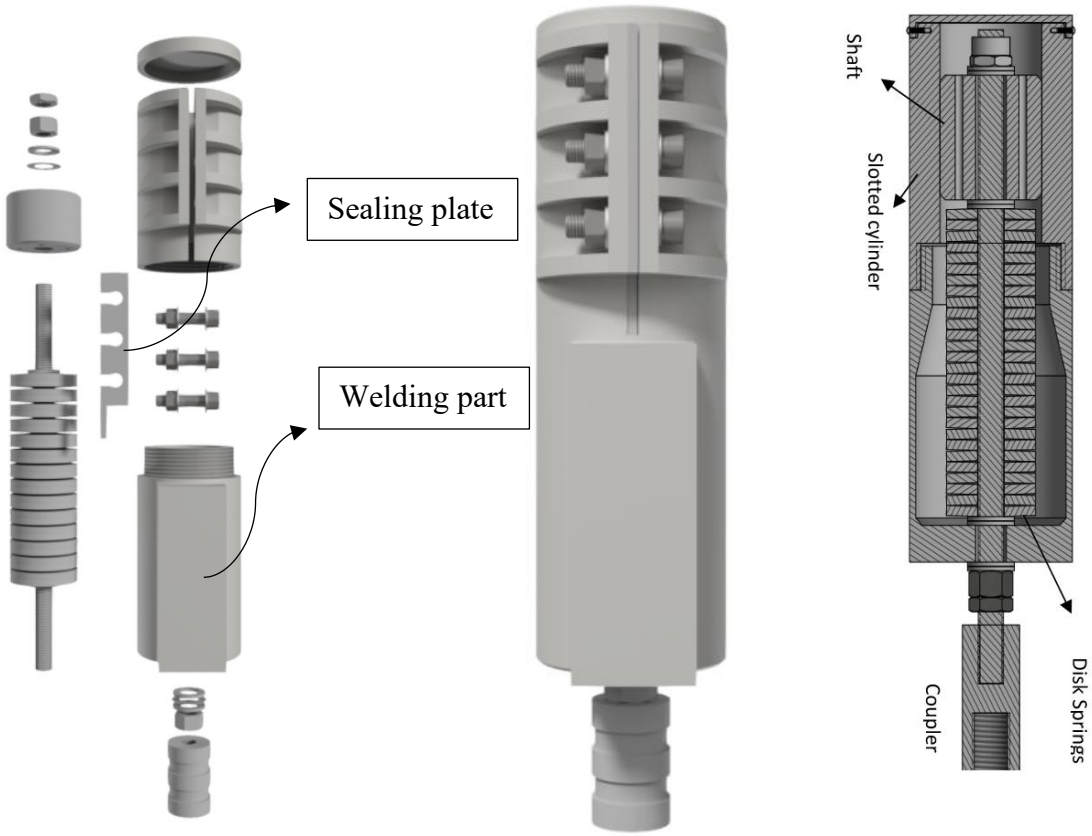

Figure 6-6: Refined RSFD Design Tailored for Tank Connection Applications

Furthermore, for a robust foundation connection, the rod of the RSFD can be linked to an anchor bolt embedded in the foundation through a mechanical coupler. This coupling mechanism ensures a strong and reliable connection, essential for the damper's performance under seismic loads. These design enhancements collectively contribute to the RSFD's improved efficacy and practicality in seismic resilience applications.

The connection to steel tanks envisages to be as below detail. The RSFD to be welded to side of tank as depicted below:

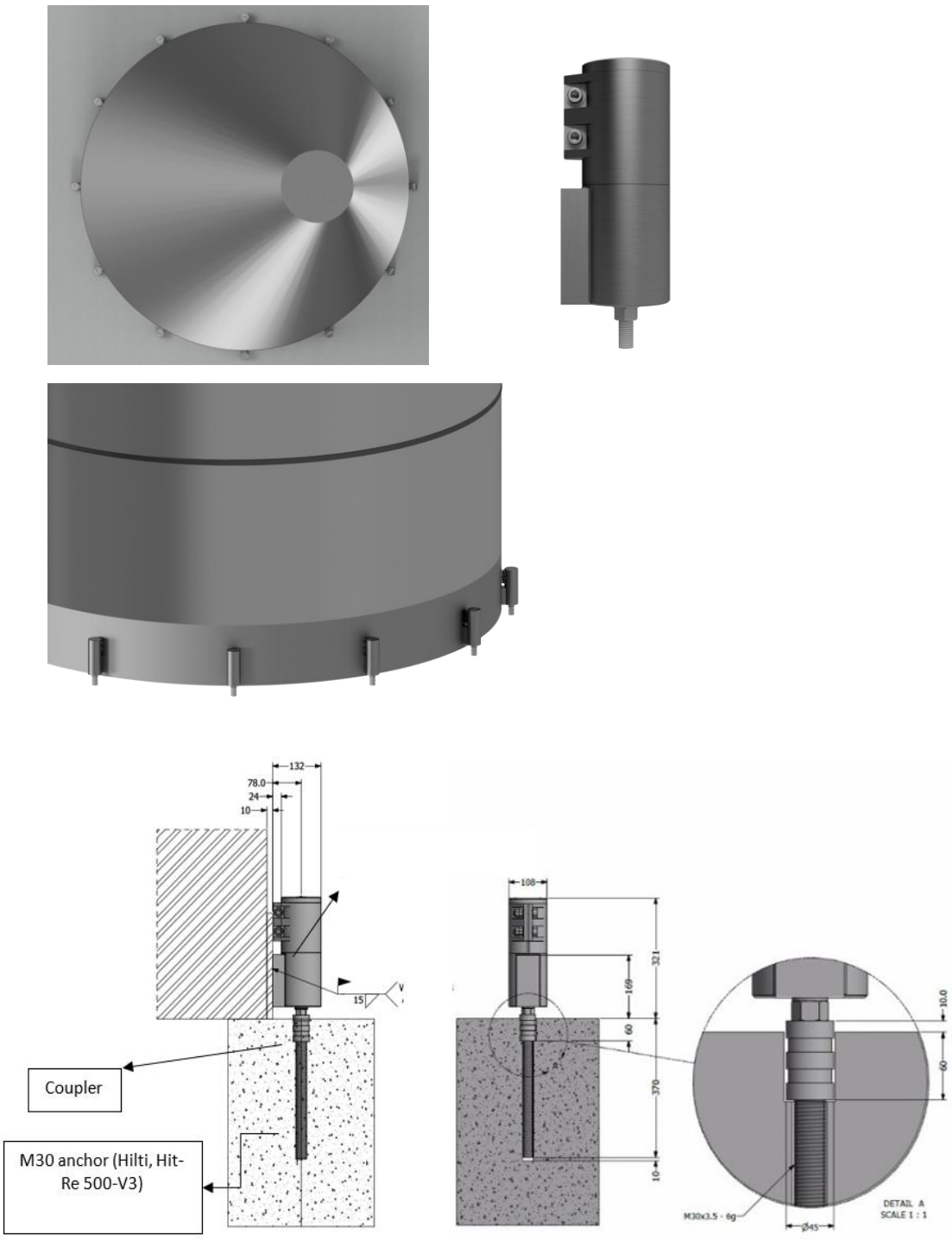

Figure 6-7: RSFD connection detail and customization for tank application integration

The design of the Resilient Slip Friction Damper (RSFD) includes versatile connection details that can be adjusted to accommodate existing tanks, an example shown in figures 6-8 to 6-10. This adaptability ensures that the RSFD can be effectively integrated with a variety of tank designs. Additionally, the RSFD's performance characteristics can be fine-tuned to align with the principles of capacity design, taking into account the existing

connection capacities of the tanks. This tuning process allows for a tailored approach to enhancing seismic resilience, ensuring that the RSFD complements and reinforces the structural integrity of the existing tank infrastructure.

Figure 6-8: Example of existing tank connections

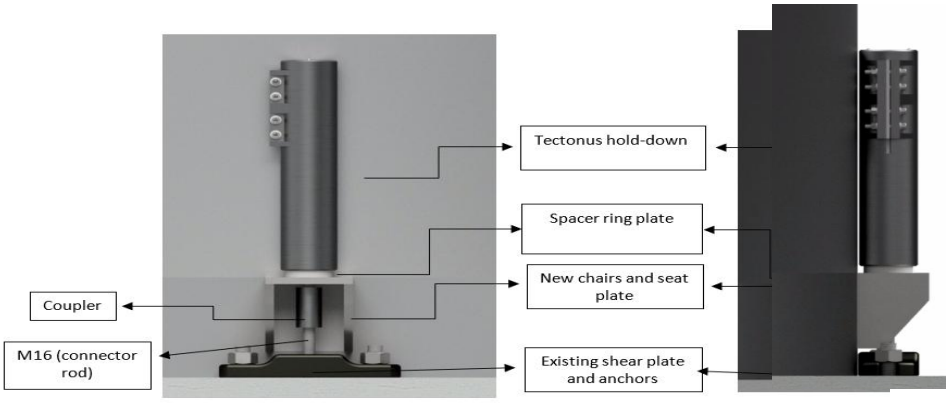

Figure 6-9: Customized detailing of RSFD for practical application in existing cases

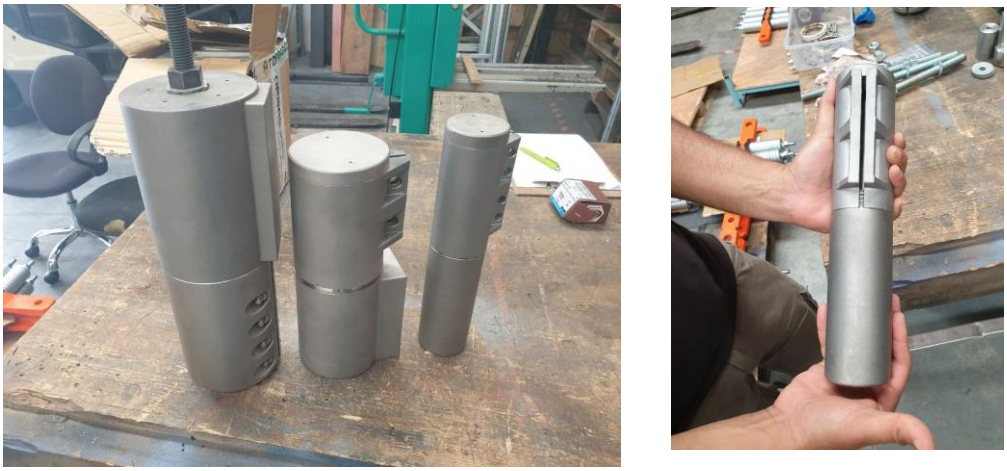

Figure 6-10: Scaled variations of RSFD tailored to tank conditions and capacity design specifications

In the process of optimizing RSFD, a critical aspect is ensuring that the tuning of the joint adheres to the specified service load requirements. This is essential to prevent any undesired sliding or displacement of the joint when it is subjected to normal service loads. The tuning process involves calibrating the joint's characteristics, such as its frictional resistance and pre-stress levels, to align with the operational loads typically encountered during regular use. This calibration ensures that the RSFD joint remains stable and functional under routine conditions, thereby maintaining the structural integrity and reliability of the system it supports. A tested sample and results shown in figure 6-11.

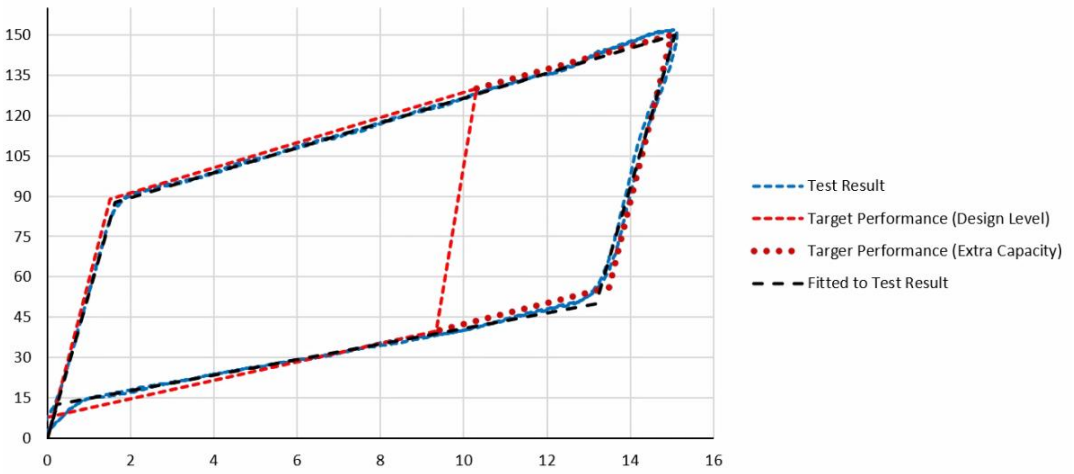

Figure 6-11: Hysteresis loop of tested RSFD

6.3. Case Studies of RSFD Implementation

The Resilient Slip Friction Damper (RSFD) concept has been increasingly recognized and adopted within the wine and dairy industry as a strategic and resilient solution aimed at safeguarding assets. The following section provides a detailed examination of various case studies where this concept has been successfully implemented.

The table presented below provides a summary of the reduction factors achieved by this system compared to the conventional rod system, as evidenced in several analysed real case studies. This compilation offers a critical academic comparison, highlighting the enhanced performance and efficiency of the innovative system in mitigating seismic forces and optimizing structural resilience in practical applications.

Table 6-1:summary of analysed real case studies

Project	K_f Factor (RSFD)	K_f Factor (Rod)	H/D	Seismic Force Reduction
125 KL Wine Tank	0.52	0.77	1.9	33%
175 KL Wine Tank	0.54	0.77	2.2	29%
310 KL Wine tank	0. 5	0.77	1.7	35%
250 KL Dairy Silo	0.46	0.86	3.6	52%

6.3.1. Case Study 1: 310 KL Wine Tanks

The 310 wine tank project represents a real-world application, providing a concrete example to assess the effectiveness of the Resilient Slip Friction Device (RSFD) as an anchorage system (Figure 6-12). This practical implementation serves as a crucial study in contrasting the RSFD with traditional anchorage systems. The project highlights the RSFD's capabilities in enhancing seismic resilience, especially in industrial settings where seismic impacts are a significant concern. By focusing on this tangible project, the study offers insights into how the RSFD can effectively reduce seismic-induced structural damages and maintain operational integrity in large storage tanks, demonstrating its practical advantages in terms of safety and cost-efficiency.

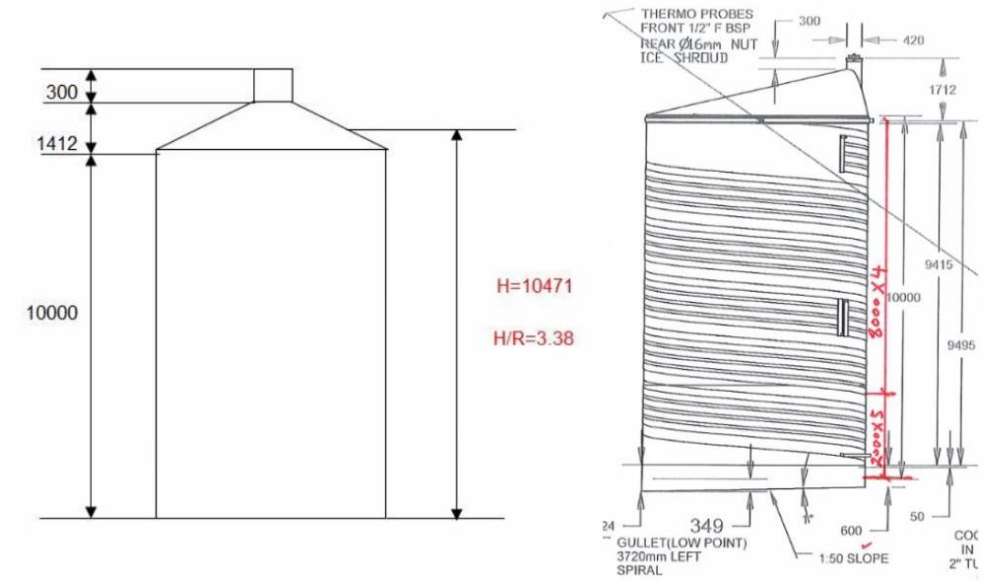

Figure 6-12: Schematic view of 310 KL wine tank

Table 6-2:Overview of Tank Specifications and Seismic Design Parameters

Tank volume	310 KL
Tank Height	10471 mm
Tank diameter	6200 mm

Hazard Factor	0.33
Soil Type	D
Importance Level	2
Design Life	50 Years
S_p	1
μ (Necked Rod AS)	2
μ (RSFD AS)	6
N (D,T)	1
Return Period	1
Weight of shell and roof	99 KN
Content Weight (Wine-Full)	337.9 KN

To examine the dynamic effects, a non-linear dynamic time-history analysis was conducted using a suite of seven pairs of ground motions (Figure 6-13). These motions were scaled to align with the NZS.1170.5 spectrum, considering a return period of $R\mu$ = 1, soil type D, and Z = 0.33.

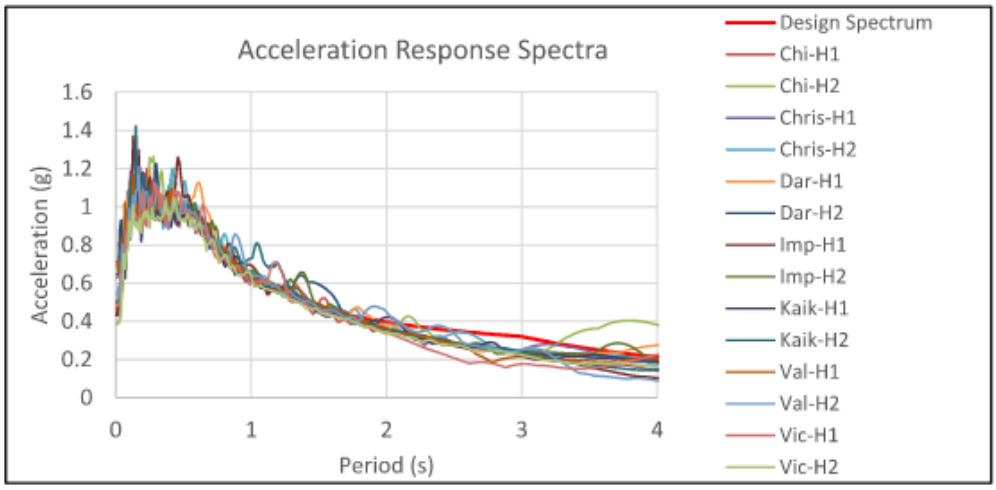

Figure 6-13: Scaled selected ground motions

As shown in Figure 6-14, the RSFD performance has been modeled based on following flag-shape through the friction spring link element in ETABS software.

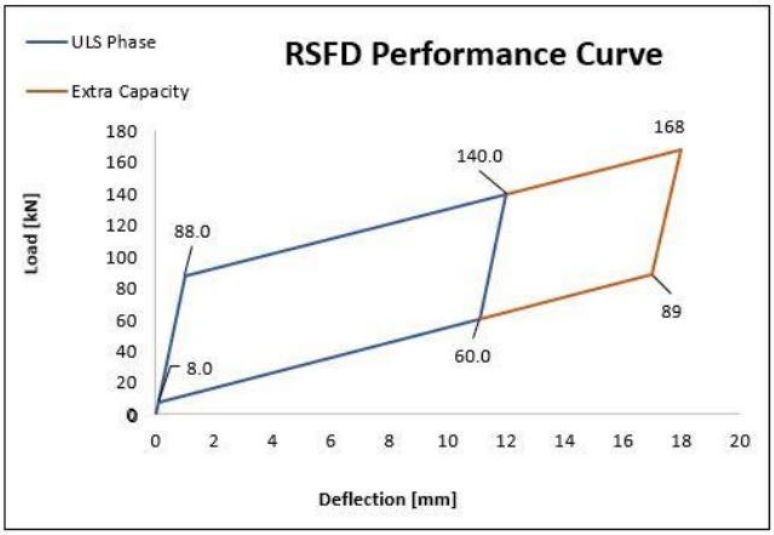

Figure 6-14: RSFD hysteresis performance

In order to augment the resilience of the RSFD, the joint's maximum deflection capacity was deliberately engineered to reach 18 mm, as indicated by the red line in Figure 8-14. This capacity represents a 50% increase over the Ultimate Limit State (ULS) deflection, which stands at 12 mm. Subsequently, the joint's maximum force capacity was established at 168 kN, amounting to 120% of the predetermined design force capacity of 140 kN. As a consequence, the resultant over-strength factor for the capacity design of both the tank barrel and the foundation is determined to be 1.2.

The implementation of the RSFD in this project led to a reduction in the overturning moment by 40% compared to the traditional necked rod system. This reduction was

quantified by a decrease in the kf value from 0.75 (with a μ value of 2) to 0.46. However, for the purposes of this project, a slightly more conservative kf value of 0.52 was chosen. This value is cautiously higher than those suggested by the Time-history and Pushover analyses. The project employed 12 RSFD units, each with a force capacity of 140 kN at the Ultimate Limit State (ULS) level, corresponding to a 12 mm deflection. These units were utilized in the tank anchorage system.

The RSFD in this study was engineered to possess a deflection capacity of 1.5 times the Ultimate Limit State (ΔULS) deflection, equating to 18 mm. Observing a 20% increase in the RSFD force from the design displacement at ΔULS to the maximum displacement, the overstrength factor (OSF) is determined to be 1.2. This is slightly lower than the 1.25 OSF characteristic of necked rods. Consequently, the ultimate force imposed on the RSFDs is calculated to be 168 kN, derived from 1.2 times the base value of 140 kN. In the design of both the tank barrel and the foundation for this project, an OSF of 1.2 has been adopted.

Considering the reduced demand transferred to the tank system, the design of the tank barrel can incorporate thinner plates, presenting a cost-effective solution. Additionally, the diminished overturning moment exerted on the foundation implies a potential for material savings. This approach not only enhances the structural integrity of the system but also contributes to economic efficiency in terms of material utilization and overall construction costs.

6.3.2. Case Study 2: 175KL Wine Tanks

In another practical case study, a 175 KL wine tank was specifically designed for a winery located in Blenheim (Figure 6-15). The specifications of this project are summarized as follows:

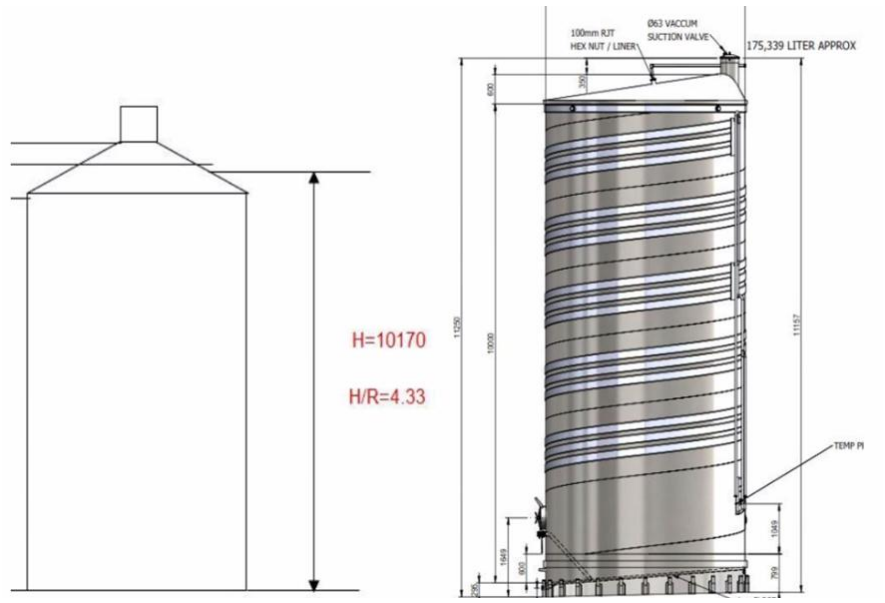

Figure 6-15: Schematic view of 175 KL wine tank

Table 6-3:Overview of Tank Specifications and Seismic Design Parameters

Tank volume (KL)	175
Tank Height (mm)	10170
Tank diameter (mm)	4700

Hazard Factor	0.33
Soil Type	d
Importance Level	2
Design Life	50
Sp	1
Kf (Necked-Rod AS)	0.767
Kf (RSFD AS)	0.5
N	1
Return Period	1
Vessel Empty Weight (kg)	99KN
Content Weight (Wine-Full) (kg)	337KN

The comparative analysis conducted is based on the average outcomes derived from employing a suite of seven pairs of ground motions. As a result of this analysis, the Kf factor for the RSFD anchorage system was determined to be 0.77. This is in contrast to the Kf factor of 0.54, which was observed for the necked rod anchorage system. An RSFD system was implemented as the anchorage mechanism for the wine tank shown below.

Figure 6-16: Implemented RSFD as anchorage system for wine tanks

6.4. Case Study 2: 125KL Wine Tank

In a similar practical example, a 125 KL wine tank was custom-designed for a winery, demonstrating the adaptability and scalability of such projects to meet specific needs. The detailed specifications for this project are outlined below. This case highlights the tailored approach in designing and engineering wine tanks to suit the unique requirements and capacities desired by different wineries.

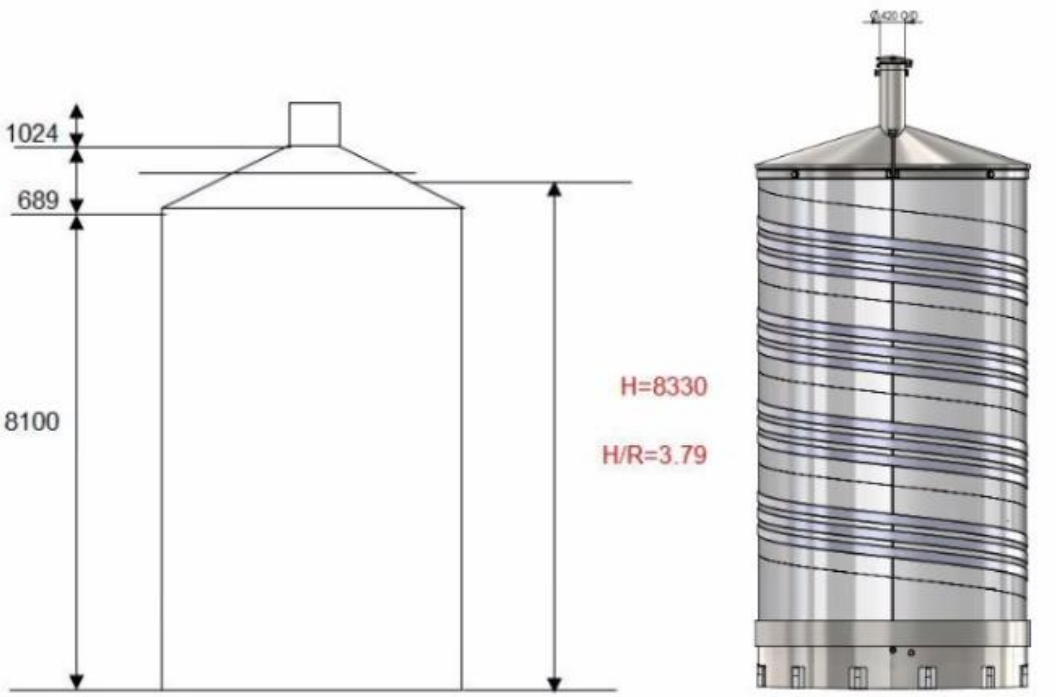

Figure 6-17: Schematic view of 125 KL wine tank

Table 6-4:Overview of Tank Specifications and Seismic Design Parameters

Tank volume (KL)	125
Tank Height (mm)	8330
Tank diameter (mm)	4400

Hazard Factor	0.33
Soil Type	d
Importance Level	2
Design Life	50
Sp	1
Kf (Necked-Rod AS)	0.77
Kf (RSFD AS)	0.52
N	1
Return Period	1
Vessel Empty Weight (kg)	7600
Content Weight (Wine-Full) (kg)	136250

Consistent with other studies, the comparative analysis for this project was also based on averages obtained from using a suite of seven pairs of ground motions. The analysis revealed that the Kf factor for the RSFD anchorage system was established at 0.77. This figure stands in contrast to a Kf factor of 0.52, which was noted for the conventional necked rod anchorage system, highlighting the differences in performance between the two systems. An RSFD system was implemented as the anchorage mechanism for the wine tank shown below.

Figure 6-18: Implemented RSFD as anchorage system for wine tanks

6.5. Case Study 2:250 kL Dairy Tank

The Resilient Slip Friction Damper (RSFD) system demonstrates a broad applicability across various sectors utilizing steel cylindrical tanks. The adaptability of this system is further exemplified in the subsequent case study focused on the dairy industry. This particular case involves the implementation of the RSFD system in a slender dairy tank (Figure 6-19), providing an insight into the system's flexibility and effectiveness for diverse tank designs.

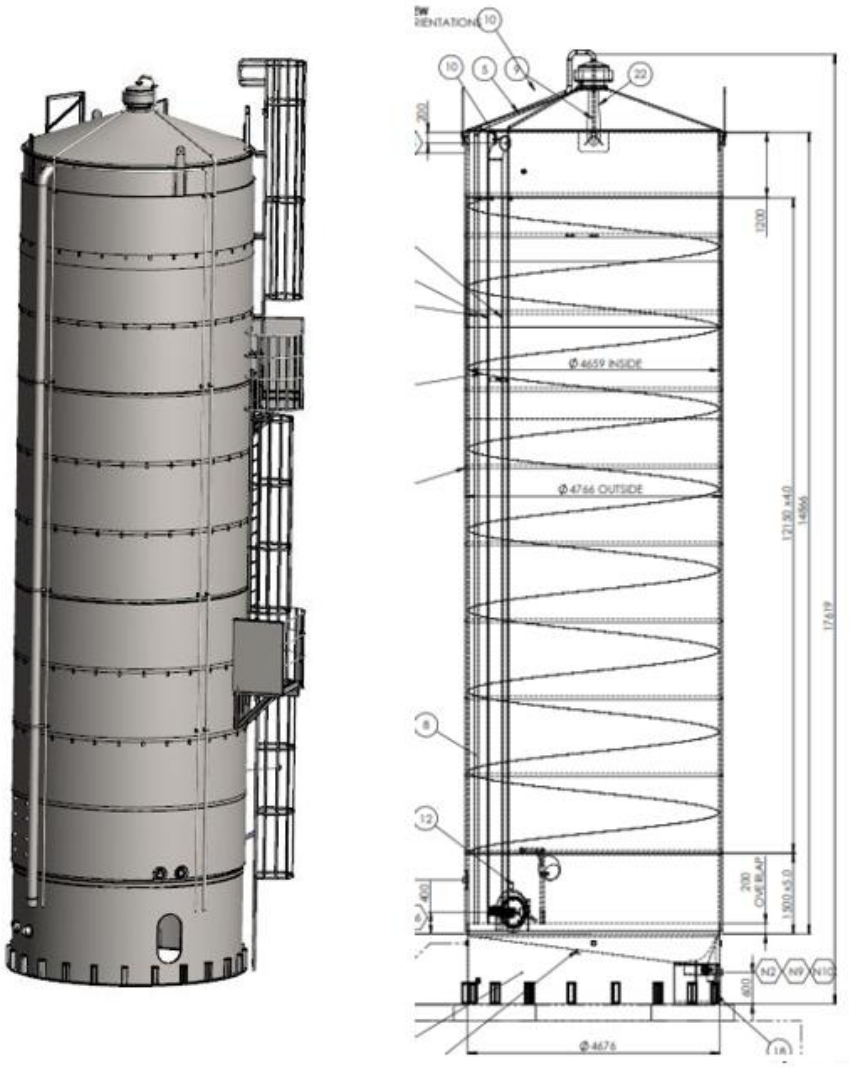

Figure 6-19: Schematic view of 125 KL wine tank

Table 6-5:Overview of Tank Specifications and Seismic Design Parameters

Seismic Factor	
Ru	0.75
Z	0.16
Soil Type	D

Tank Specs		
Diameter	4659	mm
Height	14866	mm
Skirt height	1700	mm
Skirt thickness	6	mm
First tier (1500 mm)	4	mm
Upper tiers	3	mm

The tank's wall and foundation in this project were designed to withstand seismic forces that are 46% lower when using the RSFD system, which has a Kf factor of 0.43. This is in comparison to a higher Kf factor of 0.77 associated with the traditional rod anchorage system.

6.6. References

1. Mohammadi Darani, F., Zarnani, P., Quenneville, P.J.H., & AUT Ventures Limited. (2021). Structural Connector. United States Patent Application Pub. No. US 2021/0123257 A1.

Chapter 7: Earthquake-proofing of Storage Tanks: Using an Innovative Damage-free Anchorage System

K. Sahami[1], P. Zarnani[2], P. Quenneville[3]

(1) PhD student, Dept of Built Environment Engineering, Auckland University of Technology, New Zealand, kaveh.sahami@aut.ac.nz
(2) Lecturer, Dept of Built Environment Engineering, Auckland University of Technology, New Zealand, pouyan.zarnani@aut.ac.nz
(3) Professor, Dept of Civil and Environmental Engineering, University of Auckland, New Zealand, p.quenneville@auckland.ac.nz

Paper published at 17th World Conference on Earthquake Engineering, 17WCEE.

7.1. Abstract

The enhancement of seismic performance for liquid containers, notably strategic tanks or those containing valuable substances used in industries like winery, dairy, or petrochemicals, has become a focal point in recent years due to the damages and economic losses experienced after severe events. Liquid storage systems, typically anchored to the ground with a limited number of connections, are considered structures with minimal redundancy. Consequently, in these structures, the details of the connections are crucial design factors influencing the force and deflection demands during seismic events. Traditional connections cause tanks to be either fully restrained or freely rocking, often resulting in high forces due to a lack of ductility or substantial displacement demands leading to damage. However, a novel approach involves using partially restrained connections to control both deflection and force at desired levels.

This study introduces a new anchorage system that employs the recently developed Resilient Slip Friction Dampers (RSFDs) as ductile, self-centring hold-downs for liquid storage tanks. This innovative, tension-only, damage-free anchorage mechanism mitigates earthquake forces transmitted to storage tanks by dissipating energy through friction, unlike other common ductile yielding hold-downs. The self-centring feature of this damper also limits the rocking motion of the tank and restores it to its original position, which is crucial for tanks with significant height-to-base aspect ratios. Consequently, this system does not require post-event maintenance and can withstand potential aftershocks. Conventional ductile systems, such as necked rod and buckling

restrained anchorage systems, often have sacrificial elements that experience damage leading to strength and stiffness degradation or even failure in severe cases. While buckling restrained systems were proposed to address this issue, they introduced a new problem by inducing resisting force in the reverse cycle, creating a high compression zone in the tank body and increasing vulnerability to buckling. Essentially, such systems merely transfer the buckling risk from the connections to the tank's barrel.

In this paper, we first conducted experimental component testing to demonstrate the performance of the RSFD. Then, based on these results, to introduce and compare the RSFD anchorage system with other ductile concepts (necked-rod and buckling-restrained systems), we investigated a case study of steel cylindrical storage tanks. An Incremental Dynamic Analysis (IDA) time history analysis was performed, and the results, based on the average of seven ground motions, are presented. This damage-free, tension-only, self-centring mechanism offers more design flexibility than other systems and significantly reduces the force transmitted. Additionally, the paper discusses why a tension-only mechanism should be an essential feature of an anchorage system to prevent buckling failure.

Keywords: RSFD, Resilient Slip Friction Joint, Self-centring, Storage tanks, Energy dissipation

7.2. Introduction

Above-ground cylindrical steel liquid storage tanks are extensively used in various industries, ranging from the petrochemical industry for storage and processing of liquids or liquid-like materials such as oil and liquefied natural gas, to the winery and dairy industries [1]. Depending on the type of liquid and preservation conditions, the design, shape, and volume of these storage tanks vary.

The earliest study of tank behaviour dates back to the work of Housner [2], who pioneered a methodology for assessing seismic actions on storage tanks. In his initial studies, tanks were assumed to be rigid, and the hydrodynamic effect of the liquid was considered in two separate actions: impulsive and sloshing motion. This methodology formed the basis of the American Petroleum Institute (API) Standard provisions (2003, 2007), as well as the New Zealand standards (NZSEE 1986 Red Book and Seismic Design of Storage Tanks NZSEE 2009) [3]. Significant damage to liquid storage tanks during the Chile earthquake in 1960, the Alaska earthquake in 1964, and the Parkfield earthquake in 1966

prompted researchers to thoroughly investigate the causes. They discovered that hydrodynamic pressure significantly depends on the flexible behaviour of tank walls (Veletsos and Yang 1977 [4]; Haroun and Housner 1981 [5]). Veletsos treated the liquid tank as a cantilever beam under horizontal earthquake forces, extending Housner's formulation to consider barrel flexibility and decoupling the impulsive and convective components of liquid motion by their frequency of movement. These factors, dependent on the tank's flexibility and the liquid level, could alter the hydrodynamic pressure pattern along the storage wall and base plate.

Veletsos and Tang (1990) [6] and Malhotra (1995) [7] continued this line of study. Fischer and Rammerstorfer et al. (1979) [8] then considered these findings to propose a design approach for the seismic response of anchored and unanchored liquid storage tanks. Their results were incorporated into Part 4 of Eurocode 8, Annex A (European Committee for Standardization 2006b), providing engineers with guidelines for designing cylindrical tanks. API 650 (American Petroleum Institute 2007) is a standard that focuses on the general design of liquid storage tanks. Specifically, Appendix E of API 650 is dedicated to seismic design, offering provisions for determining seismic actions on containers and calculating tank strength.

The New Zealand Seismic Tank Design Recommendations (Priestley et al. 1986 [9]), first published in 1986, offered pioneering recommendations for seismic tank design, collating existing information from research papers and codes into uniform recommendations covering a range of tank configurations and contents. The NZSEE guidelines were updated in 2009 [3], retaining the same general performance criteria as the Red Book, but with major changes including:

- Adoption of seismic load derivation from NZS 1170.5, the current national standard for seismic loads for buildings in New Zealand.
- A procedure for assessing an appropriate return period factor, Ru.
- Application of a correction factor based on ductility and damping applicable to tank behaviour.
- Limited ductility permitted in steel tanks on grade, generally reducing load demands from previous guidelines.
- Integration with other international design codes.

For this study, the NZSEE 2009 guidelines were employed for the primary design of the steel tank.

7.3. RSFD as an Anchorage System

The Resilient Slip Friction Damper (RSFD) is a friction-based connection featuring a self-centring capability, which enables it to return to its original position after a full expansion phase. The following figure illustrates the components of this connection. This damper, introduced and patented by Darani et al. (2018) [10], exhibits a flag-shaped hysteresis curve. Its stiffness, strength, and nonlinearity are derived from disk springs aligned with a friction mechanism. The friction in the RSFD is generated by clamping the slotted cylinder to the inner shaft using bolts. This induced friction force not only dissipates the input energy but also contributes to the required slip force. The damper's stiffness and self-centring feature are dependent on the disk spring, which is pre-stressed to overcome friction in the reverse cycle, thereby providing the system's resiliency. In this study, the patented RSFD design has been modified to suit tank anchorage storage systems. Figure 6-1 shows the hysteresis performance of the redesigned joint, demonstrating its compatibility and effectiveness in this application.

The following figure represents the constituents of this connection.

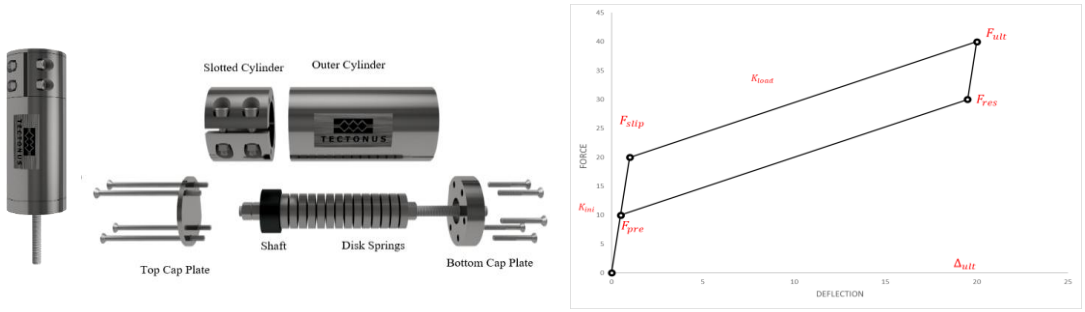

Figure 7-1: RSFD, Assembly of RSFD Joint, RSFD hysteresis behaviour

To verify the performance of RSFD, a component joint with an ultimate capacity of 40 KN and 15 mm deflection has been manufactured and successfully tested. As can be seen in Figure 6-2, the cyclic result represents the fully self-centring hysteresis of the joint.

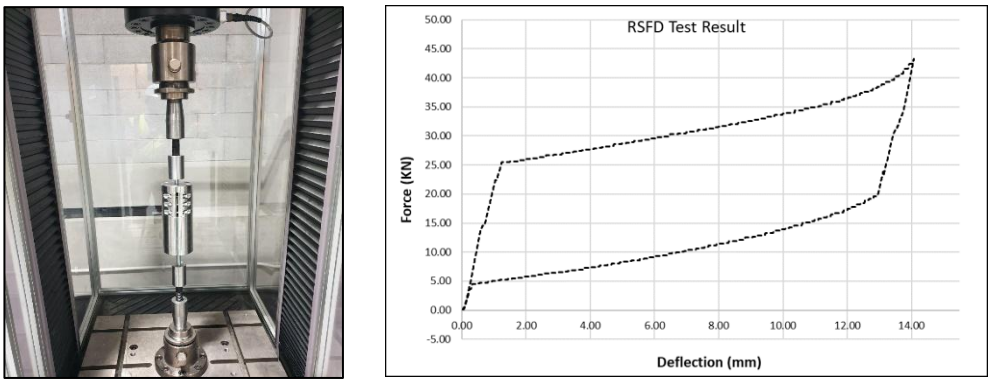

Figure 7-2: Manufactured RSFD connection for cyclic test

7.4. Advantage of Ductile, Tension Only Connections in Storage Tanks System

Conventional anchorage systems (standard or necked rod) experience damage (buckling) in reverse cycle caused strength and stiffness degradation. This flexibility could be satisfied by rod o even the base plate of tanks.

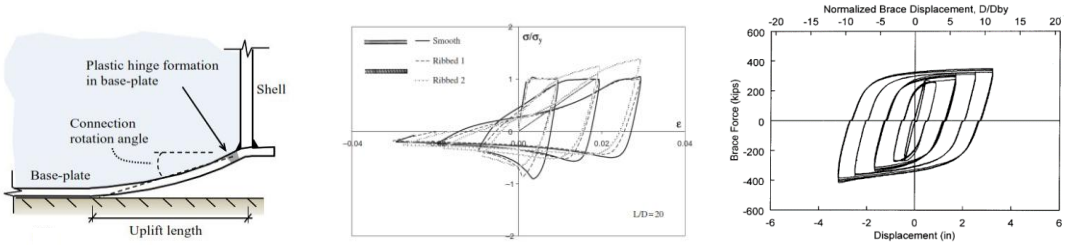

a b c

Figure 7-3: (a) Plastic hinge in the base plate during the uplift [11]; (b) Hysteresis performance of the necked rod [12]; (c) Bucking-restrained mechanism [13]

Stiffness and strength degradation in base connection means different path in each cycle, increment in displacement demand and eventually rupture in the worst-case scenarios. Ductility in such systems comes from material nonlinearity so every component must be checked and then replaced if required when an earthquake strike. To address this issue, the idea of bucking-restrained mechanism (similar to BRB performance) has been proposed. However, such a performance in tanks anchorage system means the possibility of residual displacement and a need for an external force to bring the tank back when weight resisting moment is not enough. In this situation, two possible scenarios could happen:

- The reverse cycle cannot concur buckling force so there would be residual displacement in base connection.

- The returning force is at a higher level compared to resisting force, so could bring it back, but create a high compression zone in-tank body at the gripping end, which could lead to barrel buckling. So the thickness of the barrel around the high-stress zone must increase to control the buckling mode. That means while the buckling of the anchorage has been controlled, buckling is transferred to the barrel.

Figure 6-4 represents the two possible situations. When there is just a rod, buckling mode of the anchorage system dominates as a weak chain of the system. In rod with sleeve (control bucking mechanism), tank body at the gripping point would be the fuse. Another issue with buckling-restrained connection is lack of enough rotational stiffness due to the sleeve part, which also causes additional induced stress in the tank body.

Figure 7-4: Reported damage in Kaikoura earthquake; (a,b) Barrel buckling; (c) Rod rupture [14]

7.5. Case Study (Steel Cylindrical Storage Tank)

In this research, the performance of anchorage systems in three different cases, including necked rod, buckling-restrained and RSFD anchorage system have been investigated. Assumed seismic coefficients according to NZSEE(2009) for a steel cylindrical tank of twelve-meter height, four-meter diameter and average thickness of 3 are summarized in table 6-1:

Table 7-1: Design Parameters

Hazard Factor	0.4
Soil Type	D
Importance Level	1
Design Life	50 Years

$\mathbf{S_p}$	1
$\boldsymbol{\mu}$	2
$\mathbf{N(D,T)}$	1
Return Period	1

Anchorage system contains 32 $\emptyset 20$ grade of 8.8 necked rods attached with the symmetric arrangement to the skirt. Considering the ductility factor of two and overstrength factor 1.25, the base shear and overturning moment are calculated as 1330 KN and 7425 KN.m. Following the code design approach, considering the flexible and rigid part of the impulsive mode, the seismic mass has been distributed in their corresponded equivalent heights.

$V_i = C_h(T_i)\, N(T_i.D)\, m_i\, g\;\; S_p\, Z\, R_u\, k_f$ Equation 7-1

$C_h(T_i)$: spectral shape factor for the site subsoil type and the relevant mode

$N(T_i.D)$: near-fault factor

m_i : the equivalent mass of tank and contents responding in particular mode of vibration considered.

Z: is seismic zone hazard factor,

R_u : return period factor for the ultimate limit state with tank importance level as determined by Table 6-1

S_p: structural performance factor, to be taken as 1.0.

$k_f(\mu, \varepsilon)$: force reduction due to ductility the effect of damping. This parameter used to compare the effectiveness of the anchorage system performances. Necked Rod Backbone for numerical modelling has been achieved from the result of FEM software (SeismoStruct 2020) based on Menegotto-Pinto steel model verified with .. for rod 100 mm of $\emptyset 20$.

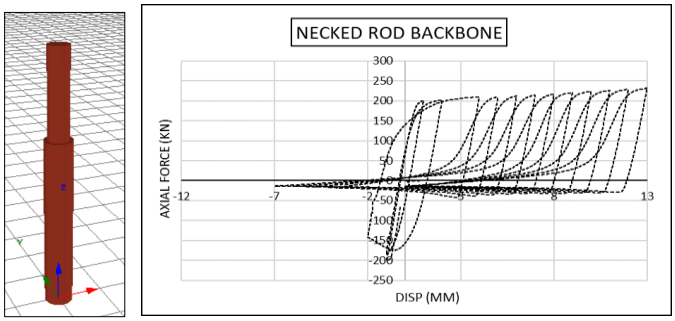

Figure 7-5: Backbone for rod M20 with a length of 100 mm

For the Restrained-Buckling Anchorage System (AS), the calculation of the yielding point is similar to that of the Necked-Rod AS. However, for the RSFD AS, the ductility is provided by the disk spring, which remains undamaged even after the slipping point is reached. Therefore, the only limitation for the slip force in the RSFD AS is to meet the requirements of the service limit state and wind action. In this study, the slip force is considered to be half of the ultimate capacity for the RSFD AS. The hysteretic responses of a single joint and the entire tank for the three anchorage concepts are illustrated as follows:

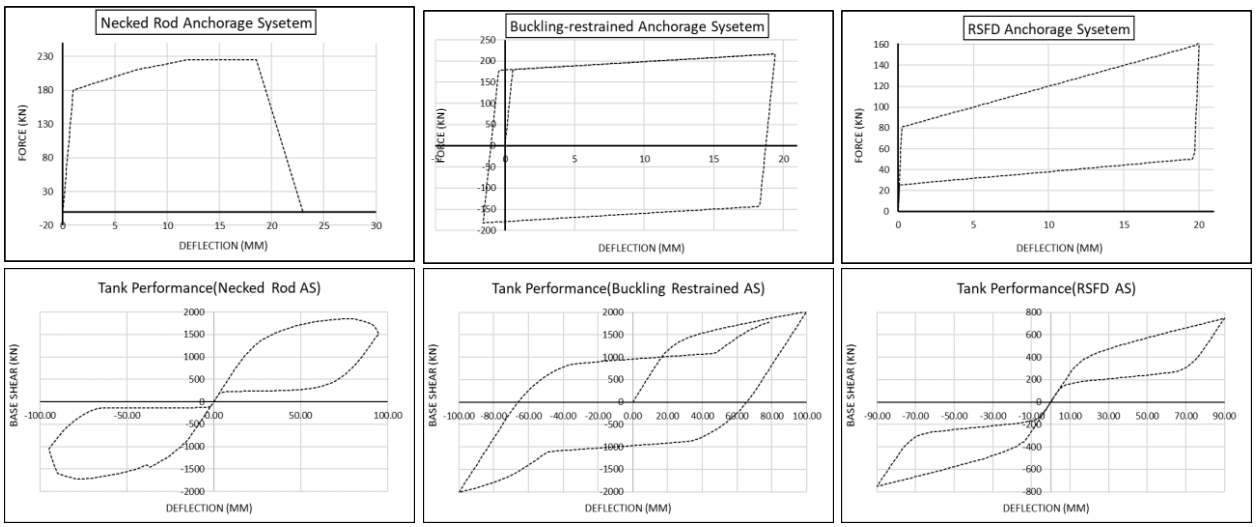

Figure 7-6: The hysteresis behaviour of joints and tanks for three introduced mechanism

7.6. Seismic Performance of Different Anchorage Systems

For non-linear dynamic time-history analyses, a suite of seven ground motions have been scaled to match NZS.1170.5 spectrum with the return period of $R_{\mu} = 1$, soil type D and $Z = 0.4$. The records and scale factors are presented in Figure 6-7.

Earthquake ground motion	PGA
El Centro (1951)	0.3
Landers (1992)	0.74
Northridge (1994)	0.61
Kobe (1995)	0.35
Chi-Chi (1999)	0.36
Bam (2003)	0.16
Christchurch (2011)	0.1

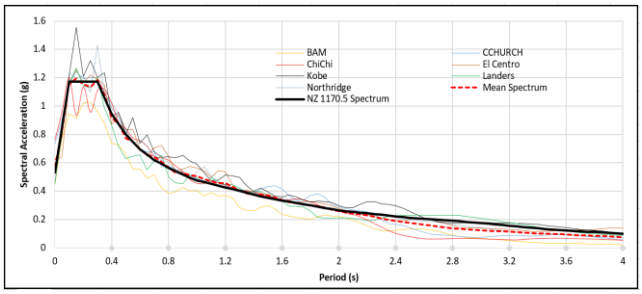

Figure 7-7: PGA and mean spectrum of selected ground motions

In this study, the increment factors for the Incremental Dynamic Analysis (IDA) are selected based on the return periods recommended in NZS 1170.5. This approach is intended to be representative of various scenarios involving different importance factors and annual probabilities of exceedance. Furthermore, all results are presented as averages from seven of the aforementioned records. The calculated averages of base shear, ranging from scale factors of 0.25 for Service Level Seismic (SLS) to three times the Ultimate Limit State (ULS) level, are derived as follows:

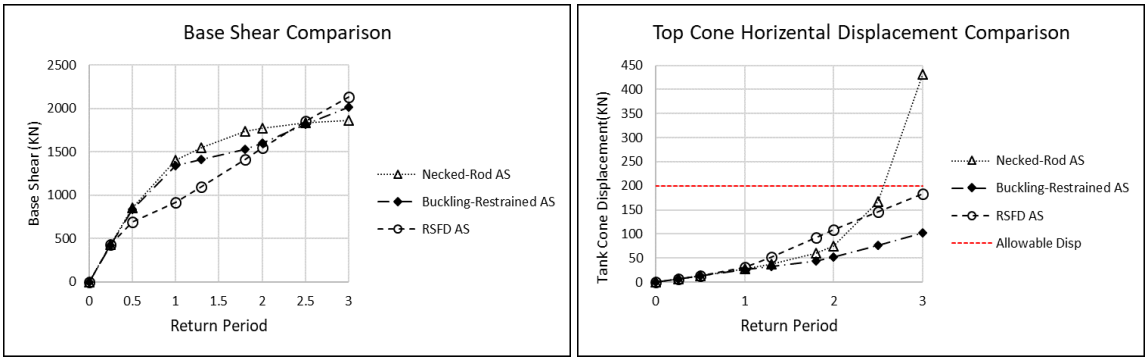

Figure 7-8: Base shears and top tank's cone displacements subjected to seven selected records

As observed, the necked-rod system has a k_f value of 0.8, as recommended by NZSEE (2009), corresponding to an equivalent ductility factor (μ) of 2. This value is almost identical to that of the buckling-restrained anchorage system. However, for the RSFD system, the k_f value is 0.53, indicating a force reduction of approximately 33% compared to the other two mechanisms. At the Service Level Seismic (SLS) level (R_μ=1), the force level remains below the slippage point, indicating that the considered slip force is adequate. Overall, the results are influenced by the effective stiffness and damping ratio of the systems.

In the higher range of scale factors, particularly beyond 2, the buckling-restrained system offers a higher range of damping, resulting in a lower range of transmitted force. While this range may not be practical for tank design, it is noteworthy. However, the increased damping provided by the nonlinearity of material typically leads to damage and residual

displacement in the connections. In the case of the necked-rod system, higher scale factors could lead to rupture due to stiffness and strength degradation.

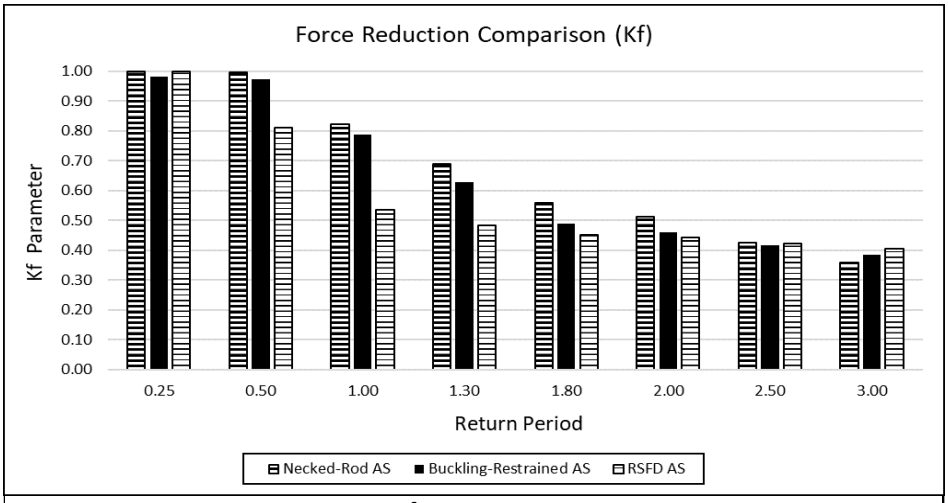

Kf Comparison			
Scale Factor	Necked-Rod AS	Buckling-Restrained AS	RSFD AS
0.25	1.00	0.98	1.00
0.50	1.00	0.97	0.81
1.00	0.82	0.79	0.53
1.30	0.69	0.63	0.48
1.80	0.56	0.49	0.45
2.00	0.51	0.46	0.44
2.50	0.43	0.42	0.42
3.00	0.36	0.38	0.40

Figure 7-9: k_f based on NZSEE 2009 [5]

Another crucial aspect in the design of seismic-resistant tanks involves controlling tank displacement. This is especially important when considering other equipment attached to the tanks, such as catwalks and pipelines. The top cone displacements for both anchorage systems are illustrated in Figure 6-10. In this study, the upper allowable limit for maximum horizontal displacement, as recommended by the API, is set at 200 mm. As the results indicate for $R_\mu = 1$ the top cone displacement is almost the same across all cases. However, as the scale factors increase, a noticeable difference in displacement emerges. The hysteresis performances of the tank subjected Kobe record under two scale factors of $R_\mu = 1$ & 2.5 are depicted in the following figures:

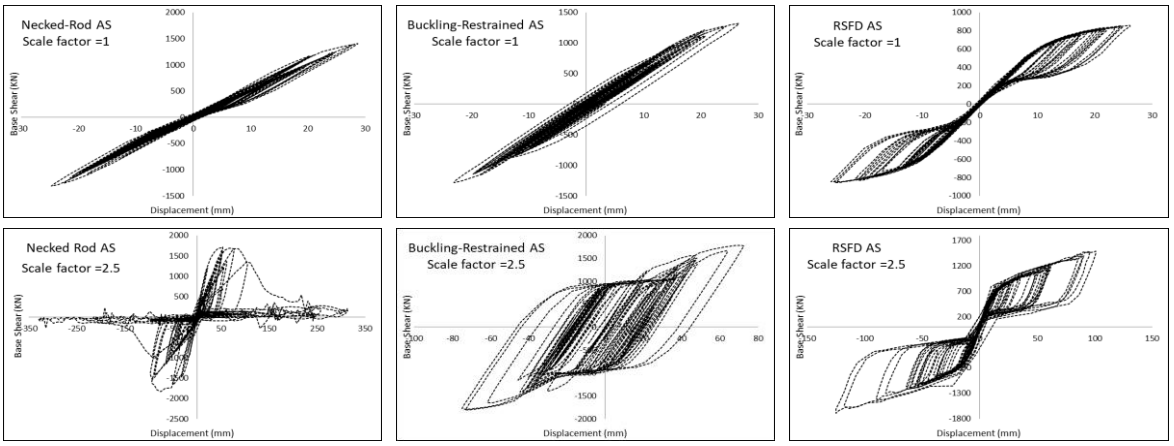

Figure 7-10: Tank hysteresis for the investigated anchorage systems subjected to Kobe record

7.7. RSFD Design and Over-Strength Factor

Considering the result of the time history analysis for the case with $R_\mu = 1$, which is particularly relevant for dairy and winery storage tanks, the specifications for the Resilient Slip Friction Damper (RSFD) have been determined. In this scenario, a k_f value of 0.53 is achieved for the RSFD, as opposed to the previously considered value of 0.8. This adjustment in the RSFD specifications reflects the specific seismic requirements for these types of storage tanks.

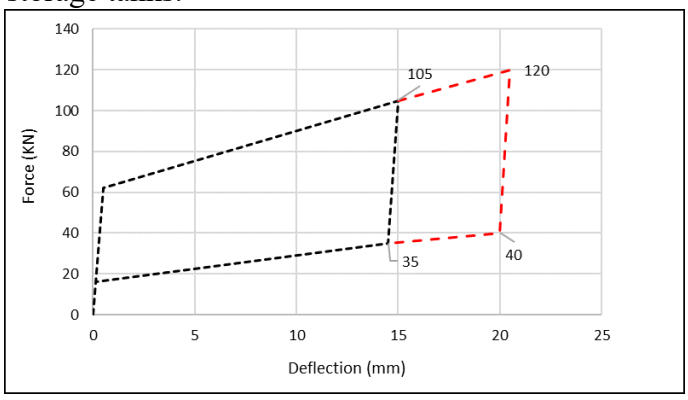

Figure 7-11: RSFD Re-designed force-displacement capacity

To accommodate the deflection capacity required for the Maximum Considered Earthquake (MCE) level, and considering a scale factor in comparison to the Ultimate Limit State (ULS) level, the joint deflection capacity for the RSFD system is designed to be 20 mm. This results in an over-strength factor of 1.15, which is crucial for designing the tank's barrel. In comparison, the over-strength factors for the necked-rod and buckling-restrained mechanisms are typically 1.25 and 1.4, respectively. It should be noted that all comparisons are based on the assumption of damage occurring in the sacrificial elements of the necked-rod or buckling-restrained systems.

Recent consecutive strong ground motions, such as those experienced in Kaikoura, New Zealand (2016) and California, US (2019), have underscored the importance of minimizing the time and cost required for the rehabilitation of structures. This is particularly crucial for structures like storage tanks, which typically have a lower degree of redundancy and are therefore more sensitive to seismic events.

7.8. RSFD Slip Force

In the initial design phase of the RSFD system, the slip forces were set to be half of the ultimate capacity at the Ultimate Limit State (ULS) level. However, given that this anchorage system possesses self-centring capabilities, the slip force can be adjusted as long as the system does not experience slippage before reaching the Service Level Seismic (SLS) earthquake level and during wind-induced effects. A lower slip force results in reduced effective stiffness and increased damping, both of which decrease the forces transmitted to the structure. However, this also leads to an increase in deflection levels. To assess the impact of varying slip force ranges, several scenarios were defined and analysed. The results of these evaluations are presented as follows:

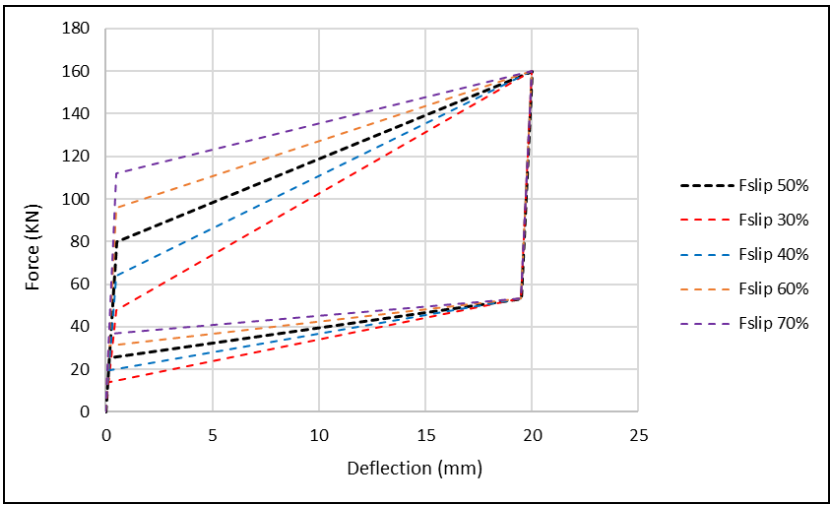

Flip/Fult	Kf	Base Shear (KN)	Top Cone Disp (mm)
30%	0.49	855	43.0
40%	0.52	888	35.4
50%	0.53	918	31.5
60%	0.57	983	28.8
70%	0.63	1071	28.2
80%	0.68	1158	28.4
90%	0.73	1242	28.2

Figure 7-12: RSFD hysteresis behaviour with different slip force and comparison of different varieties of slip force

The observed trends are illustrated in the Figure 6-13. It is noted that increasing the slip force results in a decreased force reduction within the system. However, for higher levels (exceeding 60%), the tank displacements converge and stabilize at the same level.

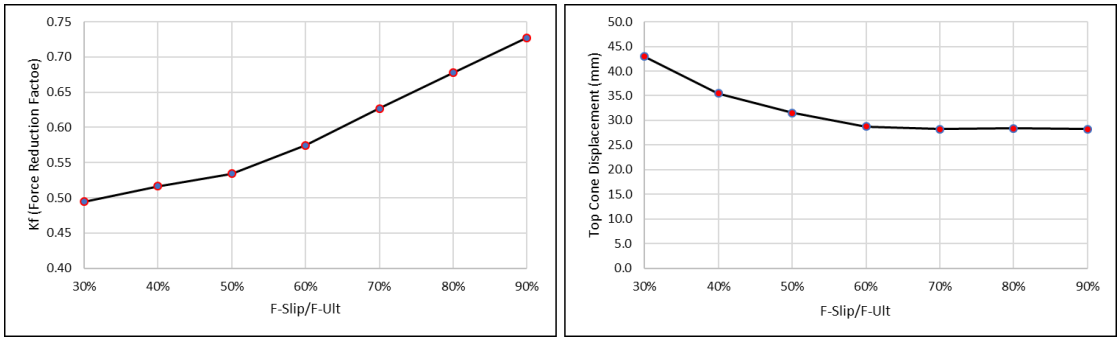

Figure 7-13: k_f and displacement of the tank for different slip force ratio

7.9. RSFD Dissipation Input Energy

As discussed, the damping energy capability significantly influences both the force reduction factor and the deflection demand. Figure 6-14 includes graphs that display the cumulative energy dissipated by the RSFD during an earthquake. As shown, nearly half of the input energy to the structure is dissipated by the connections through a safe friction mechanism, which results in no damage to the anchorage connectors. To provide a comparative analysis, Figure 6-15 illustrates the cumulative energy dissipated by other systems in relation to the total input energy. These results are based on the average of the selected records. It is revealed that for scale factors less than 1.5, the RSFD, having a lower slipping point, can offer a higher damping rate compared to other systems. However, for higher scale factors, buckling-restrained systems dissipate more energy.

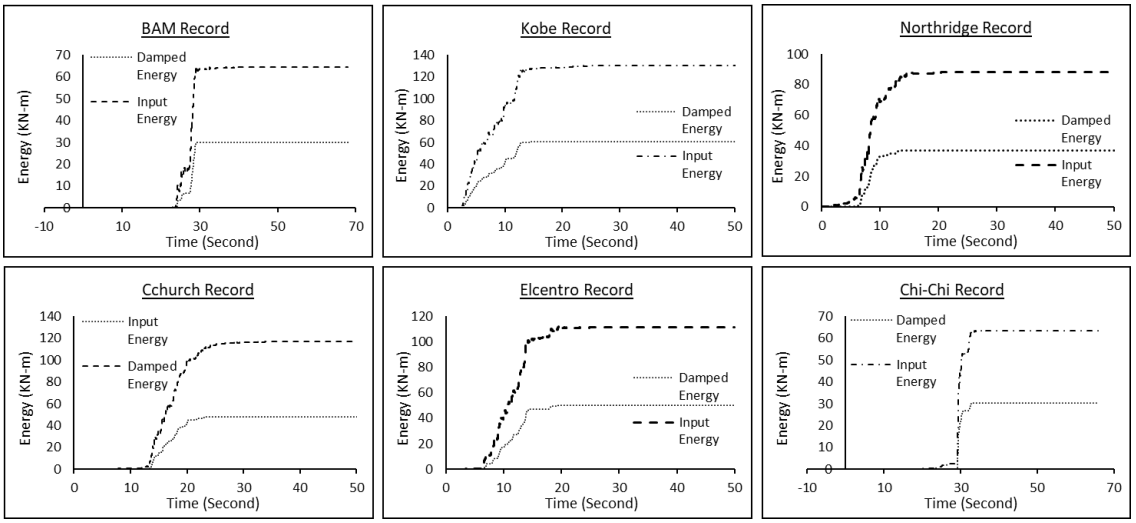

Figure 7-14: Comparison of accumulative dissipated energy by the connections to the total input energy

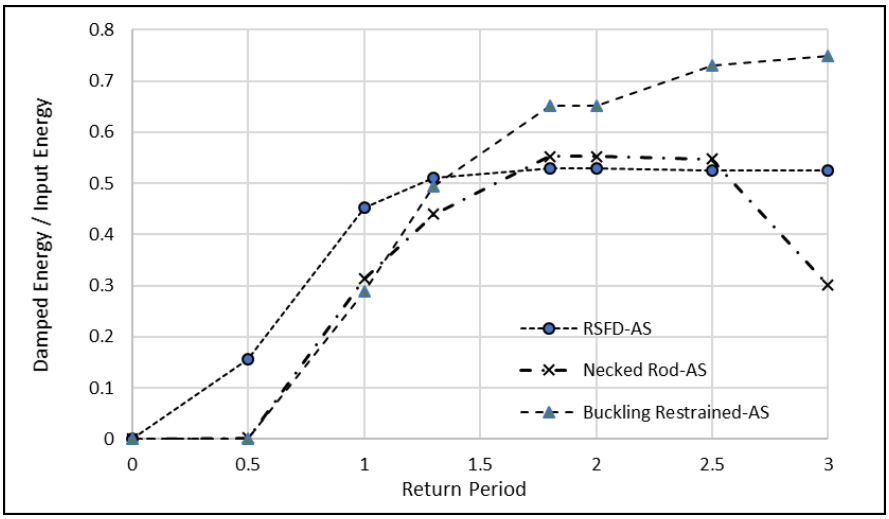

Figure 7-15: Comparison of dissipated energy to total input energy in different anchorage systems

7.10. Residual Displacement of Different Anchorage Systems

In the case of the RSFD anchorage system, there is no residual displacement observed post-earthquake. For the necked-rod system, as long as the tank avoids rupture and collapse during the seismic event, it is expected to return to its original position due to the weight moment, since the unloading stiffness is negligible. However, residual drift is a concern for the buckling-restrained system, as it requires a significant restoring force to reposition the structure.

The results, based on the average of all seven ground motions, are summarized in Table 6-2. This table presents the maximum, minimum, and average values of residual displacement, along with the ratio of residual to maximum displacement, specifically considering the connections. The data indicate that at least 30% of the maximum displacement remains as residual drifts in the connections, necessitating external force post-earthquake to reposition the storage tanks. Furthermore, the findings suggest that damage is not limited to a small number of joints at the corners undergoing rocking motion. A considerable number of connections may require replacement after seismic events.

Table 7-2: The displacement demand of buckling-restrained joints

Ru	Links Max Displacement (mm)	Links Min Displacement (mm)	Links Average Displacement (mm)	Links Ratio of Residual Displacement to Displacement
1	1.98	0.69	1.44	0.31
1.3	3.61	1.46	2.62	0.39
1.5	4.79	1.98	3.55	0.40
1.8	7.07	2.89	5.35	0.35
2	8.82	3.66	6.75	0.33

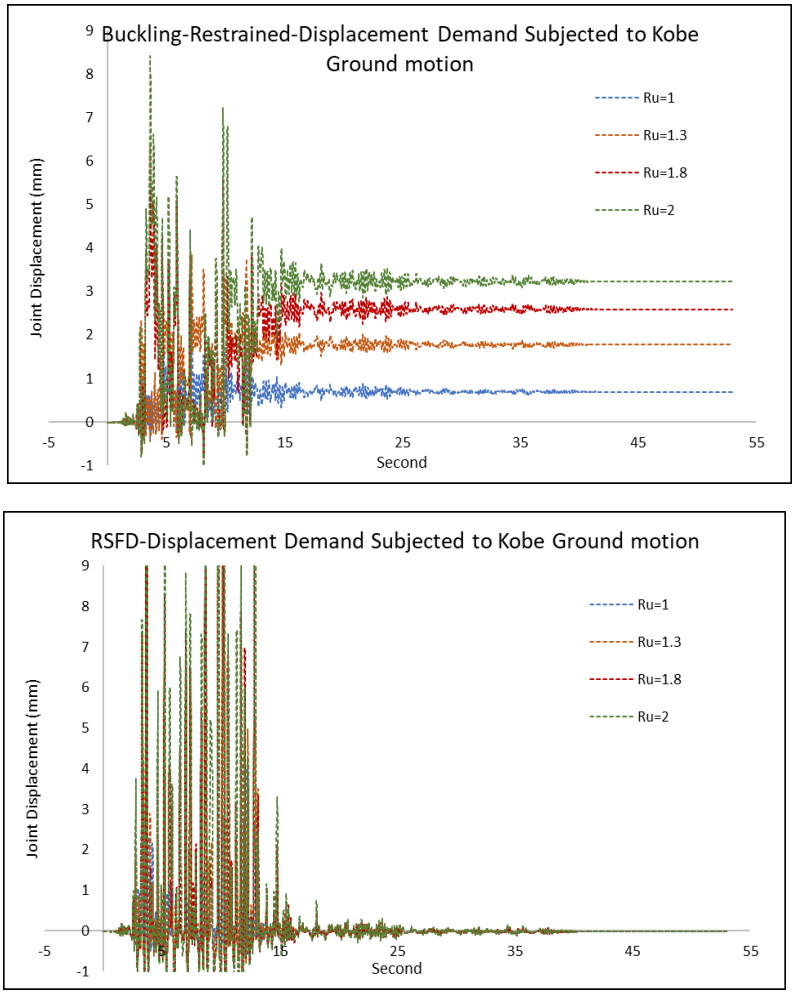

Figure 7-16: Time history of buckling-restrained and RSFD joint subjected to Kobe record

7.11. Conclusion

In this paper, we introduce a new generation of self-centring friction dampers (RSFDs) as an anchorage system for steel cylindrical storage tanks. Building on the RSFD patent, a component joint was redesigned, experimentally tested, and its performance both analytically and numerically evaluated. A case study involving a cylindrical tank with an aspect ratio of three was conducted to compare the performance of the RSFD with two conventional ductile anchorage systems: the necked-rod and buckling-restrained systems.

The paper discusses the importance of tension-only performance in anchorage systems. This feature is crucial to prevent the introduction of a compression zone at the gripping point on the tank body, which can lead to buckling issues in the barrel plate. The RSFD (for $R_\mu = 1$) reduces the overturning moment ($k_f = 0.53$)by 33% more than the other two systems while maintaining a similar displacement demand. The overstrength factor for the RSFD system, accommodating 20 mm displacement demand, is 1.15 compared to 1.25 for necked rods and 1.4 for buckling-restrained connections.

Analyzing a range of RSFD slip force ratios, it was observed that displacement demands for slip forces above 60% are almost at the same level, while k_f increases. Therefore, this range is recommended as the upper limit for slip forces. Lower slip forces also imply greater energy dissipation, with the RSFD system exhibiting a higher dissipation ratio at a 50% ratio compared to other systems.

The RSFD stands out as the only damage-free mechanism without stiffness or strength degradation. As long as the force demand remains below the design level, the entire system stays within safe margins, preparing the tank for potential aftershocks or future seismic events. Thus, the RSFD is unique in its self-centring capabilities, offering long-term cost savings as the only damage-free anchorage system.

It should be highlighted that, in line with other ground-motion-based studies and with respect to the outcomes of time-history analyses, the results presented herein are influenced by the selection of earthquake records and may vary if different ground motions, source regions, or scaling approaches are adopted.

7.12. References

1. Vamvatsikos, D., & Cornell, C. A. (2002). Incremental dynamic analysis. *Earthquake Engineering & Structural Dynamics, 31*(3), 491-514.
2. Vathi, M., & Karamanos, S. A. Liquid storage tanks: Seismic analysis. In *Encyclopedia of Earthquake Engineering*.
3. Housner, G. W. (1957). Dynamic pressures on accelerated fluid containers. *Bulletin of the Seismological Society of America, 47*(1), 15-35.
4. New Zealand Society for Earthquake Engineering (NZSEE). (2009). Seismic design of storage tanks.

5. Veletsos, A. S., & Veletsos, A. S. (1977). Earthquake response of liquid-storage tanks.
6. Haroun, M. A., & Housner, G. W. (1981). Seismic design of liquid storage tanks. *Journal of the Technical Councils of ASCE, 107*(1), 191-207.
7. Veletsos, A. S., & Tang, Y. (1990). Soil-structure interaction effects for laterally excited liquid storage tanks. *Earthquake Engineering & Structural Dynamics, 19*(4), 473-496.
8. Malhotra, P. K. (1995). Base uplifting analysis of flexibly supported liquid-storage tanks. *Earthquake Engineering & Structural Dynamics, 24*(12), 1591-1607.
9. Fischer, D. (1979). Dynamic fluid effects in liquid-filled flexible cylindrical tanks. *Earthquake Engineering & Structural Dynamics, 7*(6), 587-601.
10. New Zealand National Society for Earthquake Engineering, & Priestley, M. J. N. (1986). Seismic design of storage tanks: Recommendations of a study group of the New Zealand National Society for Earthquake Engineering. The Society.
11. Darani, F. M., Zarnani, P., Haemmerle, E., Hashemi, A., & Quenneville, P. (2018). "Application of New Resilient Slip Friction Joint for Seismic Damage Avoidance Design of Rocking Concrete Shear Walls." New Zealand Society for Earthquake Engineering (NZSEE) Conference.
12. Prinz, G. S., Nussbaumer, A., & Cortes, G. (2012). Fatigue analysis of unanchored steel liquid storage tank shell-to-base connections during earthquake induced uplift. In *Proceedings of the 15th World Conference on Earthquake Engineering* (15WCEE).
13. Prota, A., De Cicco, F., & Cosenza, E. (2009). Cyclic behaviour of smooth steel reinforcing bars: Experimental analysis and modeling issues. *Journal of Earthquake Engineering, 13*(4), 500-519.
14. Fahnestock, L. A., Sause, R., & Ricles, J. M. (2006). Analytical and large-scale experimental studies of earthquake-resistant buckling-restrained braced frame systems. *ATLSS Reports, Report No. 06-01*.
15. Loporcaro, G., Dizhur, D., Simkin, G., Garrettson, M., Palermo, A., & Ingham, J. (2017). Performance of winery facilities during the 14 November 2016 Kaikoura earthquake. *Bulletin of the New Zealand Society for Earthquake Engineering, 50*.

Chapter 8: Using an Innovative Seismic Resilient Anchorage System for Industrial Tanks and Vessels

K. Sahami[1], P. Zarnani[2], P. Quenneville[3]

(1) PhD student, Dept of Built Environment Engineering, Auckland University of Technology, New Zealand, kaveh.sahami@aut.ac.nz
(2) Lecturer, Dept of Built Environment Engineering, Auckland University of Technology, New Zealand, pouyan.zarnani@aut.ac.nz
(3) Professor, Dept of Civil and Environmental Engineering, University of Auckland, New Zealand, p.quenneville@auckland.ac.nz

Paper published at Pressure Vessels & Piping Conference PVP2021.

8.1. Abstract

Conventional storage tanks are either fully restrained by hold-down connections or left unanchored, allowing free rocking motion during an earthquake. This often results in high seismic forces due to a lack of ductility, or significant displacement demands from uplift, leading to tank damage. However, a more efficient approach could be using partially restrained connections to control both the deflection and force at desired levels.

In this paper, we introduce an innovative anchorage system that employs the Resilient Slip Friction Damper (RSFD) as a ductile, self-centring hold-down mechanism. This new, tension-only, damage-free anchorage system mitigates the seismic forces transmitted to storage tanks by dissipating the input energy through friction, without experiencing any damage, in contrast to other common ductile yielding hold-downs.

In this study, based on the numerical modeling of the tanks and the performance of the hold-downs (validated experimentally), a comparison has been conducted between the RSFD anchorage system and other ductile concepts, such as necked-rod and buckling-restrained systems. This comparison considers three case studies with different tank aspect ratios. The proposed system is capable of considerably decreasing the transmitted force, leading to a reduced seismic demand for designing both the tank barrel and the foundation.

Keywords: Tank anchorage system, Seismic hold-down, Self-centring Friction damper, Resilient Slip Friction Dampers, RSFD

8.2. Introduction

Aboveground cylindrical steel liquid storage tanks are widely used in various industries, ranging from petrochemical to winery, dairy, food, and beverage, to store and process liquid or liquid-like materials [1].

The initial study of tank behaviour dates back to Housner's work [2], which introduced a methodology for identifying seismic actions in storage tanks. In these early studies, tanks were assumed to be rigid, and the hydrodynamic effect of the liquid was accounted for through two distinct actions: impulsive and sloshing motion. This methodology formed the basis of several standards, including the American Petroleum Institute (API) provisions [3] and the NZSEE Guideline for Seismic Design of Storage Tanks [4]. The extensive damage to liquid storage tanks from the Chile earthquake in 1960, the Alaska earthquake in 1964, and the Parkfield earthquake in 1966 spurred further research. It was discovered that hydrodynamic pressure significantly depends on the tank wall's flexibility [5]. Veletsos and Yu [5] approached the liquid tank as a cantilever beam under the horizontal forces of an earthquake, expanding on Housner's formulation to include the effects of barrel flexibility. They decoupled the impulsive and convective parts of liquid motion based on their movement frequencies, noting that these factors depend on the tank's flexibility and the height of the liquid level, which could alter the hydrodynamic pressure pattern along the storage wall and base plate.

These effects were further studied by Veletsos and Tang [6]. Subsequently, Fischer et al. in 1979 [7] presented a design approach for the seismic response of both anchored and unanchored liquid storage tanks, with their results being incorporated into Part 4 of Eurocode 8, Annex A, by the European Committee for Standardization for the design of cylindrical tanks.

API 650, a standard developed by the American Petroleum Institute for the general design of liquid storage tanks, is widely used in the petrochemical industry for designing and constructing petrochemical reservoirs and facilities. Appendix E of API 650 specifically addresses seismic design, offering provisions for determining seismic actions on containers and calculating tank strength.

According to API 650 and ASCE 7 [8], tanks can be self-anchored or mechanically anchored, but there are limited details on the types of anchorage systems. The New Zealand Seismic Design of Storage Tanks, NZSEE 2009 [4], further refines mechanical

anchor systems based on their ductility and energy-damping capabilities. For instance, if ductility is provided through a necked-rod anchorage system, the tank can be designed with a lower reduction factor compared to a standard rod system. Enhancing the seismic performance of liquid containers, particularly strategic tanks or those containing valuable contents in industries like petrochemical, winery, or dairy, has gained increased attention in recent years due to damages and economic losses in seismic events [9,14].

Post-earthquake damage assessments of wineries in Marlborough, New Zealand, were conducted following the 2013 Seddon earthquake (Mw 6.5), the 2013 Lake Grassmere earthquake (Mw 6.6), and the 2016 Kaikoura earthquake (Mw 7.8). The findings indicated that in 2013, 47% of tank anchors sustained damage, the highest proportion among all failure types observed. In the 2016 earthquake, this figure reduced to 23%, showing improvement in the hold-down systems implemented post-2013. However, damage to the barrel and cone increased from 28% and 14% in 2013 to 54% and 43%, respectively, in 2016. These figures suggest that while hold-downs performed better, damage shifted to other parts, contradicting the intended failure hierarchy. Thus, proper detailing and reliable performance of an anchorage system are crucial for protecting steel storage tanks and their contents.

The aim of this study is to introduce a damage-free hold-down mechanism to reduce the seismic demand on cylindrical steel storage tanks. This system uses a friction mechanism to absorb the input energy, rendering it damage-free at the design level.

8.3. Resilient Slip Friction Damper (RSFD)

The Resilient Slip Friction Damper (RSFD) is a friction-based connection that features self-centring capabilities, enabling it to return to its original position after fully expanding. Figure 7-1 illustrates the components of this proposed device. The internal shaft is clamped by an outer cylinder using a series of bolts, which provide the necessary friction. The slip force in the damper is determined by the prestressing force in the clamping bolts and the stacked disk springs. The self-centring functionality of this connection is dependent on the disk springs, which are pre-stressed to overcome the resisting friction in reverse cycles, thus ensuring the system's resilience. This damper, introduced and patented by Darani et al. [10], exhibits a flag-shaped hysteresis response. It addresses the limitations of conventional solutions by eliminating the need for post-event maintenance and enhancing the system’s ability to withstand aftershocks.

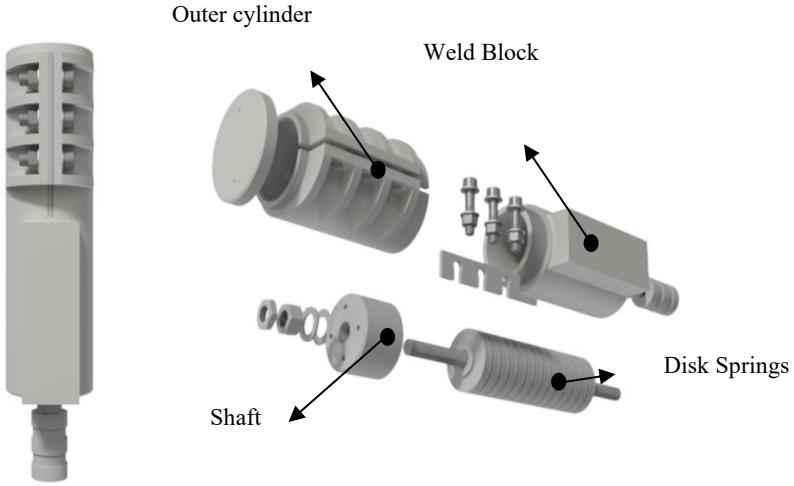

Figure 8-1: 150 KN RSFD

The hysteresis performance of the RSFD system is illustrated in Figure 2. The stiffness following the slip event can be adjusted by modifying the specifications of the disk springs. The enclosed area depicted in Figure 7-2 represents the energy absorbed by the friction mechanism. For this study, we have redesigned the original version of the RSFD for outdoor applications, making it compatible with tank hold-down connections.

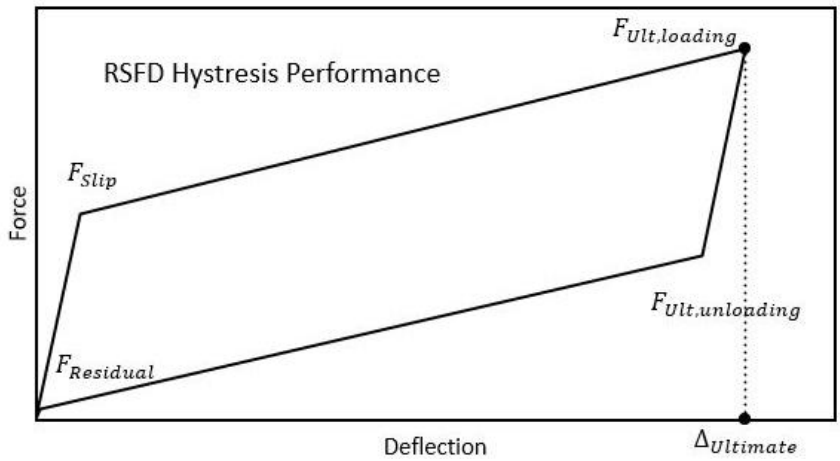

Figure 8-2: RSFD hysteresis performance

8.4. Experimental Test

To validate the performance of the RSFD, a component joint was manufactured with an ultimate capacity of approximately 45 KN and a deflection limit of 15 mm. This

joint has been successfully tested, as depicted in Figure 7-3. The results from the cyclic tests demonstrate the joint's fully self-centring response.

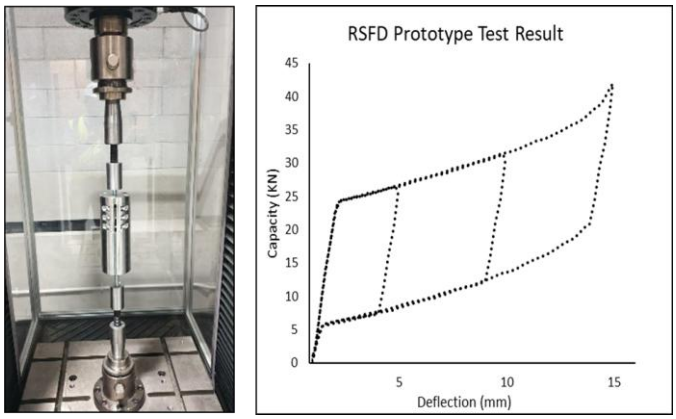

Figure 8-3: RSFD test setup and performance test result [11]

Figure 7-4 presents the test results of the recent version of an RSFD, which is designed with a 150KN capacity and 15 mm deflection for a 175KL wine tank. In this version, a block has been incorporated to facilitate direct welding of the joint to the tank skirt.

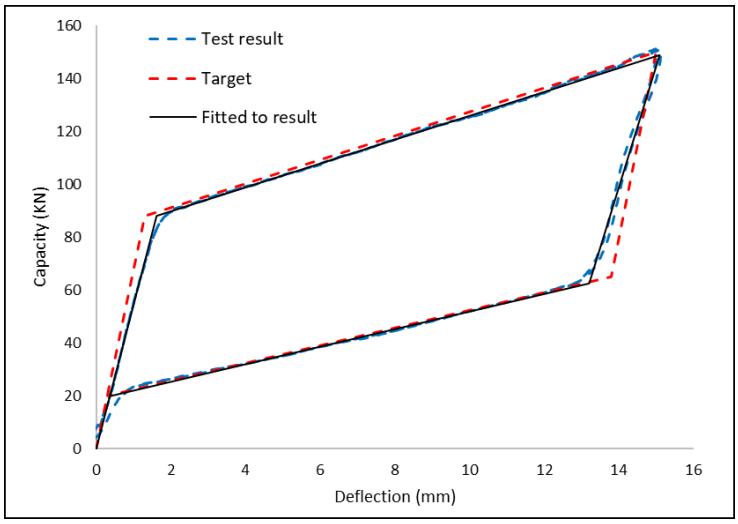

Figure 8-4: Test result of 150 KN RSFD

At the design stage, the target performance was represented by a dashed-red line, while the experimental test result is shown with a dashed-blue line. A curve fitted to these experimental results is depicted in black. As demonstrated in Figure 7-4, the predicted performance closely aligns with the actual performance observed in the test.

8.5. Conventional Ductile Hold-down Mechanisms

Conventional anchorage systems typically comprise a rod anchored to the foundation, which acts as a sacrificial fuse to mitigate damage propagation. Buckling-restrained anchorage systems represent a new generation of these systems. In these advanced

systems, the buckling mode of the rod is controlled to prevent it from buckling when the elongated rod is subjected to compression in the reverse cycle.

8.6. Necked-rod Anchorage System

Figure 7-5 illustrates the hysteresis performance of two types of rods - ribbed and smooth - each with a length-over-diameter ratio of 20 [12]. In this figure, it is shown that a standard rod, including a necked rod, tends to buckle in the reverse cycle. This buckling causes strength and stiffness degradation, a phenomenon known as pinching (as depicted in Figure 7-5). Such degradation leads to varying performance paths in each cycle, an increase in displacement demand, and ultimately, the potential rupture of the rod due to low-cycle fatigue. The ductility in these systems is derived from material nonlinearity. Therefore, after an earthquake, these hold-downs must be inspected and replaced if necessary.

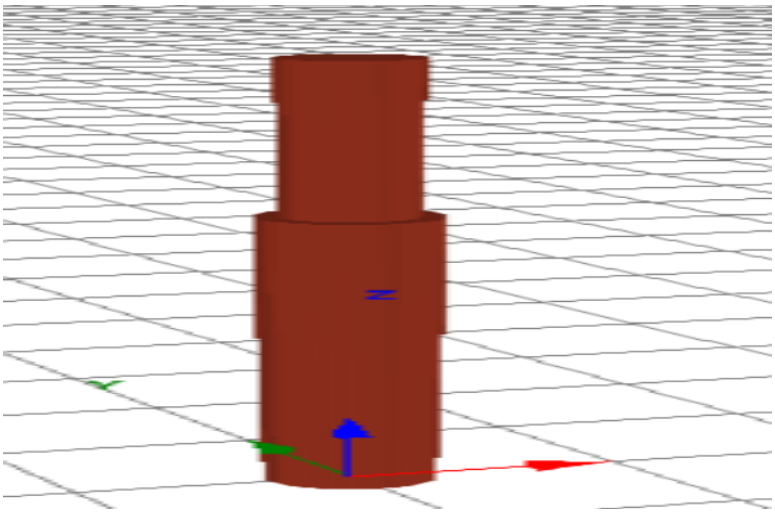

Figure 8-5: Hysteresis performance of the necked rod [12]

8.7. Buckling-Restrained System

Buckling-restrained mechanisms have been developed to control the buckling of the rod in anchorage systems. Typically, this is achieved by enclosing the rod within a sleeve. As depicted in Figure 7-6, this design prevents performance degradation, allowing the connection to maintain load-carrying capacity in both tension and compression.

In tank anchorage systems, such performance implies a potential for residual displacement after severe seismic events. Under these circumstances, two possible scenarios may arise:

- The reverse cycle may not be sufficient to overcome the buckling force of the rod, resulting in residual displacement at the base connection.
- If the returning force is greater than the resisting force, it could reposition the connection but at the cost of creating a high-stress zone on the tank body at the gripping end. This stress might lead to barrel damage. To prevent such failure, the barrel's thickness around the high-stress zone should be increased.

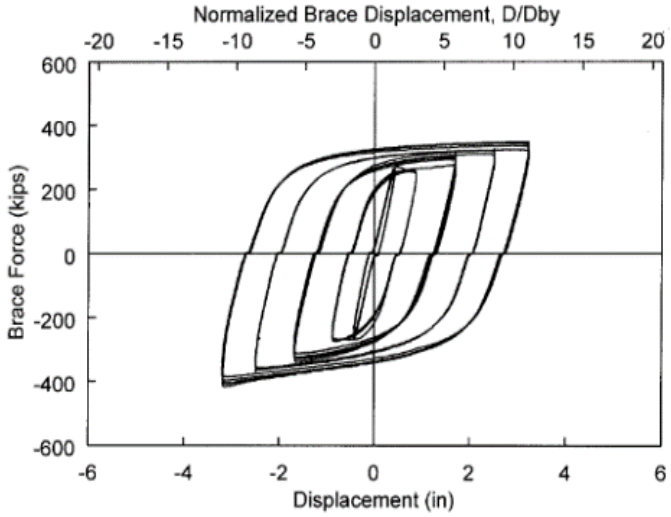

Figure 8-6: Bucking-restrained rod behaviour [13]

8.8. Case Studies

In this research, the performance of necked-rod, buckling-restrained and RSFD anchorage systems have been investigated through three case studies as per the specifications below:

Table 8-1: Case studies tank specifications

Case Study	Capacity (m^3)	H (m)	D (m)	H/D
Case study 1	395	5	10	0.5
Case study 2	295	15	5	3
Case study 3	490	25	5	5

The tanks in these studies are assumed to be located in a zone with a site class of D and a seismic use group I=1. For each scenario, the hold-downs are specifically designed to satisfy the required overturning moment as per the standards set forth in API 650:

$$A_i = \mathrm{S_{DS}}\left(\frac{I}{R_{\mathrm{wi}}}\right) \qquad \text{Equation 8-1}$$

$$T_c \leq T_L: A_c = \mathrm{KS_{D1}}\left(\frac{1}{T_c}\right)\left(\frac{I}{R_{\mathrm{wc}}}\right) \qquad \text{Equation 8-2}$$

$$T_c > T_L: A_c = \mathrm{KS_{D1}}\left(\frac{T_L}{T_c^2}\right)\left(\frac{I}{R_{\mathrm{wc}}}\right) \quad \text{Equation 8-3}$$

$$M_{\mathrm{rw}} = \sqrt{[A_i(W_i X_i + \mathrm{W}_s X_s + \mathrm{W}_r X_r)]^2 + [A_c(W_c X_c)]^2} \quad \text{Equation 8-4}$$

A_i, A_c: Impulsive and convective design response spectrum acceleration coefficient, %g

T_c:Natural period of the convective (sloshing) mode of behaviour of the liquid, seconds

T_L:Regional-dependent transition period for longer period ground motion, seconds

S_{DS}, S_{D1}: The design, 5% damped, spectral response acceleration parameter at 0.2 seconds and one second

I:Importance factor

R_{wi}, $\mathrm{R_{wc}}$: Force reduction factor for the impulsive and convective mode

K: Coefficient to adjust the spectral acceleration from 5 % to 0.5 % damping

S_{D1}: he design, 5 % damped, spectral response acceleration parameter at one second

W_i,W_s,W_r,W_c: Impulsive portion of the liquid weight, weight of tank shell, fixed tank roof, convective portion of the liquid weight

X_i, X_c: Effective Impulsive, convective height

X_s, X_r: Height from the bottom of the tank shell to the roof, shell center of gravity

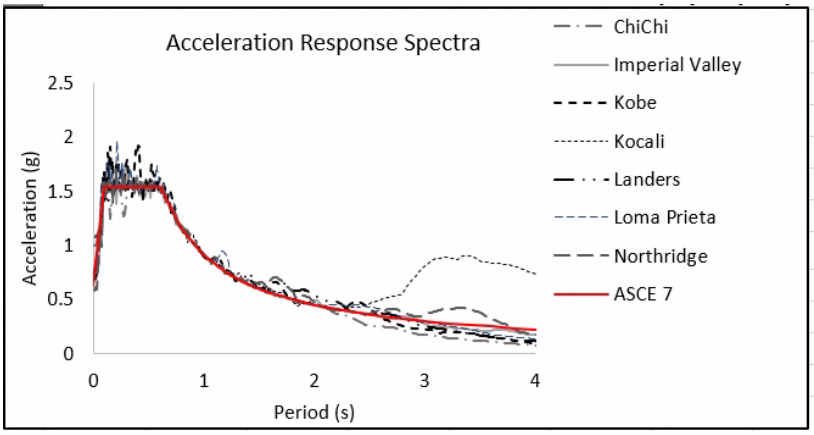

Figure 8-7: Scaled selected ground motions

In subsequent steps, the performance of the tanks was analysed using Nonlinear Time History Analysis (NLTHA). For this analysis, we employed a spring-mass analogy. To conduct the NLTHA, a suite of seven ground motions was scaled to align with the ASCE 7 spectrum, as shown in Figure 7-7. In this study, the walls of the tanks were designed to remain within the elastic range during seismic events, with ductility being provided exclusively through the hold-down system.

8.9. Results and Discussions

The response modification factor (R) constitutes of three terms of ductility (R_μ),damping (R_β) and over-strength factor (R_Ω)[3]:

$$R=R_\mu R_\beta R_\Omega \qquad \text{Equation 8-5}$$

The effectiveness of hold-down systems is quantified in terms of the R factor, which reflects the transmitted forces. Thus, the performance of various anchorage systems is compared based on the resulting R factors. Another crucial parameter is the over-strength factor, which is derived from the R factor and used for the capacity design of connections, the tank body, and the foundation to ensure the intended hierarchy of failure is observed. According to ASCE 7, the over-strength factor for a mechanical anchor system is set at 2. The comparisons presented in the following sections are based on the average results obtained from the selected ground motions.

8.10. Results of Necked-Rod Anchorage System

For the necked-rod system, the hold-downs specifications are summarised in Table 7-2:

Table 8-2: Necked-rod hold-down specifications

Case	Num of hold-downs	Fy (Mpa)	Necked-rod diameter (mm)
Case study 1	20	300	22
Case study 2	28	300	40
Case study 3	46	500	40

The backbones for the necked-rods were derived using results from the FEM software SeismoStruct 2020, and these results were verified with the findings in [12] for rods with a length of 100 mm. An example of this can be seen with the M22 rod, whose backbone is illustrated in Figure 7-8.

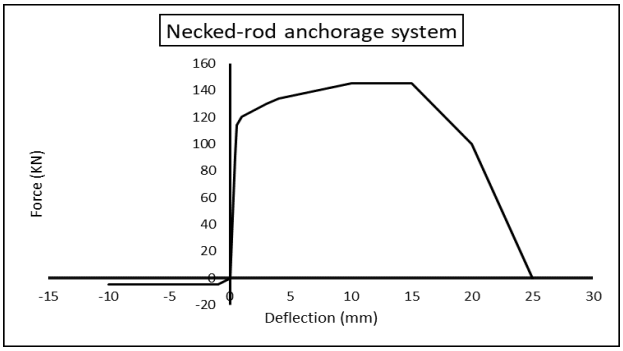

Figure 8-8: The backbone extracted from the hysteresis curve (M22 G300)

In Case Study 2, as an example, we analysed a tank equipped with 28 M40 hold-downs. Figure 7-9 illustrates the tank's hysteretic loop, where the tank was subjected to reversed monotonic loading actions up to the overturning moment demand specified at the design level. The $R_\mu R_\zeta$ factor is calculated based on the ratio of the force demand in an elastic case to that in the assumed ductile system. The R_Ω factor is determined from the ratio of the ultimate force demand (obtained from the analysis) to the yield force established at the design stage (as per the code guidelines).To determine the R_Ω, he records were scaled to match the overturning moment in a fully elastic hold-down system, addressing any potential discrepancies between the numerical results and the code-prescribed values.

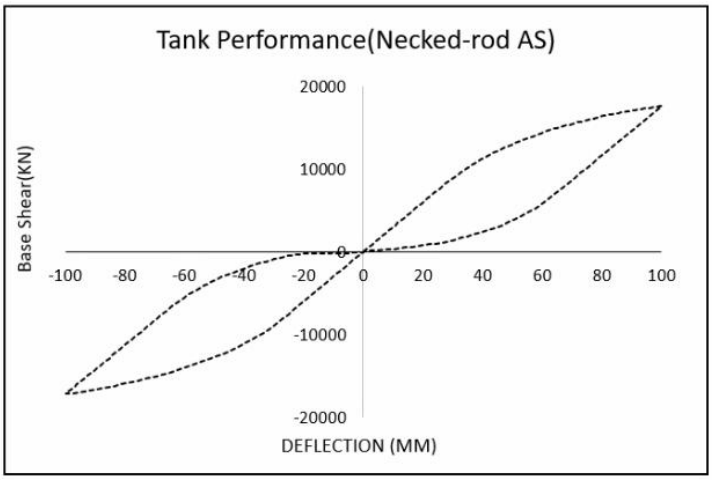

Figure 8-9: The hysteretic response of the tank in Case study 2 (295KL) with 28*M40 necked-rod

The summary of the calculated R factors consisting of $R_\mu R_\zeta$ and R_Ω are illustrated in Table 7-3 for the necked rod system:

Table 8-3: Necked-rod response modification factor

	R (design)	$R_\mu R_\zeta$	R_Ω	$R = R_\mu R_\zeta R_\Omega$
Case study 1	4	1.26	3	3.8
Case study 2	4	1.54	2.61	4.0
Case study 3	4	1.56	2.46	3.9

As illustrated, the R factor is nearly consistent with the rate assumed by the code. However, the R_Ω factors exceed 2, indicating that the actual proportions of ductility, damping, and over-strength factor do not align with the initial assumptions. This discrepancy results in a higher level of force being transferred to the tank body, its connections, and the foundation. For instance, Figure 7-10 shows the hysteresis response of a 490KL tank subjected to the Kocali earthquake.

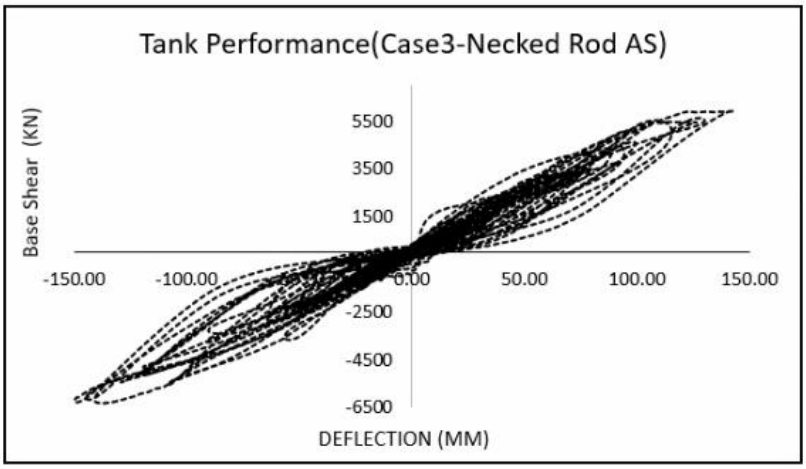

Figure 8-10: The hysteresis response of the tank in Case study 3 (490KL) subjected to Kocali earthquake with 40xM40 necked-rod

8.11. Results of Buckling-Restrained System

In the case of buckling-restrained rods, the calculation of the yielding point follows the same methodology as that for necked rods. In this study, for each of the case studies, a range of R factors between 4 to 6 has been considered.

Table 8-4: buckling-restrained hold-down specifications

Case	R factor	Num of hold-downs	Design capacity (KN)
Case study 1	4	16	118
Case study 1	5	14	118
Case study 1	6	10	118
Case study 2	4	28	295
Case study 2	5	22	295
Case study 2	6	18	295
Case study 3	4	76	295
Case study 3	5	62	295
Case study 3	6	50	295

In the following figures, the backbone of a 295 KN buckling-restrained rod and the result of a pushover analysis of a 295KL tank with 22 hold-downs have been depicted:

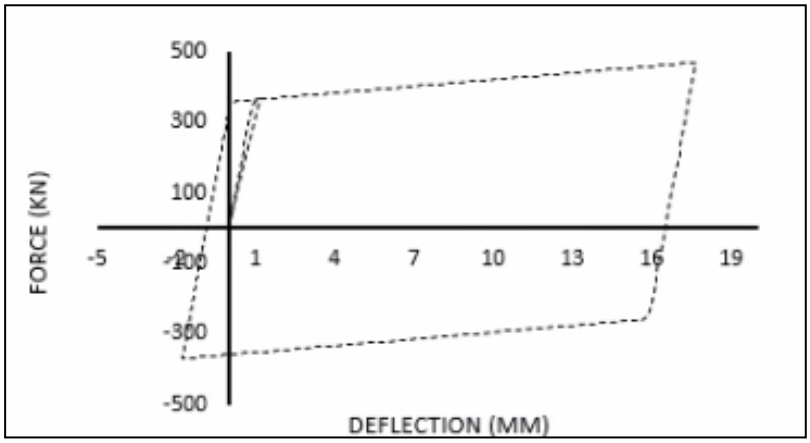

Figure 8-11: The hysteresis behaviour of the buckling-restrained rod used in Case studies 2 and 3

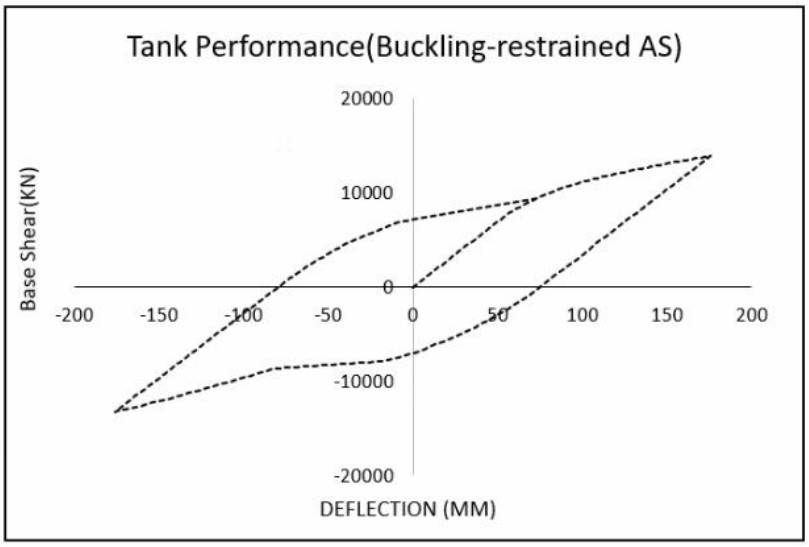

Figure 8-12: The hysteretic response of tank in Case study 2 with 22 of 295 KN capacity buckling-restrained hold-downs

The $R_\mu R_\zeta$ and R_Ω factors derived for this concept are illustrated in Table 7-5. Similar to the necked-rod system, the contribution of the over-strength factor in the R factors is predominantly higher than the assumed value (R_Ω=2), with the exception of Case Studies 2 and 3, which were designed with an R factor of 2. It is also important to note that an increase in the R factor leads to a corresponding increase in the over-strength factor, potentially compromising the safety of the tank designs, especially for broader tanks (e.g., Case Study 1). Therefore, in such scenarios, given that the code restricts the over-strength factor to a maximum of 2, it is necessary to adjust the R factor downwards to prevent damage to the tank and foundation.

Table 8-5: Buckling-restrained hold-down response modification factors

Case	R (design)	$R_\mu R_\zeta$	R_Ω	$R = R_\mu R_\zeta R_\Omega$
Case study 1	4	1.25	3.16	4.0
Case study 1	5	1.29	3.7	4.8
Case study 1	6	1.33	4.2	5.6
Case study 2	4	1.8	2.1	3.8
Case study 2	5	2.05	2.4	4.9
Case study 2	6	2.34	2.53	5.9
Case study 3	4	1.95	2.05	4.0
Case study 3	5	2.06	2.38	4.9
Case study 3	6	2.33	2.53	5.9

As an illustration of the hysteresis behaviour of a tank equipped with buckling-restrained rods, consider the response of the tank in Case Study 3. This study involved a 490KL tank with 50 hold-downs, which was subjected to the Kocali earthquake record. The resulting hysteresis response is depicted in Figure 7-13.

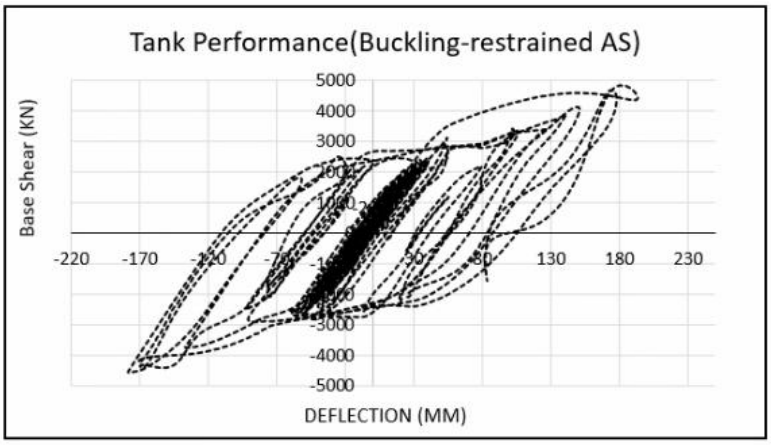

Figure 8-13: The hysteresis response of the tank in Case study 3 (490KL) subjected to Kocali earthquake with 50 buckling-restrained anchorages

8.12. Results of RSFD Anchorage System

The performance of the RSFD is adaptable, allowing for the efficient slip force for each case study to be determined based on the results of numerical analyses. This tunability means that the RSFD connections can be specifically adjusted to meet the deflection limits required by different types of tanks or industry standards. The RSFD connections in this study have been designed with the ultimate limit state in mind, according to the details provided below:

Table 8-6: RSFD hold-down specifications

Case	Num of hold-downs	Design capacity (KN)
Case study 1	14	200
Case study 2	22	300
Case study 3	44	360

As illustrative examples, the responses of an RSFD and the corresponding tank in Case Study 2 are depicted in Figures 7-14 and 15. In the scenarios being studied, the slipping force for the RSFD has been designed to be half of its ultimate force capacity.

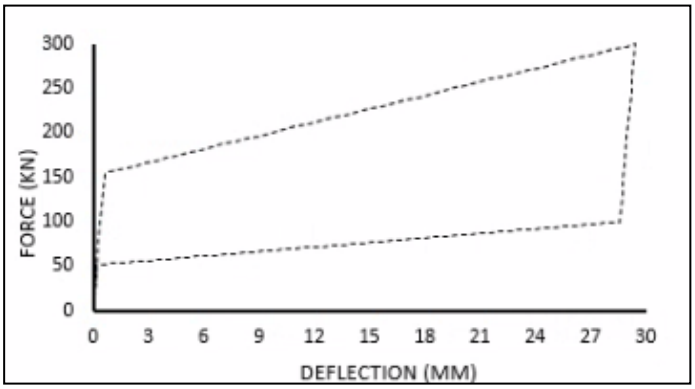

Figure 8-14: The hysteresis behaviour of RSFD used in Case study 2

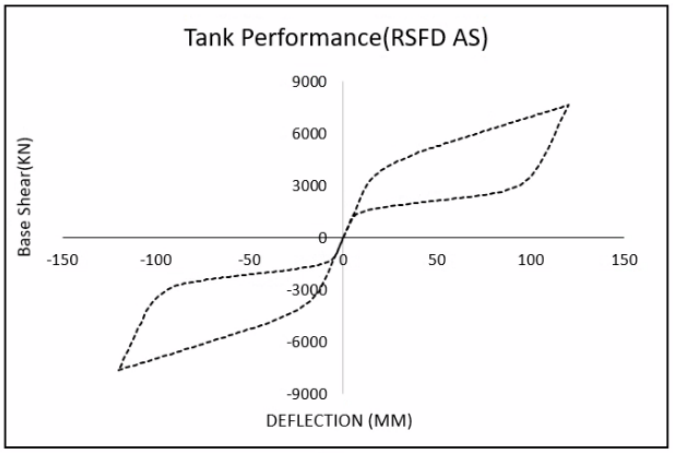

Figure 8-15: The hysteretic response of tank in Case study 2 equipped with 22 RSFDs

Accordingly, the R factors for the RSFD anchorage system are reported in Table 7-7:

Table 7: RSFD hold-down response modification factor

Case	$R_\mu R_\zeta$	$1.4R_\mu R_\zeta$	R_Ω	$R = 1.4\, R_\mu R_\zeta R_\Omega$
Case study 1	1.35	1.89	2	3.8
Case study 2	2.41	3.37	2	6.7
Case study 3	2.75	3.85	2	7.7

To align the R factor of RSFD with the allowable stress design basis of API 650, a conversion factor of 1.4 has been applied to adjust the RSFD's R factor from the strength

design level. In the case of RSFD, the assumed over-strength factor reflects the ratio of the force at the design level to the slip force of the tank. In this study, we've tuned this ratio to be 50%, which yields an over-strength factor of 2. To demonstrate the response of a tank equipped with RSFD hold-downs during seismic activity, Figure 7-16 reports the hysteresis performance of a 490KL tank in Case Study 3, which is equipped with 44 RSFDs.

The resulting over-strength factors for all systems examined in this study are compared in Figure 7-17. It is observed that the conventional anchorage systems achieve the over-strength factor of 2 primarily in cases involving higher aspect ratio tanks with buckling-restrained rods designed for an R value of 4.

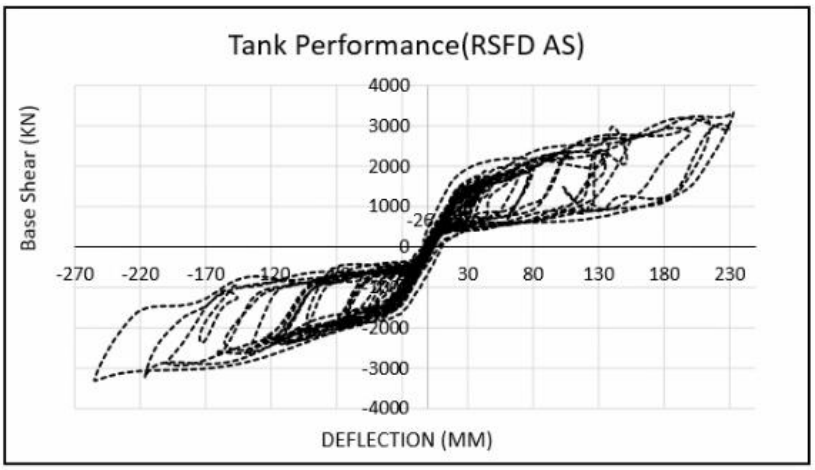

Figure 8-16: The 490KL tank hysteresis response subjected to Kocali record with 44 RSFD anchorages.

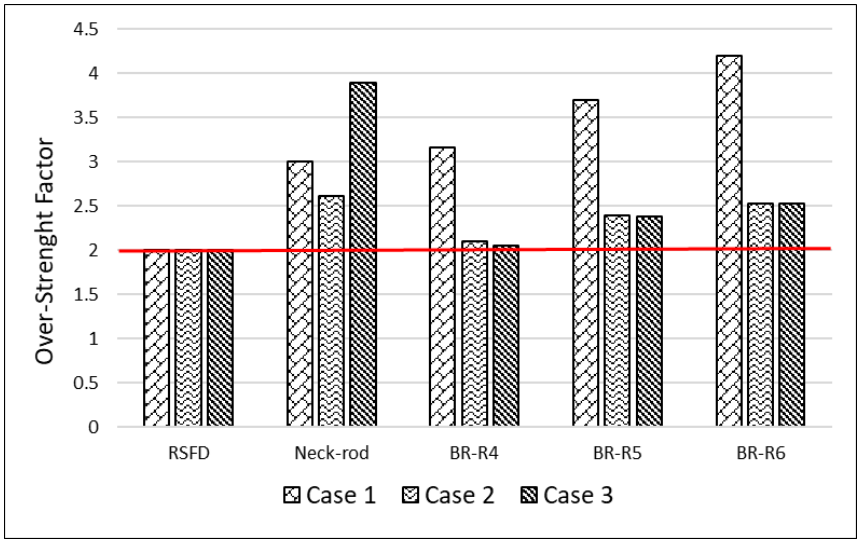

Figure 8-17: Comparison of over-strength factors

Figure 7-18 displays the ratio of R_Ω to R for all the cases studied. This ratio serves as an indicator for evaluating the demand of the overturning moment required in the design of the tank, its connections, and the foundation. Tanks equipped with RSFDs can be designed to withstand at least 30% less seismic demand. Specifically, in Case Studies 1 and 2, the use of RSFDs resulted in a reduction of overturning moment by approximately 30% and 70%, respectively. For Case Study 3, it was observed that the overturning moment demand for systems using necked-rod and buckling-restrained rods is more than double that of the RSFD system.

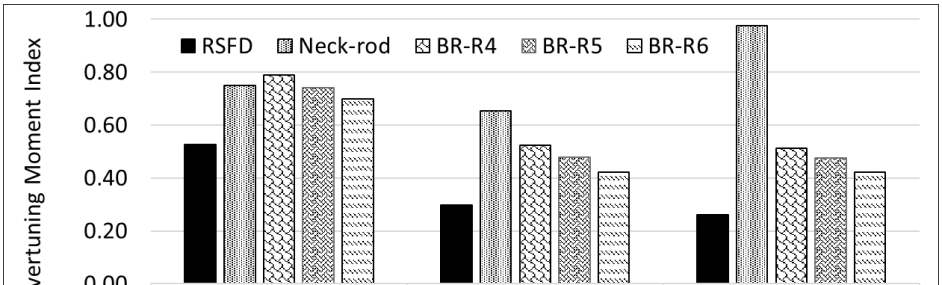

	Case 1	Case 2	Case 3
RSFD	0.53	0.30	0.26
Neck-rod	0.75	0.65	0.98
BR-R4	0.79	0.53	0.51
BR-R5	0.74	0.48	0.48
BR-R6	0.70	0.42	0.42

Figure 8-18: Comparison of overturning moment indices

8.13. Residual Displacement

The RSFD anchorage system is designed to be resilient, effectively restoring a tank to its original position after seismic events. In contrast, the necked-rod anchorage system is likely to buckle during the reverse cycle, although the weight of the tank and its contents can potentially overcome this resistance and reposition the tank. However, residual displacement is a concern with buckling-restrained systems. The extent of this issue is highlighted in Table 7-8, which reports the percentage of residual displacement in the buckling-restrained system as a ratio of its maximum displacement. On average, approximately 32% of the maximum displacement remains as residual deflection in the connections, necessitating external force application post-seismic event to reposition the storage tanks to their initial state.

Table 8-7: Average of residual deflection to maximum displacement in the buckling-restrained hold-downs

R	4	5	6
Case study 1	30%	39%	46%
Case study 2	19%	24%	31%
Case study 3	21%	26%	35%

8.14. Importance of Post-Event Immediate Recovery

Mechanically anchored steel tanks are typically structures with minimal redundancy, anchored to the ground using a limited number of connections. As such, the performance of these hold-downs plays a critical role in determining the level of force and deflection experienced during seismic events. Rod-based anchorage systems, designed to yield at certain stress levels to provide ductility, necessitate immediate recovery after an earthquake. This recovery period leaves the tanks unarmed and highly vulnerable to subsequent seismic activities, including aftershocks.

This vulnerability was notably observed following the Kaikōura earthquake in New Zealand in 2016. In response, a range of winery facilities in the Marlborough region were equipped with tri-axial accelerometers to monitor seismic excitations during aftershocks [13]. This instrumentation aimed to better understand the tanks' responses to such events and aid in developing more resilient anchorage systems.

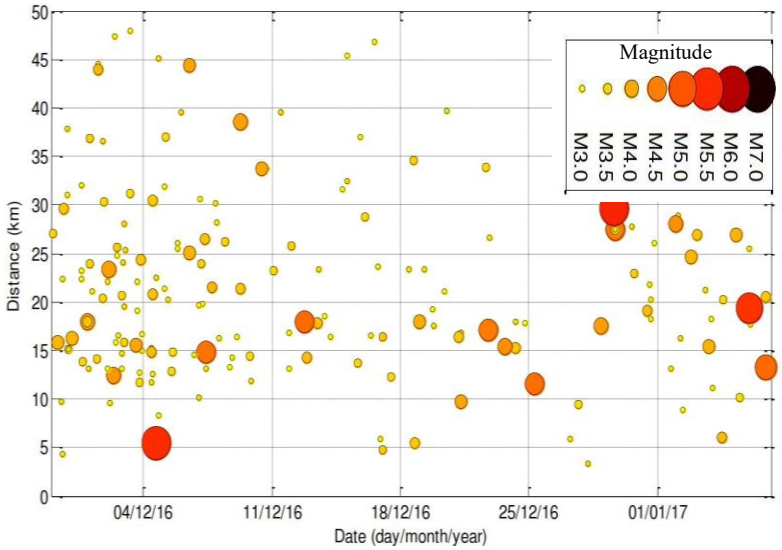

Figure 8-19: Aftershocks recorded from 28 November 2016 to 7 January 2017 - Magnitude of aftershocks within 50 km of Seddon [13]

The accelerometers installed at the winery facilities recorded at least 40 aftershocks, which induced medium to significant levels of shaking in various structures, as evidenced in Figure 7-19. Notably, the most substantial recorded seismic activity occurred during an MW5.49 earthquake on December 4, 2016. This earthquake's epicenter was less than 10 km away from many of the instrumented storage tanks. During this particular event, the recorded accelerations indicated a significant amplification of the acceleration response at the height of numerous storage tanks [13], underscoring the vulnerability of these structures to seismic activity.

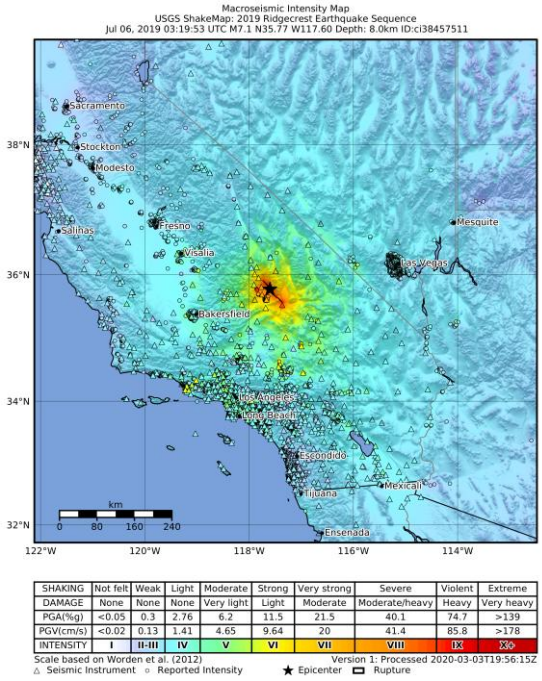

Figure 8-20: ShakeMap for the M7.1 July 5, 2019 Earthquake near Ridgecrest [14]

The magnitude 7.1 earthquake near Searles Valley in eastern California, which occurred approximately 34 hours after a magnitude 6.4 foreshock on July 4, 2019 [14], as depicted in Figure 7-20, exemplifies the challenges faced by tanks using conventional hold-down systems during seismic events. Such events underscore the critical importance of incorporating damage-free connectors in these systems.

Tables 9 and 10 detail the percentages of hold-downs that reached deflections of 10 mm and 20 mm, respectively. A deflection of 10 mm is considered as indicative of reaching 50% of the rupture threshold. The results show that, especially in broader tanks and those designed for an R factor greater than 5, a significant number of rod-based anchors at the design level may fail, leaving the tanks vulnerable to subsequent seismic events. This highlights the necessity for immediate post-event inspections and retrofitting operations.

Implementing damage-free, self-centring connections in these structures can significantly enhance the reliability of the resisting system and minimize the need for post-event maintenance.

Table 8-8: Percentage of hold-downs reached to 10 mm deflection

Case	Necked-Rod	Buckling-restrained Rod		
	R=4	R=4	R=5	R=6
Case study 1	68%	40%	95%	100%
Case study 2	49%	0%	22%	49%
Case study 3	29%	0%	23%	70%

Table 8-9: Percentage of hold-downs reached to 20 mm deflection

Case	Necked-Rod	Buckling-restrained Rod		
	R=4	R=4	R=5	R=6
Case study 1	43%	11%	45%	85%
Case study 2	5%	0%	0%	5%
Case study 3	2%	0%	1%	14%

8.15. Conclusion

In this paper, a new generation of self-centring friction damper (RSFD) has been introduced as a seismic resilient anchorage system for steel cylindrical storage tanks. For this application, a RSFD prototype has been designed and experimentally tested and its performance analytically and numerically investigated. To investigate the performance of this new hold-down system, three cylindrical tanks with different aspect ratios of 0.5, 3 and 5 have been employed and the results were compared with the conventional ductile anchorage systems including necked-rod and buckling-restrained anchorages.

In conventional anchorage systems, even though the R factors assumed at the design stage are verified by the results, there are discrepancies on the assumptions of $R_\mu R_\zeta$ and R_Ω. That means while such a design is safe for designing hold-downs but not for the tank and foundation. In conventional anchorage systems, R_Ω=2 can be satisfied just in case of having buckling-restrained system which is designed for the R factor of 2.

Comparing all the studied cases, the tanks equipped with RSFD system can be designed at least for 30% less overturning moment which could even further increase for the tanks with higher aspect ratios.

This paper also discussed the importance of the need for an immediate recovery after a seismic event especially for the necked-rod system and bucking-restrained systems. The RSFD is the only damage-free hold-down mechanism for storage tanks with no stiffness or strength degradation at the design level. The tank equipped with RSFDs can withstand the possible aftershocks or next seismic event, therefore, a unique long term seismic solution minimizing the repair costs and business interruption.

It should be highlighted that, in line with other ground-motion-based studies and with respect to the outcomes of time-history analyses, the results presented herein are influenced by the selection of earthquake records and may vary if different ground motions, source regions, or scaling approaches are adopted.

8.16. References

1. Vathi, M., et al. (2017). Performance criteria for liquid storage tanks and piping systems subjected to seismic loading. Journal of Pressure Vessel Technology, 139(5).
2. Housner, G. W. (1957). Dynamic pressures on accelerated fluid containers. Bulletin of the Seismological Society of America, 47(1), 15-35.
3. American Petroleum Institute. (2020). Welded steel tanks for oil storage. (API Standard 650, 13th ed.).
4. New Zealand Society for Earthquake Engineering. (2009). Seismic design of storage tanks. Wellington, New Zealand.
5. Veletsos, A., et al. (1977). Earthquake response of liquid storage tank. In Advances in Civil Engineering Through Engineering Mechanics: Proceedings of the Engineering Mechanics Division Specialty Conference (pp. 1-24). Raleigh, N.C.: ASCE, New York, N.Y.
6. Veletsos, A., et al. (1990). Soil-structure interaction effects for laterally excited liquid storage tanks. Earthquake Engineering & Structural Dynamics, 19(4), 473-496.
7. Fischer, F. D. (1979). Dynamic fluid effects in liquid-filled flexible cylindrical tanks. Earthquake Engineering & Structural Dynamics, 7(6), 587-601.
8. ASCE/SEI (Structural Engineering Institute). (2007). Minimum design loads for buildings and other structures. ASCE/SEI 7-16. Reston, VA: California Geological Survey. Special Report 237, Sacramento, CA.

9. Yazdanian, M., et al. (2020). Damage to flat-based wine storage tanks in the 2013 and 2016 New Zealand earthquakes. Journal of Constructional Steel Research, 168, 105983.
10. Darani, F. M., Zarnani, P., Haemmerle, E., Hashemi, A., & Quenneville, P. (2018). Application of new resilient slip friction joint for seismic damage avoidance design of rocking concrete shear walls. In New Zealand Society for Earthquake Engineering (NZSEE) Conference.
11. Sahami, K., et al. (2020). Innovative damage-free anchorage system for cylindrical steel storage tanks. In 17th World Conference on Earthquake Engineering.
12. Prota, A., et al. (2009). Cyclic behaviour of smooth steel reinforcing bars: Experimental analysis and modelling issues. Journal of Earthquake Engineering, 13(4), 500-519.
13. Fahnestock, L. A., Sause, R., & Ricles, J. M. (2006). Analytical and large-scale experimental studies of earthquake-resistant buckling-restrained braced frame systems. ATLSS Reports, Report No. 06-01.
14. Dizhur, D., Simkin, G., Giaretton, M., Loporcaro, G., Palermo, A., & Ingham, J. (2017). Performance of winery facilities during the 14 November 2016 Kaikōura Earthquake. Bulletin of the New Zealand Society for Earthquake Engineering, 50(2).

Chapter 9: Conclusions and Future Studies

This chapter presents a summary of the materials covered in the preceding chapters. It highlights the primary motivations and objectives of the research, along with the methodologies employed to achieve these aims. Additionally, it reviews the conclusions drawn from each chapter, demonstrating how they collectively contribute to the overall goals of the study. Based on the assumptions and variations considered to meet the study objectives, this chapter also identifies key areas for future research and investigation on the topic.

9.1. Summary and concluding remarks

This research investigated the seismic performance of two applications of rocking systems equipped with self-centring friction dampers: rocking panel walls and cylindrical steel liquid storage tanks. Chapter 1 outlined the motivation behind this thesis and the criteria initially targeted to be achieved. Chapter 2 elaborated on the relevant previous work and key findings, including the studies on rocking walls and frames assumed to serve as the main lateral load resisting system of structures, as well as rocking steel cylindrical tanks for which the lateral resistance depends on the performance of the anchorage system.

The research aimed to develop new seismic solutions with energy dissipation and restoring force capabilities. The focus was on enhancing seismic resilience by integrating self-centring friction dampers into the rocking systems of both cylindrical steel liquid storage tanks and rocking panel walls. This approach aimed to offer more options for systems designed to perform as low-damage structures, potentially providing advantages that are well-suited to specific conditions.

In Chapter 3, the concept of rocking concrete shear walls with self-centring friction dampers was introduced and discussed. The primary objective was to achieve a controlled rocking mechanism as the main lateral system for buildings, minimizing residual drift. The proposed system consisted of rocking walls attached to boundary columns through the shear links designed as self-centring friction dampers. This system can be applied to both single and coupled shear walls, with the Rotational-RSFJ functioning as both a shear link and an energy dissipation device.

To evaluate the seismic performance of this system, a five-story prototype building with single and coupled rocking shear walls equipped with R-RSFJs was analysed. The results from the time history analysis, using seven ground motions, confirmed the efficiency of the proposed system. The structure exhibited full self-centring capabilities, met inter-story drift limits for both ULS and MCE, and showed a reduction in maximum bending demands. Additionally, the potential for isolating the walls in stories to mitigate higher mode effects was explored. Isolating the walls led to reductions in base shear, maximum bending moment, and maximum roof displacement.

In Chapter 4, we explored the integration of RSFJs as shear links to connect the braced frame to boundary columns. Unlike conventional rocking systems that use post-tensioning technology for restoring force and yielding fuses for added damping, this study employed the RSFJs as an efficient alternative. To evaluate the performance of this proposed system, we investigated the seismic behaviour of a five-storey office building, comparing it with conventional braced frames and LRB base isolation systems. The results from nonlinear time history analysis of seven ground motions indicated that the rocking system equipped with the RSFJ technology could potentially enhance the dynamic performance of the structure compared to the conventional braced frame. The new rocking system appeared to be highly effective in reducing base shear and overturning moment, which are crucial factors in designing rocking braced frames. The proposed mechanism met the inter-storey drift limitations with minimal residual drift. It offers advantages for taller structures, applicable to rocking frames, due to its load distribution and potential for multiple rocking levels.

Chapter 5 reported the results of an experimental test conducted to validate the proposed concept of incorporating RSFJs as shear links in a rocking system. A single panel wall was designed to withstand approximately 100kN of lateral load with a maximum drift of 2.5%, adhering to New Zealand building codes. The RSFJs were designed based on equations derived from earlier analytical studies and were tested to confirm their performance. The experiment consisted of three phases: cyclic loading in the in-plane direction to simulate seismic shaking, out-of-plane shaking to test deflection compatibility and pushing the system to the ultimate actuator stroke to observe the possible failure mode. The test setup included a single rocking wall with adjacent rocking columns, and the dimensions were tailored to fit the AUT laboratory spatial constraints.

The experimental setup utilized six RSFJs as shear links mounted on both sides of the wall, with steel columns providing structural support. The RSFJs and column connections were designed as pins to allow free rotation in response to wall movement. The test setup aimed to replicate real-world conditions, with instrumentation placed to measure displacements and ensure the actuator motion to be remained centered.

The results from the pull-push tests demonstrated that the overall wall and RSFJ performance were as expected. In the in-plane direction, the system produced a flag-shaped hysteresis loop, indicative of effective energy dissipation and damping characteristics. The RSFJs successfully replicated the damping rate predicted by the theoretical models, confirming their capability to provide both restoring force and energy dissipation during seismic events.

A range of frequencies were tested, including 0.1 Hz, 0.25 Hz, and 0.35 Hz. The results indicated that the system hysteretic performance remained stable across these frequencies, showing minimal impact on the overall behaviour of this new rocking system.

When tested for the out-of-plane deflection, the system movement was mostly free, with minimal contribution from the RSFJs. This behaviour suggested that the wall and columns could rotate around their bases with little resistance, primarily due to the friction provided by the shimming plates filling the gap between the concrete wall and base plates. The RSFJs were not significantly engaged in this direction, indicating that the in-plane energy dissipation and restoring force remained as their primary role.

The motivation behind Chapter 6 was to propose an alternative solution to address the associated damages reported in conventional anchored tank systems. The proposed solution aimed to regulate the movement and prevent the tank collapse. This system supposed to offer an improved alternative to existing systems, which often incur damage due to plastic deformation and require replacement after severe seismic events. Central to this novel approach was the introduction of new supplemental damping and ductility, which results in reduction of the seismic load demand to transmitted tank components.

To meet these challenges, a Resilient Slip Friction Damper (RSFD) was utilized to create a connection between cylindrical tanks and their foundations. A prototype RSFD

demonstrated successful performance in cyclic testing, achieved the intended flag-shaped hysteresis behaviour. This innovative damper system has been successfully implemented in real-world projects, enhancing the seismic resilience of steel storage tanks. It offers low damage solution with advantages of installation simplicity and cost-efficiency.

Chapter 7 focused on a published paper reporting the results of a case study involving a cylindrical tank with an aspect ratio of three. The study compared the performance of the RSFD with two conventional ductile anchorage systems: the necked-rod and buckling-restrained systems. The analysis highlighted the importance of tension-only performance in anchorage systems to prevent the introduction of compression zones at the gripping points on the tank body, which could lead to buckling issues. The RSFD system demonstrated an impactful reduction in overturning moment compared to the other two systems while maintaining a similar displacement demand. The overstrength factor for the RSFD system was 1.15, compared to 1.25 for necked rods and 1.4 for buckling-restrained connections.

The study also analysed various RSFD slip force ratios and found that when the slip forces exceeded a certain threshold, the displacement demands remained stable while k_f increased. This suggested an optimal upper limit for the slip forces. The RSFD stood out as a low-damage mechanism as long as the force demand remained below the design level, preparing the tank for potential aftershocks or future seismic events.

In Chapter 8, based on the API 650 standards, the performance of proposed anchorage systems was investigated and compared to other conventional systems. To evaluate this new hold-down system, three cylindrical tanks with aspect ratios of 0.5, 3, and 5 were used, and the results were compared with other conventional anchorage systems. In conventional systems, while the R factors assumed at the design stage were validated, the contribution of $R_\mu R_\zeta$ and R_Ω factors seemed not to be perfectly correlated. This means that, although such designs are safe for hold-downs, they may not offer the same level of safety for the tank and foundation as a higher over-strength factor may be required.

The comparative analysis across all the studied cases revealed that the tanks equipped with the RSFD system can be designed to withstand at least 30% less overturning moment. Such design benefit could be potentially increasing for the tanks with higher aspect ratios. The paper also highlighted the critical need for immediate recovery after a seismic event, in the cases of necked-rod and buckling-restrained systems. The tanks

equipped with RSFDs, given their mechanical behaviour, can withstand aftershocks or subsequent seismic events, offering a long-term seismic solution that minimises the repair costs and business interruption.

It should be noted that, where time-history analyses are undertaken in this thesis, and in line with other ground-motion-based studies, the results presented herein are influenced by the selection of earthquake records and may vary if different ground motions, source regions, or scaling approaches are adopted; this should be carefully considered by engineers and researchers when interpreting the findings.

9.2. Future works

The primary aim of this study was to validate new concepts that could be potentially adopted as low-damage solutions for controlled rocking systems. While rocking systems have historical roots in ancient buildings, certain aspects still require a better understanding allowing them to be widely accepted as the main lateral system in modern structures. This understanding could be enhanced through more practical testing that includes detailed simulations of real structures. The following items outline ideas for the next generation of research that warrant further exploration:

- Future research could focus on experimentally testing the effectiveness of splitting rocking frames or walls in height, as numerical models have shown this approach to be effective in addressing higher mode effects. Calibration of numerical models to achieve accurate outcome predictions could be a key target.
- Future research could pay more attention to the effects of vertical acceleration in rocking systems, as the rocking motion involves the collision of walls or frames with the ground. This factor could be critical in buildings with sensitive acceleration facilities, such as hospitals, laboratories, and data centers, where equipment and operations are susceptible to vertical shocks. Understanding the effects of vertical acceleration on these systems and developing design strategies to mitigate potential issues is essential to ensure the safety and functionality of such facilities during and after seismic events.
- Since the performance of such systems relies on the behaviour of damper devices, tuning and performance behaviour of these devices are crucial for the overall performance of the building. Future studies could investigate the distribution, possible tolerances of stiffness, strength, and damping contributions of these devices. Understanding tolerances and variations could help optimizing the design.

- As discussed in Chapter 5, there is room for further study on the soil-structure interaction of rocking systems. Several studies have investigated the dependency of superstructures on soil conditions. Similar to base isolation systems, it would be worthwhile to explore how rocking systems, which make structures more flexible and control deflection, interact with various soil conditions.
- Further studies could explore the connection of rocking frames or walls to diaphragms for load-bearing systems. Practical tests could focus on the deflection compatibility of conventional concrete flooring connections, which are assumed to be less complex. This could help to understand the overall structural behaviour and optimize the load-bearing applications, advancing the field of seismic engineering.
- A comprehensive study could aim to determine the ductility factor of rocking systems as a function of height. This would provide recommendations for ductility factors and damping ratios. A range of time history analyses could cover various scenarios to enhance our understanding.
- A few previous studies have focused on the performance of liquid tank structure with various base connections using shake table testing. Given the complexity of the interaction between liquid and tank walls and the impact of the rigidity of base connections, further experimental tests could provide valuable insights. These tests could help to calibrate the damping and ductility factors currently used in practical applications.
- There are opportunities for further research to explore the sustainability of controlled rocking systems with self-centring damper devices, focusing on their low-damage design and its impact on the components sizes. This study could examine how the reduced seismic load demand could result in less use of materials by smaller sizes, thus decreasing the embodied carbon emissions. Additionally, assess how the extended lifespan of these structures reduces the demand for repairs, replacements or new construction, which typically has a high carbon footprint due to material production, transportation, and installation (ie, lower whole-life carbon emission)

These research suggestions present opportunities for advancing the field of seismic engineering by improving our understanding of rocking systems and well optimising their performance and components design.

Appendix 1: Structural Drawings of the test setup and RC Frame

- In-plane setup

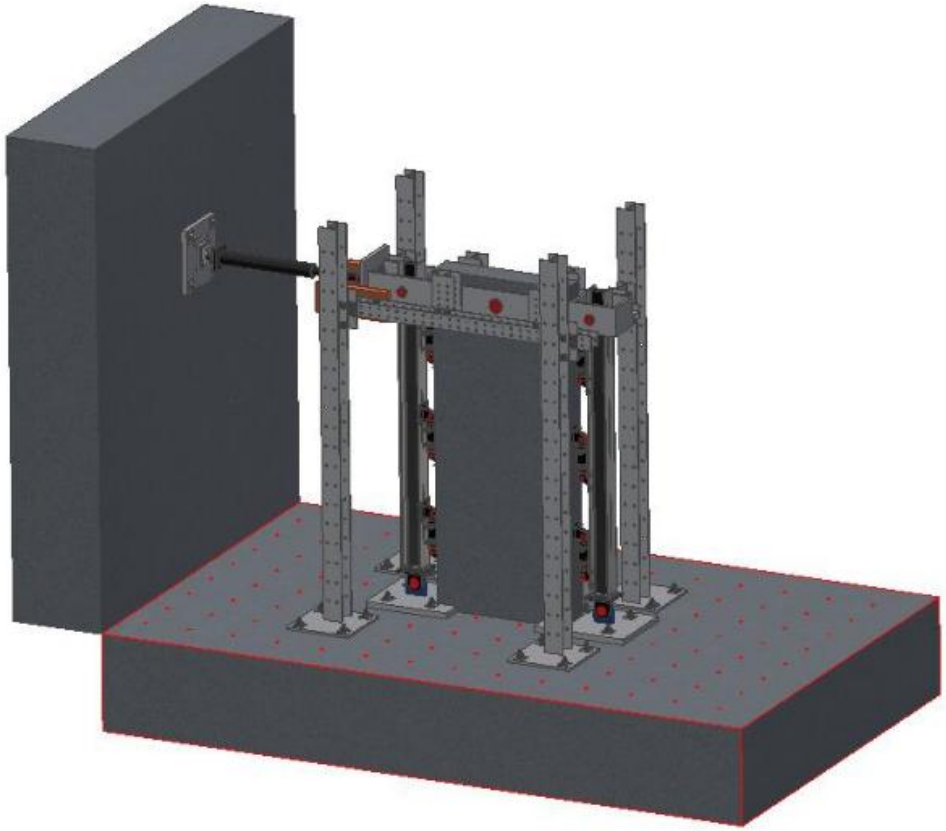

- Out-of-plane setup

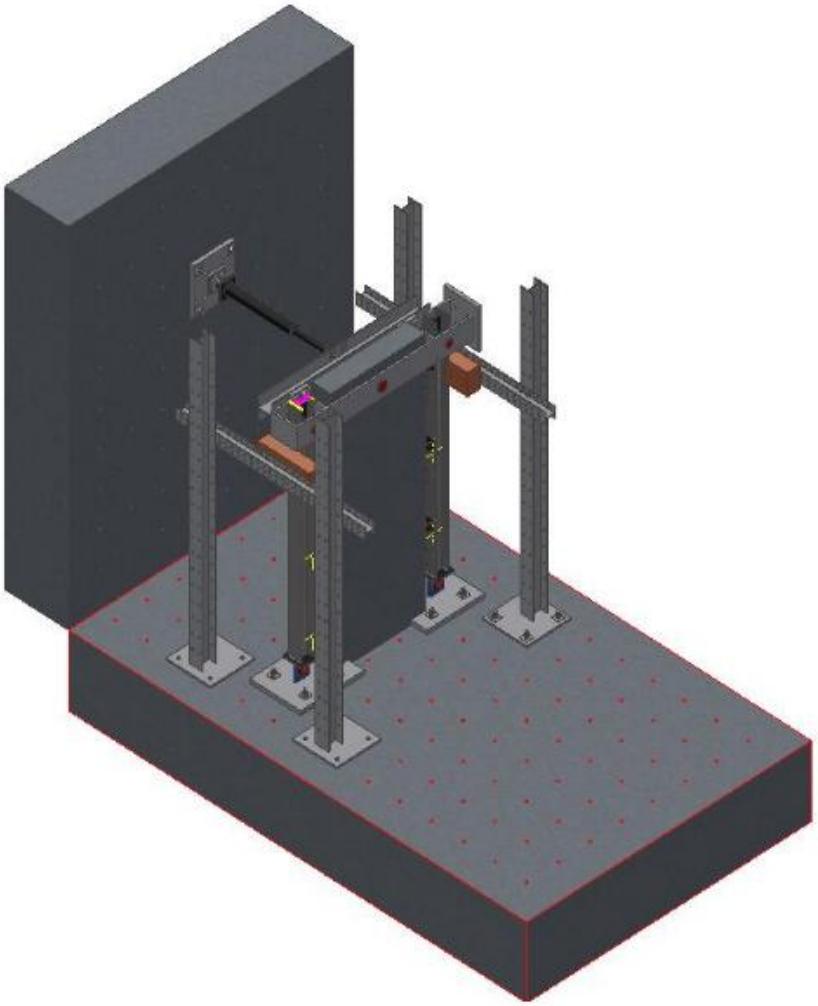

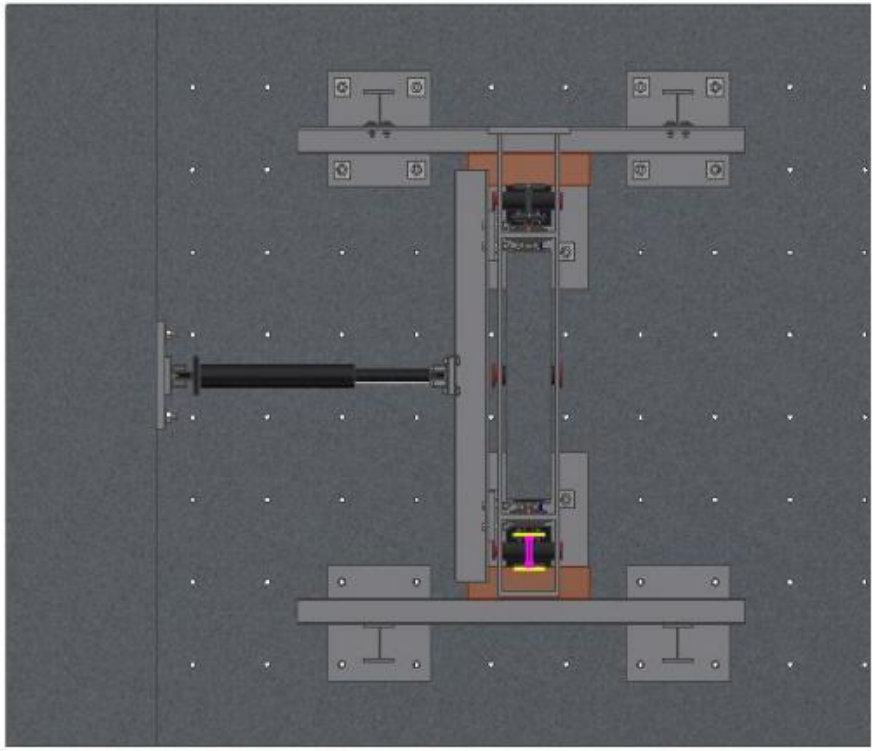

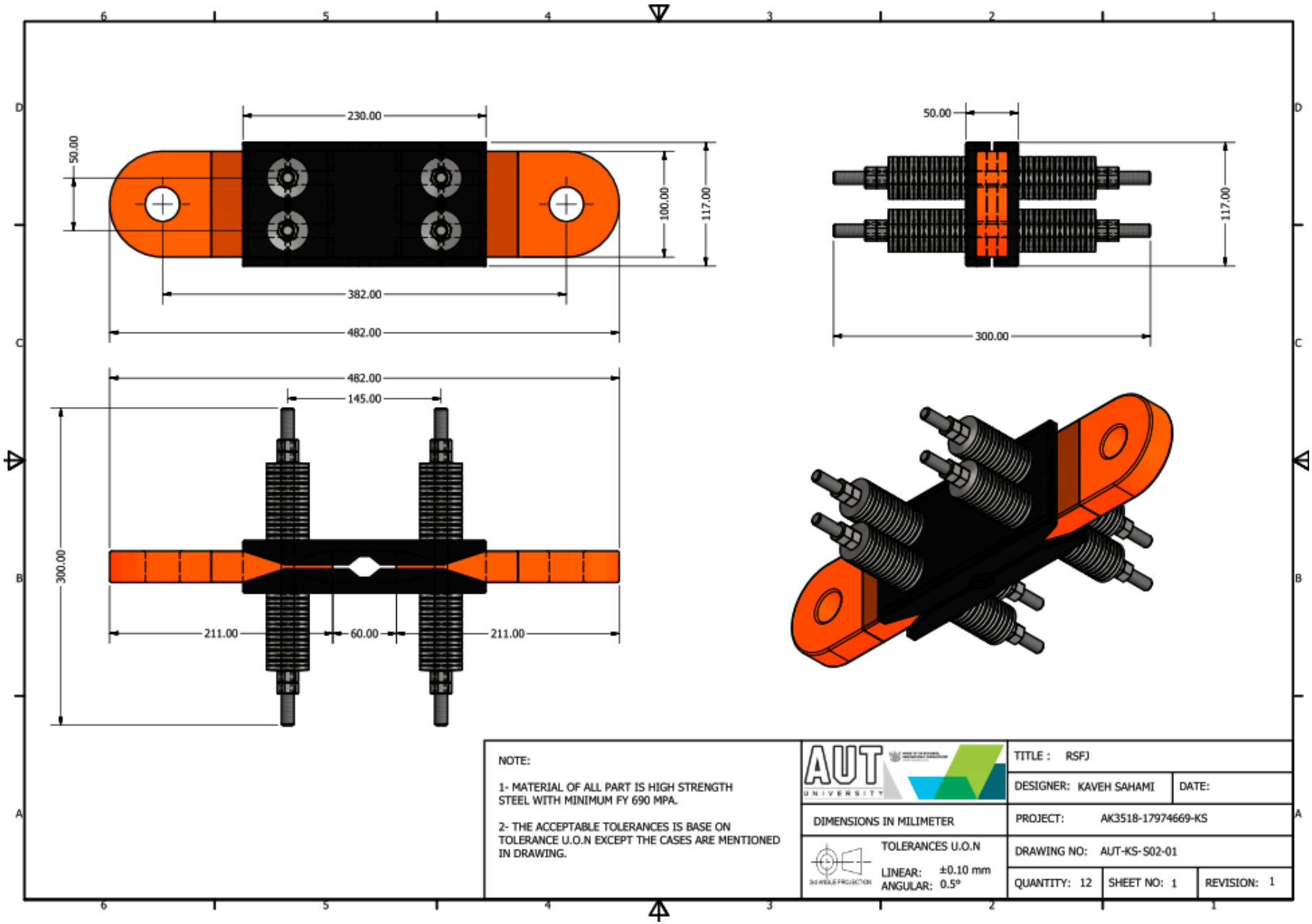
230.00
50.00
100.00
117.00
382.00
482.00
50.00
117.00
300.00
482.00
145.00
300.00
211.00
60.00
211.00
NOTE:
1- MATERIAL OF ALL PART IS HIGH STRENGTH STEEL WITH MINIMUM FY 690 MPA.
2- THE ACCEPTABLE TOLERANCES IS BASE ON TOLERANCE U.O.N EXCEPT THE CASES ARE MENTIONED IN DRAWING.
AUT UNIVERSITY
TITLE : RSFJ
DESIGNER: KAVEH SAHAMI
DATE:
DIMENSIONS IN MILIMETER
PROJECT: AK3518-17974669-KS
TOLERANCES U.O.N
LINEAR: ±0.10 mm
ANGULAR: 0.5°
DRAWING NO: AUT-KS-S02-01
QUANTITY: 12
SHEET NO: 1
REVISION: 1

- **RSFJ components**

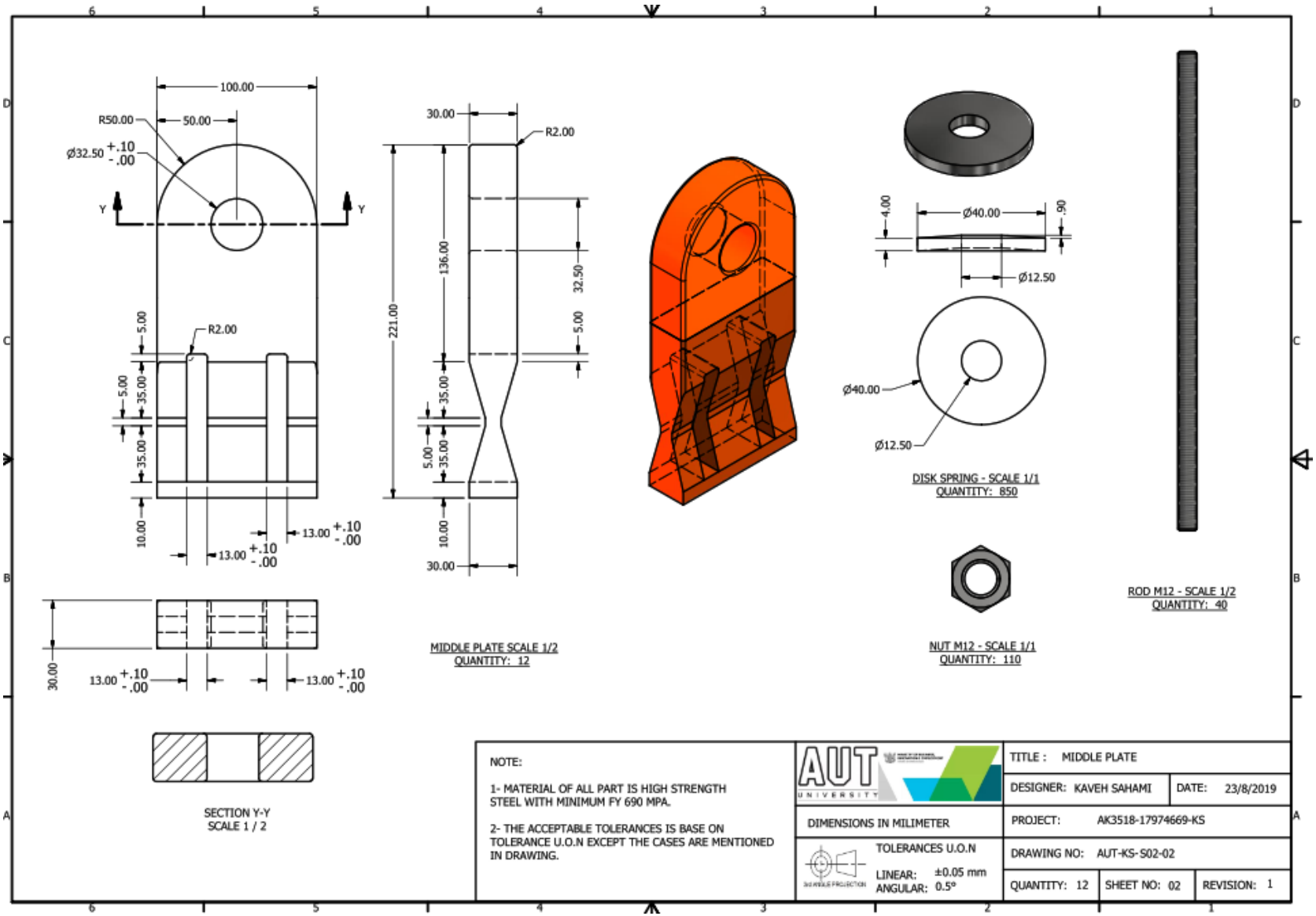

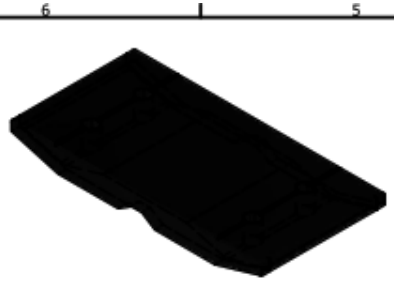

CAP PLATE ATTACHED EDGES - Scale 1/3

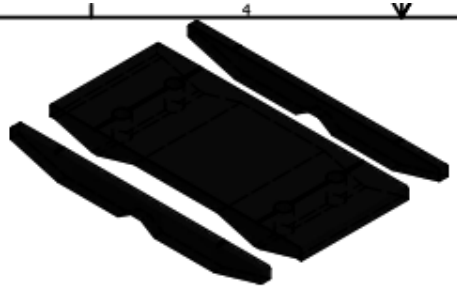

Cap Plate attched Edge plate - Scale 1/3

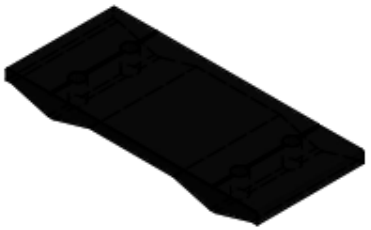

Cap Plate - Scale 1/3

Edge plate - Scale 1/3

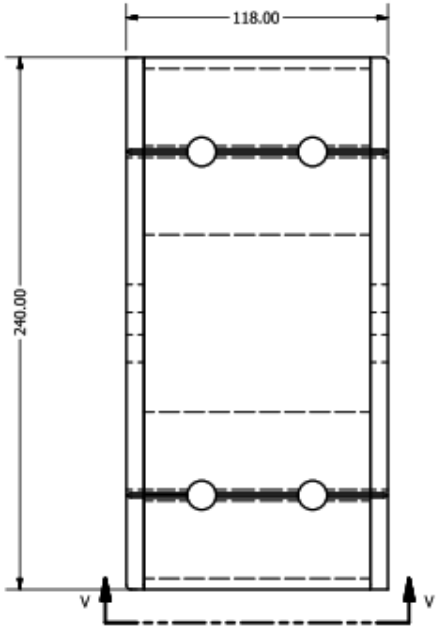

CAP PLATE ATTACHED EDGES - Scale 1/2
QUANTITY:12

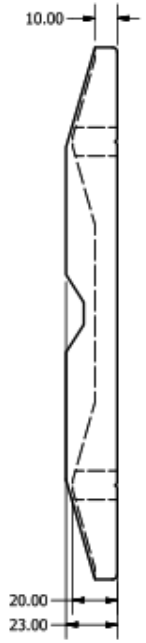

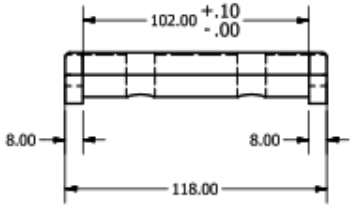

VIEW V-V
SCALE 1 / 2

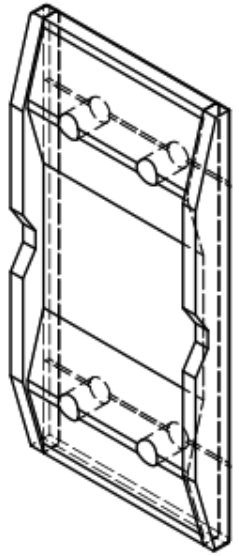

NOTE:

1- MATERIAL OF ALL PART IS HIGH STRENGTH STEEL WITH MINIMUM FY 690 MPA.

2- THE ACCEPTABLE TOLERANCES IS BASE ON TOLERANCE U.O.N EXCEPT THE CASES ARE MENTIONED IN DRAWING.

AUT UNIVERSITY

DIMENSIONS IN MILIMETER

TOLERANCES U.O.N
LINEAR: ±0.10 mm
ANGULAR: 0.5°

TITLE : CAP PLATE		
DESIGNER: KAVEH SAHAMI	DATE: 23/8/2019	
PROJECT: AK3518-17974669-KS		
DRAWING NO: AUT-KS-S02-03		
QUANTITY: 12	SHEET NO: 03	REVISION: 1

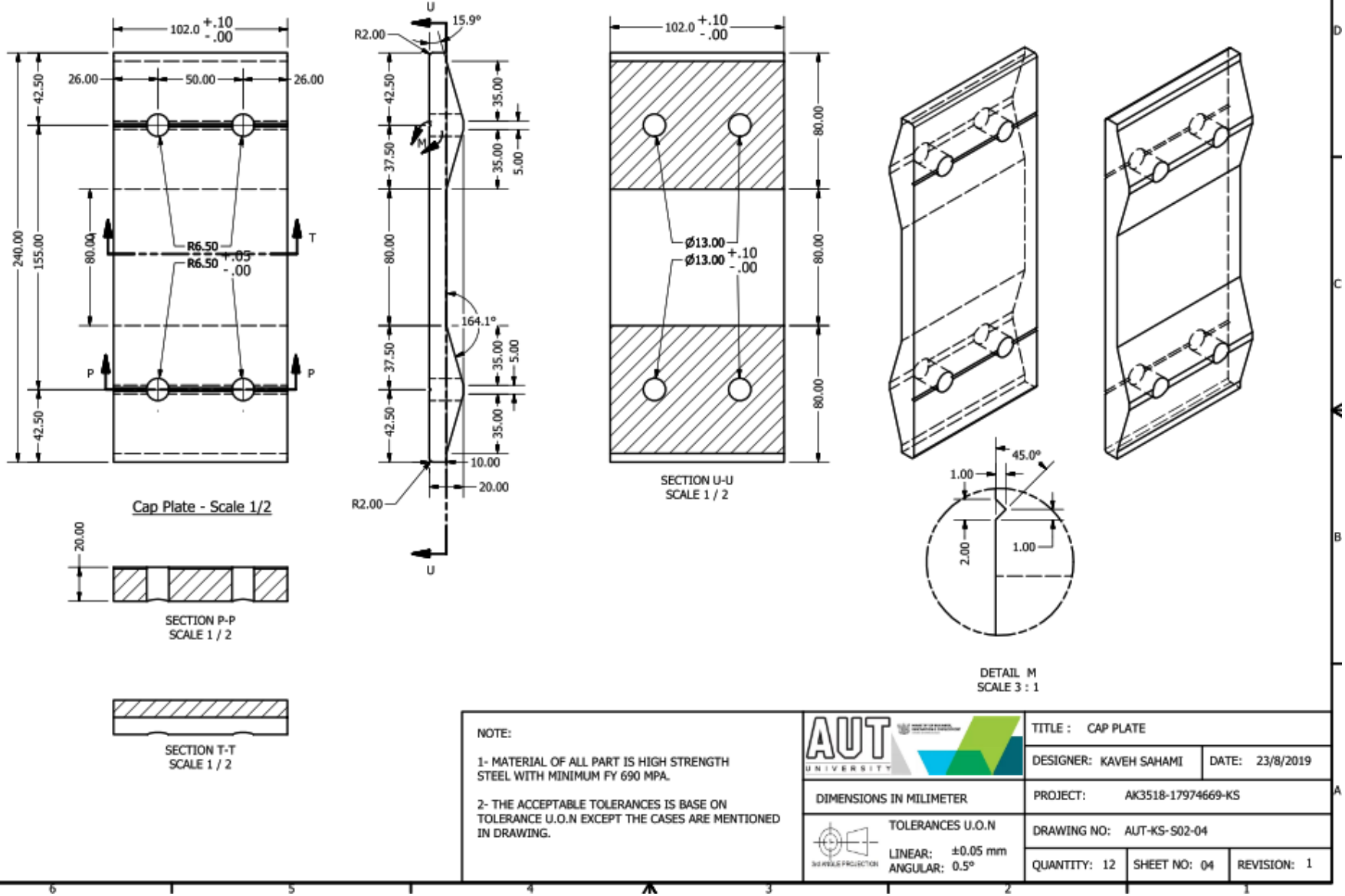
102.0 +.10 -.00
26.00
50.00
26.00
42.50
240.00
155.00
80.00
R6.50
R6.50 +.03 -.00
T
P
P
42.50
Cap Plate - Scale 1/2
U
15.9°
R2.00
42.50
37.50
80.00
164.1°
37.50
42.50
35.00
35.00
5.00
35.00
5.00
10.00
20.00
R2.00
U
102.0 +.10 -.00
80.00
80.00
80.00
80.00
Ø13.00
Ø13.00 +.10 -.00
SECTION U-U
SCALE 1 / 2
45.0°
1.00
2.00
1.00
DETAIL M
SCALE 3 : 1
20.00
SECTION P-P
SCALE 1 / 2
SECTION T-T
SCALE 1 / 2
NOTE:
1- MATERIAL OF ALL PART IS HIGH STRENGTH STEEL WITH MINIMUM FY 690 MPA.
2- THE ACCEPTABLE TOLERANCES IS BASE ON TOLERANCE U.O.N EXCEPT THE CASES ARE MENTIONED IN DRAWING.
AUT UNIVERSITY
DIMENSIONS IN MILIMETER
TOLERANCES U.O.N
LINEAR: ±0.05 mm
ANGULAR: 0.5°
TITLE : CAP PLATE
DESIGNER: KAVEH SAHAMI
DATE: 23/8/2019
PROJECT: AK3518-17974669-KS
DRAWING NO: AUT-KS-S02-04
QUANTITY: 12
SHEET NO: 04
REVISION: 1

- **Concrete shear wall components**

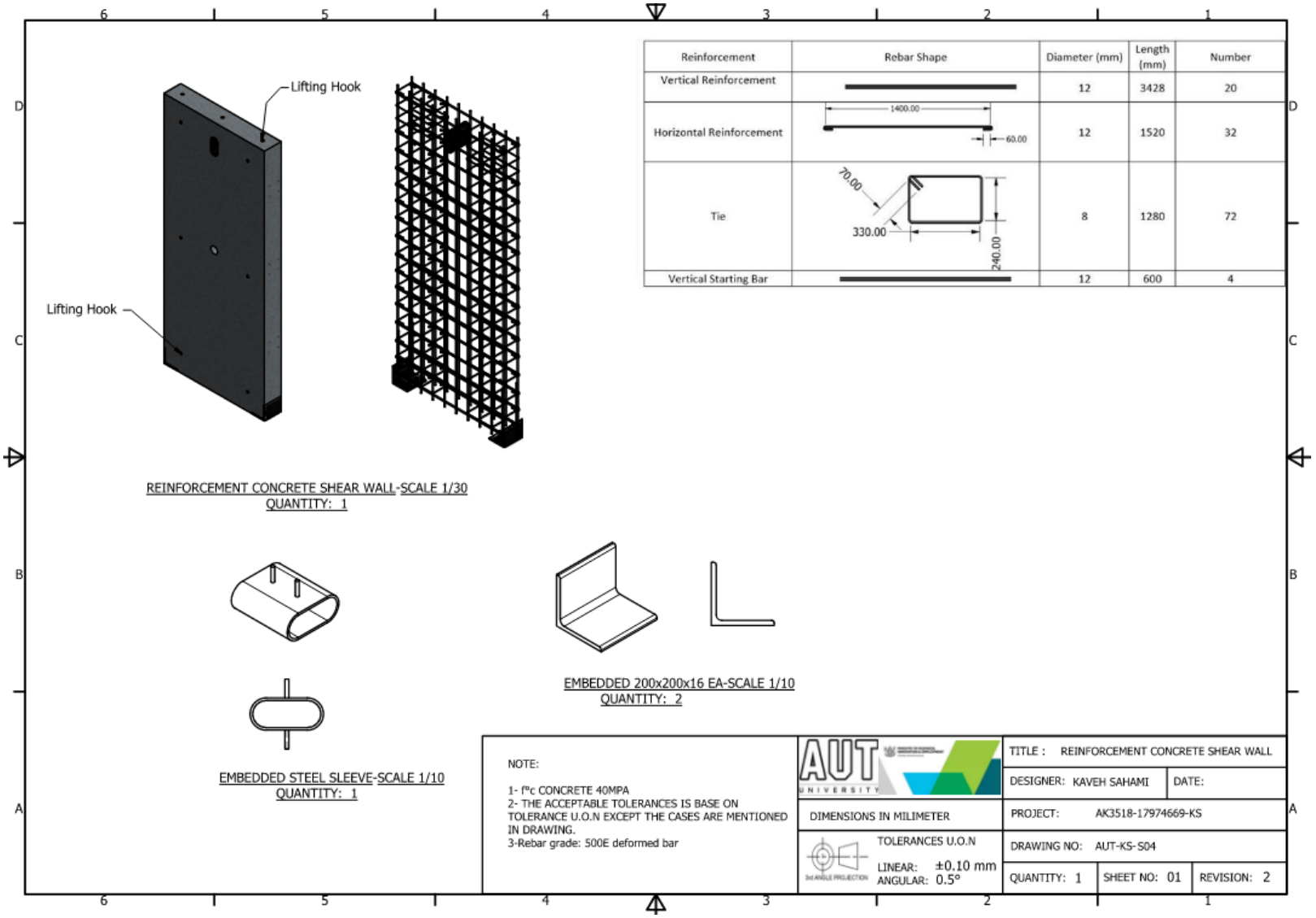

Reinforcement	Rebar Shape	Diameter (mm)	Length (mm)	Number
Vertical Reinforcement		12	3428	20
Horizontal Reinforcement	1400.00, 60.00	12	1520	32
Tie	70.00, 330.00, 240.00	8	1280	72
Vertical Starting Bar		12	600	4

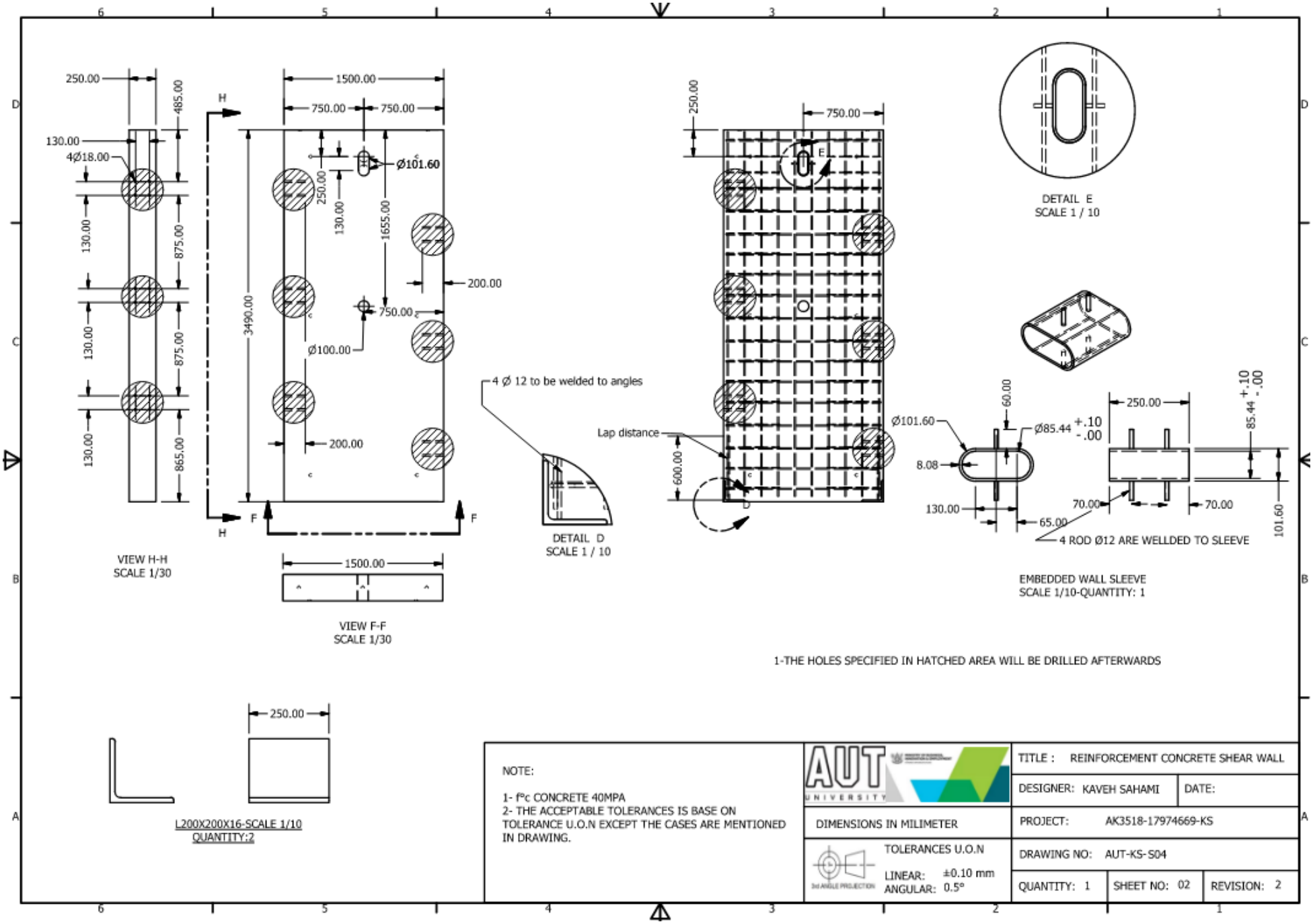

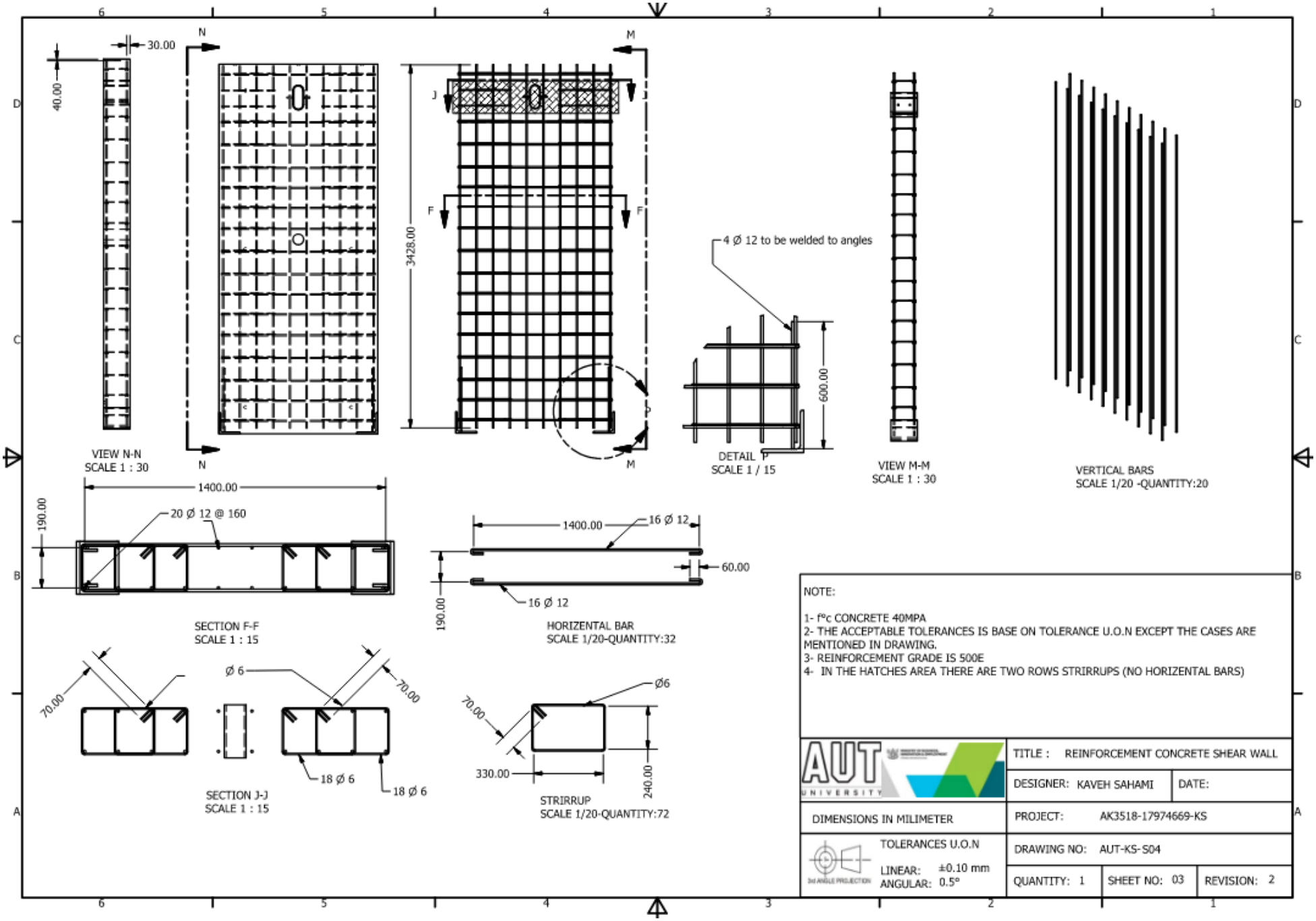

NOTE:

1- f°c CONCRETE 40MPA
2- THE ACCEPTABLE TOLERANCES IS BASE ON TOLERANCE U.O.N EXCEPT THE CASES ARE MENTIONED IN DRAWING.
3- REINFORCEMENT GRADE IS 500E
4- IN THE HATCHES AREA THERE ARE TWO ROWS STRIRRUPS (NO HORIZENTAL BARS)

AUT UNIVERSITY	TITLE : REINFORCEMENT CONCRETE SHEAR WALL	
	DESIGNER: KAVEH SAHAMI	DATE:
DIMENSIONS IN MILIMETER	PROJECT: AK3518-17974669-KS	
TOLERANCES U.O.N LINEAR: ±0.10 mm ANGULAR: 0.5°	DRAWING NO: AUT-KS-S04	
	QUANTITY: 1 / SHEET NO: 03	REVISION: 2

- **Steel column and associated connections**

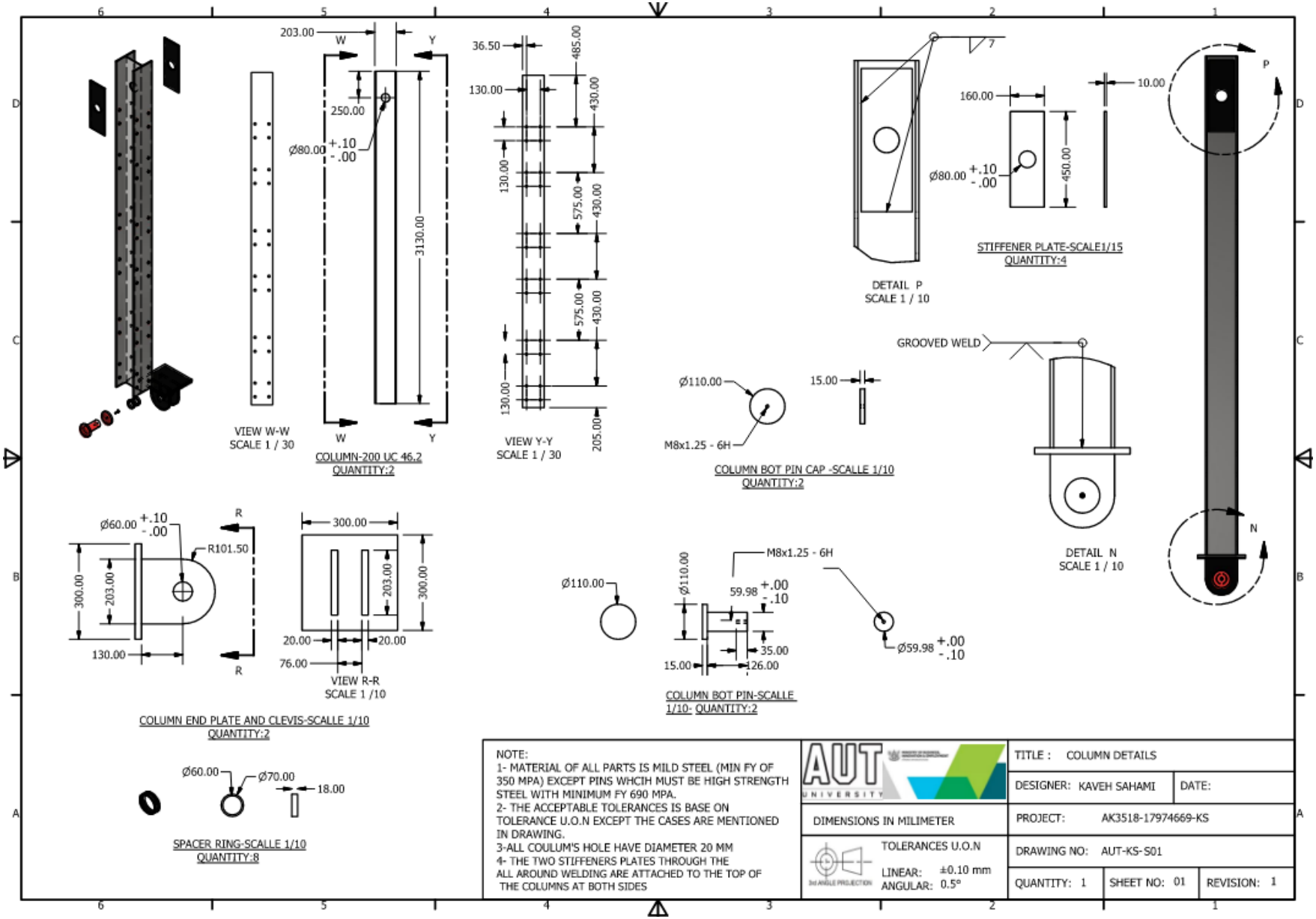

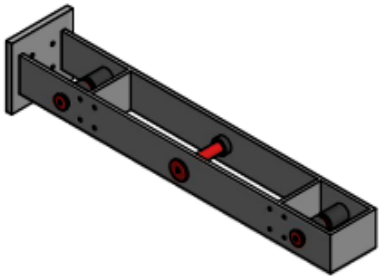

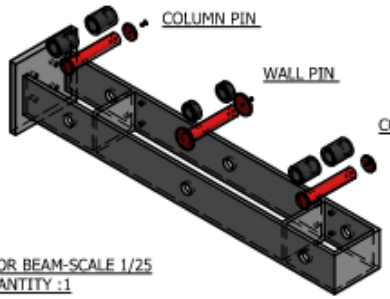

CONNECTOR BEAM-SCALE 1/25
QUANTITY :1

VIEW W-W
SCALE 1 / 15

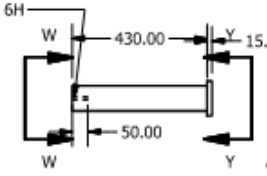

COLUMN PIN -SCALE 1/15
QUANTITY:2

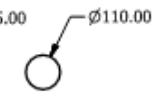

VIEW Y-Y
SCALE 1 / 15

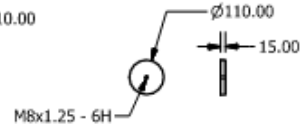

COLUMN PIN CAP -SCALE 1/15
QUANTITY:2

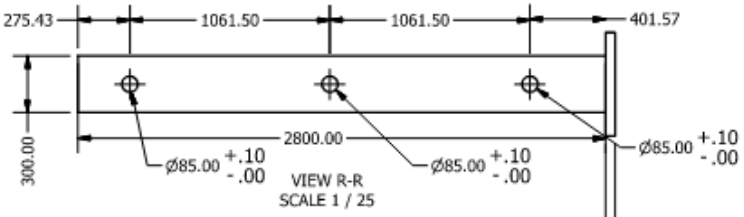

VIEW R-R
SCALE 1 / 25

VIEW AA-AA
SCALE 1 / 15

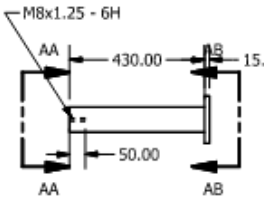

WALL PIN-SCALE 1/15
QUANTITY:1

VIEW AB-AB
SCALE 1 / 15

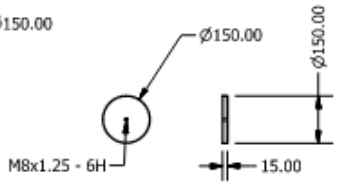

WALL PIN CAP -SCALE 1/15
QUANTITY :1

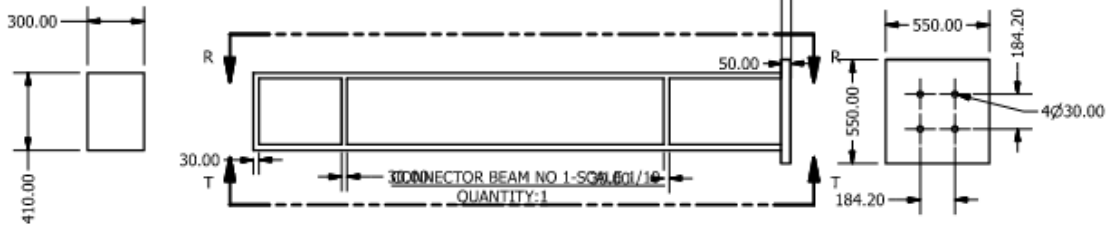

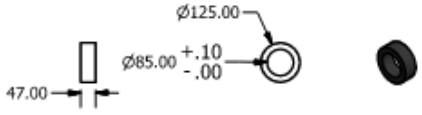

SLEEVE WALL PIN -SCALE 1/15
QUANTITY:2

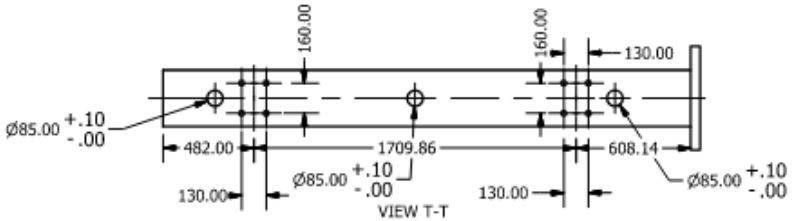

VIEW T-T
SCALE 1 / 25

SLEEVE COLUMN PIN-SCALE 1/15
QUANTITY:4

NOTE:
1- MATERIAL OF ALL PARTS IS MILD STEEL (MIN FY OF 350 MPA) EXCEPT PINS WHCIH MUST BE HIGH STRENGTH STEEL WITH MINIMUM FY 690 MPA.
2- THE ACCEPTABLE TOLERANCES IS BASE ON TOLERANCE U.O.N EXCEPT THE CASES ARE MENTIONED IN DRAWING.

AUT UNIVERSITY	TITLE : CONNECTOR BEAM	
	DESIGNER: KAVEH SAHAMI	DATE:
DIMENSIONS IN MILIMETER	PROJECT: AK3518-17974669-KS	
TOLERANCES U.O.N LINEAR: ±0.10 mm ANGULAR: 0.5°	DRAWING NO: AUT-KS-S02	
	QUANTITY: 1 / SHEET NO: 02	REVISION: 1

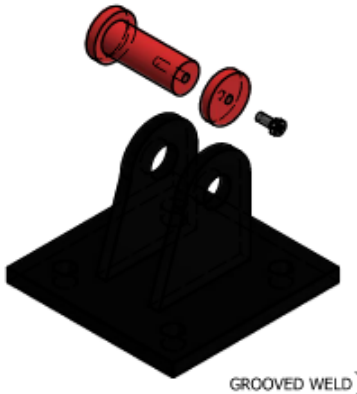

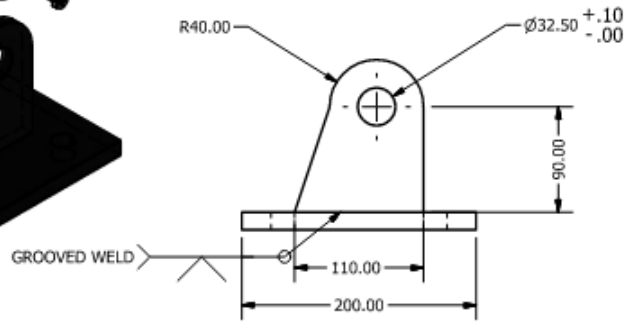

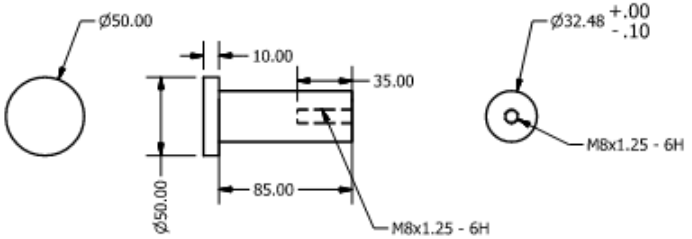

RSFJ PIN-SCALE 1/4
QUANTITY: 12

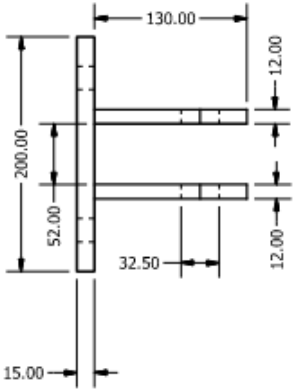

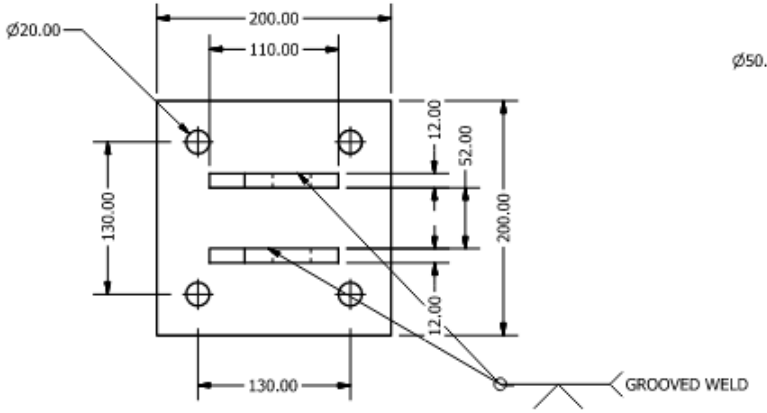

RSFJ CLEVIS AND END PLATE-SCALE 1/4
QUANTITY: 12

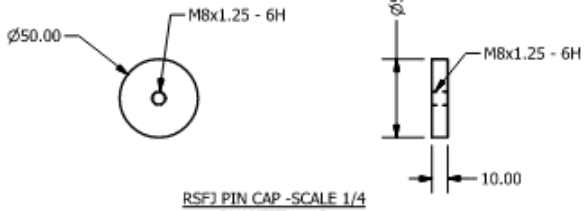

RSFJ PIN CAP -SCALE 1/4
QUANTITY: 12

NOTE:
1- MATERIAL OF ALL PARTS IS MILD STEEL (MIN FY OF 350 MPA) EXCEPT PINS WHCIH MUST BE HIGH STRENGTH STEEL WITH MINIMUM FY 690 MPA.
2- THE ACCEPTABLE TOLERANCES IS BASE ON TOLERANCE U.O.N EXCEPT THE CASES ARE MENTIONED IN DRAWING.

AUT UNIVERSITY	TITLE : RSFJ CONNECTION	
	DESIGNER: KAVEH SAHAMI	DATE:
DIMENSIONS IN MILIMETER	PROJECT: AK3518-17974669-KS	
TOLERANCES U.O.N LINEAR: ±0.10 mm ANGULAR: 0.5°	DRAWING NO: AUT-KS-S03	
	QUANTITY: 1	SHEET NO: 03 REVISION: 1

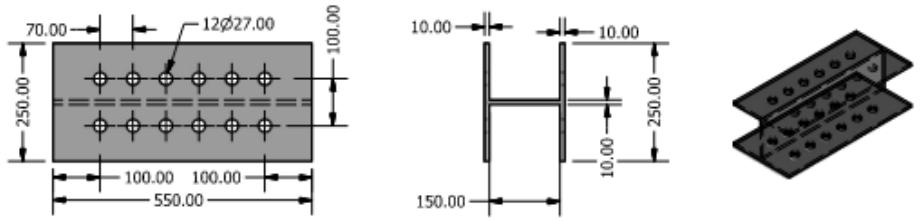

SUPPORT BEAM 01-SCALE 1/10
QUANTITY:4

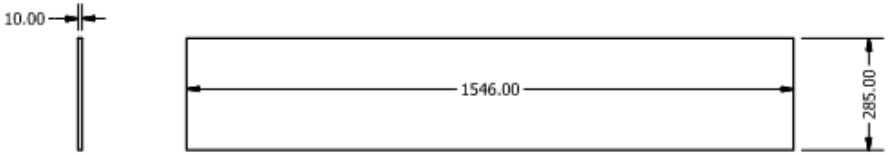

FILLER PLATE 01-SCALE 1/12
QUANTITY: 1

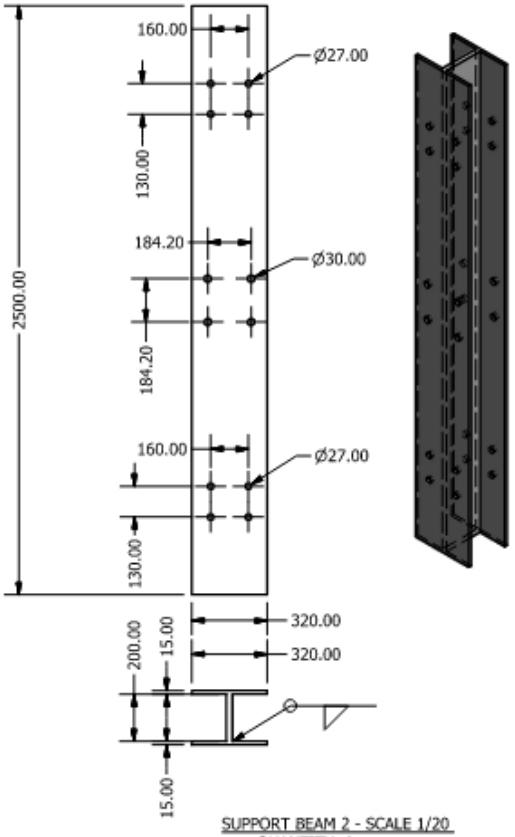

SUPPORT BEAM 2 - SCALE 1/20
QUANTITY: 1

NOTE:
1- MATERIAL OF ALL PARTS IS MILD STEEL (MIN FY OF 350 MPA) EXCEPT PINS WHCIH MUST BE HIGH STRENGTH STEEL WITH MINIMUM FY 690 MPA.
2- THE ACCEPTABLE TOLERANCES IS BASE ON TOLERANCE U.O.N EXCEPT THE CASES ARE MENTIONED IN DRAWING.

AUT UNIVERSITY	TITLE : COLUMN	
	DESIGNER: KAVEH SAHAMI	DATE:
DIMENSIONS IN MILIMETER	PROJECT: AK3518-17974669-KS	
TOLERANCES U.O.N LINEAR: ±0.10 mm ANGULAR: 0.5°	DRAWING NO: AUT-KS-S04	
	QUANTITY: 1	SHEET NO: 04 REVISION: 1

BASE PLATE 01
SCALE 1/15 - QUANTITY: 1

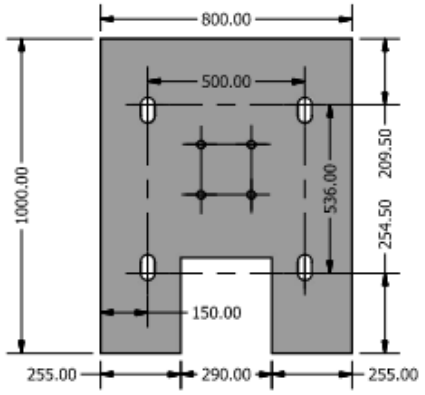

BASE PLATE 02
SCALE 1/15 - QUANTITY: 1

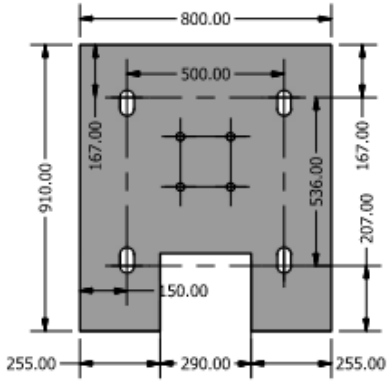

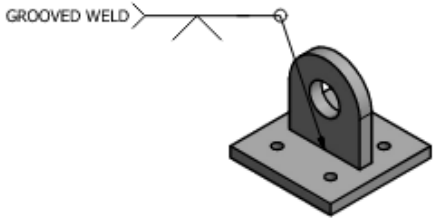

BASE PLATE CLEVIS
SCALE 1/10 - QUANTITY: 2

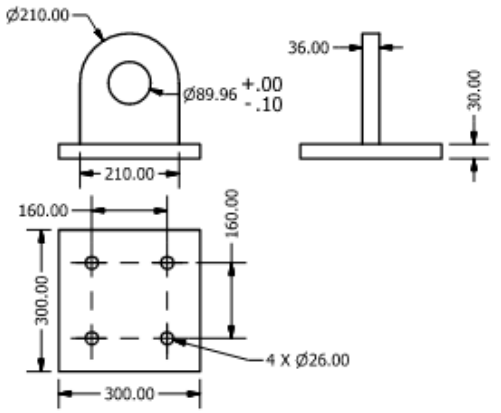

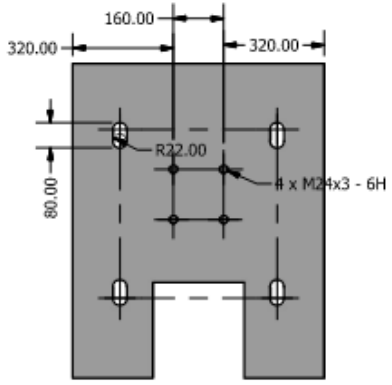

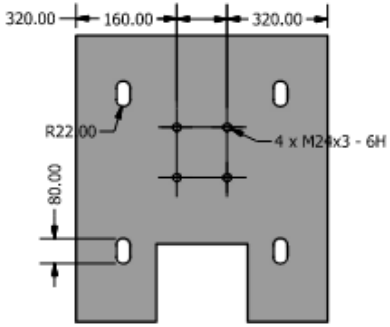

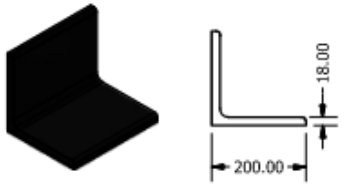

L20X20X12-SCALE 1/10
QUANTITY:2

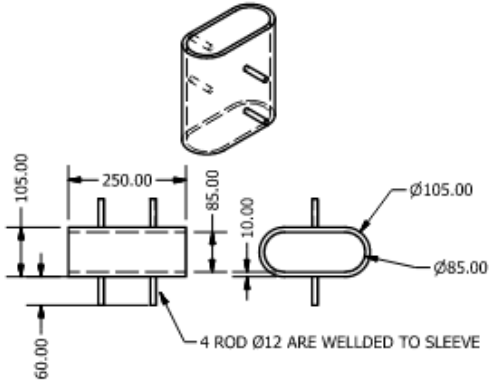

EMBEDDED WALL SLEEVE
SCALE 1/10-QUANTITY: 1

NOTE:
1- MATERIAL OF ALL PARTS IS MILD STEEL (MIN FY OF 350 MPA) EXCEPT PINS WHCIH MUST BE HIGH STRENGTH STEEL WITH MINIMUM FY 690 MPA.
2- THE ACCEPTABLE TOLERANCES IS BASE ON TOLERANCE U.O.N EXCEPT THE CASES ARE MENTIONED IN DRAWING.

AUT UNIVERSITY	TITLE : COLUMN BASE PLATE	
	DESIGNER: KAVEH SAHAMI	DATE:
DIMENSIONS IN MILIMETER	PROJECT: AK3518-17974669-KS	
TOLERANCES U.O.N LINEAR: ±0.10 mm ANGULAR: 0.5°	DRAWING NO: AUT-KS-S05	
	QUANTITY: 1 / SHEET NO: 05	REVISION: 1

- **Prototype Development of the Resilient Slip Friction Device (RSFD)**

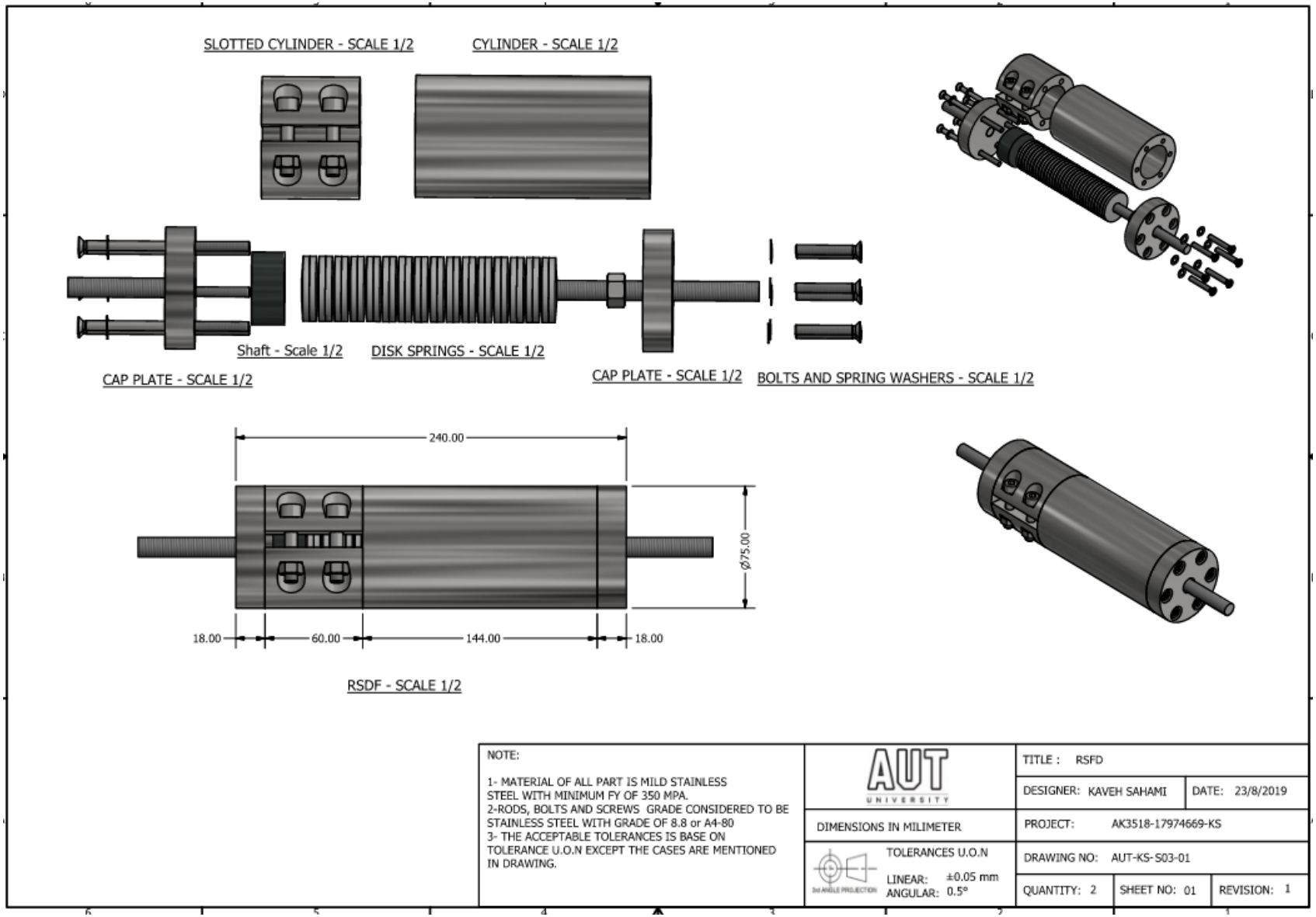

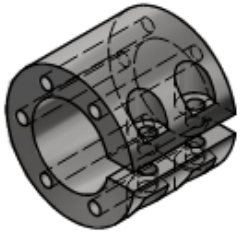

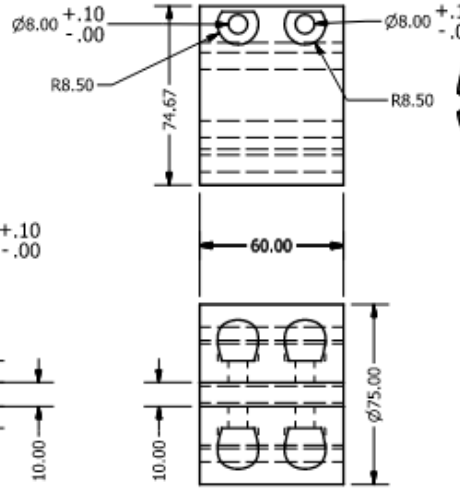

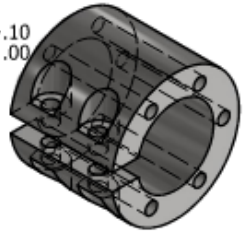

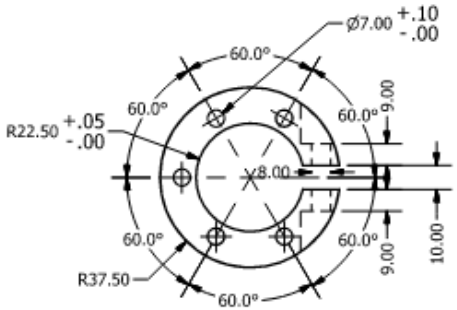

SLOTTED CYLINDER - SCALE 1/2
QUANTITY:2

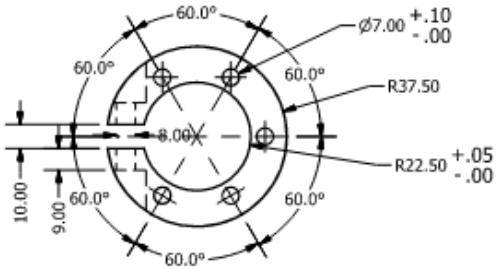

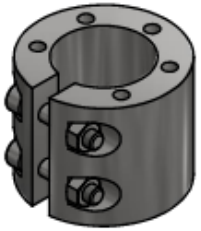

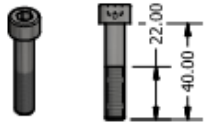

BOLT M8 SOCKET HEAD
SCALE 1/2, QUANTITY : 8

-

WASHER M8 - SCALE 1/2
QUANTITY : 8

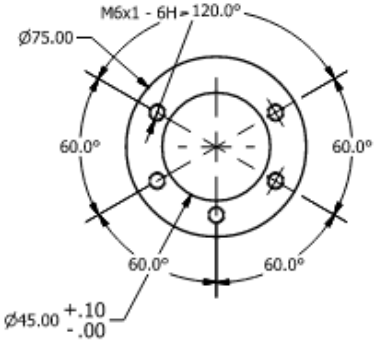

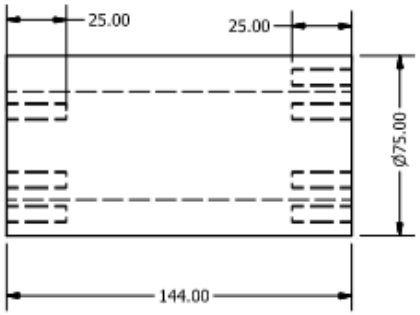

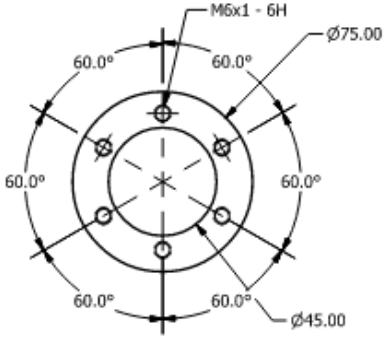

CYLINDER - SCALE 1/2
QUANITITY : 2

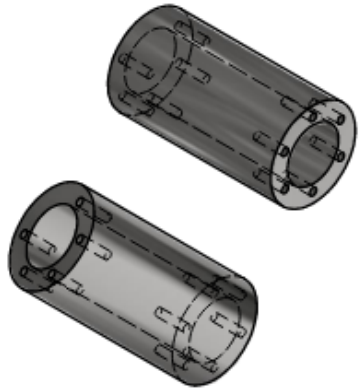

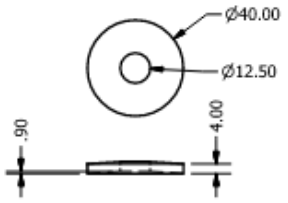

DISK SPRING - SCALE 1/2
QUANITITY : 80

NOTE:

1- MATERIAL OF ALL PART IS MILD STAINLESS STEEL WITH MINIMUM FY OF 350 MPA.
2-RODS, BOLTS AND SCREWS GRADE CONSIDERED TO BE STAINLESS STEEL WITH GRADE OF 8.8 or A4-80
3- THE ACCEPTABLE TOLERANCES IS BASE ON TOLERANCE U.O.N EXCEPT THE CASES ARE MENTIONED IN DRAWING.

AUT UNIVERSITY

DIMENSIONS IN MILIMETER

TOLERANCES U.O.N
LINEAR: ±0.05 mm
ANGULAR: 0.5°

TITLE : RSFD CYLINDERS		
DESIGNER: KAVEH SAHAMI	DATE: 23/8/2019	
PROJECT: AK3518-17974669-KS		
DRAWING NO: AUT-KS-S03-02		
QUANTITY: 12	SHEET NO: 02	REVISION: 1

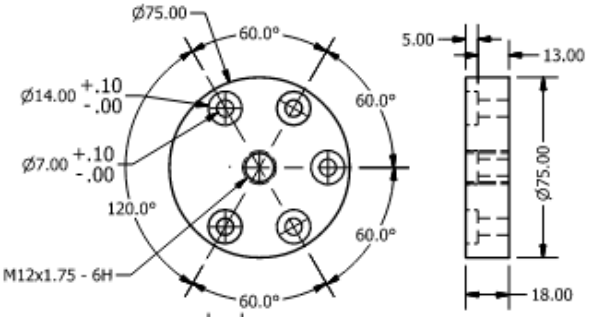

CAP PLATE - SCALE 1/2
QUANTITY: 2

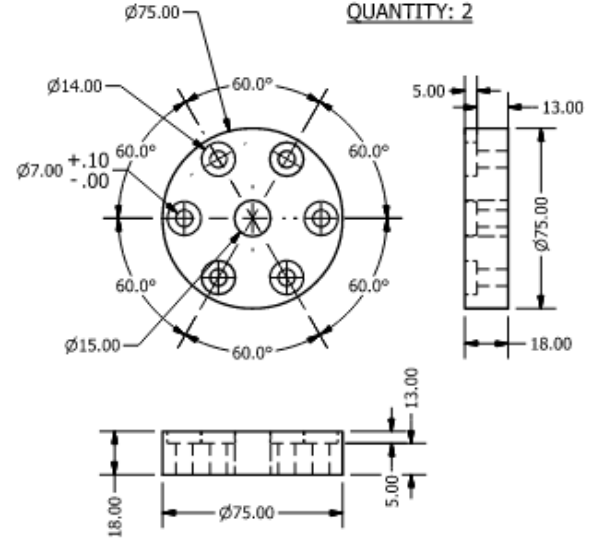

CAP PLATE - SCALE 1/2
QUANTITY: 2

WASHER SPRING M6 - SCALE 1/2
QUANTITY: 45

NUT M12-SCALE 1/2-
QUANTITY: 10

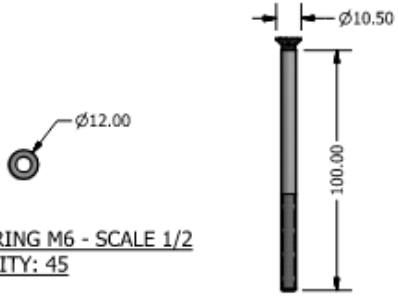

COUNTERSUNK SCREW M6 GRADE 8.8
SCALE 1/2-QUANTITY: 20

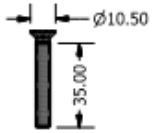

COUNTERSUNK SCREW M6 GRADE 8.8
SCALE 1/2-QUANTITY: 24

ROD M12 (GRADE: 8.8)
SCALE 1/2-QUANTITY: 4

ROD M12 (GRADE 8.8)
SCALE 1/2-QUANTITY: 4

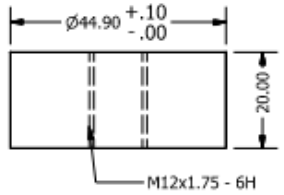

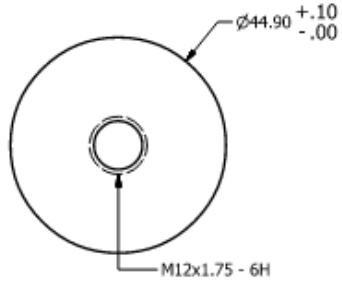

SHAFT - SCALE 1/2
QUANTITY: 2

NOTE:

1- MATERIAL OF ALL PART IS MILD STAINLESS STEEL WITH MINIMUM FY OF 350 MPA.
2-RODS, BOLTS AND SCREWS GRADE CONSIDERED TO BE STAINLESS STEEL WITH GRADE OF 8.8 or A4-80
3- THE ACCEPTABLE TOLERANCES IS BASE ON TOLERANCE U.O.N EXCEPT THE CASES ARE MENTIONED IN DRAWING.

AUT UNIVERSITY

DIMENSIONS IN MILIMETER

TOLERANCES U.O.N
LINEAR: ±0.05 mm
ANGULAR: 0.5°

TITLE : RSFD CYLINDERS		
DESIGNER: KAVEH SAHAMI	DATE: 23/8/2019	
PROJECT: AK3518-17974669-KS		
DRAWING NO: AUT-KS-S03-03		
QUANTITY: 12	SHEET NO: 03	REVISION: 1

- **Enhanced RSFD Prototype for Commercial Seismic Resilience Projects**